Cenomanian–Turonian Radiolarians of Northern Turkey and the Crimean Mountains

L. G. Bragina

Geological Institute, Russian Academy of Sciences, Pyzhevskii per. 7, Moscow, 119017 Russia

e-mail: bragin.n.@mail.ru

Received December 5, 2003

Contents

Vol. 38, Suppl. 4, 2004

The supplement is published only in English by MAIK "Nauka/Interperiodica" (Russia).
Paleontological Journal ISSN 0031-0301.

Paleontological Journal, Vol. 38, Suppl. 4, 2004, pp. S325–S456.

Abstract—The Middle Cenomanian–Early Turonian radiolarians are studied from two sections of the central Pontic Mountains (northern Turkey) and three sections of the Crimean Mountains. The type section of the Tomalar Formation (Turkey) contains a Middle–Early Cenomanian assemblage with *Dactyliosphaera silviae*, correlative to the upper part of the *Dactyliosphaera silviae* Zone in the western Mediterranean. The Ürküt section (Turkey) yielded a rich assemblage with species characteristic of the *Dactyliosphaera silviae* Zone. In the Crimean Mountains there are two radiolarian assemblages (from the base upward): (1) *Triactoma parva–Patulibracchium ingens* Assemblage (Late Cenomanian), which corresponds to the upper part of the *Dactyliosphaera silviae* Zone, and (2) *Alievium superbum* Assemblage (Early Turonian), which corresponds to the *Alievium superbum* circumtropical Zone. These radiolarian assemblages are compared with those known from the literature, and the stratigraphic ranges of these radiolarians are revised. Descriptions of 193 species belonging to 4 orders, 28 families, and 77 genera are given. These include 1 genus and 3 species that were previously erected by the author and descriptions of 1 new genus and 36 new species. Diagnoses of 5 genera and 28 species are emended. Most of the stratigraphic and geographic ranges of these radiolarians are more precisely delimited.

Key words: Radiolaria, Nassellaria, Spumellaria, stratigraphy, Upper Cretaceous, Crimean Mountains, northern Turkey, systematics.

INTRODUCTION

Radiolarians, earlier thought to be of little stratigraphical significance, have become important in detailed subdivision and correlation of markedly dislocated strata of mobile belts. Great progress has been made in the stratigraphy of the Mesozoic and Paleozoic siliceous rocks despite their puzzling structures and genesis and the fact that they contain virtually no fossils other than radiolarians.

This is also true for Cretaceous deposits. The pioneering publications by Foreman (1968) and Pessagno (1971a, 1971b, 1973), which described some families and lower taxa of Cretaceous radiolarians and made a preliminary analysis of their stratigraphic ranges in the reference sections, were shortly followed by the first publications on radiolarian zonation of the Cretaceous (Riedel and Sanfilippo, 1974; Foreman, 1975; Pessagno, 1976; Schaaf, 1981). The great potential of such zonation became evident as early as the 1970s, despite the fact that their resolution was then low. Subsequently, radiolarian zonations of higher resolution were established in the Mediterranean region for the Lower Cretaceous (Jud, 1994; Baumgartner *et al.*, 1995) and the upper Lower–lower Upper Cretaceous (Barremian–Turonian) (Erbacher, 1994; O'Dogherty, 1994).

These zonations should be applied to those areas of the Mediterranean mobile belt in which radiolarians have been of little or no use in Cretaceous stratigraphy. For example, in areas such as the Crimea and northern Turkey, radiolarians may be valuable for regional stratigraphy and useful in establishing interregional correlations between radiolarian biostratigraphic units and in improving knowledge of the stratigraphic and geographic ranges of some radiolarian taxa.

The previous papers on Cretaceous radiolarian assemblages dealt mainly with those taxa that were recorded from deep oceanic deposits and deepwater siliceous and siliceous–carbonate rock strata of mobile belts. Radiolarians from relatively shallow-water or moderately deepwater carbonate–terrigenous deposits of mobile belts and their peripheral zones, i.e., those regions in which the reference sections of the Cretaceous System were based on other groups of fossils, have received little study. Future study of radiolarians from these regions may yield more accurate data on the distribution and stratigraphic potential of some taxa, thus providing a baseline for refined stratigraphic zonation and correlation and paleoecological and paleobiogeographic reconstructions. Finally, they should fill considerable gaps in our present knowledge of ancient radiolarian diversity.

The purpose of this work is to study the Cenomanian–Turonian radiolarians of northern Turkey and the Crimean Mountains. Both of these regions belong to the Mediterranean mobile belt, within which this stratigraphic interval is most reliably subdivided by radiolarians. The Crimea lies on the periphery of this belt. The Crimean sections are composed of rocks that formed in much shallower waters than the oceanic waters of the Tethys, and are characterized by various fossil groups including, as shown below, representative radiolarian assemblages. The sections from northern Turkey are typical of the central Mediterranean belt, being intermediate between the Crimean sections and the type areas of the Middle Cretaceous radiolarian zones of central Italy and southern Spain. The radiolarian assemblages of both the Crimea and northern Turkey are taxonomically diverse and can be examined in detail owing to their good state of preservation. This permits evaluation of the theoretical and practical importance of radiolarians for general and regional stratigraphy and makes a considerable contribution to

our knowledge of the paleobiology, systematics, and paleobiogeography of Cretaceous radiolarians.

CHAPTER 1. CENOMANIAN–TURONIAN SECTIONS OF NORTHERN TURKEY AND THE CRIMEAN MOUNTAINS

In this chapter, the reference sections of the Cenomanian and Turonian of northern Turkey and the Crimean Mountains are studied. These sections exhibit the geological development of these regions in sufficient detail, and are characterized throughout by ortho- and parastratigraphic faunal groups. Representative radiolarian assemblages have been discovered at many stratigraphic levels. Material from the sections of northern Turkey and the Crimean Mountains is supplemented by V.S. Vishnevskaya's material from central Italy, and by published data (Erbacher, 1994; O'Dogherty, 1994; Salvini and Marcucci Passerini, 1998; Khan *et al.*, 1999).

NORTHERN TURKEY

The Cenomanian and Turonian deposits of northern Turkey are widely developed within the Rhodope–Pontic Block (Sengor, 1984), where they lie in depressions on the metamorphosed Precambrian basement or in confusedly dislocated Paleozoic–Lower Mesozoic deposits and are overlain by younger strata. One such depression is the Devrekâni basin in the central Pontic Mountains, which represents a synclinal structure filled with Upper Cretaceous–Cenozoic deposits (Tunoglu, 1991, 1994). The Upper Cretaceous is represented by the carbonate–terrigenous Tomalar Formation, which unconformably overlies either apparently Precambrian metamorphic deposits or Upper Jurassic limestones (Fig. 1). The formation includes calciturbidites and olistostromal horizons. The absence of macrofaunal fossils suggests deep-water sedimentation at the base of the continental slope. No radiolarian investigations have previously been made here. Radiolarians have now been discovered in the type section of the formation near the village of Tomalar in the central part of the Devrekâni basin. The section is described below from the base upward (Fig. 2).

The Tomalar Section

In the central part of the Devrekâni basin, the Tomalar Formation unconformably lies on gray massive Upper Jurassic limestones. Because of unconformity, which is associated with a fault, not all basal beds of the formation are fully represented in the stratotype section. The following beds are exposed above the tectonic contact.

Bed 1. Interbedding of light gray and red flaggy mudstones with gray and yellowish gray conchoidal mudstones. Burrows of mud-eaters occur occasionally in the red mudstones and are abundant in the gray and yellowish gray mudstones. The following radiolarians were found 25.5 m above the bed base (Sample 73): *Acanthocircus impolitus* O'Dogherty, *A. horridus* (Squinabol), *Archaeocenosphaera ? mellifera* O'Dogherty, *Cavaspongia euganea* (Squinabol), *Crucella irwini* Pessagno, *C. messinae* Pessagno, *Dactyliodiscus spinosus* sp. nov., *Dactyliosphaera silviae* Squinabol, *Halesium quadratum* Pessagno, *H. sexangulum* Pessagno, *Hexapyramis pantanellii* Squinabol, *Orbiculiforma ovoidea* sp. nov., *Paronaella spica* sp. nov., *Patellula verteroensis* (Pessagno), *Patulibracchium ingens* (Lipman), *P. woodlandensis* Pessagno, *Phaseliforma carinata* Pessagno, *Pseudoaulophacus lenticulatus* (White), *P. putahensis* Pessagno, *Pyramispongia glascockensis* Pessagno, *Savaryella quadra* (Foreman), *Staurosphaeretta longispina* Squinabol, *Amphipyndax stocki* (Campbell et Clark), *Archaeodictyomitra (?) speciosa* sp. nov., *Distylocapsa squama* O'Dogherty, *Holocryptocanium barbui* Dumitrica, *Novixitus weyli* Schmidt-Effing, *Petasiforma foremanae* Pessagno, *P. glascockensis* Pessagno, *Pogonias ? hirsutus* (Squinabol), *Pseudoeucyrtis spinosa* (Squinabol), *Squinabollum fossile* (Squinabol), *Stichomitra communis* Squinabol, *Thanarla gracilis* (Squinabol), *T. veneta* (Squinabol), *Torculum coronatum* (Squinabol), and *Tubilustrium guttaeformis* (Bragina). In addition to these species, Sample 75 (30.5 m above the bed base) contains *Acaeniotyle macrospina* (Squinabol), *Alievium sculptus* (Squinabol), *Cavaspongia californiaensis* Pessagno, *Crucella aster* (Lipman), *Paronaella spica* sp. nov., *Phaseliforma ovum* Jud, *Savaryella quadra* (Foreman), *Staurosphaeretta longispina* Squinabol, *Triactoma cellulosa* Foreman, *Vitorfus campbelli* Pessagno, *Archaeodictyomitra sliteri* Pessagno, *Cryptamphorella conara* (Foreman), *C. sphaerica* (White), *Diacanthocapsa antiqua* (Squinabol), *Distylocapsa veneta* (Squinabol), *Novixitus dengoi* Schmidt-Effing, *Rhopalosyringium euganeum* (Squinabol), *Rotaforma hessi* Pessagno, and *Xitus spicularius* (Aliev). The overlying layer of olive brown mudstones is 4 m thick. Sample 77, located 36.5 m above the bed base and, correspondingly, 1 m below the bed top, has yielded the following radiolarians: *Acaeniotyle diaphorogona* Foreman, *Archaeocenosphaera ? mellifera* O'Dogherty, *Archaeospongoprunum cortinaensis* Pessagno, *Becus regius* O'Dogherty, *Crucella cachensis* Pessagno, *C. irwini* Pessagno, *C. messinae* Pessagno, *Dactyliodiscus longispinus* (Squinabol), *Dactyliosphaera silviae* Squinabol, *Godia tomalarea* sp. nov., *Halesium quadratum* Pessagno, *Hexapyramis pantanellii* Squinabol, *Patellula verteroensis* (Pessagno), *Pseudoacanthosphaera magnifica* (Squinabol), *Pseudoaulophacus praefloresensis* Pessagno, *Quinquecapsularia ombonii* (Squinabol), *Q. grandiloqua* O'Dogherty, *Savaryella quadra* (Foreman), *Staurosphaeretta longispina* (Squinabol), *S. wisniowskii* (Squinabol), *Afens liriodes* Riedel et Sanfilippo, *Amphipyndax stocki* (Campbell et Clark), *Archaeodictyomitra sliteri* Pessagno, *A. (?) speciosa* sp. nov.,

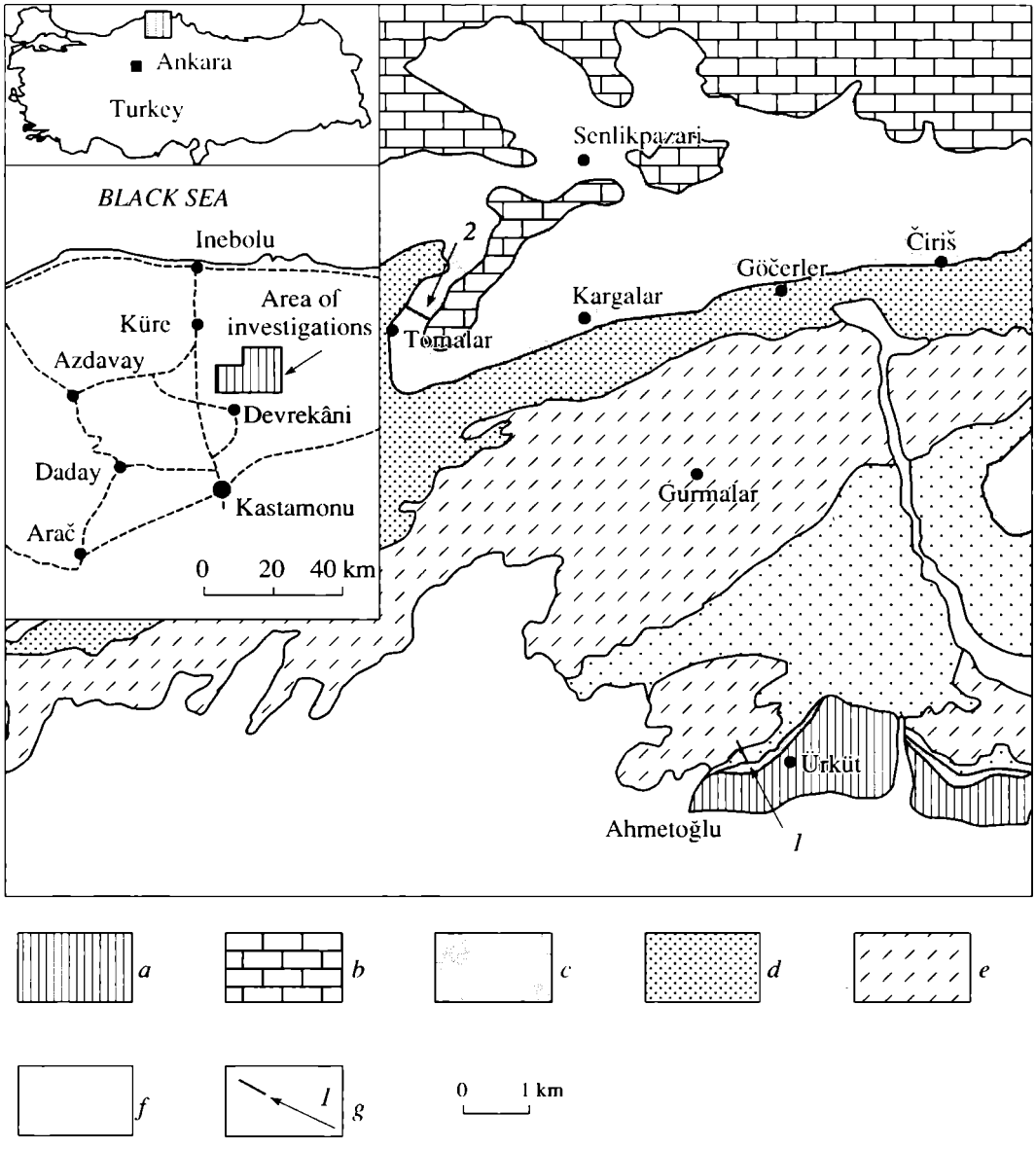

Fig. 1. Geological structure of the Devrekâni Basin in the central Pontic Mountains, northern Turkey (Tunoğlu, 1994; Bragin *et al.*, 2001). Designations: (*a*) Precambrian metamorphites; (*b*) Jurassic carbonate–terrigenous deposits; (*c*) Incigez and Tomalar formations, Upper Cretaceous; (*d*) Davutlar Formation, Upper Maastrichtian–Paleogene; (*e*) Gürleyikdere and Gurmalar formations, Paleogene; (*f*) Quaternary; and (*g*) sections: (*1*) Ürküt and (*2*) Tomalar.

Cryptamphorella conara (Foreman), *Dictyomitra montisserei* (Squinabol), *D. napaensis* Pessagno, *Distylocapsa squama* O'Dogherty, *D. veneta* (Squinabol), *Holocryptocanium barbui* Dumitrica, *Microsciadiocapsa monticelloensis* Pessagno, *Novixitus dengoi* Schmidt-Effing, *N. weyli* Schmidt-Effing, *Pogonias ? hirsutus* (Squinabol), *Pseudodictyomitra nakasekoi* Taketani, *P. pseudomacrocephala* (Squinabol), *Rhopalosyringium euganeum* (Squinabol), *Squinabollum fossile* (Squinabol), *Stichomitra communis* Squinabol, *Thanarla veneta* (Squinabol), *Tubilustrium transmontanum* O'Dogherty, *Xitus spicularius* (Aliev), and *X. spinosus* (Squinabol). 37.5 m.

Bed 2. Red flaggy clayey limestones interbedded with red–green tuffaceous limestones. 4 m.

Bed 3. Olistostromal breccia consisting of subrounded fragments of gray limestones, red jaspers, and gray cherts. 5 m.

Bed 4. Pink clayey limestones. 1 m.

Bed 5. Gray thinly laminated calcareous sandstones. 6 m.

Bed 6. Light gray clayey limestones with marl interbeds. 10 m.

Bed 7. Pink gray siliceous and clayey limestones. 30 m.

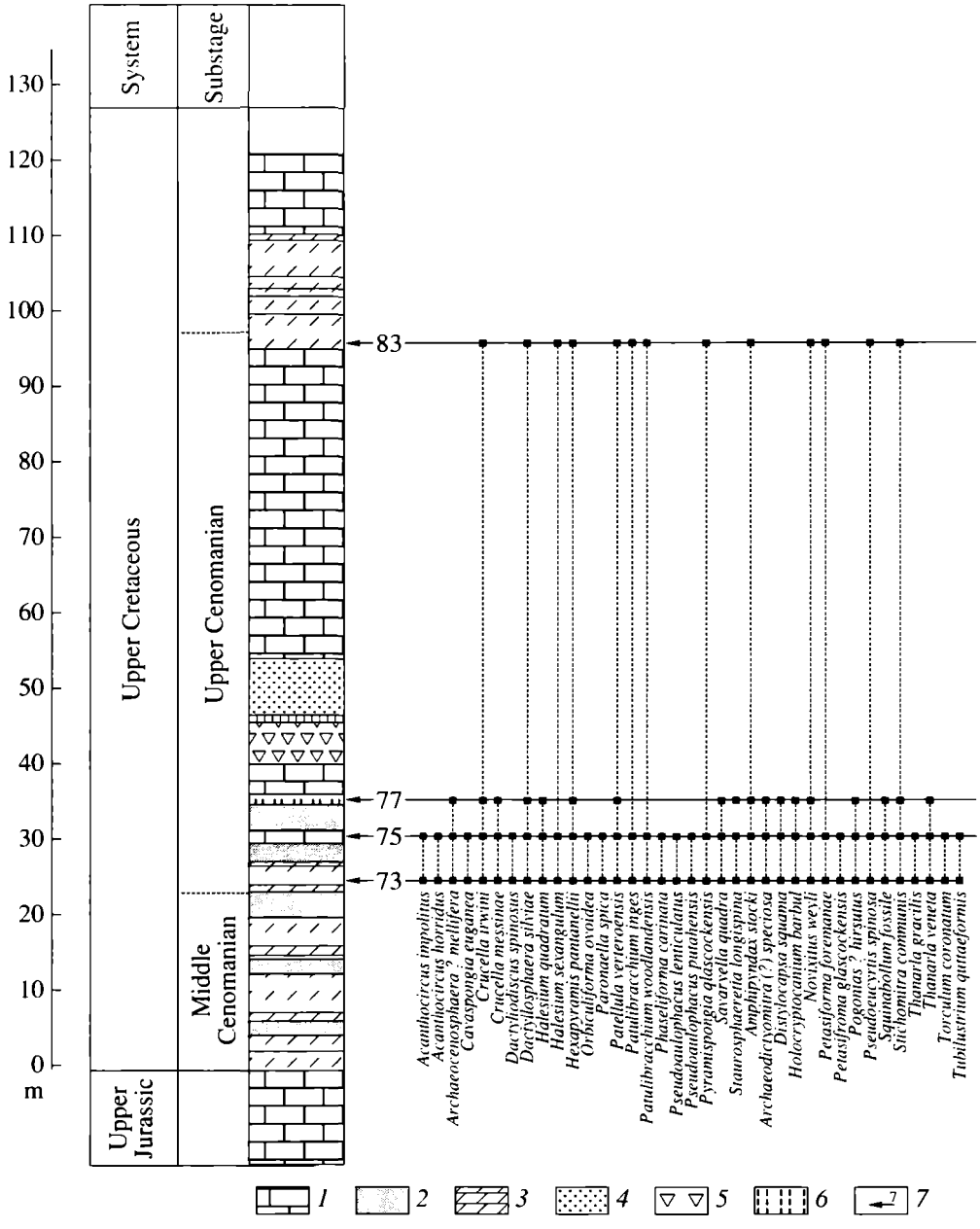

Fig. 2. Distribution of the main radiolarian species in the Tomalar section (central Pontic Mountains, northern Turkey); the levels of radiolarian samples are to the right of the stratigraphic column. Designations (*1*) limestone, (*2*) clay, (*3*) marl, (*4*) sandstone, (*5*) olistostromal breccia, (*6*) chert, and (*7*) radiolarian samples and their numbers.

Bed 8. Pinkish gray clayey–calcareous cherts and cherty marls. Radiolarians *Alievium sculptus* (Squinabol), *Archaeospongoprunum pontidum* sp. nov., *Crucella cachensis* Pessagno, *C. irwini* Pessagno, *Dactyliodiscus lenticulatus* (Jud), *D. longispinus* (Squinabol), *Dactyliosphaera silviae* Squinabol, *Dicroa rara* (Squinabol), *Halesium sexangulum* Pessagno, *Hexapyramis pantanellii* Squinabol, *Patellula verteroensis* (Pessagno), *Patulibracchium ingens* (Lipman), *P. californiaensis* Pessagno, *P. woodlandensis* Pessagno, *Phaseliforma ovum* Jud, *Pyramispongia glascockensis* Pessagno, *Amphipyndax stocki* (Campbell et Clark), *Archaeodictyomitra simplex* Pessagno, *Diacanthocapsa antiqua* (Squinabol), *D. ancus* (Foreman), *Dictyomitra napaensis* Pessagno, *Microsciadiocapsa monticelloensis* Pessagno, *Mita (?) cypraea* sp. nov., *Novixitus dengoi* Schmidt-Effing, *N. weyli* Schmidt-Effing, *Petasiforma foremanae* Pessagno, *Pseudodictyomitra nakasekoi* Taketani, *P. quasilodogaensis* sp. nov., *Pseudoeucyrtis spinosa* (Squinabol), *Stichomitra communis* Squinabol, *Trisyringium echitonicum* (Aliev), and *Xitus spicularius* (Aliev) were found 3 m above the bed base (Sample 83). 15 m.

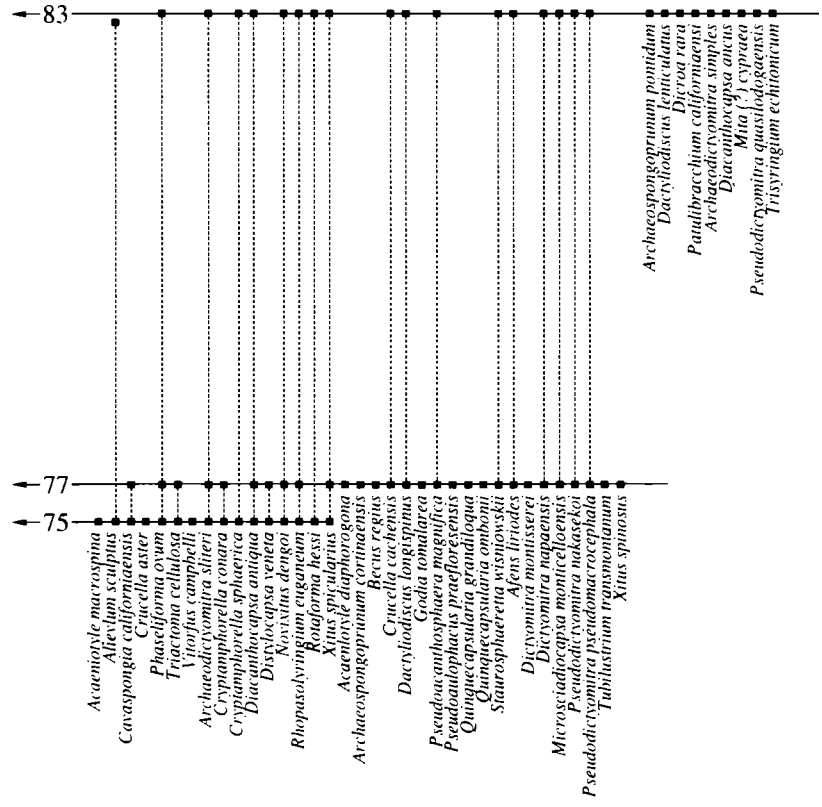

Fig. 2. (Contd.)

Bed 9. White and light gray clayey limestones and marls. 10 m.

Bed 10. Gray and dark gray clays and marls. Apparent thickness. about 5 m.

The Tomalar Formation has a slightly different structure in the Ürküt section of the southern part of the Devrekâni Basin, where it is represented by the siliceous–clayey facies (Fig. 3). The section is described below from the base upward.

The Ürküt section

Bed 1. Gneisses cut by diorite–porphyrite dykes.

The Tomalar Formation

Bed 2. The eroded surface of the gneisses is unconformably overlain by light greenish gray opoka-like cherts (5–10 cm), which are rhythmically interbedded with yellowish olive gray siliceous siltstones (7–15 cm). In the lower part of the bed, Samples 54–56 have yielded the Middle Cenomanian foraminifers *Rotalipora reicheli* Mornod, *R. brotzeni* (Sigal), *R. deeckei* (Franke), *Brittonella portsdownensis* (Williams-Mitchel), *Hedbergella delrioensis* (Carsey), and *H. trochoidea* Gandolfi (identified by O.A. Korchagin), and Sample 55 has yielded the radiolarians *Acaeniotyle diaphorogona* (Foreman), *A. macrospina* (Squinabol), *A. umbilicata* (Rüst), *Acanthocircus impolitus* O'Dogherty, *A. horridus* (Squinabol), *A. hueyi* (Pessagno), *A. moorei* (Foreman), *A. polymorphus* (Squinabol), *Alievium sculptus* (Squinabol), *Archaeocenosphaera ? mellifera* O'Dogherty, *Archaeospongoprunum cortinaensis* Pessagno, *A. klingi* Pessagno, *Becus horridus* (Squinabol), *Cavaspongia antelopensis* Pessagno, *C. californiaensis* Pessagno, *C. euganea* (Squinabol),

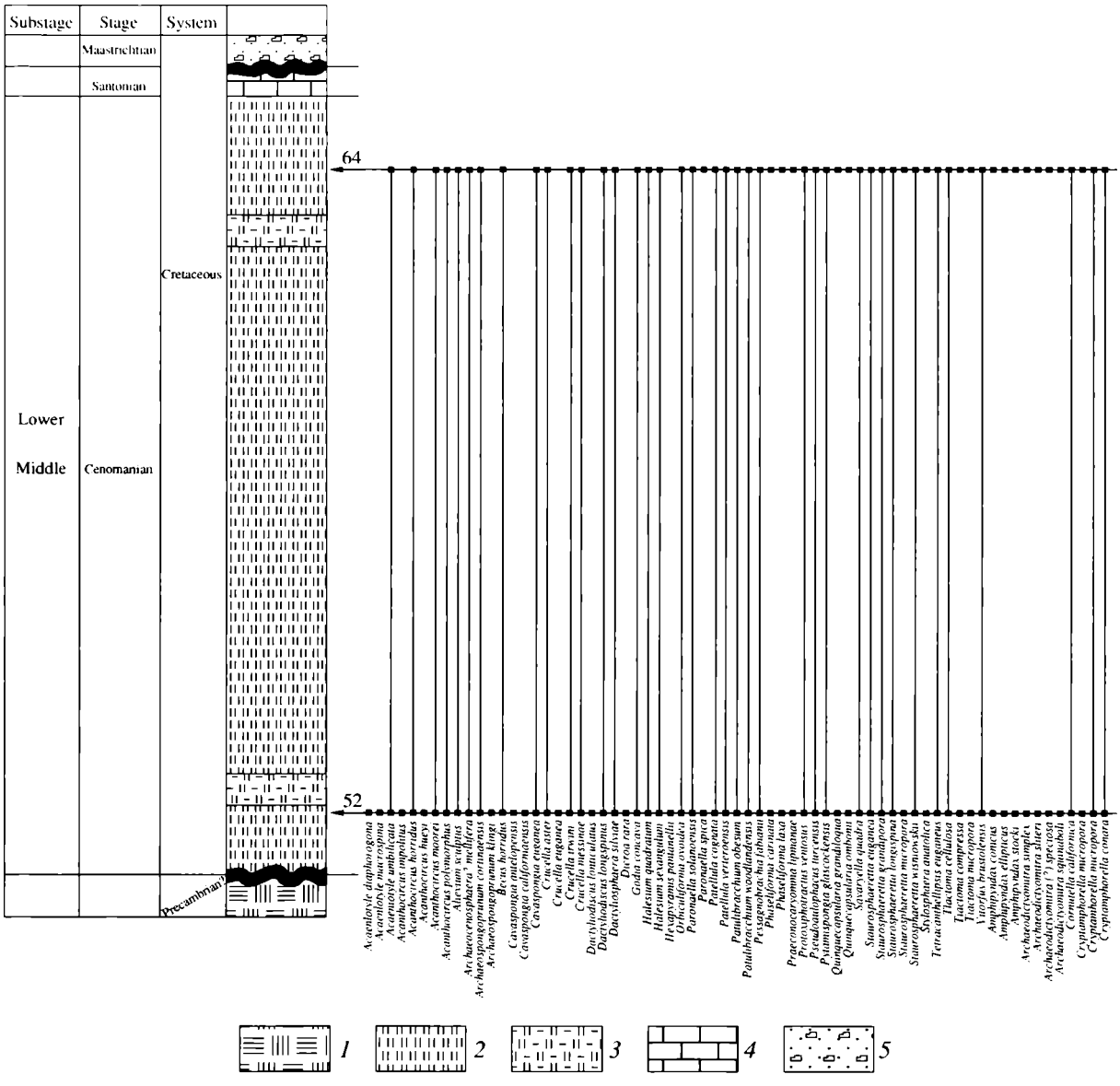

Fig. 3. The Cenomanian section at the Ürküt settlement (central Pontic Mountains, northern Turkey). Designations: (*1*) gneiss, (*2*) chert, (*3*) siliceous mudstone, (*4*) limestone, and (*5*) sandstone and conglomerate; radiolarian samples and their numbers are shown to the right of the column.

Crucella aster (Lipman), *Cr. euganea* (Squinabol), *C. irwini* Pessagno, *C. messinae* Pessagno, *Dactyliodiscus lenticulatus* (Jud), *D. longispinus* (Squinabol), *Dactyliosphaera silviae* Squinabol, *Dicroa rara* (Squinabol), *Godia concava* (Li et Wu), *Halesium quadratum* Pessagno, *H. sexangulum* Pessagno, *Hexapyramis pantanellii* Squinabol, *Orbiculiforma ovoidea* sp. nov., *Paronaella solanoensis* Pessagno, *P. spica* sp. nov., *Patellula cognata* O'Dogherty, *P. verteroensis* (Pessagno), *Patulibracchium obesum* Pessagno, *P. woodlandensis* Pessagno, *Pessagnobrachia fabianii* (Squinabol), *Phaseliforma carinata* Pessagno, *P. laxa* Pessagno, *Praeconocaryomma lipmanae* Pessagno, *Protoxiphotractus ventosus* O'Dogherty, *Pseudoaulophacus turcensis* sp. nov., *Pyramispongia glascockensis* Pessagno, *Quinquecapsularia grandiloqua* O'Dogherty, *Q. ombonii* O'Dogherty, *Savaryella quadra* (Foreman), *Staurosphaeretta euganea* (Squinabol), *S. grandipora* (Squinabol), *S. longispina* (Squinabol), *S. micropora* sp. nov., *S. wisniowskii* (Squinabol), *Stylosphaera anatolica* sp. nov., *Tetracanthellipsis euganeus* Squinabol, *Triactoma cellulosa* Foreman, *T. compressa* (Squinabol), *T. micropora* sp. nov., *Vitorfus brustolensis* (Squinabol), *Amphipyndax stocki* (Campbell et Clark), *A. ellipticus* Nakaseko et Nishimura, *A. conicus* Nakaseko et Nishimura, *Archaeodictyomitra simplex* Pessagno, *A. sliteri* (Squinabol), *A. (?) speciosa* sp. nov., *A. squinaboli* Pessagno, *Cornutella*

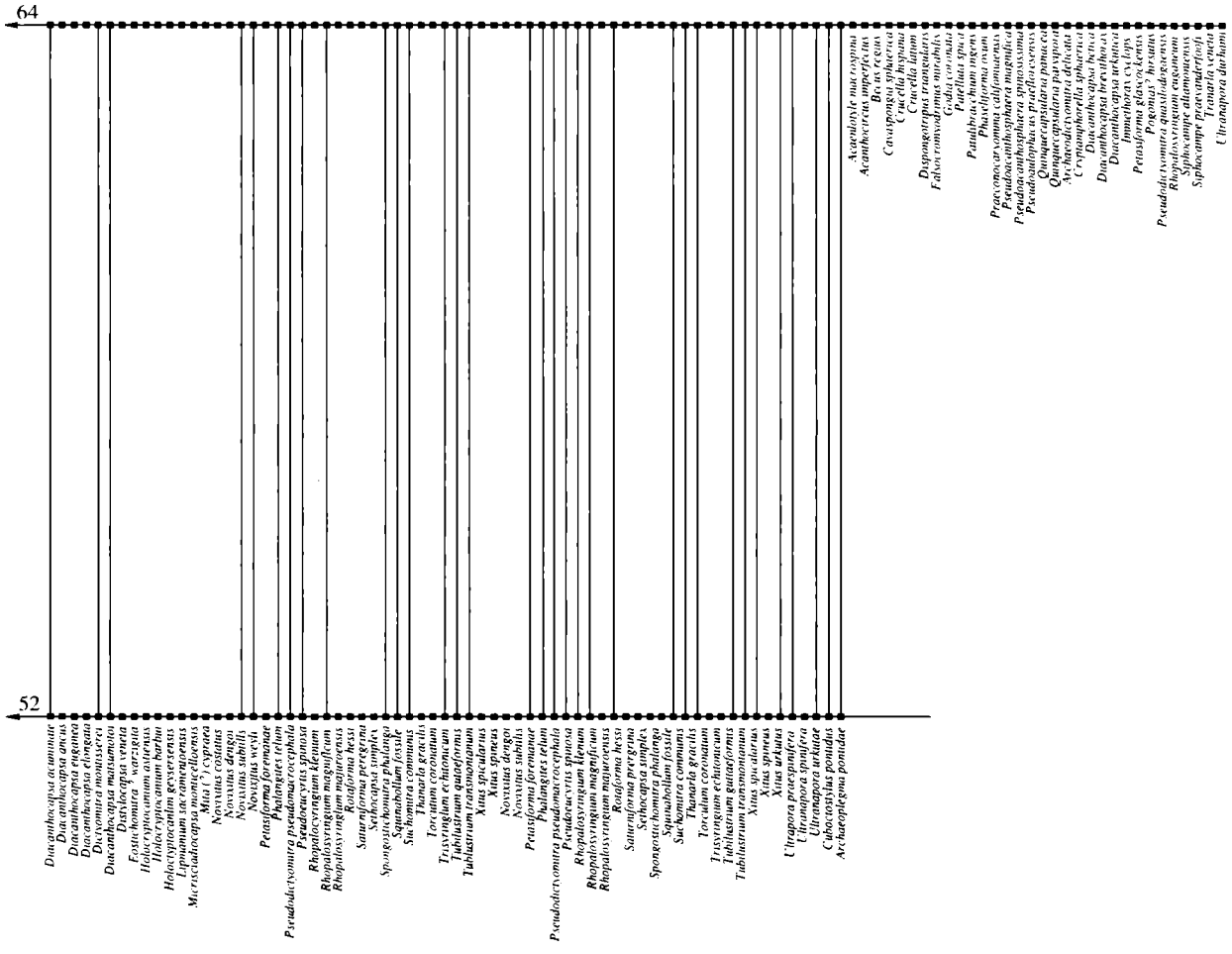

Fig. 3. (Contd.)

californica Campbell et Clark, *Cryptamphorella micropora* sp. nov., *C. conara* (Foreman), *Diacanthocapsa acuminata* Dumitrica, *D. ancus* (Foreman), *D. euganea* Squinabol, *D. matsumotoi* (Taketani), *D. elongata* sp. nov., *Dictyomitra montisserei* (Squinabol), *Distylocapsa veneta* (Squinabol), *Eostichomitra warzigita* Empson-Morin, *Holocryptocanium astiensis* Pessagno, *H. barbui* Dumitrica, *H. geysersensis* Pessagno, *Lipmanium sacramentoensis* Pessagno, *Microsciadiocapsa monticelloensis* Pessagno, *Mita (?) cypraea* sp. nov., *Novixitus dengoi* Schmidt-Effing, *N. weyli* Schmidt-Effing, *N. costatus* sp. nov., *N. subtilis* sp. nov., *Petasiforma foremanae* Pessagno, *Phalangites telum* O'Dogherty, *Pseudodictyomitra pseudomacrocephala* (Squinabol), *Pseudoeucyrtis spinosa* (Squinabol), *Rhopalosyringium kleinum* Empson-Morin, *R. magnificum* Campbell et Clark, *R. majuroensis* Schaaf, *Rotaforma hessi* Pessagno, *Saturniforma peregrina* Pessagno, *Spongostichomitra phalanga* O'Dogherty, *Squinabollum fossile* (Squinabol), *Stichomitra communis* Squinabol, *Thanarla gracilis* (Squinabol), *Torculum coronatum* (Squinabol), *Trisyringium echitonicum* (Aliev), *Tubilustrium guttaeformis* (Bragina), *T. transmontanum* O'Dogherty, *Xitus spicularius* (Aliev), *X. spineus* Pessagno, *X. urkutus* sp. nov., *Ultranapora praespinifera* Pessagno, *Ultranapora spinifera* Pessagno, *U. urkutae* sp. nov., *Cuboctostylus pontidus* sp. nov., and *Archaeoplegma pontidae* gen. et sp. nov. The middle part of the bed contains the Late Cenomanian foraminifers *Rotalipora cushmani* (Morrow) and *Dicarinella* sp. (identified by O.A. Korchagin). The upper part (Sample 64) has yielded the following radiolarians: *Acaeniotyle macrospina* (Squinabol), *A. umbilicata* (Rüst), *Acanthocircus horridus* (Squin-

abol), *A. imperfectus* sp. nov., *A. moorei* (Foreman), *A. polymorphus* (Squinabol), *Alievium sculptus* (Squinabol), *Archaeospongoprunum cortinaensis* Pessagno, *Archaeocenosphaera ? mellifera* O'Dogherty, *Becus horridus* (Squinabol), *B. regius* O'Dogherty, *Cavaspongia euganea* (Squinabol), *C. sphaerica* O'Dogherty, *Crucella aster* (Lipman), *C. hispana* O'Dogherty, *C. irwini* Pessagno, *C. latum* (Lipman), *C. messinae* Pessagno, *Dactyliodiscus longispinus* (Squinabol), *Dactyliosphaera silviae* Squinabol, *Dispongotripus triangularis* (Squinabol), *Falsocromyodrimus mirabilis* (Squinabol), *Godia concava* (Li et Wu), *G. coronata* (Tumanda), *Halesium quadratum* Pessagno, *H. sexangulum* Pessagno, *Paronaella solanoensis* Pessagno, *Patellula cognata* O'Dogherty, *P. verteroensis* (Pessagno), *P. spica* O'Dogherty, *Patulibracchium ingens* (Lipman), *P. obesum* Pessagno, *P. woodlandensis* Pessagno, *Pessagnobrachia fabianii* (Squinabol), *Phaseliforma ovum* Jud, *Praeconocaryomma californiaensis* Pessagno, *Protoxiphotractus ventosus* O'Dogherty, *Pseudoacanthosphaera magnifica* (Squinabol), *P. spinosissima* (Squinabol), *Pseudoaulophacus praefloresensis* Pessagno, *P. turcensis* sp. nov., *Pyramispongia glascockensis* Pessagno, *Quinquecapsularia panacea* O'Dogherty, *Q. parvipora* (Squinabol), *Savaryella quadra* (Foreman), *Staurosphaeretta euganea* (Squinabol), *S. grandipora* (Squinabol), *S. longispina* (Squinabol), *S. wisniowskii* (Squinabol), *Tetracanthellipsis euganeus* Squinabol, *Triactoma cellulosa* Foreman, *Vitorfus brustolensis* (Squinabol), *Amphipyndax stocki* (Campbell et Clark), *Archaeodictyomitra delicata* sp. nov., *Cornutella californica* Campbell et Clark, *Cryptamphorella sphaerica* (White), *C. conara* (Foreman), *Diacanthocapsa acuminata* Dumitrica, *D. ancus* (Foreman), *D. betica* O'Dogherty, *D. brevithorax* Dumitrica, *D. urkutica* sp. nov., *Dictyomitra montisserei* (Squinabol), *Distylocapsa veneta* (Squinabol), *Immersothorax cyclops* Dumitrica, *Novixitus weyli* Schmidt-Effing, *Petasiforma foremanae* Pessagno, *P. glascockensis* Pessagno, *Pogonias ? hirsutus* (Squinabol), *Pseudodictyomitra pseudomacrocephala* (Squinabol), *P. quasilodogaensis* sp. nov., *Pseudoeucyrtis spinosa* (Squinabol), *Rhopalosyringium euganeum* (Squinabol), *R. kleinum* Empson-Morin, *R. majuroensis* Schaaf, *Siphocampe praevanderhoofi* sp. nov., *Squinabollum fossile* (Squinabol), *Stichomitra communis* Squinabol, *Thanarla gracilis* (Squinabol), *T. veneta* (Squinabol), *Tubilustrium guttaeformis* (Bragina), *T. transmontanum* O'Dogherty, *Xitus spicularius* (Aliev), *Ultranapora durhami* Pessagno, *U. praespinifera* Pessagno, *U. urkutae* sp. nov., *Cuboctostylus pontidus* sp. nov., and *Archaeoplegma pontidae* gen. et sp. nov. 10 m.

Bed 3. White and light gray clayey limestones. 0–0.5 m.

The Davutlar Formation

Bed 4. Conglomerates of well-rounded medium-sized granite–diorite–gneiss pebbles passing up the section into coarse- and medium-grained polymictic sandstones. Upper Maastrichtian (Tunoglu, 1991; Bragin *et al.*, 2001).

THE CRIMEAN MOUNTAINS

The Crimea is a fragment of the Late Cimmerian folded system in the north of the extensive Alpine–Mediterranean fold belt (*Geological ...*, 1989). In the southwestern Crimea is the Kacha Upland, where Upper Cretaceous deposits overlie the middle–upper parts of the Upper Albian without angular unconformity, but with a small hiatus. The cuesta relief facilitates investigations of the continuous Cretaceous sequences. The most complete Upper Cretaceous sections are located in the Bodrak–Alma interfluve, near the Moscow University's geology field center (Fig. 4). The sections between the villages of Trudolyubovka and Verkhorech'e have been selected as regional standard reference sections (Naidin and Alekseev, 1980; Naidin *et al.*, 1981). In the Crimean Mountains, Upper Cretaceous biostratigraphy is based on inoceramids (*Atlas ...*, 1959; Kopaevich and Walaszczyk, 1990), ammonites (*Atlas ...*, 1959; Naidin and Alekseev, 1980), and planktonic and benthic foraminifers (*Atlas ...*, 1959; Maslakova and Voloshina, 1969; Dolitskaya, 1972; Naidin *et al.*, 1981; Kopaevich, 1996; Alekseev *et al.*, 1997; Kuz'micheva, 2000a, 2000b; Podobina, 2000). The Upper Cretaceous zonation of the Crimea was developed based on calcareous nannofossils in the 1970s (Shumenko and Stetsenko, 1978). The area under study was part of the European paleobiogeographic region in the Late Cretaceous (*Geological ...*, 1989). It is therefore not surprising that zonations developed for western Europe were widely used in the Crimean Mountains. The aforementioned sections have been described and subdivided into lithological members (Naidin and Alekseev, 1980; Naidin *et al.*, 1981). These members, with their biostratigraphic markers (Kuz'micheva, 2001, 200b), are used in the subsequent discussion.

I studied radiolarians from three sections: Mt. Sel'-Bukhra, Aksudere Gully, and Mt. Belaya (Fig. 4). Radiolarian samples were collected at closely spaced levels to cover every lithological variety, especially at boundaries, where samples were taken from the top of the underlying bed and from the base of the overlying bed. Special attention was paid to interbeds of finer-grained lithological varieties, particularly siliceous ones. In such cases samples were taken10 cm apart or closer.

The Sel'-Bukhra Mountain Section

The reference section is an outcrop on the southern slope of Mt. Sel'-Bukhra that reveals the following

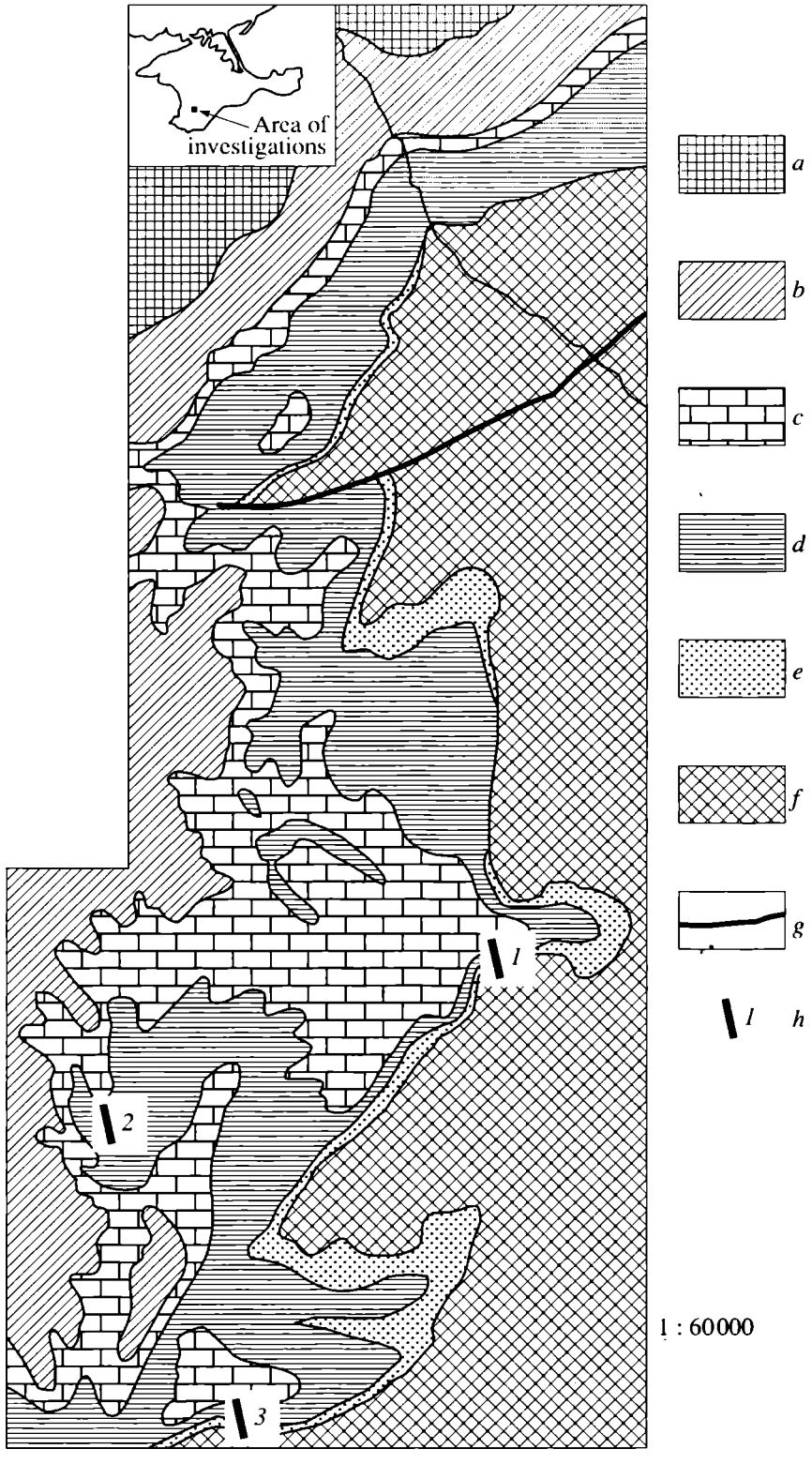

Fig. 4. Geological structure of the Kacha Upland (the Crimean Mountains): (*a*) Paleogene; (*b*) Santonian–Maastrichtian; (*c*) Upper Turonian–Coniacian; (*d*) Cenomanian and Lower Turonian; (*e*) Upper Albian; (*f*) pre-Upper Albian; (*g*) faults; and (*h*) sections studied: (*1*) Sel'-Bukhra, (*2*) Aksudere; and (*3*) Belaya.

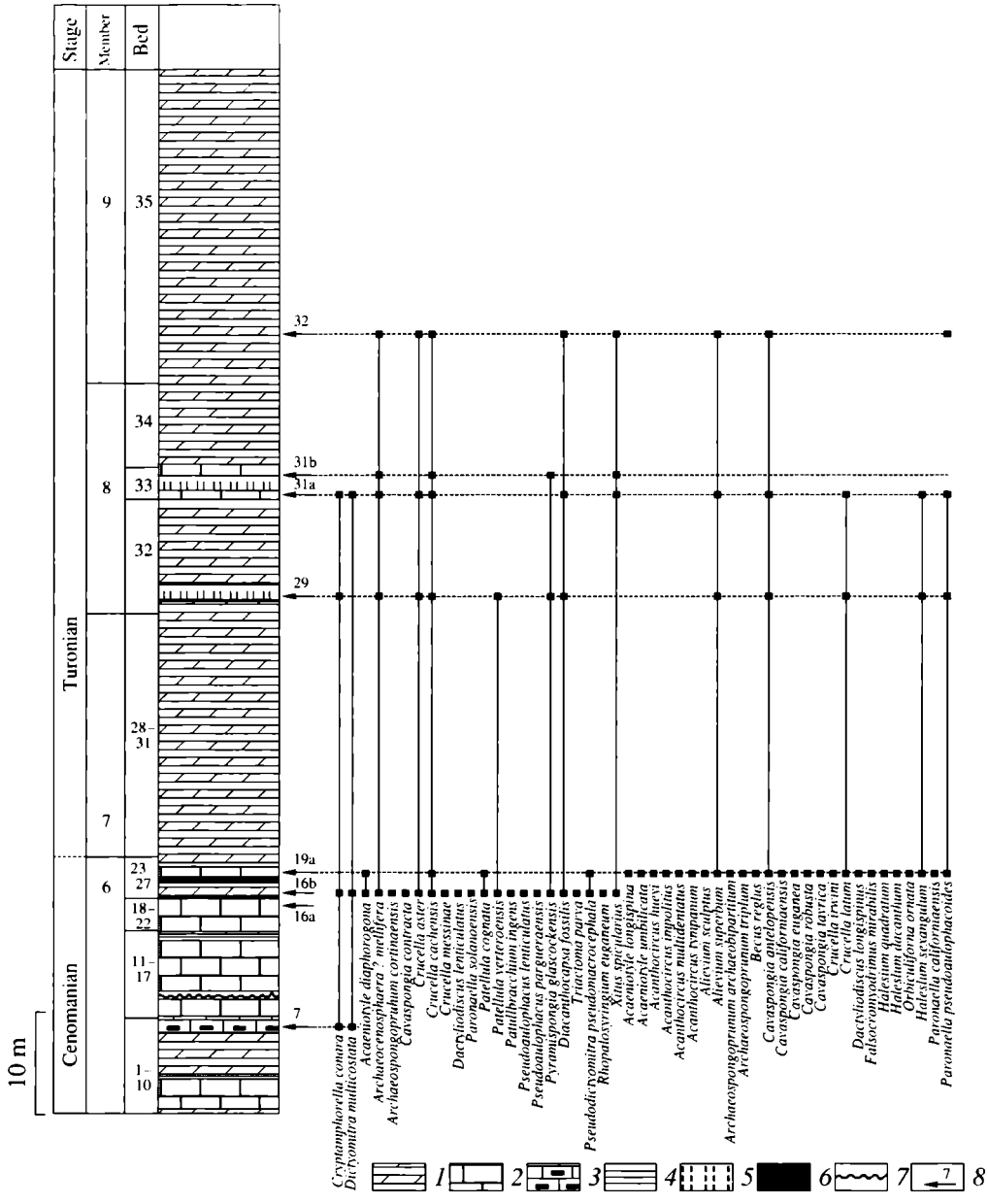

Fig. 5. Distribution of the radiolarian species in the Sel'-Bukhra section. Designations: (*1*) calcareous marl, (*2*) chalk-like limestone, (*3*) clay limestone, (*4*) marlaceous platy limestone, (*5*) chert interbeds, (*6*) marl with carbonaceous detritus, (*7*) erosion, and (*8*) sample number.

Upper Cenomanian–Lower Turonian beds (from the base upward) (Fig. 5):

Member 6, Upper Cenomanian

Member 6-2, *Rotalipora cushmani foraminiferal* Zone

Bed 1. Light gray to white, chalky massive limestone. 0.4 m.

Bed 2. Light yellowish gray, platy, slightly ferruginous marl (virtually limestone). 0.1 m.

Bed 3. Chalky white limestone similar to that of Bed 1. 0.3 m.

Bed 4. White chalky flaggy clayey limestone. 0.5 m.

Bed 5. White chalky massive limestone. 0.7 m.

Bed 6. Interbedding of light yellowish gray chalky flaggy limestone, light yellowish gray platy marl, and light gray calcareous thin-layered shaly clay. 0.3 m.

Bed 7. White chalky massive limestone. 0.3 m.

Bed 8. Interbedding of white platy and yellowish gray foliated, heavily clay marls. 0.4 m.

Bed 9. White chalky massive limestone. 0.7 m.

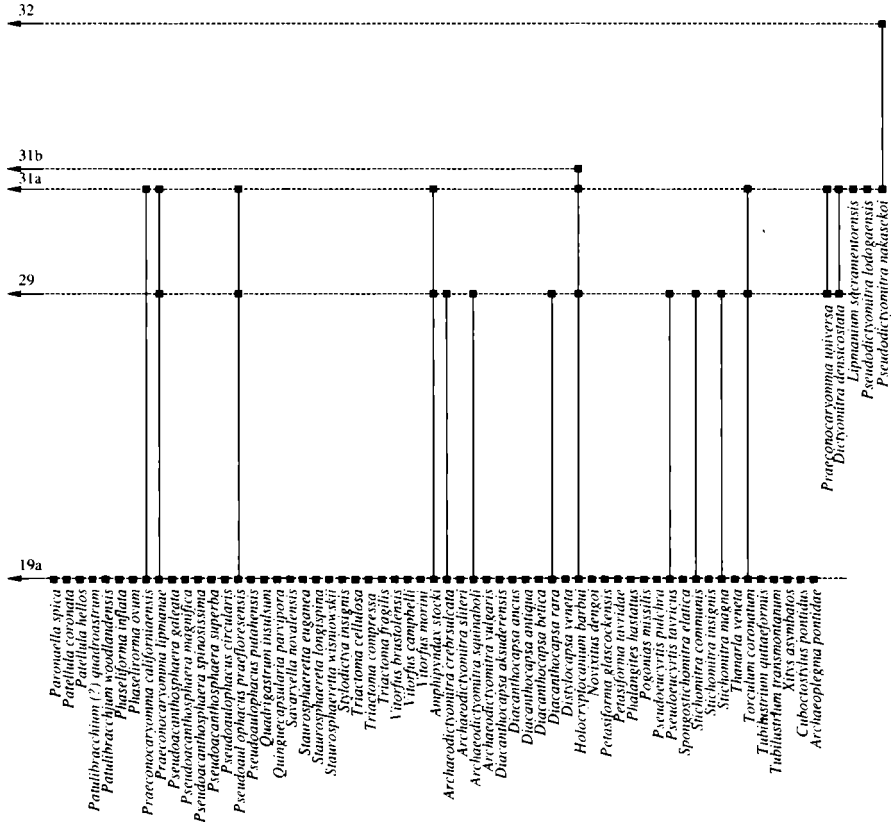

Fig. 5. (Contd.)

Bed 10. White clayey and light gray platy limestone with yellowish gray marl interbeds. Isolated specimens of poorly preserved radiolarians including only two identifiable species: *Cryptamphorella conara* (Foreman) and *Dictyomitra multicostata* Zittel (Sample 7). The last occurrence of the zonal species *Rotalipora cusmani* of the *Rotalipora cusmani* Zone and the first occurrence of *Whiteinella archaeocretacea* Pessagno. 1 m.

Member 6-3. *Whiteinella archaeocretacea* foraminiferal Zone

Bed 11. White yellowish gray chalky massive limestone. Considerable changes in foraminiferal assemblages. The bed is marked by *Whiteinella archaeocretacea* Pessagno. 0.6 m.

Bed 12. Yellowish gray chalk with fragments of underlying limestone lies on the uneven eroded surface of Bed 11. 0.03 m.

Bed 13. Olive brown, greenish gray, plastic, mottled clay lies on the uneven surface of Bed 12 and gives way to foliated clay up the section. 0.25 m.

Bed 14. Light gray flaggy silty limestone. 0.1 m.

Bed 15. Light gray to yellowish gray platy marly limestone with interbeds of bluish gray marl with ferruginous pyrite concretions. 0.8 m.

Bed 16. White massive hard siliceous limestone. The middle part of the bed (Sample 16a) contains fragments of radiolarian skeletons of *Acaeniotyle dia-*

phorogona Foreman, *Archaeocenosphaera ? mellifera* O'Dogherty, *Archaeospongoprunum cortinaensis* Pessagno, *Cavaspongia contracta* O'Dogherty, *Crucella aster* (Lipman), *C. cachensis* Pessagno, *C. messinae* Pessagno, *Dactyliodiscus lenticulatus* (Jud), *Paronaella solanoensis* Pessagno, *Patellula verteroensis* (Pessagno), *P. cognata* O'Dogherty, *Patulibracchium ingens* (Lipman), *Pseudoaulophacus lenticulatus* (White), *P. pargueraensis* (Pessagno), *Pyramispongia glascockensis* Pessagno, *Triactoma parva* Foreman, *Cryptamphorella conara* (Foreman), *Diacanthocapsa fossilis* (Squinabol), *Dictyomitra multicostata* Zittel, *Obesacapsula* ex gr. *O. marroensis* Pessagno, *Pseudodictyomitra pseudomacrocephala* (Squinabol), *Rhopalosyringium euganeum* (Squinabol), and *Xitus spicularius* (Aliev). 0.2 m.

Bed 17. Light yellowish gray, slightly platy, laminated limestones with interbeds of yellowish gray marls. 0.3 m.

Bed 18. Light gray massive, weakly silty limestone. 0.1 m.

Bed 19. Light gray marly limestones with flaggy limestone interbeds. Sample 16b, taken at the bed top, contains all radiolarian species of Sample 16a. 1.2 m.

Bed 20. Bluish gray, weakly laminated, vaguely platy–splintered marls rich in carbonaceous detritus. They are related to the anoxic event at the Cenomanian–Turonian boundary. 0.2 m.

Member 7, Lower Turonian

The *Quadrum gartneri* nannoplankton Zone

The *Whiteinella archaeocretacea* foraminiferal Zone

Bed 21. Light yellowish gray splintered marls with separate rounded concretions of pyrite. *Dicarinella hagni* (Scheibnerova) at the base. 0.25 m.

Bed 22. White to light gray, aphanitic, hard, massive, indistinctly platy limestone, heavily silicified in plates. At the base (Samples 19a, 19b), there is a very rich radiolarian assemblage, which, in addition to almost all species listed above, contains *Acaeniotyle diaphorogona* Foreman, *A. longispina* (Squinabol), *A. umbilicata* (Rust), *Acanthocircus hueyi* (Pessagno), *A. impolitus* O'Dogherty, *A. multidentatus* (Squinabol), *A. tympanum* O'Dogherty, *Alievium sculptus* (Squinabol), *A. superbum* (Squinabol), *Archaeospongoprunum archaeobipartitum* sp. nov., *A. triplum* Pessagno, *Becus regius* O'Dogherty, *Cavaspongia antelopensis* Pessagno, *C. californiaensis* Pessagno, *C. euganea* (Squinabol), *C. robusta* sp. nov., *C. tavrica* sp. nov., *Crucella cachensis* Pessagno, *C. irwini* Pessagno, *C. latum* (Lipman), *Dactyliodiscus longispinus* (Squinabol), *Falsocromyodrimus mirabilis* (Squinabol), *Halesium diacanthum* (Squinabol), *H. quadratum* Pessagno, *H. sexangulum* Pessagno, *Orbiculiforma ornata* sp. nov., *Paronaella californiaensis* (Pessagno), *P. pseudoaulophacoides* O'Dogherty, *P. spica* sp. nov., *Patellula cognata* O'Dogherty, *P. coronata* (Tumanda), *P. helios* (Squinabol), *Patulibracchium (?) quadroastrum* Bragina, *P. woodlandensis* Pessagno, *Phaseliforma inflata* sp. nov., *P. ovum* Jud, *Pogonias missilis* O'Dogherty, *Praeconocaryomma californiaensis* Pessagno, *P. lipmanae* Pessagno, *Pseudoacanthosphaera galeata* O'Dogherty, *P. magnifica* (Squinabol), *P. spinosissima* (Squinabol), *P. superba* (Squinabol), *Pseudoaulophacus circularis* sp. nov., *P. praefloresensis* Pessagno, *P. putahensis* Pessagno, *Quadrigastrum insulsum* O'Dogherty, *Quinquecapsularia parvipora* (Squinabol), *Savaryella novalensis* (Squinabol), *Staurosphaeretta euganea* (Squinabol), *S. longispina* (Squinabol), *S. wisniowskii* (Squinabol), *Stylodictya insignis* Campbell et Clark, *Triactoma cellulosa* Foreman, *T. compressa* (Squinabol), *T. fragilis* Bragina, *Vitorfus brustolensis* (Squinabol), *V. campbelli* Pessagno, *V. morini* Empson-Morin, *Amphipyndax stocki* (Campbell et Clark), *Archaeodictyomitra crebrisulcata* (Squinabol), *A. sliteri* (Squinabol), *A. squinaboli* Pessagno, *A. vulgaris* Pessagno, *Diacanthocapsa ancus* (Foreman), *D. aksuderensis* sp. nov., *D. antiqua* (Squinabol), *D. betica* O'Dogherty, *D. rara* Squinabol, *Distylocapsa veneta* (Squinabol), *Holocryptocanium barbui* Dumitrica, *Novixitus dengoi* Schmidt-Effing, *Petasiforma glascockensis* Pessagno, *P. tavridae* sp. nov., *Phalangites hastatus* O'Dogherty, *Pogonias missilis* O'Dogherty, *Pseudodictyomitra pseudomacrocephala* (Squinabol), *Pseudoeucyrtis pulchra* (Squinabol), *P. tavricus* sp. nov., *Spongostichomitra elatica* (Aliev), *Stichomitra communis* Squinabol, *S. insignis* (Squinabol), *S. magna* Squinabol, *Thanarla veneta* (Squinabol), *Torculum coronatum* (Squinabol), *Tubilustrium guttaeformis* (Bragina), *T. transmontanum* O'Dogherty, *Xitus asymbatos* (Foreman), *Cuboctostylus pontidus* sp. nov., and *Archaeoplegma pontidae* gen. et sp. nov. 0.4 m.

The foraminiferal zone of *Praeglobotruncana oraviensis*

Bed 23. Light gray marly, indistinctly platy limestones. The foraminiferal assemblage *"Helvetoglobotruncana helvetica"* with *Praeglobotruncana oraviensis* Scheibnerova. 0.3 m.

Bed 24. Almost white and light gray massive clay limestones. 0.1 m.

Bed 25. Light gray platy marly limestones. 0.3 m.

Bed 26. White massive limestone. 0.35 m.

Bed 27. Light gray indistinctly platy marls. 1 m.

Bed 28. Yellowish gray dense, laminated calcareous clay. 0.15 m.

Bed 29. Interbedding of light yellowish gray platy, dense marly limestones and light gray marls with ferruginous interbeds. 1.2 m.

Bed 30. Light gray to almost white, platy-splintered, calcareous, occasionally chalky marls. 8.5 m.

Bed 31. Light yellowish gray to grayish white, dense, distinctly platy (about 20 cm thick on average), chalky marls. 3.5 m.

Member 8, Lower Turonian

Bed 32. Platy (up to 2 mm) calcareous–siliceous marls with a basal horizon (up to 3 cm) of variously silicified radiolarites (Sample 29), which contains remains of radiolarians *Alievium superbum* (Squinabol), *Archaeocenosphaera ? mellifera* O'Dogherty, *Cavaspongia antelopensis* Pessagno, *Crucella aster* (Lipman), *C. cachensis* Pessagno, *C. latum* (Lipman), *Orbiculiforma ornata* sp. nov., *Paronaella pseudoaulophacoides* (O'Dogherty), *Patellula verteroensis* (Pessagno), *Praeconocaryomma lipmanae* Pessagno, *P. universa* Pessagno, *Pseudoaulophacus praefloresensis* Pessagno, *Pyramispongia glascockensis* Pessagno, *Amphipyndax stocki* (Campbell et Clark), *Archaeodictyomitra squinaboli* Pessagno, *Cryptamphorella conara* (Foreman), *Dictyomitra densicostata* Pessagno, *Holocryptocanium barbui* Dumitrica, *Stichomitra communis* Squinabol, and *Torculum coronatum* (Squinabol). 6 m.

Bed 33. Platy chalky limestones with interbeds of platy chalky marls, which include interbeds of cherts, which contain (Sample 31a) remains of radiolarians *Alievium superbum* (Squinabol), *Archaeocenosphaera ? mellifera* O'Dogherty, *Cavaspongia antelopensis* Pessagno, *Crucella aster* (Lipman), *C. cachensis* Pessagno, *C. latum* (Lipman), *Orbiculiforma ornata* sp. nov., *Praeconocaryomma californiaensis* Pessagno, *P. lipmanae* Pessagno, *P. universa* Pessagno, *Pseudoaulophacus praefloresensis* Pessagno, *Paronaella pseudoaulophacoides* O'Dogherty, *Pyramispongia glascockensis* Pessagno, *Amphipyndax stocki* (Campbell et Clark), *Cryptamphorella conara* (Foreman), *Dictyomitra densicostata* Pessagno, *D. multicostata* Zittel, *Holocryptocanium barbui* Dumitrica, *Lipmanium sacramentoensis* Pessagno, *Pseudodictyomitra nakasekoi* Taketani, *P. lodogaensis* Pessagno, *Torculum coronatum* (Squinabol), and *Xitus spicularius* (Aliev). 2 m.

Bed 34. Yellow gray and white platy marls with separate chert concretions. The chert interbeds (Sample 31b) contain remains of radiolarians *Archaeocenosphaera ? mellifera* O'Dogherty, *Cavaspongia euganea* (Squinabol), *Crucella cachensis* Pessagno, *Pyramispongia glascockensis* Pessagno, *Holocryptocanium barbui* Dumitrica, and *Xitus spicularius* (Aliev). 4 m.

Member 9

Bed 35. Light gray, white, and yellowish gray platy marls with frequent chert concretions. The following radiolarians were found 4 m above the bed base (Sample 32): *Alievium superbum* (Squinabol), *Archaeocenosphaera ? mellifera* O'Dogherty, *Cavaspongia antelopensis* Pessagno, *Crucella aster* (Lipman), *C. cachensis* Pessagno, *Paronaella pseudoaulophacoides* (O'Dogherty), *Pyramispongia glascockensis* Pessagno, *Pseudodictyomitra nakasekoi* Taketani, and *Xitus spicularius* (Aliev). 13 m.

Members 7–9 correspond to the *Quadrum gartneri* nannoplanktonic Zone of the Lower Turonian of Europe. They are overlain by Upper Turonian limestones.

The Aksudere Gully Section

The lower part of the Aksudere Gully section corresponds to the Sel'-Bukhra Mountain section. This section embraces the interval up to the Coniacian (Fig. 6) and includes the following strata (from the base upward):

Member 6-2, Upper Cenomanian

The *Rotalipora cushmani* foraminiferal Zone

Bed 1. White chalky, massive limestone with *Rotalipora cushmani* (Morrow). Apparent thickness 0.5 m.

Member 6-3

The *Whiteinella archaeocretacea* foraminiferal Zone

Bed 2. Greenish brown dense clay. 0.3 m.

Bed 3. Red brown laminated flaggy clay. 0.25 m.

Bed 4. Dark gray and brownish gray, weakly bioturbated clay stained with iron oxide. 0.05 m.

Member 7, Lower Turonian

The *Quadrum gartneri* nannoplanktonic Zone

The *Whiteinella archaeocretacea* foraminiferal Zone

Bed 5. Light gray and yellowish gray, calcareous silty clay containing a foraminiferal assemblage with *Dicarinella hagni*. 0.1 m.

Bed 6. Gray and light gray flaggy dense clayey marls, ferruginous in places. 0.2 m.

Bed 7. Gray and yellow gray loose platy clayey marl with ferruginous interbeds. 0.35 m.

Bed 8. Dark to light gray platy marls with intercalations of brown to light bluish gray foliated marl stained with iron oxide after pyrite concretions at the top. It gradually passes into the overlying bed. 0.7 m.

Bed 9. Indistinctly platy marly limestone of light gray color with dark gray spots. The first occurrence of foraminifer species *Praeglobotruncana oraviensis* Scheibnerova. 0.35 m.

Bed 10. Light gray, weakly clayey, dense, chalky limestone. 0.25 m.

Bed 11. Light brownish gray platy marls with dark gray spots and burrows of mud-eaters. 0.25 m.

Bed 12. Grayish white dense splintered weakly clayey marl. 0.3 m.

Bed 13. Light yellowish gray dense indistinctly platy clayey marl. 1.2 m.

Bed 14. Light gray, indistinctly platy to massive marly, micaceous limestone. 0.25 m.

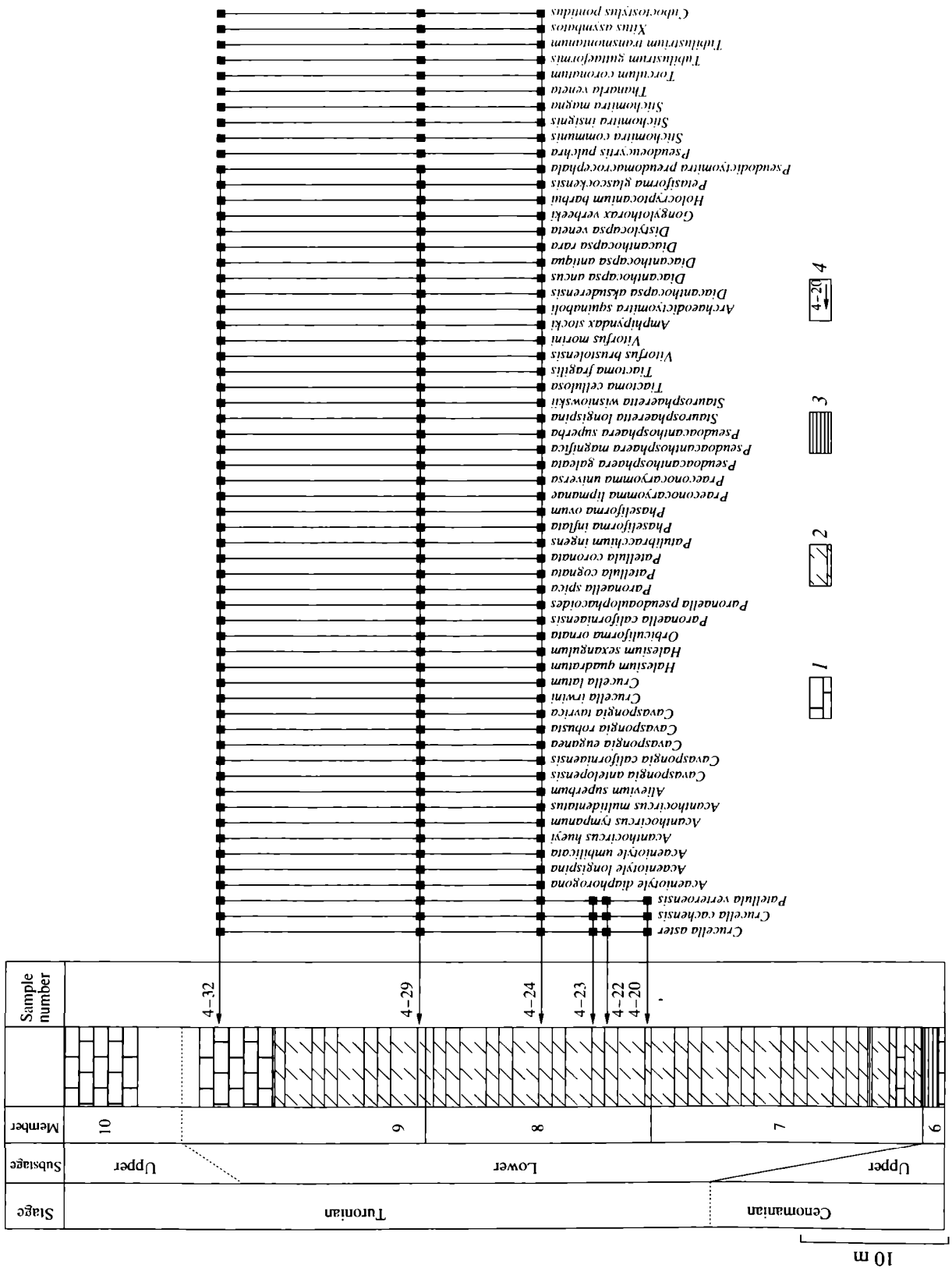

Fig. 6. Distribution of radiolarian species in the Aksudere section. Designations: (*1*) limestone, (*2*) marl, (*3*) clay, and (*4*) sample number.

Bed 15. Light gray indistinctly platy dense calcareous marl. 1.2 m.

Bed 16. Light gray and white, chalky, dense, platy marl. 0.45 m.

Bed 17. Light gray and white chalky, indistinctly platy, splintered marl. 2 m.

Bed 18. Light gray and light yellowish gray platy marl. 2.5 m.

Bed 19. Gray dense platy marl. 2.5 m.

Bed 20. Light yellowish gray indistinctly platy marl. 4 m.

Bed 21. Light yellowish gray indistinctly platy dense marl. 1 m.

Bed 22. Light yellowish gray to white platy marl. 1 m.

Member 8

Bed 23. A member of eluviated and fragmentarily exposed light gray, white, light yellowish gray, indistinctly flaggy, splintered, occasionally platy marls stained with iron oxide and including separate chert concretions. The interval from the base up to 3.8 m contains the radiolarians *Crucella aster* (Lipman), *C. cachensis* Pessagno, and *Patellula verteroensis* (Pessagno). The following radiolarians were found 4 m above the base (Sample 4-24a): *Acaeniotyle diaphorogona* Foreman, *A. longispina* (Squinabol), *A. umbilicata* (Rüst), *Acanthocircus hueyi* (Pessagno), *A. multidentatus* (Squinabol), *A. tympanum* O'Dogherty, *Alievium superbum* (Squinabol), *Cavaspongia antelopensis* Pessagno, *C. californiaensis* Pessagno, *C. euganea* (Squinabol), *C. robusta* sp. nov., *C. tavrica* sp. nov., *Crucella aster* (Lipman), *C. cachensis* Pessagno, *C. irwini* Pessagno, *C. latum* (Lipman), *Halesium quadratum* Pessagno, *H. sexangulum* Pessagno, *Orbiculiforma ornata* sp. nov., *Paronaella californiaensis* (Pessagno), *P. pseudoaulophacoides* O'Dogherty, *P. spica* sp. nov., *Patellula cognata* O'Dogherty, *P. coronata* (Tumanda), *Patellula verteroensis* (Pessagno), *Patulibracchium ingens* (Lipman), *Phaseliforma inflata* sp. nov., *P. ovum* Jud, *Praeconocaryomma universa* Pessagno, *P. lipmanae* Pessagno, *Pseudoacanthosphaera galeata* O'Dogherty, *P. magnifica* (Squinabol), *P. superba* (Squinabol), *Staurosphaeretta longispina* (Squinabol), *S. wisniowskii* (Squinabol), *Triactoma cellulosa* Foreman, *T. fragilis* Bragina, *Vitorfus brustolensis* (Squinabol), *V. morini* Empson-Morin, *Amphipyndax stocki* (Campbell et Clark), *Archaeodictyomitra squinaboli* Pessagno, *Diacanthocapsa ancus* (Foreman), *D. aksuderensis* sp. nov., *D. antiqua* (Squinabol), *D. rara* Squinabol, *Distylocapsa veneta* (Squinabol), *Gongylothorax verbeeki* (Tan Sin Hok), *Holocryptocanium barbui* Dumitrica, *Petasiforma glascockensis* Pessagno, *Pseudodictyomitra pseudomacrocephala* (Squinabol), *Pseudoeucyrtis pulchra* (Squinabol), *Stichomitra communis* Squinabol, *S. insignis* (Squinabol), *S. magna* Squinabol, *Thanarla veneta* (Squinabol), *Torculum coronatum* (Squinabol), *Tubilustrium guttaeformis* (Bragina), *T. transmontanum* O'Dogherty, *Xitus asymbatos* (Foreman), and *Cuboctostylus pontidus* sp. nov. 15 m.

Member 9

Bed 24. Light gray and white chalky marls, occasionally siliceous, with chert concretions and intercalations. The latter contain a radiolarian assemblage equivalent to that of Bed 23. 10 m.

Bed 25. Light yellowish gray and white, marly, platy limestones with gray and white chert nodules. Chert intercalations contain a radiolarian assemblage equivalent to that of Bed 24. Apparent thickness 5 m.

The interval of 4 m is unexposed.

Member 10. The Upper Turonian

Bed 26. White massive limestones with stylolites. Apparent thickness 5 m.

The Belaya Mountain Section

The section is located on the southern slope of Mt. Belaya (Fig. 7). The following members are exposed from the base upward.

Member 6-2. The Upper Cenomanian

The *Rotalipora cushmani* foraminiferal Zone

Bed 1. White dense, hard, homogenous limestone with thin ferruginous interbeds. The last occurrence of *Rotalipora cushmani*. The presence of an impoverished radiolarian assemblage with *Pyramispongia glascockensis* Pessagno, *Archaeocenosphaera ? mellifera* O'Dogherty, and *Pseudoaulophacus colburni* Pessagno. Apparent thickness. 0.2 m.

Member 6-3

The *Whiteinella archaeocretacea* foraminiferal Zone

Bed 2. Red brown (greenish at the base), laminated, calcareous-ferruginous clay. 1 m.

Bed 3. Greenish gray laminated calcareous clay. 0.3 m.

Bed 4. Greenish gray dense clayey limestone, homogenous in the lower part and lenticular-layered in the upper part, with interbeds of dark and light gray material and thin ferruginous interlayers. 0.8 m.

Bed 5. Light gray (lighter yellowish at the top), homogenous, ferruginous, calcareous clay. 0.18 m.

Bed 6. Red brown ferruginous clay. The radiolarian assemblage is identical to that of Bed 1. 0.015 m.

Bed 7. Light brown and dark gray laminated clay with ferruginous interbeds. In the upper part, the radiolarian assemblage is identical to that of Bed 1. 0.9 m.

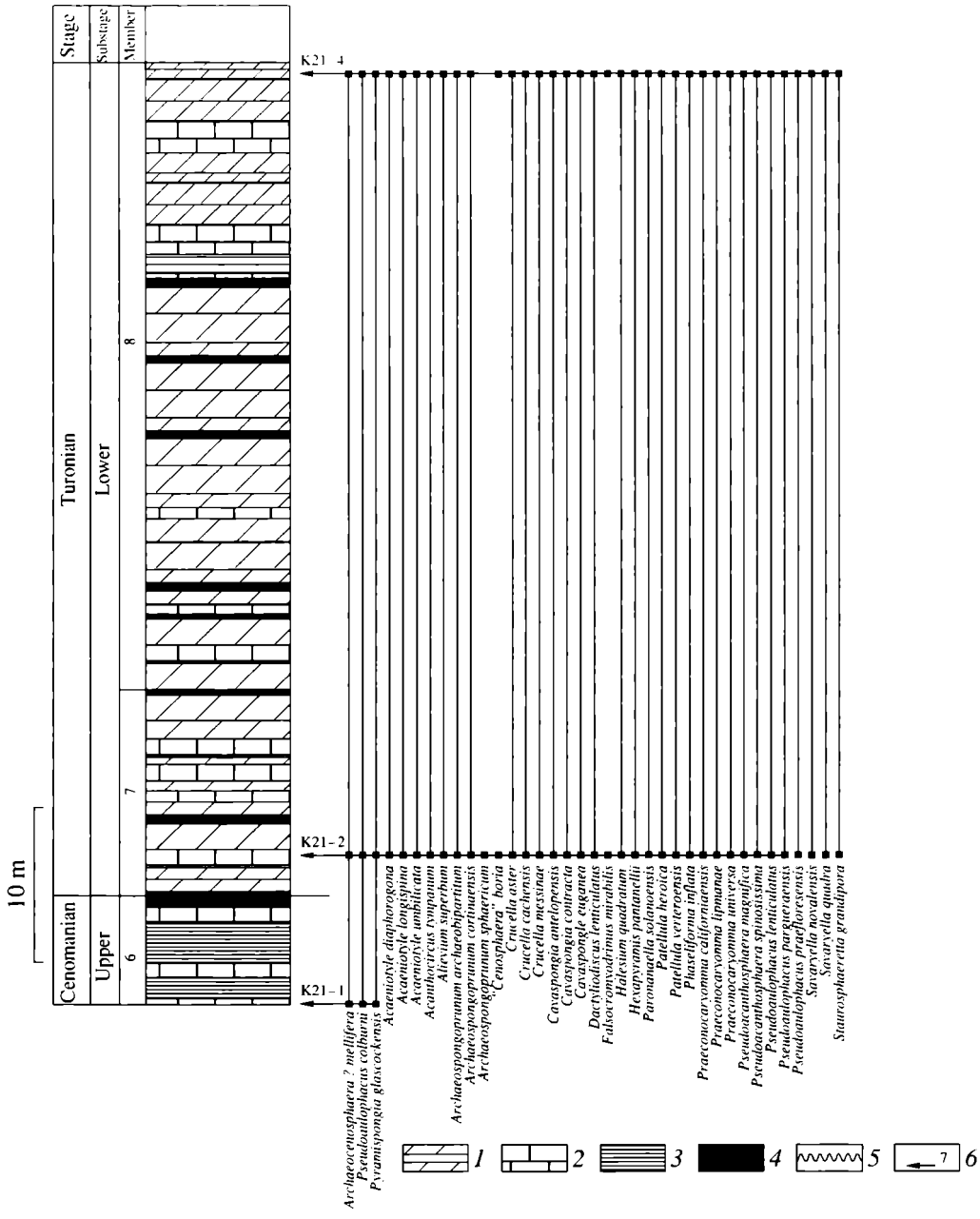

Fig. 7. Distribution of radiolarian species in the Belaya Mountain section. Designations: (*1*) calcareous marl, (*2*) chalk-like limestone, (*3*) clay, (*4*) marls with carbonaceous detritus, (*5*) erosion, and (*6*) sample number.

Bed 8. Interbedding of black, light brown, and dark gray clayey limestones. The basal and topmost interbeds are ferruginous. 0.5 m.

Member 7, Lower Turonian

The *Whiteinella archaeocretacea* foraminiferal Zone

Bed 9. Light gray, heterogeneous, lenticular–tabular, bioturbated clayey limestones are stained with light and dark gray material and form dense and massive or platy interbeds, which show a rubbly weathered surface. The first occurrences of the foraminiferal species *Dicarinella hagni* (at the base) and the zonal nannoplankton species *Quadrum gartneri* characteristic of the Lower Turonian (0.1 m above the base). 0.2 m.

Bed 10. Greenish white, dense, calcareous, slightly silicified limestones containing glauconite. 0.5 m.

The *Praeglobotruncana oraviensis* foraminiferal Zone

Bed 11. Yellowish greenish white, heterogeneous, bioturbated, occasionally ferruginous limestones, which become cleaner and whiter towards the top. They include massive dense limestones interbedded with

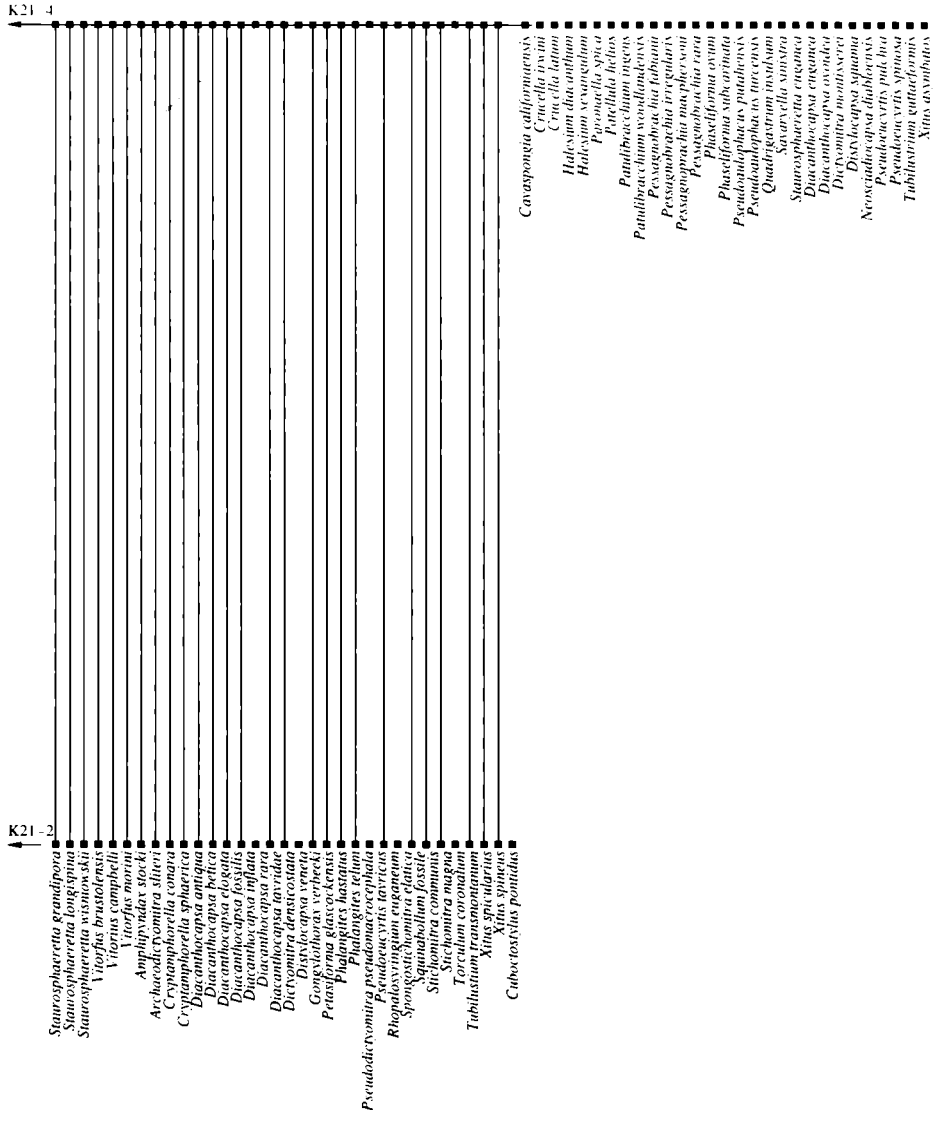

Fig. 7. (Contd.)

more clayey platy varieties. The following radiolarians were found 1 m above the bed base (Sample K21-2): *Acaeniotyle diaphorogona* Foreman, *A. longispina* (Squinabol), *A. umbilicata* Rüst, *Acanthocircus tympanum* O'Dogherty, *Alievium superbum* (Squinabol), *Archaeocenosphaera ? mellifera* O'Dogherty, *Archaeospongoprunum archaeobipartitum* sp. nov., *A. cortinaensis* Pessagno, *A. sphaericum* sp. nov., *"Cenosphaera" boria* Pessagno, *Crucella aster* (Lipman), *C. cachensis* Pessagno, *C. messinae* Pessagno, *Cavasponga antelopensis* Pessagno, *C. contracta* O'Dogherty, *C. euganea* (Squinabol), *Dactyliodiscus lenticulatus* (Jud), *Falsocromyodrymus mirabilis* (Squinabol), *Halesium quadratum* Pessagno, *Hexapyramis pantanellii* Squinabol, *Paronaella solanoensis* Pessagno, *Patellula heroica* O'Dogherty, *P. verteroensis* (Pessagno), *Phaseliforma inflata* sp. nov., *Praeconocaryomma californiaensis* Pessagno, *P. lipmanae* Pessagno, *P. universa* Pessagno, *Pseudoacanthosphaera magnifica* (Squinabol), *P. spinosissima* (Squinabol), *Pseudoaulophacus lenticulatus* (White), *P. pargueraensis* Pessagno, *P. praefloresensis* Pessagno, *Pyramispongia glascockensis* Pessagno, *Savaryella quadra* (Foreman), *S. novalensis* O'Dogherty, *Staurosphaeretta grandipora* (Squinabol), *S. longispina* (Squinabol), *S. wisniowskii* (Squinabol), *Vitorfus brustolensis* (Squinabol), *V. campbelli* Pessagno, *V. morini* Empson-Morin, *Amphipyndax stocki* (Campbell et Clark), *Archaeodictyomitra sliteri* Pessagno, *Cryptamphorella conara* (Foreman), *C. sphaerica* (White), *Diacanthocapsa antiqua* (Squinabol), *D. betica* O'Dogherty, *D. elongata* sp. nov., *D. fossilis* (Squinabol), *D. inflata* sp. nov.,

D. rara Squinabol, *D. tavridae* sp. nov., *Dictyomitra densicostata* Pessagno, *Distylocapsa veneta* (Squinabol), *Gongylothorax verbeeki* (Tan Sin Hok), *Petasiforma glascockensis* Pessagno, *Phalangites hastatus* O'Dogherty, *P. telum* O'Dogherty, *Pseudodictyomitra pseudomacrocephala* (Squinabol), *Pseudoeucyrtis tavricus* sp. nov., *Rhopalosyringium euganeum* (Squinabol), *Spongostichomitra elatica* (Aliev), *Squinabollum fossile* (Squinabol), *Stichomitra communis* Squinabol, *S. magna* Squinabol, *Torculum coronatum* (Squinabol), *Tubilustrium transmontanum* O'Dogherty, *Xitus spicularius* (Aliev), *X. spineus* Pessagno, and *Cuboctostylus pontidus* sp. nov. The first occurrence of the zonal foraminiferal species *Praeglobotruncana oraviensis* Scheibnerova was also recorded at this level. 2 m.

Bed 12. White and light yellowish gray, platy marls with white chalky limestone interbeds. 1 m.

Bed 13. Interbedding of white chalky limestones (20–30 cm) with light bluish gray, heavily clayey marls (30–40 cm) enclosing limonitized pyrite concretions. 4 m.

Bed 14. White chalky flaggy limestones with thin marl interbeds. 1.5 m.

Member 8

Bed 15. White platy marls. In the upper part (1 m below the top), there is a horizon of marls (Sample K21-4) with abundant easily observable radiolarians: *Acaeniotyle diaphorogona* Foreman, *A. longispina* (Squinabol), *A. umbilicata* Rüst, *Acanthocircus tympanum* O'Dogherty, *Alievium superbum* (Squinabol), *Archaeocenosphaera ? mellifera* O'Dogherty, *Archaeospongoprunum archaeobipartitum* sp. nov., *A. cortinaensis* Pessagno, *Crucella aster* (Lipman), *C. cachensis* Pessagno, *C. irwini* Pessagno, *C. latum* (Lipman), *C. messinae* Pessagno, *Cavaspongia antelopensis* Pessagno, *C. californiaensis* Pessagno, *C. contracta* O'Dogherty, *C. euganea* (Squinabol), *Dactyliodiscus lenticulatus* (Jud), *Halesium diacanthum* (Squinabol), *H. quadratum* Pessagno, *H. sexangulum* Pessagno, *Hexapyramis pantanellii* Squinabol, *Paronaella spica* sp. nov., *P. solanoensis* Pessagno, *Patellula helios* (Squinabol), *P. heroica* O'Dogherty, *P. verteroensis* Pessagno, *Patulibracchium ingens* (Lipman), *P. woodlandensis* Pessagno, *Pessagnobrachia fabianii* (Squinabol), *P. irregularis* (Squinabol), *P. macphersoni* O'Dogherty, *P. rara* (Squinabol), *Phaseliforma inflata* sp. nov., *P. ovum* Jud, *P. subcarinata* Pessagno, *Praeconocaryomma californiaensis* Pessagno, *P. lipmanae* Pessagno, *P. universa* Pessagno, *Pseudoaulophacus praefloresensis* Pessagno, *P. putahensis* Pessagno, *P. turcensis* sp. nov., *Pseudoacanthosphaera magnifica* (Squinabol), *P. spinosissima* (Squinabol), *Pseudoaulophacus lenticulatus* (White), *P. pargueraensis* Pessagno, *P. praefloresensis* Pessagno, *Pyramispongia glascockensis* Pessagno, *Quadrigastrum insulsum* O'Dogherty, *Savaryella quadra* (Foreman), *S. novalensis* O'Dogherty, *S. sinistra* O'Dogherty, *Staurosphaeretta euganea* (Squinabol), *S. grandipora* (Squinabol), *S. longispina* (Squinabol), *S. wisniowskii* (Squinabol), *Vitorfus brustolensis* (Squinabol), *V. campbelli* Pessagno, *V. morini* Empson-Morin, *Amphipyndax stocki* (Campbell et Clark), *Archaeodictyomitra sliteri* Pessagno, *Cryptamphorella conara* (Foreman), *C. sphaerica* (White), *Diacanthocapsa antiqua* (Squinabol), *D. betica* O'Dogherty, *D. elongata* sp. nov., *D. euganea* Squinabol, *D. fossilis* (Squinabol), *D. inflata* sp. nov., *D. ovoidea* Dumitrica, *D. rara* Squinabol, *Dictyomitra densicostata* Pessagno, *D. montisserei* (Squinabol), *Distylocapsa squama* O'Dogherty, *D. veneta* (Squinabol), *Neosciadiocapsa diabloensis* Pessagno, *Petasiforma glascockensis* Pessagno, *Phalangites hastatus* O'Dogherty, *P. telum* O'Dogherty, *Pseudodictyomitra pseudomacrocephala* (Squinabol), *Pseudoeucyrtis pulchra* (Squinabol), *P. spinosa* (Squinabol), *Rhopalosyringium euganeum* (Squinabol), *Squinabollum fossile* (Squinabol), *Stichomitra communis* Squinabol, *S. magna* Squinabol, *Tubilustrium guttaeformis* (Bragina), *T. transmontanum* O'Dogherty, *Xitus asymbatos* (Foreman), *X. spicularius* (Aliev), and *X. spineus* Pessagno. 18 m.

Bed 16. Light yellowish gray platy marl. Apparent thickness. 1.1 m.

CHAPTER 2. THE CENOMANIAN–TURONIAN RADIOLARIAN ASSEMBLAGES OF NORTHERN TURKEY AND THE CRIMEAN MOUNTAINS AND THEIR STRATIGRAPHIC SIGNIFICANCE

The basic principles of Cretaceous stratigraphy were developed in western Europe. Standard ammonite zonation was the major biostratigraphic tool (Kennedy, 1984). By the mid-Cretaceous, however, ammonites had lost their significance because of an increasingly greater degree of provincialism (Naidin *et al.*, 1981). In the biostratigraphy of the Turonian and younger strata, inoceramids became the most important group (*Atlas* ..., 1992, 1993; Pergament, 1978; Matsumoto, 1977).

The marine realm can be divided into three paleobiogeographic realms based on macrofauna development; these are the Pacific, Tethyan, and Paratethyan (Boreal or European) (*Geological* ..., 1989). Two different stratigraphic schemes have been developed for the Paratethyan and Tethyan realms, and, more recently, a new zonal scheme that is thought to be applicable to both realms has been proposed (Kennedy, 1984). A detailed correlation of Middle Cretaceous strata within the European and Pacific realms was developed in the 1970s (Hancock *et al.*, 1977; Kennedy and Hancock, 1977). The Pacific macrofauna is too endemic to be positively correlated with that of the Tethyan.

There is no standard Upper Cretaceous radiolarian zonation that can provide interregional correlations. In

practice, radiolarians are used in combination with other fossil groups. The best studied Late Cretaceous radiolarians are those from the fairly complete marine sequences of the Pacific (Moore, 1973; Foreman, 1973, 1975; Schaaf, 1981) and the Atlantic (Thurow, 1988; Schaaf, 1985). The first composite radiolarian zonation for the northwestern Pacific, northwestern Atlantic, Indian Ocean, and the Caribbean basin was proposed by Riedel and Sanfilippo (1974). A number of zonal schemes appeared in the mid-1980s (Sanfilippo and Riedel, 1985; Schaaf, 1985). Investigations of nonmarine sequences have resulted in local radiolarian zonations for Japan (Taketani, 1982; Tumanda, 1989), the Californian coast (Pessagno, 1976), Romania (Dumitrica, 1975), and the Caucasus (Vishnevskaya, 1993). The resolution of these schemes varies from one to two or three zones per stage. Difficulties in correlation of radiolarian assemblages from different tropical regions are mainly due to their inadequate knowledge. Usually, taxonomic studies of the assemblages have been restricted to revealing index species and some characteristic species (Riedel and Sanfilippo, 1974; Marcucci *et al.*, 1991; Marcucci and Gardin, 1992; Pignotti, 1994). Recent studies have revealed the very high diversity of Late Cretaceous tropical radiolarian assemblages. The most representative of these assemblages are the thoroughly studied Mediterranean assemblages (Erbacher, 1994; O'Dogherty, 1994; Khan *et al.*, 1999; Salvini and Marcucci Passerini, 1998; Squinabol, 1903, 1904). The regional radiolarian zonation for the Cenomanian–Turonian of the Mediterranean that has recently been developed by O'Dogherty (1994) has yet to be adapted to many other regions. This paper pays special attention to the correlation of northern Turkish sections with the Mediterranean radiolarian zones.

In contrast to the deep-water Italian and Spanish assemblages, little is known about radiolarian assemblages from shallower water facies. The present study aims to fill this gap.

NORTHERN TURKEY

The Upper Cretaceous deposits of northern Turkey are represented by relatively deep-water marine facies typical of the axial areas of the Mediterranean belt. These are predominantly carbonate and terrigenous-carbonate flysch and, occasionally, olistostromes in the western and central Pontic Mountains and thick volcanogenic sediments in the eastern Pontic Mountains. The stratigraphy of the Upper Cretaceous of Turkey is mainly based on planktonic foraminifers and nannoplankton and gives comparatively low level of resolution. The Coniacian and Campanian stages have not been recognized with certainty in the Devrekâni Basin. No precise correlations have been made between the neighboring areas of the Pontic Mountains and other Mediterranean regions.

It is now important to study the taxonomic diversity and characteristic assemblages of radiolarians in this region, and to correlate them with those of other Mediterranean regions.

The highest taxonomic diversity of Middle Cenomanian radiolarians has been recorded in relatively deep-water siliceous deposits of the Ürküt section, in which radiolarians are associated with planktonic foraminifers. This section has yielded more than 120 species (see the table following chapter 2); most of the newly described species come from this section. The assemblages contain species typical of the western Mediterranean *Dactyliosphaera silviae* Zone (O'Dogherty, 1994), such as *Acaeniotyle macrospina, Becus horridus, Cavaspongia antelopensis, C. californiaensis, C. euganea, Crucella irwini, C. messinae, Dactyliodiscus longispinus, Dactyliosphaera silviae, Dicroa rara, Hexapyramis pantanellii, Pyramispongia glascockensis, Quinquecapsularia grandiloqua, Vitorfus brustolensis, Distylocapsa veneta, Novixitus dengoi, Phalangites telum, Spongostichomitra phalanga, Squinabollum fossile*, and many others. A similar but less diverse assemblage correlative to that of the upper part of *Dactyliosphaera silviae* Zone has been yielded by the Tomalar section of the Devrekâni basin (Fig. 8).

In Italy and Spain, the *Dactyliosphaera silviae* Zone may be subdivided into two subzones: *Patellula spica* and *Guttacapsa biacuta* (O'Dogherty, 1994) (Fig. 8). However, the absence of these species from the Turkish sections prevents the recognition of these subzones in northern Turkey. Therefore, *Patellula spica* and *Guttacapsa biacuta* are not entirely appropriate index species.

A characteristic feature of the Cenomanian assemblages of the Devrekâni basin is the presence of distinctive large Orosphaeridae (*Archaeoplegma pontidae* gen. et sp. nov.) and Entactinaria (*Cuboctostylus pontidus* sp. nov.). In addition, these assemblages were the first in the Cenomanian of the Mediterranean to yield abundant *Archaeospongoprunum*, which were previously described from the Cenomanian of North America (Pessagno, 1976).

THE CRIMEAN MOUNTAINS

The present study of the Late Cretaceous radiolarians of the Crimean Mountains aims to estimate the degree of their provincialism and to determine whether or not O'Dogherty's zonation of the Tethys (1994) is applicable to this region.

Previous studies of the Upper Cretaceous deposits of the Crimean Mountains (Bragina, 1999a) have revealed a succession of radiolarian assemblages the faunal composition of which varies considerably through the succession, thus allowing the recognition and correlation of radiolarian-based biostratigraphic units. Beds with radiolarians have been established in accordance with the commonly accepted procedure: the lower boundary is defined by the first occurrences of

Species composition of the Cenomanian–Turonian radiolarian assemblages of northern Turkey and the Crimean Mountains

Radiolarian species \ Sample	Turkey						Crimea						
	Ürküt			Tomalar			Sel'-Bukhra				Aksu-dere	Belaya	
	55	64	73	75	77	83	16a	19	29	32	4-24	K21-2	K21-4
Saturniforma peregrina	●												
Rotaforma hessi	●			●									
Petasiforma foremanae	●	●	●	●		●		●					
Petasiforma glascockensis		●	●	●				●			●	●	●
Petasiforma tavridae								●					
Lipmanium sacramentoensis	●								●	●			
Neosciadiocapsa diabloensis													●
Microsciadiocapsa monticelloensis	●				●	●							
Ultranapora durhami		●											
Ultranapora praespinifera	●	●											
Ultranapora spinifera	●												
Ultranapora urkutae	●	●											
Rhopalosyringium euganeum		●		●	●		●					●	●
Rhopalosyringium kleinum	●	●											
Rhopalosyringium magnificum	●												
Rhopalosyringium majuroensis	●	●											
Distylocapsa squama			●	●	●			●					●
Distylocapsa veneta	●	●		●	●			●			●	●	●
Torculum coronatum	●		●	●				●	●	●	●	●	
Phalangites hastatus								●				●	●
Phalangites telum	●							●				●	●
Xitus asymbatos								●			●		●
Xitus spicularius	●	●		●	●	●	●			●		●	●
Xitus spineus	●				●							●	●
Xitus urkutus	●												
Novixitus costatus	●												
Novixitus dengoi	●			●	●	●		●					
Novixitus subtilis	●												
Novixitus urkutus	●												
Novixitus weyli	●	●	●		●	●							
Pseudodictyomitra pseudomacrocephala	●	●			●		●	●			●	●	●
Pseudodictyomitra nakasekoi					●	●				●			
Pseudodictyomitra quasilodogaensis		●				●							
Pseudodictyomitra lodogaensis										●			
Mita (?) cypraea	●					●							
Thanarla gracilis	●	●	●										
Thanarla veneta		●	●		●			●			●		
Archaeodictyomitra crebrisulcata								●					
Archaeodictyomitra delicata		●											
Archaeodictyomitra simplex	●					●							
Archaeodictyomitra sliteri	●			●	●			●				●	●
Archaeodictyomitra (?) speciosa	●		●	●	●								
Archaeodictyomitra squinaboli	●							●	●		●		

Table. (Contd.)

Radiolarian species \ Sample	Turkey						Crimea						
	Ürküt			Tomalar			Sel'-Bukhra				Aksu-dere	Belaya	
	55	64	73	75	77	83	16a	19	29	32	4-24	K21-2	K21-4
Archaeodictyomitra vulgaris								●					
Dictyomitra densicostata									●			●	●
Dictyomitra montiserrei	●	●			●								●
Dictyomitra multicostata							●			●			
Dictyomitra napaensis					●	●							
Stichomitra communis	●	●	●		●	●		●	●		●	●	●
Stichomitra insignis								●			●		
Stichomitra magna								●			●	●	●
Stichomitra manifesta								●					
Eostichomitra warzigita	●												
Amphipyndax stocki	●	●	●		●	●		●	●	●	●	●	●
Amphipyndax ellipticus	●												
Amphipyndax conicus	●												
Holocryptocanium astiensis	●												
Holocryptocanium barbui	●		●		●			●	●		●		
Holocryptocanium geysersensis	●												
Diacanthocapsa acuminata	●	●											
Diacanthocapsa aksuderensis											●		
Diacanthocapsa ancus	●	●				●		●			●		
Diacanthocapsa antiqua				●		●		●			●	●	●
Diacanthocapsa betica		●						●				●	●
Diacanthocapsa brevithorax	●												
Diacanthocapsa elongata	●											●	●
Diacanthocapsa euganea	●												●
Diacanthocapsa fossilis							●					●	●
Diacanthocapsa inflata												●	●
Diacanthocapsa matsumotoi	●												
Diacanthocapsa rara								●			●	●	●
Diacanthocapsa ovoidea			●	●									
Diacanthocapsa tavridae												●	
Diacanthocapsa urkutica		●											
Cryptamphorella conara	●	●		●	●		●		●			●	
Cryptamphorella micropora	●												
Cryptamphorella sphaerica		●		●								●	
Immersothorax cyclops		●											
Squinabollum fossile	●	●	●		●							●	
Sethocapsa simplex	●												
Trisyringium echitonicum	●					●							
Pogonias missilis								●					
Pogonias (?) hirsutus		●	●		●								
Siphocampe altamontensis		●											
Siphocampe praevanderhoofi		●											
Tubilustrium guttaeformis	●	●	●					●			●		●

Table. (Contd.)

Radiolarian species \ Sample	Turkey						Crimea						
	Ürküt			Tomalar			Sel'-Bukhra				Aksu-dere	Belaya	
	55	64	73	75	77	83	16a	19	29	32	4-24	K21-2	K21-4
Tubilustrium transmontaum	●	●			●			●			●	●	
Pseudoeucyrtis pulchra								●			●		●
Pseudoeucyrtis spinosa	●	●	●			●							●
Pseudoeucyrtis tavricus								●				●	
Spongostichomitra elatica								●				●	
Spongostichomitra phalanga	●												
Cornutella californica	●	●											
Afens liriodes					●								
Archaeocenoshaera ? mellifera	●						●		●	●		●	●
"Cenosphaera" borea	●				●								
Praeconocaryomma californiaensis		●			●			●				●	●
Praeconocaryomma lipmanae	●							●	●		●	●	●
Praeconocaryomma universa									●		●	●	●
Pseudoacanthosphaera galeata								●			●		
Pseudoacanthosphaera magnifica		●			●			●			●	●	●
Pseudoacanthosphaera spinosissima		●						●				●	●
Pseudoacanthosphaera superba					●			●			●		
Staurosphaeretta euganea		●						●					●
Staurosphaeretta grandipora	●	●	●	●	●	●						●	●
Staurosphaeretta micropora	●												
Staurosphaeretta longispina	●	●						●			●	●	●
Staurosphaeretta wisniowskii		●						●			●	●	●
Tetracanthellipsis euganeus	●	●		●									
Quinquecapsularia panacea	●	●		●									
Quinquecapsularia grandiloqua					●								
Quinquecapsularia ombonii	●												
Quinquecapsularia parvipora		●		●	●			●					
Falsocromyodrims cardulus	●												
Falsocromyodrimus mirabilis		●				●		●				●	
Hexapyramis pantanellii	●											●	●
Acaeniotyle diaphorogona	●						●	●			●	●	●
Acaeniotyle longispina	●				●			●			●	●	●
Acaeniotyle macrospina	●	●	●										
Acaeniotyle umbilicata		●						●			●	●	●
Triactoma cellulosa	●	●									●		
Triactoma compressa	●		●	●									
Triactoma fragilis											●		
Triactoma micropora	●		●	●									
Triactoma parva	●						●						
Protoxiphotractus ventosus	●	●											
Archaeospongoprunum anatolica	●												
Archaeospongoprunum archaeobipartitum								●				●	●
Archaeospongoprunum cortinaensis	●	●			●		●					●	●

Table. (Contd.)

Radiolarian species \ Sample	Turkey						Crimea						
	Ürküt			Tomalar			Sel'-Bukhra				Aksu-dere	Belaya	
	55	64	73	75	77	83	16a	19	29	32	4-24	K21-2	K21-4
Archaeospongoprunum klingi	●												
Archaeospongoprunum pontidum						●							
Archaeospongoprunum sphaericum												●	
Archaeospongoprunum triplum								●					
Paronaella pseudoaulophacoides								●	●	●	●		
Paronaella solanoensis	●	●					●					●	●
Paronaella spica	●		●	●				●			●		●
Halesium diacanthum								●					●
Halesium quadratum	●	●	●					●			●	●	●
Halesium sexangulum	●	●	●			●		●			●		●
Patulibracchium ingens		●	●			●	●				●		●
Patulibracchium californiaensis						●							
Patulibracchium obesum	●	●											
Patulibracchium woodlandensis	●	●	●			●							●
Patulibracchium (?) quadroastrum								●					
Savaryella quadra	●	●	●	●	●							●	●
Savaryella novalensis								●				●	●
Savaryella sinistra													●
Crucella aster			●	●	●								
Crucella cachensis					●	●	●	●	●	●	●	●	●
Crucella euganea	●							●					
Crucella hispana		●											
Crucella irwini	●	●	●		●	●		●			●		●
Crucella latum		●						●	●	●	●		●
Crucella messinae	●	●	●		●		●					●	●
Pessagnobrachia irregularis													●
Pessagnobrachia fabianii	●	●											●
Pessagnobrachia rara								●			●		●
Cavaspongia antelopensis	●							●	●	●	●	●	●
Cavaspongia californiaensis							●	●					●
Cavaspongia contracta							●					●	●
Cavaspongia euganea	●	●	●								●	●	●
Cavaspongia robusta								●			●		
Cavaspongia sphaerica		●											
Cavaspongia tavrica								●			●		
Pyramispongia glascockensis	●	●	●			●	●		●	●	●	●	●
Pseudoaulophacus circularis								●					
Pseudoaulophacus lenticulatus			●				●					●	●
Pseudoaulophacus parguerensis							●					●	●
Pseudoaulophacus praefloresensis		●			●			●	●	●		●	●
Pseudoaulophacus putahensis			●					●					●
Pseudoaulophacus turcensis	●	●											●
Alievium sculptus	●	●		●		●		●					

Table. (Contd.)

Radiolarian species \ Sample	Turkey						Crimea						
	Ürküt			Tomalar			Sel`-Bukhra				Aksu-dere	Belaya	
	55	64	73	75	77	83	16a	19	29	32	4-24	K21-2	K21-4
Alievium superbum								●	●	●	●	●	●
Stylodictya insignis	●							●					
Quadrigastrum insulsum								●					●
Dactyliosphaera silviae	●	●	●		●	●							
Dactyliosphaera lenticulatus	●					●	●					●	●
Dactyliosphaera longispinus	●	●			●	●		●					
Dactyliosphaera spinosus			●										
Godia concava	●	●											
Godia tomalarea			●										
Orbiculiforma ornata								●	●		●		
Orbiculiforma ovoidea	●		●										
Patellula cognata	●	●					●				●		
Patellula coronata		●									●		
Patellula helios													●
Patellula heroica												●	●
Patellula spica	●												
Patellula verteroensis	●	●	●		●	●	●		●		●	●	●
Becus horridus	●	●											
Becus regius	●	●	●								●	●	●
Dispongotripus triangularis		●											
Phaseliforma carinata	●		●										
Phaseliforma inflata								●			●	●	●
Phaseliforma laxa	●												
Phaseliforma ovum		●		●		●		●			●		●
Phaseliforma subcarinata													●
Acanthocircus imperfectus		●											
Acanthocircus impolitus	●		●					●					
Acanthocircus horridus	●	●	●										
Acanthocircus hueyi	●							●			●		
Acanthocircus moorei	●	●											
Acanthocircus multidentatus								●			●		
Acanthocircus polymorphus	●	●											
Acanthocircus tympanum								●			●	●	●
Vitorfus brustolensis	●	●						●			●	●	●
Vitorfus campbelli				●				●				●	●
Vitorfus morini								●			●	●	●
Cuboctostylus pontidus	●	●						●			●	●	●
Archaeoplegma pontidae	●	●						●					

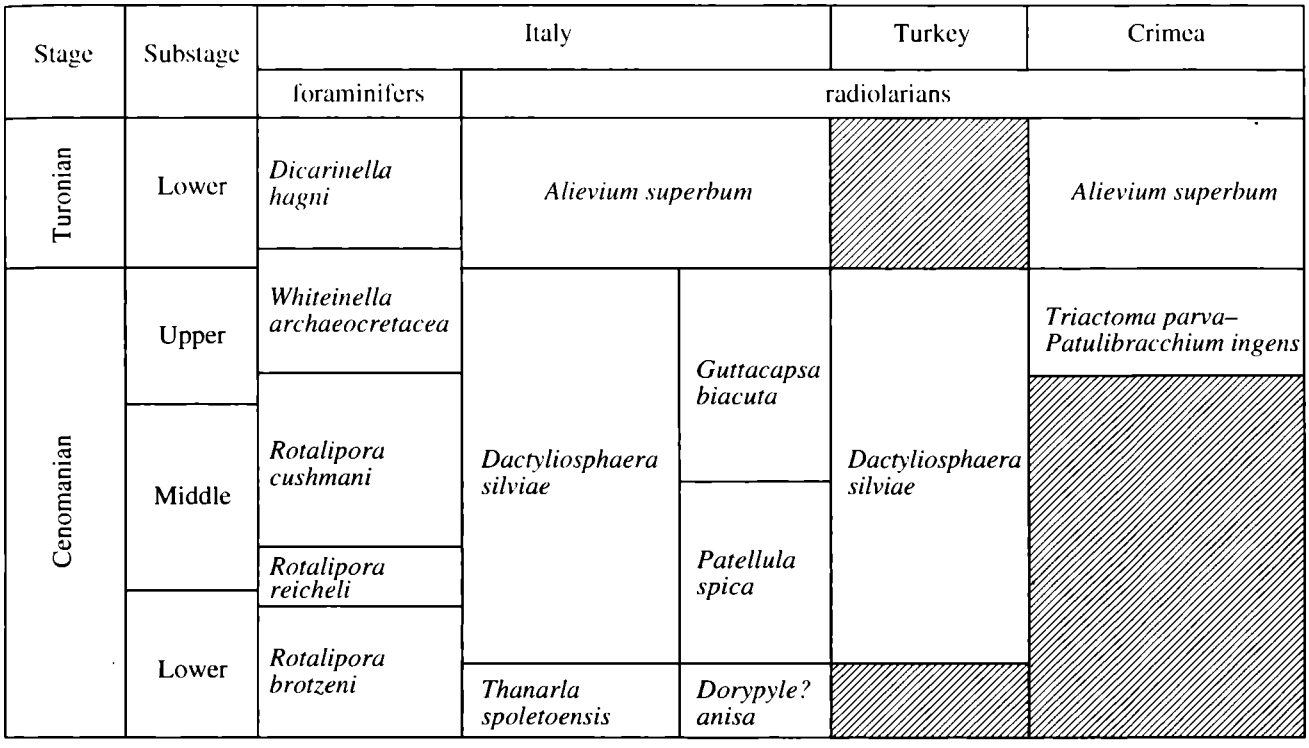

Fig. 8. Correlation of the Cenomanian–Turonian radiolarian zones of Italy, Turkey, and the Crimea.

the index species and the assemblage of associated characteristic species.

The following biostratigraphic units have been recognized in the Crimean sections (Fig. 8):

Unit 1. The Upper Cenomanian. Beds with *Triactoma parva–Patulibracchium ingens*. The upper part of Member 6-3 of the Sel'-Bukhra section. The beds are equivalent to the lower part of the foraminiferal *Whiteinella archaeocretacea* Zone of (terminal Cenomanian–lowermost Turonian) of the Crimean Mountains. The lower part of the zone belongs to the Upper Cenomanian, and the upper part—from the first occurrence of *Dicarinella hagni* (Kuz'micheva, 2000b) and above the last occurrence of *Rotalipora cushmani*—belongs to the Lower Turonian. Since these beds share the species *Acaeniotyle diaphorogona, Archaeocenosphaera ? mellifera, Cavaspongia contracta, Crucella messinae, Patellula verteroensis, Pseudodictyomitra pseudomacrocephala, Pyramispongia glascockensis*, and *Xitus spicularius*, with the Mediterranean *Dactyliosphaera silviae* Zone (the *Guttacapsa biacuta* Subzone) of O'Dogherty, (1994), they may be correlated with the latter. A large number of Early Turonian species are survivors from the Cenomanian; thus, the Lower Turonian is recognized in Italy and Spain by the presence of newly appeared species. Therefore, Beds with *Triactoma parva–Patulibracchium ingens* were ascribed to the Upper Cenomanian because of the absence of many typical Early Turonian Mediterranean species, including *Alievium superbum*, the index species of the Lower Turonian *Alievium superbum* Zone in the Mediterranean.

Some taxa recorded in Beds with *Triactoma parva–Patulibracchium ingens* have different stratigraphic ranges in the southwestern Mediterranean (Italy and Spain). Thus, *Diacanthocapsa fossilis* and *Dactyliodiscus lenticulatus* have not been found in the Mediterranean above the Middle Cenomanian (O'Dogherty, 1994). *Crucella cachensis, Paronaella solanoensis*, and *Triactoma parva*, which are restricted to the Lower Turonian in Italy and Spain, appeared in the Crimean Mountains as early as the Upper Cenomanian. *Pseudoaulophacus parqueraensis, Obesacapsula* sp. ex gr. *O. morroensis* Pessagno are typical of the Late Cenomanian of the Crimean Mountains. Some species from Beds with *Triactoma parva–Patulibracchium ingens*, e.g., *Crucella aster, Patulibracchium ingens* (= *P. inaequalum* Pessagno), occur in both warm- and cold-water assemblages.

These beds correlate with the coeval radiolarian *Rotaforma hessi* Zone of California (Pessagno, 1976) by having the species *Archaeospongoprunum cortinaensis, Crucella cachensis, Pyramispongia glascockensis*, and *Pseudodictyomitra pseudomacrocephala* in common.

Unit 2. The lowermost Turonian. The lower part of *Alievium superbum* Zone embraces the upper part of Member 7 of the Belaya Mountain section as well as the interval from the base of Member 7 through the basal part of Member 8 in the Sel'-Bukhra section. The

zone is recognized by the presence of the index species and a great number (several tens) of species characteristic of this zone in Italy (O'Dogherty, 1994). Some species (*Alievium superbum, Cavaspongia antelopensis, C. californiaensis, C. euganea, Crucella cachensis*, and *Cr. irwini*) are known from the stratotype of this zone in the Lower Turonian of California (Pessagno, 1976). The zone corresponds to the upper part of the foraminiferal *Whiteinella archaeocretacea* Zone, i.e., to the initial Lower Turonian (Kuz'micheva, 2000b). Among the macrofaunal taxa, there are scarce *Inoceramus labiatus* Schloth., which supports the Early Turonian age of the host beds.

The assemblage of the *Alievium superbum* Zone includes all species characteristic of Beds with *Triactoma parva–Patulibracchium ingens*, except for *Pseudoaulophacus pargueraensis* and *Obesacapsula* sp. ex gr. *O. morroensis*. In addition, there are a great many (more than 100) newly appeared species: *Acaeniotyle diaphorogona* Foreman, *A. longispina* (Squinabol), *A. umbilicata* (Rüst), *Acanthocircus hueyi* (Pessagno), *A. impolitus* O'Dogherty, *A. multidentatus* (Squinabol), *A. tympanum* O'Dogherty, *Alievium sculptus* (Squinabol), *A. superbum* (Squinabol), *Archaeospongoprunum archaeobipartitum* sp. nov., *A. triplum* Pessagno, *Becus regius* O'Dogherty, *Cavaspongia antelopensis* Pessagno, *C. californiaensis* Pessagno, *C. euganea* (Squinabol), *C. robusta* sp. nov., *C. tavrica* sp. nov., *Crucella cachensis* Pessagno, *C. irwini* Pessagno, *C. latum* (Lipman), *Dactyliodiscus longispinus* (Squinabol), *Falsocromyodrimus mirabilis* (Squinabol), *Halesium diacanthum* (Squinabol), *H. quadratum* Pessagno, *H. sexangulum* Pessagno, *Orbiculiforma ornata* sp. nov., *Paronaella californiaensis* (Pessagno), *P. pseudoaulophacoides* O'Dogherty, *P. spica* sp. nov., *Patellula cognata* O'Dogherty, *P. coronata* (Tumanda), *P. helios* (Squinabol), *Patulibracchium (?) quadroastrum* Bragina, *P. woodlandensis* Pessagno, *Phaseliforma inflata* sp. nov., *P. ovum* Jud, *Pogonias missilis* O'Dogherty, *Praeconocaryomma californiaensis* Pessagno, *P. lipmanae* Pessagno, *Pseudoacanthosphaera galeata* O'Dogherty, *P. magnifica* (Squinabol), *P. spinosissima* (Squinabol), *P. superba* (Squinabol), *Pseudoaulophacus circularis* sp. nov., *P. praefloresensis* Pessagno, *P. putahensis* Pessagno, *Quadrigastrum insulsum* O'Dogherty, *Quinquecapsularia parvipora* (Squinabol), *Savaryella novalensis* (Squinabol), *Staurosphaeretta euganea* (Squinabol), *S. longispina* (Squinabol), *S. wisniowskii* (Squinabol), *Stylodictya insignis* Campbell et Clark, *Triactoma cellulosa* Foreman, *T. compressa* (Squinabol), *T. fragilis* Bragina, *Vitorfus brustolensis* (Squinabol), *V. campbelli* Pessagno, *V. morini* Empson-Morin, *Amphipyndax stocki* (Campbell et Clark), *Archaeodictyomitra crebrisulcata* (Squinabol), *A. sliteri* (Squinabol), *A. squinaboli* Pessagno, *A. vulgaris* Pessagno, *Diacanthocapsa ancus* (Foreman), *D. aksuderensis* sp. nov., *D. antiqua* (Squinabol), *D. betica* O'Dogherty, *D. rara* Squinabol, *Distylocapsa veneta* (Squinabol), *Holocryptocanium barbui* Dumitrica, *Novixitus dengoi* Schmidt-Effing, *Petasiforma glascockensis* Pessagno, *P. tavridae* sp. nov., *Phalangites hastatus* O'Dogherty, *Pogonias missilis* O'Dogherty, *Pseudodictyomitra pseudomacrocephala* (Squinabol), *Pseudoeucyrtis pulchra* (Squinabol), *P. tavricus* sp. nov., *Spongostichomitra elatica* (Aliev), *Stichomitra communis* Squinabol, *S. insignis* (Squinabol), *S. magna* Squinabol, *Thanarla veneta* (Squinabol), *Torculum coronatum* (Squinabol), *Tubilustrium guttaeformis* (Bragina), *T. transmontanum* O'Dogherty, *Xitus asymbatos* (Foreman), *Cuboctostylus pontidus* sp. nov., and *Archaeoplegma pontidae* sp. nov. (table). Among the continuing species there are *Archaeocenosphaera ? mellifera, Cavaspongia contracta, C. messinae, Patellula verteroensis, Xitus spicularius*, which are characteristic of the Cenomanian–Turonian deposits of Italy and Spain. The most part (70%) of the assemblage is characteristic of the Upper Cenomanian–Lower Turonian of Italy. Many species (20% of the assemblage) were first discovered and described by O'Dogherty (1994) from Italy and Spain. However, some Cenomanian species known in Italy and Spain (e.g., *Crucella irwini* and *C. messinae*) did not appear in the Crimea until the Turonian. *Tubilustrium guttaeformis* was first described from the Lower Campanian of Cyprus (Bragina and Bragin, 1996). The presence of this species in the Early Turonian assemblage of the Crimea extends both its geochronological and spatial ranges. The species of this assemblage show only slight differences in abundance. The most abundant of them are some species of *Pseudoaulophacus* and *Archaeocenosphaera ? mellifera. Patulibracchium davisi* and *Pseudoaulophacus praefloresensis* are unknown from Italy and Spain but are characteristic of the Cenomanian–Turonian assemblages in California. *Praeconocaryomma californiaensis* and *Pseudoaulophacus floresensis* are known from the younger Coniacian–Campanian assemblages of California.

The assemblage shares 12 species (*Acanthocircus tympanum, Vitorfus campbelli, Archaeocenosphaera ? mellifera, Praeconocaryomma lipmanae, Cavaspongia antelopensis, Crucella cachensis, Dictyomitra multicostata, Pseudodictyomitra pseudomacrocephala, Amphipyndax stocki, Holocryptocanium barbui, Stichomitra communis*, and *Cryptamphorella conara*) with the Early Turonian assemblages of the Klippen Belt of the western Carpathians in Slovakia and Poland (Sykora *et al.*, 1997).

Unit 3. The upper part of the Lower Turonian. Beds with *Praeconocaryomma universa–Dictyomitra densicostata* (the upper part of the *Alievium superbum* Zone) correspond to the interval of the lower part of Member 8 through the lower part of Member 9 of the Sel'-Bukhra section and to Member 8 of the Aksudere Gully section. The beds are correlative to the Mediterranean foraminiferal zone of *Helvetoglobotruncana helvetica* of the Lower Turonian (excluding the lowermost part) (O'Dogherty, 1994) and the coeval Crimean zone of

Praeglobotruncana oraviensis (Kuz'micheva, 2000b). The radiolarian assemblage comprises 99 species: *Acaeniotyle diaphorogona* Foreman, *A. longispina* (Squinabol), *A. umbilicata* Rust, *Acanthocircus tympanum* O'Dogherty, *Alievium superbum* (Squinabol), *Archaeocenosphaera ? mellifera* O'Dogherty, *Archaeospongoprunum archaeobipartitum* sp. nov., *A. cortinaensis* Pessagno, *Cavaspongia euganea* (Squinabol), *Crucella aster* (Lipman), *C. cachensis* Pessagno, *C. irwini* Pessagno, *C. latum* (Lipman), *C. messinae* Pessagno, *Cavaspongia antelopensis* Pessagno, *C. californiaensis* Pessagno, *C. contracta* O'Dogherty, *C. euganea* (Squinabol), *Dactyliodiscus lenticulatus* (Jud), *Halesium diacanthum* (Squinabol), *H. quadratum* Pessagno, *H. sexangulum* Pessagno, *Hexapyramis pantanellii* Squinabol, *Paronaella pseudoaulophacoides* O'Dogherty, *P. spica* sp. nov., *P. solanoensis* Pessagno, *Patellula helios* (Squinabol), *P. heroica* O'Dogherty, *P. verteroensis* (Pessagno), *Patulibracchium ingens* (Lipman), *P. woodlandensis* Pessagno, *Pessagnobrachia fabianii* (Squinabol), *P. irregularis* (Squinabol), *P. macphersoni* O'Dogherty, *P. rara* (Squinabol), *Phaseliforma inflata* sp. nov., *P. ovum* Jud, *P. subcarinata* Pessagno, *Praeconocaryomma californiaensis* Pessagno, *P. lipmanae* Pessagno, *P. universa* Pessagno, *Pseudoaulophacus praefloresensis* Pessagno, *P. putahensis* Pessagno, *P. turcensis* sp. nov., *Pseudoacanthosphaera magnifica* (Squinabol), *P. spinosissima* (Squinabol), *Pseudoaulophacus lenticulatus* (White), *P. parguerensis* Pessagno, *P. praefloresensis* Pessagno, *Pyramispongia glascockensis* Pessagno, *Quadrigastrum insulsum* O'Dogherty, *Savaryella quadra* (Foreman), *S. novalensis* O'Dogherty, *S. sinistra* O'Dogherty, *Staurosphaeretta euganea* (Squinabol), *S. grandipora* (Squinabol), *S. longispina* (Squinabol), *S. wisniowskii* (Squinabol), *Vitorfus brustolensis* (Squinabol), *V. campbelli* Pessagno, *V. morini* Empson-Morin, *Amphipyndax stocki* (Campbell et Clark), *Archaeodictyomitra sliteri* Pessagno, *A. squinaboli* Pessagno, *Cryptamphorella conara* (Foreman), *C. sphaerica* (White), *Diacanthocapsa antiqua* (Squinabol), *D. betica* O'Dogherty, *D. elongata* sp. nov., *D. euganea* Squinabol, *D. fossilis* (Squinabol), *D. inflata* sp. nov., *D. ovoidea* Dumitrica, *D. rara* Squinabol, *Dictyomitra densicostata* Pessagno, *D. montisserei* (Squinabol), *D. multicostata* Zittel, *Distylocapsa squama* O'Dogherty, *D. veneta* (Squinabol), *Lipmanium sacramentoensis* Pessagno, *Neosciadiocapsa diabloensis* Pessagno, *Petasiforma glascockensis* Pessagno, *Phalangites hastatus* O'Dogherty, *P. telum* O'Dogherty, *Pseudodictyomitra pseudomacrocephala* (Squinabol), *P. nakasekoi* Taketani, *P. lodogaensis* Pessagno, *Pseudoeucyrtis pulchra* (Squinabol), *P. spinosa* (Squinabol), *Rhopalosyringium euganeum* (Squinabol), *Squinabollum fossile* (Squinabol), *Stichomitra communis* Squinabol, *S. magna* Squinabol, *Torculum coronatum* (Squinabol), *Tubilustrium guttaeformis* (Bragina), *T. transmontanum* O'Dogherty, *Xitus asymbatos* (Foreman), *X. spicularius* (Aliev), and *X. spineus* Pessagno. The majority of these species are characteristic of the Middle–Upper Cenomanian of northern Turkey and the Cenomanian–Lower Turonian of Italy and Spain. Some species (*Pseudodictyomitra lodogaensis* and *Torculum coronatum*) found in Beds with *Praeconocaryomma universa–Dictyomitra densicostata* are known from considerably older deposits (Albian–Cenomanian) of Italy and Spain (O'Dogherty, 1994).

Thus, in the Crimean Mountains, we can distinguish several Upper Cretaceous biostratigraphic units that correlate well with the coeval zones of the Mediterranean. The circumtropical *Alievium superbum* Zone (Pessagno, 1976; O'Dogherty, 1994; Salvini and Marcucci Passerini, 1998; Khan *et al.*, 1999) has been recognized in the Crimean sections. The index species of the Mediterranean zone of *Dactyliosphaera silviae* (O'Dogherty, 1994) has not been found in the Crimea despite the similarity in the taxonomic composition of the coeval assemblages.

The Cenomanian–Turonian assemblages of the Crimean Mountains (table) formed in considerably shallower water environments than those of Italy and Spain. Nevertheless, nearly 95% of the Crimean species are known from the Mediterranean (Erbacher, 1994; O'Dogherty, 1994; Pignotti, 1994; Salvini and Marcucci Passerini, 1998) and the remaining species, unknown from the Mediterranean, occur in the Cenomanian–Turonian assemblages of California (Pessagno, 1976), except for the two new Early Turonian species that are described below. O'Dogherty (1994, pl. 66, figs. 1–8) provided a photograph of one of these species (*Paronaella spica* sp. nov.), but it was incorrectly identified as *Patulibracchium grapevinensis* Pessagno. The Early Turonian assemblages show the greatest degree of taxonomic similarity to the Italian and Spanish assemblages (96% of species in common), thus representing almost the entire taxonomic diversity of the coeval Mediterranean assemblages.

Therefore, the Upper Cretaceous radiolarian zones can usually be traced throughout the Mediterranean belt from the axial zones of predominantly deep-water marine deposits, including oceanic sediments, to the peripheral areas of shelf facies, such as the Crimea. Certain difficulties arise from inadequate description of some assemblages, incomplete knowledge of the stratigraphic ranges of many taxa, and, probably, frequently inappropriate choices of index species. The difficulties can be resolved in the course of further investigations. It is evident that radiolarians have very considerable potential in the refined Upper Cretaceous biostratigraphy.

CHAPTER 3. SYSTEMATIC PALEONTOLOGY

This paper presents the first comprehensive study of radiolarian taxa in the Middle–Upper Cenomanian of northern Turkey and Upper Cenomanian–Lower Turonian of the Crimean Mountains. The radiolarian assem-

blages of these regions comprise 193 species belonging to 77 genera, 28 families, and 4 orders. The specimens are shown in 41 plates. The study emends the diagnoses of 5 genera and 28 species and extends the stratigraphic and geographic ranges of several tens of species and several genera, including one genus and three species that the author described previously. One new genus and 36 new species are described here for the first time. Diagnoses were given only for the species described and emended herein and for the genera that include these species. The specimens are measured in μm.

CLASS RADIOLARIA MÜLLER, 1855

SUBCLASS EURADIOLARIA LAMEERE, 1931

Superorder Polycystina Ehrenberg, 1838

Order Nassellaria Haeckel, 1887

Family Rotaformidae Pessagno, 1970

Genus *Saturniforma* Pessagno, 1970

Saturniforma peregrina Pessagno, 1970

Plate 1, figs. 1 and 2

Saturniforma peregrina: Pessagno, 1970, p. 20, pl. 6, figs. 3–5.

Holotype. University of Texas at Dallas, Pessagno's collection (USNM-Pessagno), no. 165496; California coast, Great Valley sequence, Locality NSF 350, Fiske Creek Formation; Upper Cretaceous, Cenomanian (Pessagno, 1970, pl. 6, fig. 3).

Occurrence. Cenomanian of California; Lower–Middle Cenomanian of northern Turkey.

Material. Nine specimens.

Genus *Rotaforma* Pessagno, 1970

Rotaforma hessi Pessagno, 1970

Plate 1, fig. 4

Rotaforma hessi: Pessagno, 1970, p. 16, pl. 3, figs. 4–6; pl. 4, figs. 1 and 2.

Holotype. USNM-Pessagno, no. 165478; California coast, Great Valley sequence, Locality NSF 350, Fiske Creek Formation; Upper Cretaceous, Cenomanian (Pessagno, 1970, pl. 3, figs. 4, 5).

Occurrence. Cenomanian of Californian; northern Turkey, Ürküt section, Lower–Middle Cenomanian.

Material. Eight specimens.

Family Neosciadiocapsidae Pessagno, 1969

Genus *Petasiforma* Pessagno, 1969, emend. herein

Petasiforma: Pessagno, 1969a, p. 411.

Type species. *Petasiforma foremanae* Pessagno, 1969; Cenomanian, Fiske Creek Formation, Antelope Shale Beds; California.

Diagnosis. Shell two-chambered, hat-shaped. Cephalis usually subspherical, non-perforate, without apical horn. Large sternal pore with tubular extension. Cephalic elements characteristic of the family. Thorax conical in proximal part, then flaring to form thoracic fringe distally. One or several well-developed concentric ridges occurring occasionally in the middle of thorax. Circular thoracic pores form transverse rows. Pores gradually increase in size from proximal to distal part up to thoracic fringe and slightly decrease toward margins of post-thoracic fringe.

Species composition. *P. foremanae* Pessagno, 1969; *P. glascockensis* Pessagno, 1969; *P. tavridae* sp. nov. Cretaceous, Tethys, Pacific.

Comparison. *Petasiforma* differs from *Neosciadiocapsa* Pessagno, 1969 in the absence of an apical horn.

Petasiforma foremanae Pessagno, 1969

Plate 1, figs. 5, 9, and 10

Petasiforma foremanae: Pessagno, 1969a, p. 411, pl. 23, figs. 6–10; Erbacher, 1994, pl. 10, fig. 8.

Sciadiocapsa speciosa: O'Dogherty, 1994, p. 229, pl. 38, fig. 19.

Holotype. USNM-Pessagno, no. 164216; California coast, Great Valley sequence, Locality NSF 350, Fiske Creek Formation, Antelope Shale Beds; Upper Cretaceous, Cenomanian (Pessagno, 1969a, pl. 23, fig. 8).

Occurrence. Cenomanian of California; Middle–Upper Cenomanian of Turkey; Turonian of the Crimean Mountains.

Material. Several tens of specimens.

Petasiforma glascockensis Pessagno, 1969

Plate 1, fig. 3; Plate 33, figs. 1–3.

Petasiforma glascockensis: Pessagno, 1969a, p. 412; pl. 23, figs. 1–5; pl. 24, figs. 1 and 2; 1976, pl. 2, figs. 2 and 3; Erbacher, 1994, pl. 10, figs. 9–11.

Sciadiocapsa speciosa: O'Dogherty, 1994, pl. 38, figs. 12 and 15.

Holotype. USNM-Pessagno, no. 164208; California coast, Great-Valley sequence, Locality NSF 350, Fiske Creek Formation; Upper Cretaceous, Cenomanian (Pessagno, 1969a, pl. 23, figs. 1–3).

Explanation of Plate 1

Figs. 1 and 2. *Saturniforma peregrina* Pessagno, 1970: (1) GIN, no. 4871/1, ×120; (2) GIN, no. 4871/2, ×200.

Fig. 3. *Petasiforma glascockensis* Pessagno, 1969, GIN, no. 4871/3, ×140.

Fig. 4. *Rotaforma hessi* Pessagno, 1970, GIN, no. 4871/4, ×180.

Figs. 5, 9, and 10. *Petasiforma foremanae* Pessagno, 1969: (5) GIN, no. 4871/5, ×200; (9) GIN, no. 4871/6, ×250; and (10) GIN, no. 4871/7, ×170.

Fig. 6. *Lipmanium sacramentoensis* Pessagno, 1969, GIN, no. 4871/8, ×300.

Figs. 7 and 8. *Microsciadiocapsa monticelloensis* Pessagno, 1969: (7) GIN, no. 4871/9, ×175, and (8) GIN, no. 4871/10, ×160.

Figs. 1–6, and 8. From the Ürküt section, sample 52; Figs. 7, 9, and 10. From the Tomalar section, sample 83.

Plate 1

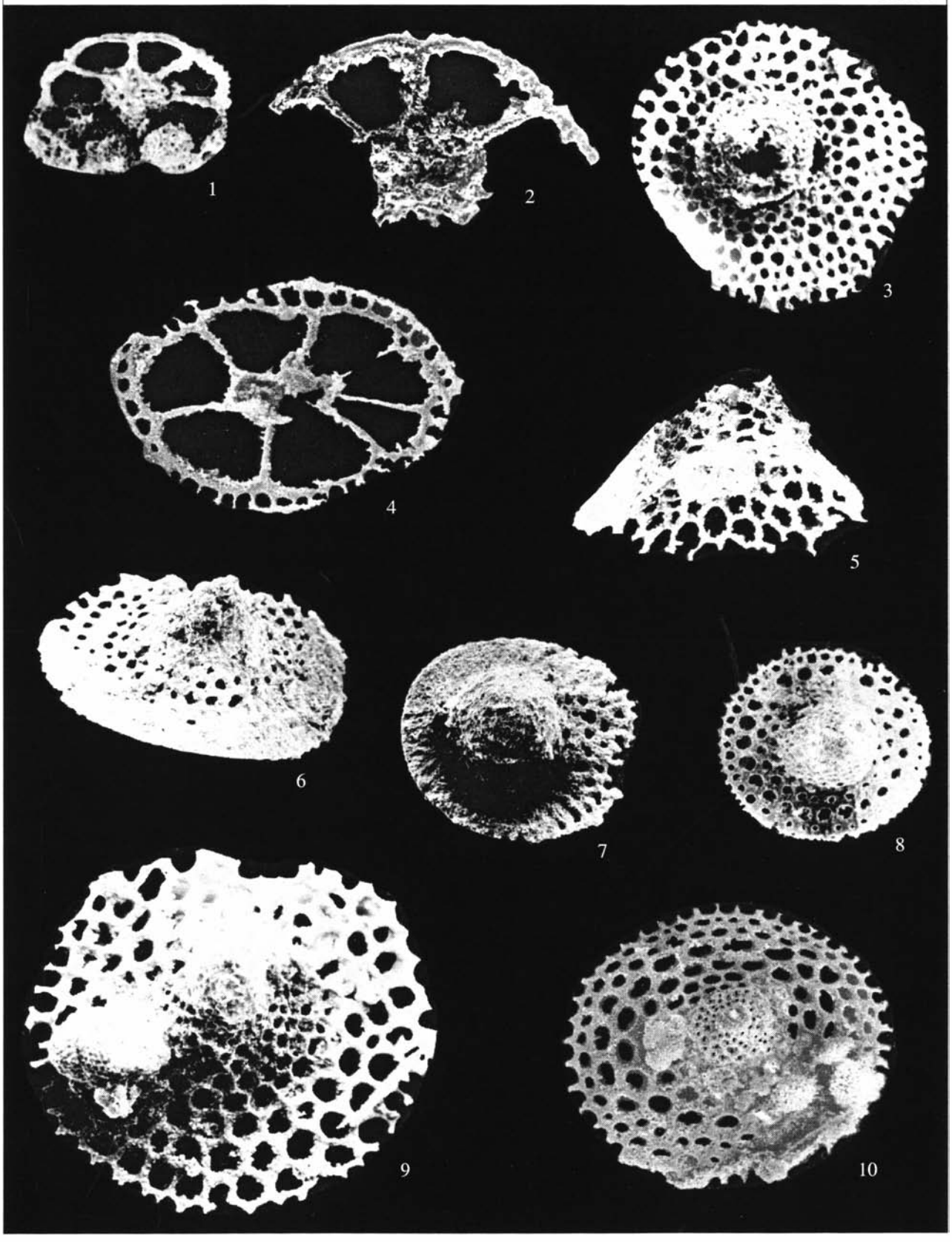

Comparison. *P. glascockensis* differs from *P. foremanae* Pessagno, 1969 in the smaller cephalis and concentric ridges bordering the thorax and post-thoracic fringe.

Occurrence. Cenomanian of California; Upper Albian–Lower Cenomanian of Italy and Spain; Upper Cenomanian of northern Turkey; Lower Turonian of the Crimean Mountains.

Material. Twenty specimens.

Petasiforma tavridae Bragina, sp. nov.

Plate 33, fig. 4

Neosciadiocapsa ex gr. *N. diabloensis*: Schaaf, 1981, pl. 25, figs. 4a and 4b; Vishnevskaya, 2001, pl. 122; figs. 27–29.

Etymology. From Tavrida, the old name of the Crimea.

Holotype. Geological Institute of the Russian Academy of Sciences (GIN), no. 4870/35; Crimean Mountains, Sel'-Bukhra section; Upper Cretaceous, Lower Turonian.

Description. The shell is small, cap-shaped. The cephalis is hemispherical, without an apical horn, pierced with randomly arranged, widely spaced pores. The cephalic wall is not usually pierced through. The thorax is sharply conical and slightly higher than the cephalis . At the transition from the thorax to the post-thoracic fringe there is a distinct constriction. The thoracic pores are commonly pierced through, arranged in a pentagonal–hexagonal pattern, and spaced closer than on the cephalis. The middle part of the post-thoracic fringe bears a ridge that is unevenly developed across the shell. The ridge divides the fringe into the proximal, sharply conical and the distal, broadly opened parts. The pores of the post-thoracic fringe are circular in cross section, arranged in a hexagonal pattern, and increase 1.5 times in size toward the distal part. The spaces between neighboring pores are equal to the pore diameter at the base and about half of the pore diameter in the distal part of the thoracic fringe. The post-thoracic fringe is slightly extended to the aperture on the opposite sides of the cephalothorax. A small portion of the post-thoracic fringe between these extended parts is arched slightly toward the aperture.

Measurements. Shell diameter, 180; cephalis diameter, 30.

Comparison. *P. tavridae* differs from *P. glascockensis* Pessagno, 1969 in having a single unevenly developed ridge and post-thoracic fringe of lesser diameter.

Material. Four complete and five fragmental specimens.

Genus *Lipmanium* Pessagno, 1969

Lipmanium sacramentoensis Pessagno, 1969

Plate 1, fig. 6

Lipmanium sacramentoensis: Pessagno, 1969a, p. 402, pl. 26, figs. 4–12.

Holotype. USNM-Pessagno, no. 164224; California coast, Great Valley sequence, Locality NSF 350, Fiske Creek Formation, Antelope Shale Beds; Upper Cretaceous, Cenomanian (Pessagno, 1969a, pl. 26, figs. 4–6).

Occurrence. Cenomanian of California; Middle–Upper Cenomanian of northern Turkey.

Material. Twelve specimens.

Genus *Microsciadiocapsa* Pessagno, 1969, emend. herein

Microsciadiocapsa: Pessagno, 1969a, p. 403.

Type species. *Microsciadiocapsa monticelloensis* Pessagno, 1969; Middle Turonian–Coniacian, Yolo Formation, California.

Diagnosis. Shell two-chambered, cap-shaped. Cephalis subspherical, with smooth and nonperforated outer surface. Short apical horn with two to four radial apical ridges at the base. Apical pores between ridges. Sternal pore well developed. Cephalic structure typical of the family. Conical thorax expands proximally to form thoracic fringe nearly orthogonal to cephalothorax. Thoracic pores usually circular. Some species bear surface costae stretching from proximal to distal part of thorax into thoracic fringe. Three to six longitudinal rows of subquadrate or rectangular pores between adjacent costae. Velum flat, completely closing aperture, and bordered with thin equatorial ridge, round in cross section.

Species composition. *M. berryessaensis* Pessagno, 1969; *M. cortinaensis* Pessagno, 1969; *M. lipmanae* Pessagno, 1969; *M. madisonae* Pessagno, 1969; *M. monticelloensis* Pessagno, 1969; *M. radiata* Pessagno, 1969; and *M. sutterensis* Pessagno, 1969; Cretaceous, Pacific, Tethys.

Comparison. The species of *Microsciadiocapsa* differ from those of *Neosciadiocapsa* Pessagno, 1969 in (1) the smaller apical horn; (2) the cephalothorax smaller in size than the thoracic fringe; and (3) the presence of costae in some species.

Microsciadiocapsa monticelloensis Pessagno, 1969

Plate 1, figs. 7 and 8

Microsciadiocapsa monticelloensis: Pessagno, 1969a, p. 407, pl. 32, figs. 3–9.

Holotype. USNM-Pessagno, no. 164243; California coast, Great Valley sequence, Locality NSF 350, Yolo Formation; Upper Cretaceous, Middle Turonian–Coniacian (Pessagno, 1969a, pl. 32, figs. 2–5).

Occurrence. Middle Turonian–Coniacian of California; Middle–Upper Cenomanian of northern Turkey.

Material. Six specimens.

Family Ultranaporidae Pessagno, 1977

Genus *Ultranapora* Pessagno, 1977

Ultranapora: Pessagno, 1977, p. 38.

Type species. *Ultranapora durhami* Pessagno, 1977; Upper Albian, Locality NSF 884, Great Valley sequence, California.

Diagnosis. Shell typical of family: shaped like conical helmet. Apical horn massive, porous at base, with well-developed vertical spine tube.

Species composition. The type species *U. durhami* Pessagno, 1977; *U. urkutae* sp. nov., and about ten more species; Cretaceous, common in the Atlantic and Tethys.

Comparison. *Ultranapora* differs from *Napora* Pessagno, 1977 in having a massive apical horn with basal porosity and tube of the vertical spine.

Ultranapora durhami Pessagno, 1977

Plate 2, fig. 7

Ultranapora durhami: Pessagno, 1977, p. 39, pl. 5, figs. 1, 3, 13, and 14; Thurow, 1988, p. 402, pl. 5, fig. 4; O'Dogherty, 1994, p. 242, pl. 42.

Holotype. USNM-Pessagno, no. 2422767; California coast, Great Valley sequence, Locality NSF 884, Lower Cretaceous, Upper Albian (Pessagno, 1977, pl. 5, figs. 1, 3, 13).

Occurrence. Upper Albian of California; Upper Cenomanian of northern Turkey.

Material. More than ten specimens.

Ultranapora praespinifera Pessagno, 1977

Plate 2, figs. 1, 3–6

Ultranapora praespinifera: Pessagno, 1977, p. 39, pl. 5, figs. 4, 9, and 10.

Holotype. USNM-Pessagno, no. 2422765; California coast, Great Valley sequence, Locality NSF 860, Lower Cretaceous, Upper Albian (Pessagno, 1977, pl. 5, fig. 8).

Occurrence. Upper Albian of California; Middle–Upper Cenomanian of northern Turkey.

Material. More than ten specimens.

Ultranapora spinifera Pessagno, 1977

Plate 2, fig. 2

Ultranapora spinifera: Pessagno, 1977, p. 39, pl. 5, figs. 5, 11, and 12.

Holotype. USNM-Pessagno, no. 242746; California coast, Great Valley sequence, Locality NSF 860, Lower Cretaceous, Upper Albian (Pessagno, 1977, pl. 5, figs. 11, 12).

Occurrence. Upper Albian of California; Middle–Upper Cenomanian of northern Turkey.

Material. Six specimens.

Ultranapora urkutae Bragina, sp. nov.

Plate 2, fig. 8

Etymology. From the Ürküt section in Turkey.

Holotype. GIN, no. 4871/18; northern Turkey, Tomalar Formation, Ürküt section, Upper Cretaceous, Middle Cenomanian.

Description. The shell is small, two-chambered, with three feet. The cephalis is sharply conical, with several (two to four) poorly developed ridges that wind from the base to the top of the cephalis. The cephalis top is reinforced with a very thick apical horn. The diameter of the horn base is equal to that of the cephalis top. The apical horn is comb-shaped, predominantly massive, with ridges and deep longitudinal grooves. In the distal part, the horn sharply narrows, loses its ridges, and becomes round in cross section. Its length is twice the height of the cephalic chamber. The thorax is barrel-shaped and twice as wide and high as the cephalis. The thoracic pores are large and form a pentagonal to hexagonal patterns. The interspaces between the pores are pentagonal to heptagonal and bear expanded spines and ridges, which partly overlap the pores. Three feet start from the proximal part of the thorax and are connected with the cephalic spicular spines—dorsal (D) and two main lateral (Lr, Ll). The feet are not connected to the distal part of the thorax, are aligned with the main axis of the test in the opposite direction to the cephalothorax and shaped like crescents that are directed to each other on the distal edge.

Measurements. Shell length, 100; foot length, 70; and apical horn length, 70.

Comparison. The new species differs from *U. durhami* Pessagno, 1977 in the thick comb-shaped apical horn, ribbed feet, and sharply conical cephalis.

Occurrence. Middle–Upper Cenomanian of Turkey, Ürküt section.

Material. Seven specimens.

Genus *Rhopalosyringium* Campbell et Clark, 1944

Rhopalosyringium euganeum (Squinabol, 1903)

Plate 3, figs. 1–4; Plate 34, figs. 3 and 4

Pterocorys euganea: Squinabol, 1903, p. 134, pl. 10, fig. 25.

Rhopalosyringium sp. A: Thurow and Kuhnt, 1986, text-fig. 9.12; Erbacher, 1994, pl. 9, fig. 6.

Rhopalosyringium sp.: Erbacher, 1994, pl. 9, fig. 6.

Rhopalosyringium euganeum: O'Dogherty, 1994, p. 162, pl. 22, figs. 7–13.

Holotype. Northern Italy, southern Venetian Alps, Colli Euganei, Teolo Series; upper Lower Cretaceous–lower Upper Cretaceous, Upper Albian–Turonian (Squinabol, 1903, pl. 10, fig. 25).

Comparison. *R. euganeum* differs from *R. elegans* (Squinabol, 1903) in having three long three-bladed spines on the thorax, while *R. elegans* has short spines which are round in cross section.

Occurrence. Middle Albian–Lower Turonian of Italy and Spain; Upper Cenomanian of northern Turkey; Upper Cenomanian–Lower Turonian of the Crimean Mountains.

Material. More than 50 specimens.

Rhopalosyringium magnificum Campbell et Clark, 1944

Plate 4, figs. 1 and 2

Rhopalosyringium magnificum: Campbell and Clark, 1944, p. 30, pl. 7, figs. 16 and 17.

Plate 2

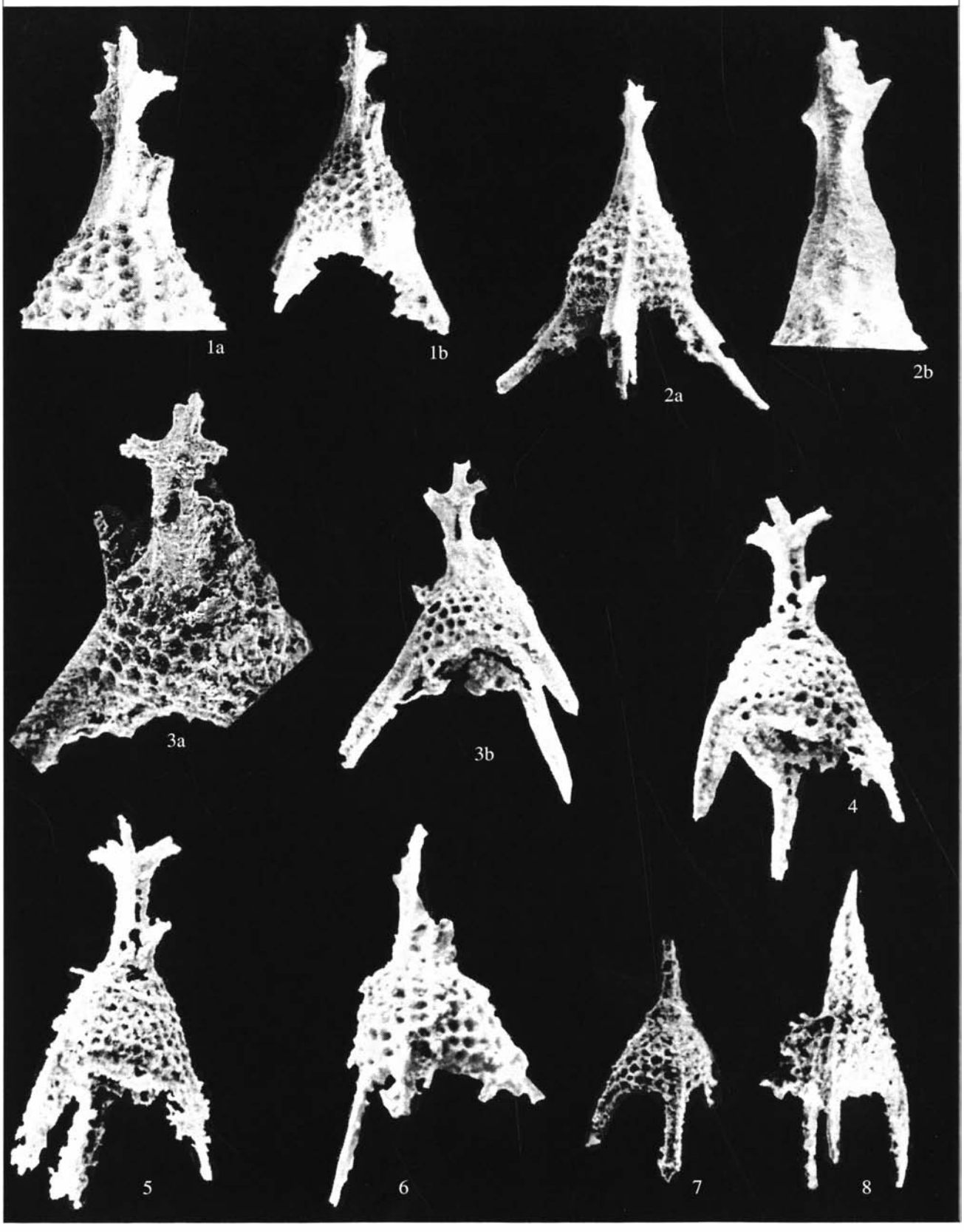

Holotype. The United States National Museum of Natural History (USNM), no. 34529; California, Teslo County, Campanian (Campbell and Clark, 1944, pl. 7, figs. 16, 17).

Occurrence. Upper Cretaceous of California, Middle–Upper Cenomanian of Turkey.

Material. More than 20 specimens.

Rhopalosyringium majuroensis Schaaf, 1981

Plate 3, figs. 7–10

Rhopalosyringium majuroensis: Schaaf, 1981, p. 437, pl. 6, figs. 2 and 3; pl. 23, fig. 5; Salvini and Marcucci Passerini, 1998, fig. 6.p.

Holotype. Institute of Geology, Strasbourg, France, no. 62-465A-29-1, 43–44 cm; Hess Rise, borehole 465A; Lower Cretaceous, Albian (Schaaf, 1981, pl. 23, fig. 5).

Occurrence. Albian of the Hess Rise; Middle–Upper Cenomanian of northern Turkey.

Material. More than 20 specimens.

Rhopalosyringium kleinum Empson-Morin, 1981

Plate 3, figs. 5 and 6; Plate 4, figs. 3 and 4

Rhopalosyringium sp. aff. *R. magnificum*: Petrushevskaya and Kozlova, 1972, p. 536, pl. 7, fig. 13.

Rhopalosyringium kleinum: Empson-Morin, 1981, p. 265, pl. 8, figs. 2A-3.

Rhopalosyringium aff. *R. kleinum*: Urquhart and Banner, 1994, fig. 4.a.

Holotype. USNM, no. 305344; Mid-Pacific Mountains, DSDP Leg 32, borehole 313; Upper Cretaceous, Campanian (Empson-Morin, 1981, pl. 8, fig. 2).

Occurrence. Upper Cretaceous of the Atlantic Ocean, Campanian of Cyprus; Middle–Upper Cenomanian of northern Turkey.

Material. More than ten specimens.

Family Eucyrtidiidae Ehrenberg, 1847

Genus *Distylocapsa* Squinabol, 1904

Distylocapsa: Squinabol, 1904, p. 225; O'Dogherty, 1994, p. 185.

Type species. *Distylocapsa nova* Squinabol, 1904; upper Lower Cretaceous–lower Upper Cretaceous, Middle Albian–Cenomanian; "red-colored" part of the Scaglia Bianca Formation, southern Venetian Alps, northern Italy.

Diagnosis. Shell fusiform, multichambered, commonly consisting of four chambers. Apical horn at the extreme top of cephalic chamber. Outer constrictions poorly developed. Shell surface covered with small spines. Aperture commonly terminated in tube with spine.

Species composition. *D. micropora* (Squinabol, 1903); *D. nova* Squinabol, 1904; *D. squama* O'Dogherty, 1994; and *D. veneta* (Squinabol, 1904); Middle Albian–Turonian of the Tethys.

Distylocapsa veneta (Squinabol, 1904), emend. herein

Plate 4, figs. 5, 7, and 8; Plate 32, fig. 7; Plate 34, fig. 5

Eusyringium venetum: Squinabol, 1904, p. 235, pl. 10, fig. 10.

? *Stichomitra* ex gr. *indonesiensis*: Dumitrica, 1975, text-fig. 2.43.

Stichomitra foraminosa: Taketani, 1982, p. 55, pl. 3, figs. 5a, 5b, 6a, and 6b.

Stichomitra sp.: Tumanda, 1989, pl. 9, fig. 13.

Distylocapsa veneta: O'Dogherty, 1994, p. 186, pl. 28, figs. 10–15.

Holotype. Northern Italy, southern Venetian Alps, "red-colored" part of the Scaglia Bianca Formation; upper Lower Cretaceous–lower Upper Cretaceous, Middle Albian–Cenomanian (Squinabol, 1904, pl. 10, fig. 10).

Description. The shell is widely fusiform and commonly comprises four or five chambers. From the first chamber onwards, the shell rapidly increases in width and, gradually, in height. The last chamber is very narrow. The cephalis is small, subspherical, with a small sharp apical horn. The shell wall is thick, with closely spaced pores. Some larger specimens show a poorly defined constriction between the post-cephalis chambers, but smaller specimens show no constrictions. The interspaces between pores look like rounded polygons and are arranged in a hexagonal and pentagonal patterns. The shell bears a rather short terminal spine.

Measurements. Shell length, 285–190; shell width, 120–100.

Comparison. *D. veneta* differs from *D. nova* Squinabol, 1904 in the absence of a long apertural tube and in the wider shell.

Occurrence. Middle Albian–Cenomanian of Italy, Romania, and Japan; Middle Turonian of northern Turkey; Lower Turonian of the Crimean Mountains.

Material. About 50 specimens.

Distylocapsa squama O'Dogherty, 1994, emend. herein

Plate 4, fig. 6

Distylocapsa squama: O'Dogherty, 1994, p. 188, pl. 28, figs. 16–21; Salvini and Marcucci Passerini, 1998, text-fig. 9s.

Explanation of Plate 2

Figs. 1, 3–6. *Ultranapora praespinifera* Pessagno, 1977: (1) GIN, no. 4871/11: (a) cephalis and apical horn, ×350, (b) general view, ×200; (3) GIN, no. 4871/12: (a) cephalis and apical horn, ×350; (b) general view, ×150; (4) GIN, no. 4871/13, ×150; (5) GIN, no. 4871/14, ×250; (6) GIN, no. 4871/15, ×200.

Fig. 2. *Ultranapora spinifera* Pessagno, 1977, GIN, no. 4871/16, (a) general view, ×150, and (b) cephalis and apical horn, ×300.

Fig. 7. *Ultranapora durhami* Pessagno, 1977, GIN, no. 4871/17, ×150.

Fig. 8. *Ultranapora urkutae* sp. nov., ×200, holotype GIN, no. 4871/18.

All specimens come from the Ürküt section.

Plate 3

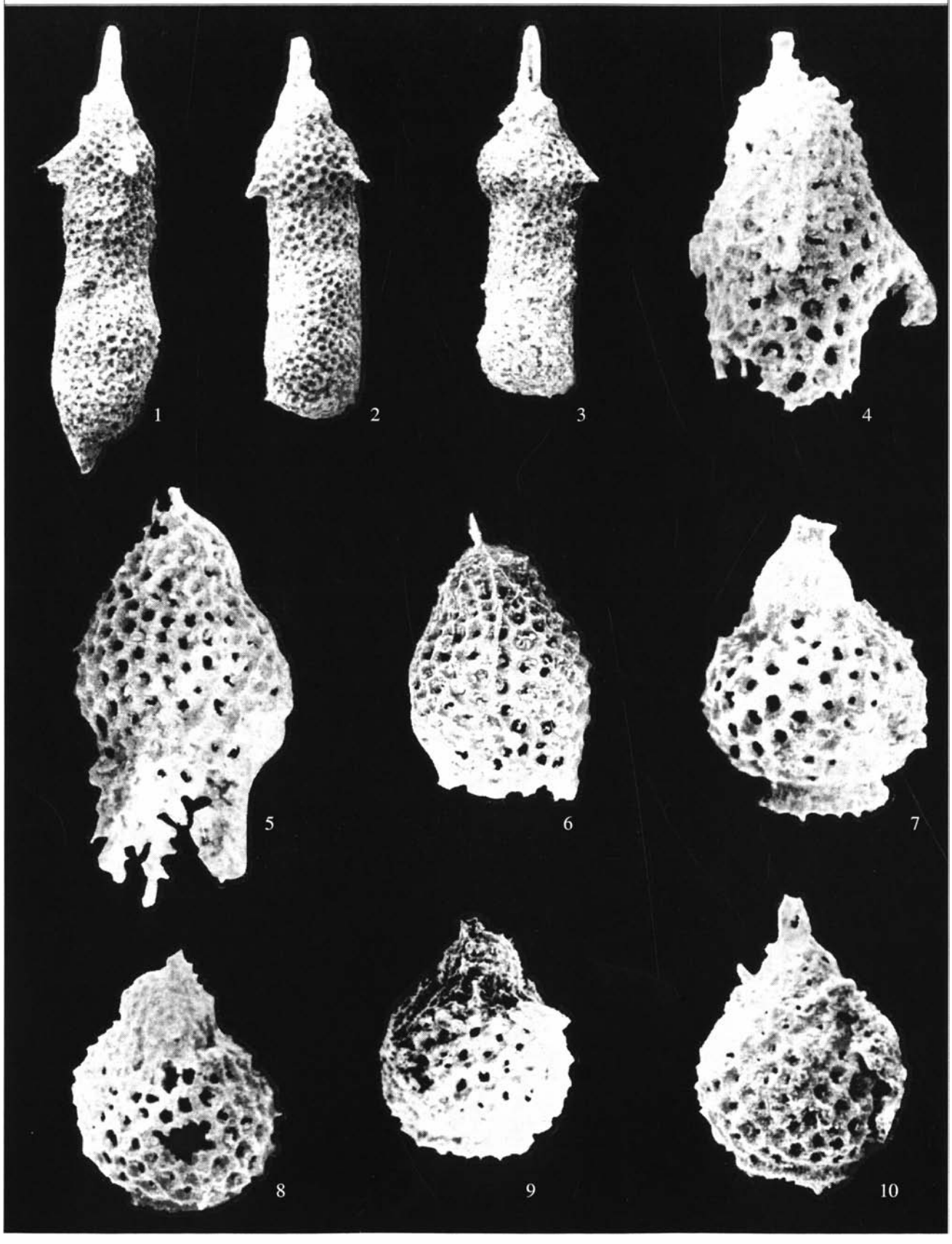

Holotype. Switzerland, University of Lausanne (UL), no. 6960; central Italy, Umbria-Marche Apennines, Locality Asv-5-43; Upper Cretaceous, Lower Turonian (O'Dogherty, 1994, pl. 28, fig. 16).

Description. The shell is fusiform and consists of four or, less frequently, five chambers. The apical horn is short, markedly tapering, and almost circular in cross section. The shell is covered with closely spaced, uniform-sized circular pores that are surrounded by interspaces arranged in hexagonal and pentagonal patterns. The surface of the shell varies from smooth to very spiny. The shell gradually thickens over a length of two-thirds of the distance between the cephalic chamber and the first post-abdominal chambers. Distally it narrows sharply to form a short terminal tube tapering in a variably developed massive spine that has three or four blades at the base and is rounded at the end.

Measurements. Shell length, 325–250; maximal shell width, 140–100; length of distal spine, 70–40.

Comparison. *D. squama* differs from *Distylocapsa veneta* (Squinabol, 1904) in having distinct small spines throughout the shell surface.

Occurrence. Upper Albian–Lower Turonian of Italy and Spain; Upper Cenomanian of northern Turkey; Lower Turonian of the Crimean Mountains.

Material. About 50 specimens.

Family Xitidae Pessagno, 1977

Genus *Torculum* O'Dogherty, 1994

Torculum coronatum (Squinabol, 1904)

Plate 4, figs. 9–12

Theoconus coronatus: Squinabol, 1904, p. 220, pl. 8, fig. 3; Kuhnt *et al.*, 1986, pl. 7, fig. Q; Thurow, 1988, p. 407, pl. 4, figs. 2–4.

Stichomitra (?) zamoraensis: Pessagno, 1976, p. 54, pl. 3, figs. 7–9; Pessagno, 1977, p. 53, pl. 9, figs. 5 and 16.

Novixitus variabilis: Nakaseko and Nishimura, 1981, p. 155, pl. 10, fig.7.

Novixitus (?) sp. A: Empson-Morin, 1984, pl. 2, fig. 11.

Novixitus (?) sp. B: Empson-Morin, 1984, pl. 2, fig. 12.

Novixitus (?) sp. C: Empson-Morin, 1984, pl. 2, fig. 13.

Novixitus sp. B: Urquhart and Banner, 1994, fig. 4.

Spongocapsula (?) zamoraensis: Schaaf, 1981, p. 438, pl. 24, figs. 2a and 2b; Taketani, 1982, p. 62, pl. 5, figs. 6a and 6b; pl. 12, figs. 12 and 13; Bak, 1993, p. 3, fig. 10; Kazintsova, 2002, pl. 2, fig. 9.

Spongocapsula coronata: Jud, 1994, p. 107, pl. 20, fig. 18.

Torculum coronatum: O'Dogherty, 1994, p. 133, pl. 12, figs. 27 and 28; pl. 14, figs. 4–29; Bragin *et al.*, 2000, figs. 4F–4I.

? *Torculum coronatum*: O'Dogherty, 1994, p. 133, pl. 14, figs. 1–3.

Theoconus spp. group: Erbacher, 1994, pl. 7, figs. 6–11; pl. 14, figs. 4 and 5.

Holotype. Northern Italy, southern Venetian Alps, "red-colored" part of the Scaglia Bianca Formation; upper Lower Cretaceous–lower Upper Cretaceous, Middle Albian–Cenomanian (Squinabol, 1904, pl. 8, fig. 3).

Remarks. This species shows considerable intraspecific variability. The shells vary widely in shape, from specimens that look like almost regular cones to those in which the middle part between the sixth and ninth chambers is strongly constricted. The shell may be broadly open toward the aperture or sacculately closed to form a slightly elongate narrow aperture. Nodes of different irregular shapes may cover either the entire shell or its minor part (the first three or four post-abdominal chambers). Nevertheless, a characteristic feature of the species is that the shell that has a distinct sharply conical proximal part (first three to five chambers) and a distal part that gradually widens.

Occurrence. Albian–Turonian, worldwide; Lower Turonian of the Crimean Mountains; Middle–Upper Cenomanian of northern Turkey.

Material. More than 20 specimens.

Genus *Phalangites* O'Dogherty, 1994

Phalangites: O'Dogherty, 1994, p. 155.

Type species. *Phalangites calamus* O'Dogherty, 1994; Upper Cretaceous, lower Cenomanian, Scaglia Bianca Formation, Umbria-Marche Apennines, central Italy.

Diagnosis. Shell consisting of four or more chambers. Apical horn usually massive. Shell usually cylindrical, slightly narrowing toward aperture. Longest specimens with closed aperture. Shell wall porous, single- or double-layered. Pores small, circular.

Species composition. *P. calamus* O'Dogherty, 1994; *P. hastatus* O'Dogherty, 1994; *P. perspicuus* (Squinabol, 1904); and *P. telum* O'Dogherty, 1994; Upper Aptian–Turonian, Tethys.

Comparison. *Phalangites* differs from *Pseudoeucyrtis* Pessagno, 1977 in having double-layered porous walls.

Phalangites hastatus O'Dogherty, 1994, emend. herein

Plate 33, figs. 9 and 10

Phalangites hastatus: O'Dogherty, 1994, p. 158, pl. 21, figs. 1–6.

Holotype. UL, no. 5820; central Italy, Umbria-Marche Apennines, Locality Asv-5-43; Upper Cretaceous, Lower Turonian (O'Dogherty, 1994, pl. 21, fig. 3).

Description. The shell is large, multicyrtoid, subcylindrical to conical, and usually consists of four to seven post-cephalic chambers. The cephalis is sharply conical and bears slitlike pores and a long stout apical

Explanation of Plate 3

Figs. 1–4. *Rhopalosyringium euganeum* (Squinabol, 1903), specimens: (1) GIN, no. 4871/19, ×200; (2) GIN, no. 4871/20, ×200; (3) GIN, no. 4871/21, ×200; (4) GIN, no. 4871/22, ×550.

Figs. 5 and 6. *Rhopalosyringium kleinum* Empson-Morin, 1981: (5) GIN, no. 4871/23; ×550, (6) GIN, no. 4871/24, ×375.

Figs. 7–10. *Rhopalosyringium majuroensis* Schaaf, 1981, specimens, ×375: (7) GIN, no. 4871/25; (8) GIN, no. 4871/26; (9) GIN, no. 4871/27; and (10) GIN, no. 4871/28.

Figs. 1–3. From the Tomalar section; Figs. 4–10. From the Ürküt section.

Plate 4

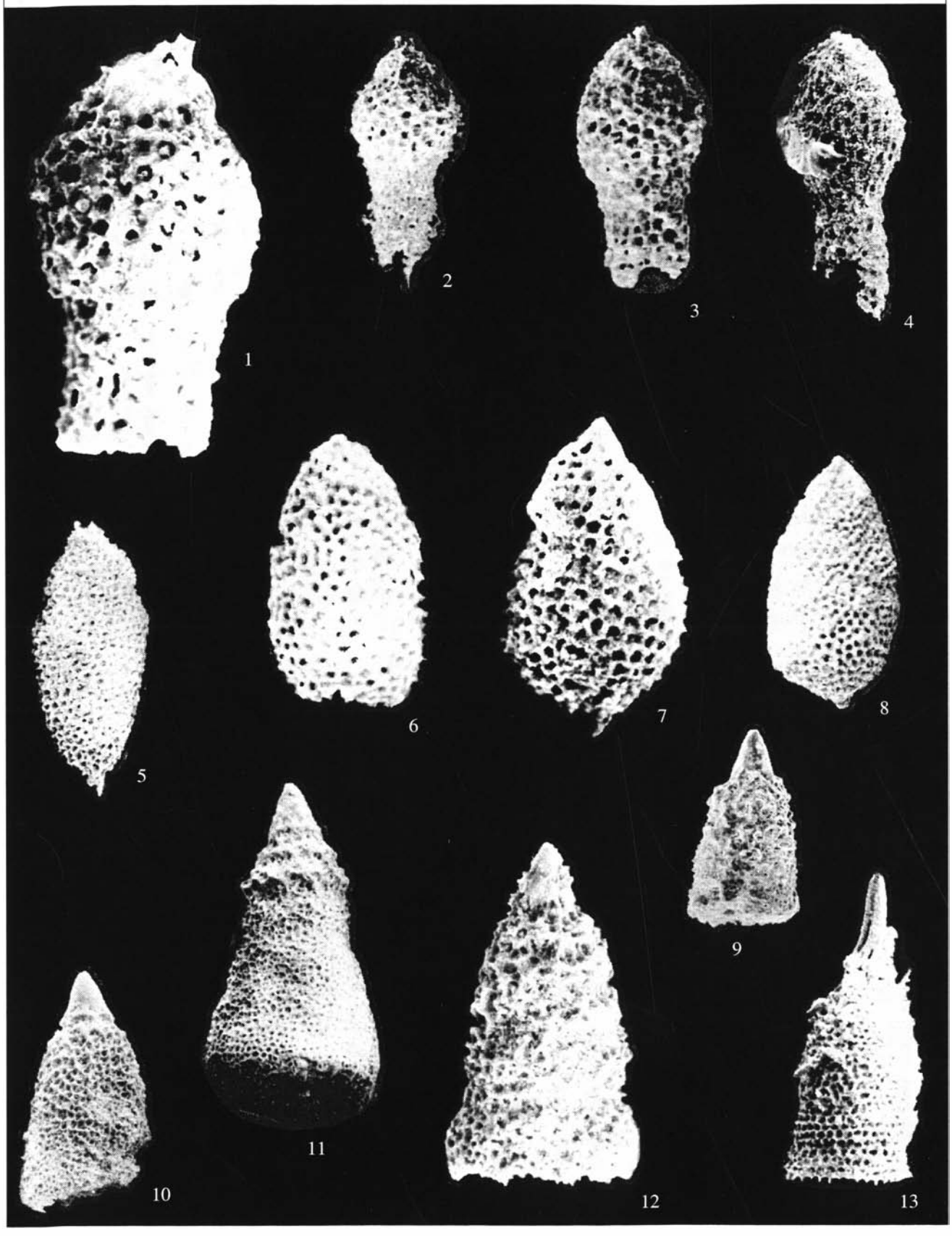

horn with prominent ribs at the base. The shell has an uneven surface covered with ridges. The shell wall is thick and consists of two lattice layers of pore frames. The inner layer consists of irregularly arranged thin rounded pore frames. The outer layer overlies the inner, with large, triangular to polygonal, occasionally irregularly arranged pore frames. The shell wall, especially in the proximal chambers, is thick and spiny. The cephalis and the base of the apical horn are usually covered by the well-developed outer lattice layer. The aperture is round and enormous.

Measurements. Shell length, 387–220; maximal shell width, 157–130; length of apical horn, 113–67.

Comparison. *Ph. hastatus* differs from *Ph. telum* O'Dogherty, 1994 in the thicker apical horn and well-defined rough-ridged shell surface.

Occurrence. Lower Turonian of Italy, Spain, and the Crimean Mountains.

Material. More than ten specimens.

Phalangites telum O'Dogherty, 1994

Plate 4, fig. 13

Phalangites telum: O'Dogherty, 1994, p. 157, pl. 20, figs. 16–23; Salvini and Marcucci Passerini, 1998, text-fig. 10.h.

Holotype. UL; central Italy, Umbria-Marche Apennines, Locality Gc-1035.10; Lower Cretaceous, Upper Albian (O'Dogherty, 1994, pl. 20, fig. 19).

Occurrence. Middle–Upper Albian of Italy and Spain; Middle–Upper Cenomanian of northern Turkey; Lower Turonian of the Crimean Mountains.

Material. More than ten specimens.

Genus *Xitus* Pessagno, 1977

Xitus: Pessagno, 1977, p. 55; O'Dogherty, 1994, p. 123.

Type species. *Xitus plenus* Pessagno, 1977; Lower Cretaceous, Upper Albian, Great Valley sequence, Locality NSF 860, California.

Diagnosis. Shell sharply conical, with apical horn. Each chamber usually with double row of small nodes. Last chambers frequently extended to form tube with large aperture, with nodes (if present) usually poorly developed.

Species composition. *Xitus plenus* Pessagno, 1977, *Xitus urkutus* sp. nov., and more than ten other species. Upper Jurassic?–Cretaceous, worldwide.

Comparison. *Xitus* differs from *Novixitus* Pessagno, 1977, in the presence of an apical horn.

Xitus asymbatos (Foreman, 1968), emend. herein

Plate 33, fig. 21

Stichomitra asymbatos: Foreman, 1968, p. 73, pl. 8, figs. 10a–10c; 1978b, p. 748, pl. 4, fig. 15; Petrushevskaya and Kozlova, 1972, p. 546, pl. 8, figs. 1–3; Dumitrica, 1975, p. 87–89, text-fig. 2, fig. 13; Taketani, 1982, p. 54, pl. 4, fig. 13; pl. 11, figs. 3 and 4.

Stichomitra asymbatos Foreman group: Riedel and Sanfilippo, 1974, p. 780, pl. 10, figs. 1–7, pl. 15, fig. 5.

? *Xitus* sp. B: Iwata and Tajika, 1986, pl. 1, fig. 12.

Xitus asymbatos: Iwata and Tajika, 1986, pl. 2, figs. 11 and 12; Kazintsova, 1993, p. 81, pl. 22, fig. 5.

Holotype. USNM, no. 158013; California, Moreno Formation, Locality 1144; Upper Cretaceous, Upper Maastrichtian (Foreman, 1968, pl. 8, figs. 10a–10c).

Description. The shell is tubercular, conical, and multichambered (7 to 11 chambers). The cephalis is relatively large, smooth, and spherical, showing no pores. It has a short stout apical horn. The thorax and subsequent chambers are barrel-shaped or truncated-conical, with the two last chambers being slightly narrower. Outer constrictions between the chambers are more or less distinct. Each chamber gradually increases in height and width. The shell wall varies in thickness. The shell surface (excluding cephalis) bears nodes that tend to form two (less frequently three) transverse rows in each chamber. Unequally developed radial and intersecting ridges extend from the top of every node. The nodes may be connected with the neighboring nodes of the same row (or the adjacent row) by ridges. The pores are small, rounded-polygonal in cross section, and arranged in pentagonal–hexagonal patterns. Both the exterior and interior surfaces of the two last chambers are usually free of nodes and have a staggered arrangement of pores. The aperture is open and has a wide tubular extension.

Measurements. Shell length, 400–200; maximal shell width, 250–80.

Comparison. *X. asymbatos* differs from *X. spicularius* (Aliev, 1965) in the large and well-developed nodes, well-developed ridges, and massive stout apical horn.

Remarks. Accuracy of specific identification is hampered by the variability of *X. asymbatos* (Foreman, 1968), which includes both specimens with and without distinct outer constrictions . In the latter case, this species can be reliably distinguished from *X. specularius*

Explanation of Plate 4

Figs. 1 and 2. *Rhopalosyringium magnificum* Campbell et Clark, 1944: (1) GIN, no. 4871/29, ×375; (2) GIN, no. 4871/30, ×200.

Figs. 3 and 4. *Rhopalosyringium kleinum* Empson-Morin, 1981: (3) GIN, no. 4871/31, ×350; (4) GIN, no. 4871/32, ×330.

Figs. 5, 7, and 8. *Distylocapsa veneta* (Squinabol, 1904), specimens: (5) GIN, no. 4871/33, ×150; (7) GIN, no. 4871/34, ×220; and (8) GIN, no. 4871/35, ×200.

Fig. 6. *Distylocapsa squama* O'Dogherty, 1994, GIN, no. 4871/36, ×200.

Figs. 9–12. *Torculum coronatum* (Squinabol, 1904), specimens: (9) GIN, no. 4871/37, ×120; (10) GIN, no. 4871/38, ×120; (11) GIN, no. 4871/39, ×150; and (12) GIN, no. 4871/40, ×200.

Fig. 13. *Phalangites telum* O'Dogherty, 1994, GIN, no. 4871/41, ×200.

All specimens come from the Ürküt section.

(Aliev, 1965) by means of well-developed xitoid nodes. Otherwise, both species have the same diagnosis.

Occurrence. Cenomanian–Maastrichtian of the world; Lower Turonian of the Crimean Mountains.

Material. More than ten specimens.

Xitus spicularius (Aliev, 1965), emend. herein

Plate 5, figs. 1–6; Plate 33, figs. 19, 20, and 22

Dictyomitra spicularia: Aliev, 1965, p. 39, pl. 6, fig. 9.

Stichomitra asymbatos: Dumitrica, 1975, text-fig. 2.13.

Xitus plenus: Pessagno, 1977, p. 55, pl. 9, figs. 15, 21, 22, and 26; pl. 12, fig. 15; Kazintsova, 1993, p. 82, pl. 5, fig. 1.

Xitus spicularius: Pessagno, 1977, p. 56, pl. 9, fig. 7; pl. 10 fig. 5; Thurow, 1988, p. 408, pl. 3, fig. 19; O'Dogherty, 1994, p. 127, pl. 11, figs. 17–31; Salvini and Marcucci Passerini, 1998, text-fig. 7.c.

Non *Xitus spicularius*: Thurow, 1988, p. 408, pl. 7, fig. 1 (= *X.* ex gr. *X. alievi* (Foreman, 1973).

Holotype. Northeastern Azerbaijan, Locality of Konagkend; Lower Cretaceous, Albian (Aliev, 1965, pl. 6, fig. 9).

Description. The shell is conical, with a rough surface, and consists of many (7 to 9) chambers. The cephalis is non-perforated, conical, and bears a short horn, usually circular in cross section. The thorax and subsequent chambers are trapezoidal. From the fourth chamber onwards, they increase rapidly in width and gradually in height. The last chamber is slightly narrower. The shell wall is quite thick. The shell surface is covered by moderate-sized nodes arranged in two transverse staggered rows on every chamber beginning from the abdomen or the first post-abdominal chamber. The upper row is usually better developed than the lower row. Occasionally, this arrangement of two rows of nodes may be disturbed, and they are not always present in every chamber. The nodes are connected by poorly defined ridges. The small rounded-polygonal pores are closely spaced and arranged in pentagonal–hexagonal patterns. The interspaces between the pores are fragile. The shell surface is rough because of abundant thin short spines located at vertices of several pores. The ridges connecting spine tips are virtually undeveloped.

Measurements. Shell length, 616–300; maximal shell width, 200–120.

Comparison. *X. spicularius* differs from *Xitus alievi* (Foreman, 1973) in (1) the conical shape of the shell, (2) well-developed short pointed apical horn, (3) less developed and occasionally irregularly spaced nodes, and (4) the absence of the change in the shell form from the broadly conical proximal part to the sharply conical middle and distal parts.

Occurrence. Albian of Azerbaijan, Italy, Spain, and Romania; Upper Albian of California; Upper Albian–Upper Turonian of southwestern Sakhalin; Middle–Upper Cenomanian of northern Turkey; Upper Cenomanian–Lower Turonian of the Crimean Mountains.

Material. More than ten specimens.

Xitus spineus Pessagno, 1977

Plate 33, fig. 23

Xitus spineus: Pessagno, 1977, p. 56, pl. 10, figs. 3, 12, 16, and 20.

Holotype. USNM-Pessagno, no. 242735; California coast, Great Valley sequence, Locality NSF 854; Lower Cretaceous, Lower Albian (Pessagno, 1977, pl. 10, figs. 2, 12, 16, 20).

Comparison. *X. spineus* differs from *X. asymbatos* (Foreman, 1968) in having a single row of nodes on the thorax and abdomen.

Occurrence. Lower Albian of California; Middle–Upper Cenomanian of northern Turkey; Lower Turonian of the Crimean Mountains.

Material. More than 20 specimens.

Xitus urkutus Bragina, sp. nov.

Plate 5, fig. 7

Etymology. From the name of the section in which the species was first found.

Holotype. GIN, no. 4871/48; northern Turkey, Tomalar Formation, Ürküt section; Upper Cretaceous, Middle Cenomanian.

Description. The shell is fusiform. The cephalis is small, broadly conical, without pores, with a very short apical horn circular in cross section. A row of oval and irregularly shaped pores separates the cephalis from the thorax. The thorax is as high as the cephalis but one-third wider. The thorax is virtually without pores and is separated from the abdomen by a row of oval pores of different sizes. The abdomen is virtually as high as the thorax and only slightly wider. The post-thoracic part of the shell is narrowly conical up to the two or three last chambers. The last chambers rapidly narrow, terminating in a narrow aperture. The post-thoracic part of the shell has small rounded-polygonal pores with polygonal and irregular pore frames. The xitoid nodes form an indistinct transverse row on the abdomen, diminishing distally to the point of disap-

Explanation of Plate 5

Figs. 1–6. *Xitus spicularius* (Aliev, 1965), specimens: (1) GIN, no. 4871/42, ×200; (2) GIN, no. 4871/43, ×175; (3) GIN, no. 4871/44, ×175; (4) GIN, no. 4871/45, ×120; (5) GIN, no. 4871/46, ×120; and (6) GIN, no. 4871/47, ×250.

Fig. 7. *Xitus urkutus* sp. nov., holotype GIN, no. 4871/48: (a) general view, ×180; and (b) cephalis and apical horn, ×550.

Figs. 8 and 9. *Novixitus costatus* sp. nov., (8) GIN, no. 4871/49, ×200; (9) holotype GIN, no. 4871/50: (a) general view, ×250, and (b) cephalic and thoracic wall, ×320.

Fig. 10. *Novixitus subtilis* sp. nov., holotype GIN, no. 4871/51, ×180.

Figs. 1 and 5. From the Tomalar section; Figs. 2–4, 6–10. From the Ürküt section.

Plate 5

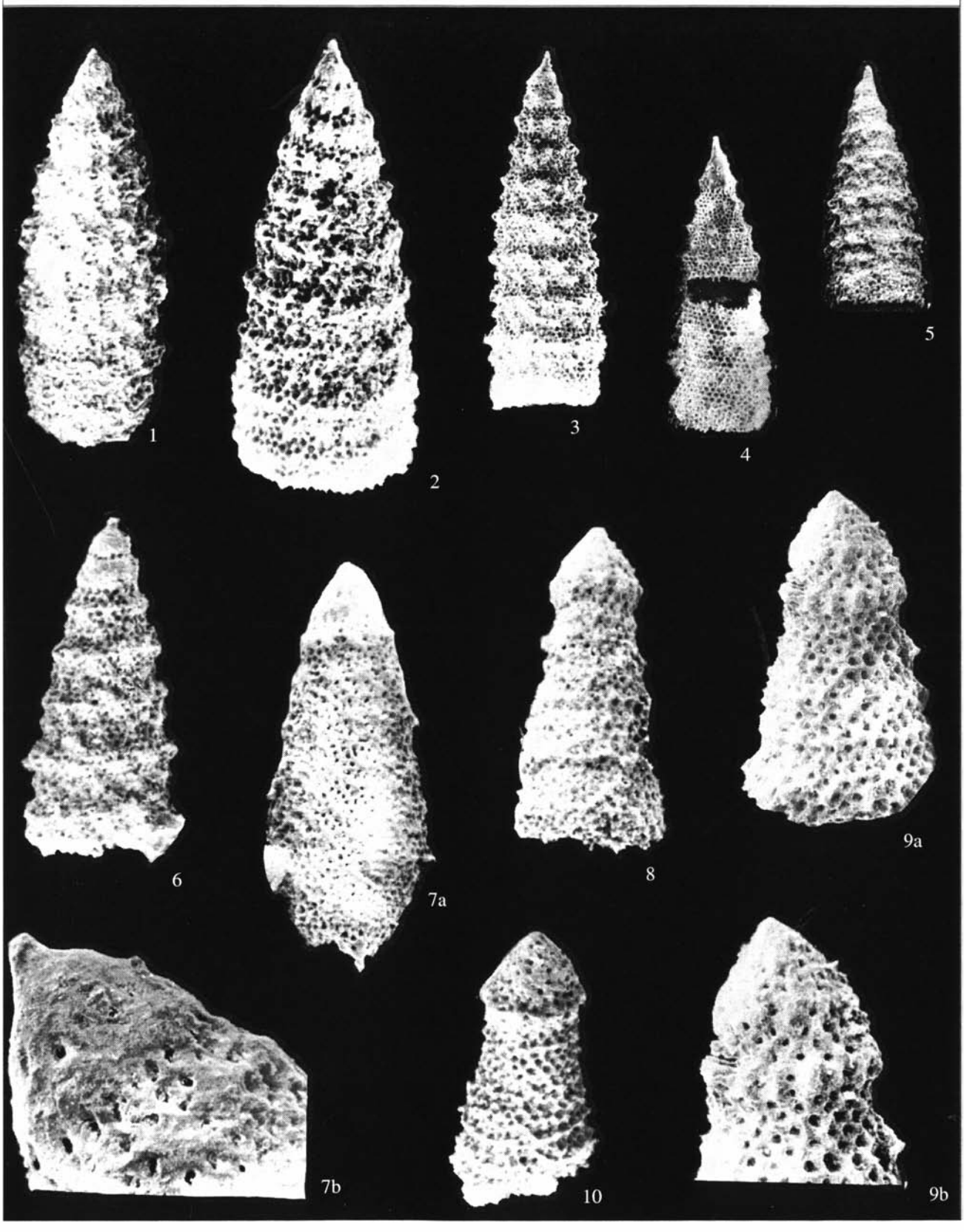

pearance. The distal part shows only rare thin ridges extending in different directions through the pore frames connecting three to five neighboring pores.

Measurements. Shell length, 150; maximal width, 60.

Comparison. *X. urkutus* differs from *X. plenus* Pessagno, 1977 in the fusiform shell and poorly developed irregular nodes.

Occurrence. Middle Cenomanian of northern Turkey, Ürküt section.

Material. Three complete and eight incomplete specimens.

Genus *Novixitus* Pessagno, 1977, emend. herein

Novixitus: Pessagno, 1977, p. 54.

Type species. *Novixitus mclaughlini* Pessagno, 1977; Upper Cretaceous, Lower Cenomanian; Locality MG 236, Franciscan Formation, California.

Diagnosis. Shell sharply conical, usually without apical horn. Cephalis without pores and separated from (usually porous) thorax by single (sometimes indistinct) row of pores. Xitoid nodes usually arranged in transverse rows. In some species some post-cephalis chambers devoid of xitoid nodes. Last post-abdominal chamber usually cylindrical and devoid of xitoid nodes. Polygonal pore frames well developed.

Species composition. *N. dengoi* Schmidt-Effing, 1980; *N. mclaughlini* Pessagno, 1977; *N. weyli* Schmidt-Effing, 1980; *N. costatus* sp. nov.; and *N. subtilis* sp. nov.; Upper Cretaceous of the Pacific, Atlantic, and Tethys oceans.

Comparison. *Novixitus* differs from representatives of *Xitus* Pessagno, 1977 in the absence of an apical horn.

Novixitus costatus Bragina, sp. nov.

Plate 5, figs. 8 and 9; Plate 34, fig. 7

Etymology. From the Latin *costatus* (costate).

Holotype. GIN, no. 4871/50; northern Turkey, Tomalar Formation, Ürküt section; Upper Cretaceous, Middle Cenomanian.

Description. The shell is narrowly conical and has a club-shaped thickening proximally. The cephalis is small, broadly conical, with a few fine, widely spaced pores. The thorax is shaped like a broad truncated cone and is connected with the cephalis without noticeable outer constrictions. The abdomen is barrel-shaped and forms, in combination with the cephalis and thorax, a club-shaped thickening. The thorax and abdomen are pierced by small, rounded to polygonal pores, with a diameter less than the distance between pores. The pore frames are polygonal (four to seven angles) and irregular in outline. The shell surface is uneven owing to variously developed spines and ridges at the vertices of several pore frames. The first one or two post-abdominal chambers are armed with massive curved ridges. The long axis of the ridges coincides with the main shell axis. The next chamber is considerably narrower, and, from this chamber on, the shell becomes narrowly conical, widening slightly toward the aperture. The narrowly conical chambers bear rounded pores and smaller, irregularly shaped ridges. The central and distal parts of the shell occasionally have a transverse row of small ridged nodes.

Measurements. Shell length, 250; maximal width, 120; maximal width of club-shaped thickening, 80.

Comparison. The new species differs from *Novixitus dengoi* Schmidt-Effing, 1980 in the club-shaped proximal part of the shell and the presence of ridges surrounding the shell under the club-shaped thickening.

Occurrence. Northern Turkey, Ürküt section, Middle Cenomanian.

Material. Four complete and ten incomplete specimens.

Novixitus dengoi Schmidt-Effing, 1980

Plate 6, figs. 2–4

Novixitus sp. *B*: Pessagno, 1977, p. 54, pl. 9, fig. 14.

Novixitus dengoi: Schmidt-Effing, 1980, p. 252, text-fig. 30; Pessagno, 1977, p. 54, pl. 9, fig. 14.

Non *Novixitus dengoi*: Erbacher, 1994, pl. 7, figs. 11 and 12 (= *Torculum* ex gr. *T. coronatus* (Squinabol, 1904)).

Non *Torculum dengoi*: O'Dogherty, 1994, p. 135, pl. 15, figs. 1–4 (= *Torculum* sp.?).

Holotype. Geological–Paleontological Institute of Münster, Abb. 30; Central America, northwestern Costa Rica, Cabo Santa Elena (cape), Rio Potrero Grande Series, locality of Capas del Sardinal; Upper Cretaceous, Cenomanian.

Explanation of Plate 6

Figs. 1, 5–8, 10, and 11. *Novixitus weyli* Schmidt-Effing, 1980, specimens: (1) GIN, no. 4871/52, ×130; (5) GIN, no. 4871/53, ×120; (6) GIN, no. 4871/54, ×130; (7) GIN, no. 4871/55, ×120; (8) GIN, no. 4871/56, ×110; (10) GIN, no. 4871/57: (*a*) wall of cephalis, thorax, and abdomen, ×200, and (*b*) general view, ×130; and (11) GIN, no. 4871/326, ×120.

Figs. 2–4. *Novixitus dengoi* Schmidt-Effing, 1980, specimens: (2) GIN, no. 4871/58, ×250; (3) GIN, no. 4871/59, ×120; and (4) GIN, no. 4871/60, ×160.

Figs. 9 and 12. *Pseudodictyomitra quasilodogaensis* sp. nov., holotype GIN, no. 4871/61: (9) general view, ×165, and (12) wall structure, ×220.

Figs. 3, 5, 8–10. From the Tomalar section; Figs. 1, 2, 4, 6, 7, and 11. From the Ürküt section.

Plate 6

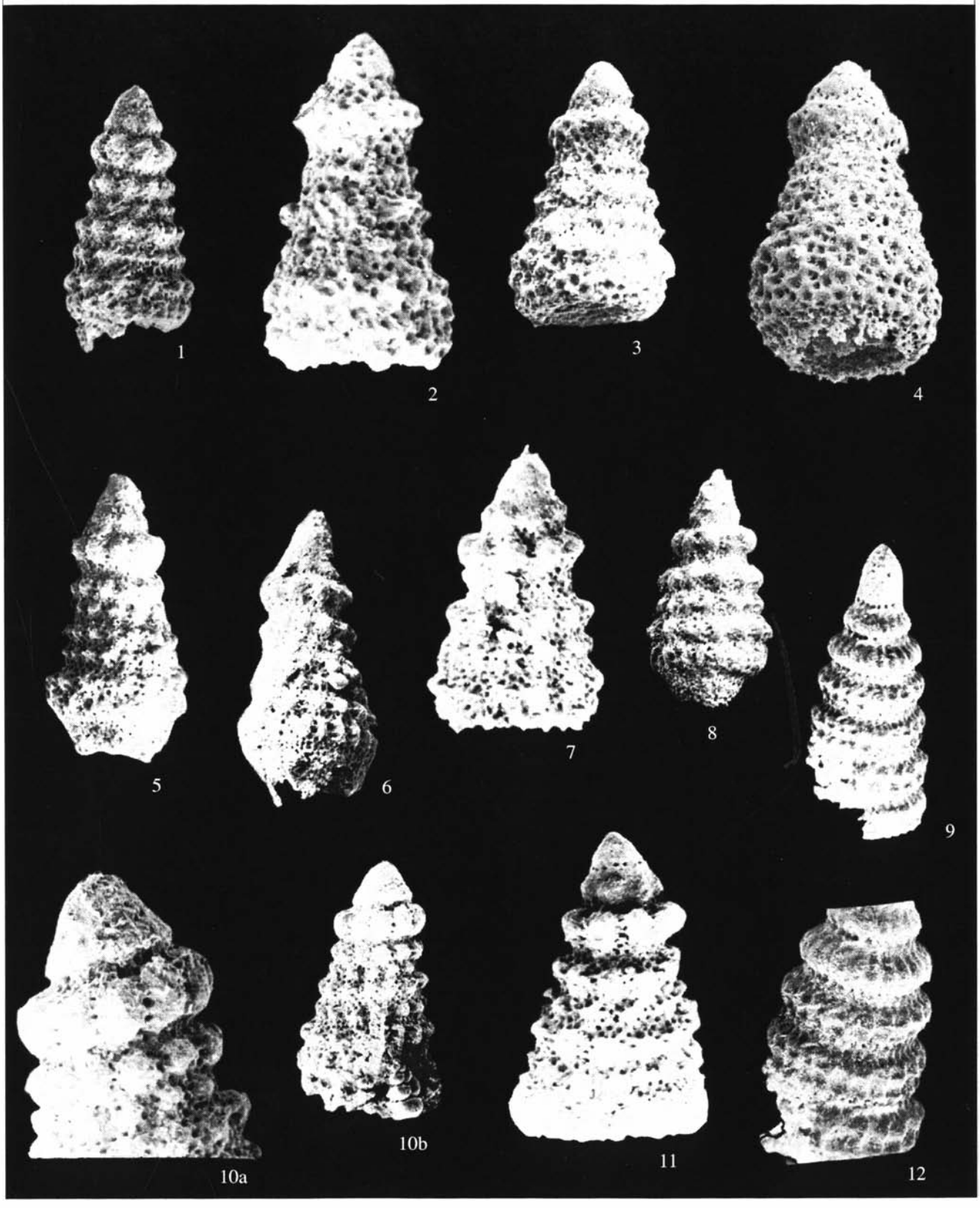

Comparison. *N. dengoi* differs from *Novixitus weyli* Schmidt-Effing, 1980 in the presence of well-defined hemispherical nodes on the abdomen.

Remarks. The most complete specimens, such as those shown in Pl. 6, fig. 4, have a bag-shaped (sacculate) apertural portion of the shell.

Occurrence. Albian–Turonian, worldwide; Middle–Upper Cenomanian of northern Turkey; Lower Turonian of the Crimean Mountains.

Material. More than ten specimens.

Novixitus subtilis Bragina, sp. nov.

Plate 5, fig. 10

Etymology. From the Latin *subtilis* (subtle).

Holotype. GIN, no. 4871/51; northern Turkey, Tomalar Formation, Ürküt section; Upper Cretaceous, Middle Cenomanian.

Description. The shell is narrowly conical and has a club-shaped thickening proximally. The cephalis is small, broadly conical, with a few fine, widely spaced pores. The thorax is shaped like a broad truncated cone connected with the cephalis without noticeable outer constrictions. The abdomen is barrel-shaped and forms, in combination with the cephalis and thorax, a club-shaped thickening. The thorax and abdomen are pierced by small, rounded to polygonal pores with a diameter less than the distance between pores. The pore frames are polygonal (four- to seven-sided) and irregular in outline. The shell surface is uneven owing to variously developed spines at the junctions of several pore frames. The next chamber is markedly narrower; however, its middle part is encircled around the entire circumference of the abdomen by a fairly high, but poorly defined and somewhat sinuous ridge. Distally the shell forms a truncate high cone widening slightly toward the aperture. The surface of this portion of the shell is pierced with rounded pores, which are spaced at a distance less than or equal to their diameter. The ridges on the pore frames of this portion of the shell are small and poorly defined in outline. The surface of the narrowly conical portion of the shell may be encircled with comblike ridges varying in number (two to five) from specimen to specimen.

Measurements. Shell length, 220; maximal width, 120; maximal width of club-shaped thickening, 90; pore diameter, 1–5.

Comparison. *N. subtilis* differs from *Novixitus mclaughlini* Pessagno, 1977, in the absence of characteristic nodes on the club-shaped and more distal parts of the shell.

Occurrence. Northern Turkey, Ürküt section, Middle Cenomanian.

Material. Seven complete and three incomplete specimens.

Novixitus weyli Schmidt-Effing, 1980

Plate 6, figs. 1, 5–8, and 10–11

Novixitus sp. *A*: Pessagno, 1977, p. 54, pl. 9, fig. 6.

Novixitus sp.: Kato and Iwata, 1989, pl. 8, fig. 10.

Novixitus weyli: Schmidt-Effing, 1980, p. 252–253, text-fig. 33; Nakaseko and Nishimura, 1981, p. 155, pl. 10, figs. 1 and 2; Taketani, 1982, p. 62, pl. 5, figs. 9a and 9b; pl. 12, fig. 11; Schaaf, 1984, p. 162–163, text-figs. 9a and 9b; Teraoka, Kurimoto, 1986, pl. 4, fig. 6; Thurow, 1988, p. 402, pl. 4, fig. 1; Bak, 1993, p. 198, pl. 4, figs. 9–11.

Pars *Novixitus weyli*: Kato and Iwata, 1989, pl. 8, fig. 9.

Non *Novixitus weyli*: Teraoka, Kurimoto, 1986, pl. 4, fig. 7 (= *N.* ex gr. *N. mclaughlini* Pessagno, 1977); Erbacher, 1994, pl. 14, figs. 7 and 8 (= *N. mclaughlini* Pessagno, 1977).

Novixitus mclaughlini: Marcucci *et al.*, 1991, text-figs. 3f and 3g; Bak, 1993, p. 198, pl. 4, fig. 8; O'Dogherty, 1994, p. 130, pl. 12, figs. 14–21; Vishnevskaya, 2001, pl. 25, fig. 5.

Holotype. Geological–Paleontological Institute of Münster, Abb. 33; Central America, northwestern Costa Rica, Cabo Santa Elena (cape), Rio Potrero Grande Series, locality of Capas del Sardinal; Upper Cretaceous, Cenomanian.

Comparison. *N. weyli* Schmidt-Effing, 1980 differs distinctly from *N. mclaughlini* Pessagno, 1977 in having an outer constriction after the first two rows of nodes (the first row is quite poorly developed in both species) and in that the chamber bearing the second row of nodes is wider than the next chamber.

Occurrence. Cenomanian–Turonian, worldwide; Middle–Upper Cenomanian of northern Turkey.

Material. More than 30 specimens.

Genus *Pseudodictyomitra* Pessagno, 1977

Pseudodictyomitra: Pessagno, 1977, p. 50.

Type species. *Pseudodictyomitra pentacolaensis* Pessagno, 1977; Upper Albian, Lower Cretaceous, Great Valley sequence, Locality NSF 860, California.

Diagnosis. Narrowly conical shell consisting of six or more post-abdominal chambers. Distal post-abdominal chamber with less distinct costae.

Comparison. *Pseudodictyomitra* differs from *Dictyomitra* Zittel, 1876 in (1) the presence of a double row of pores on each constriction between adjacent chambers from the second post-abdominal chamber onward and (2) in that the costae of adjacent chambers do not touch one another.

Species composition. In addition to the type species, more than ten species, including *P. quasilodogaensis* sp. nov.; Upper Jurassic–Cretaceous, worldwide.

Pseudodictyomitra nakasekoi Taketani, 1982

Plate 7, figs. 1–3

? *Dictyomitra tiara*: Holmes, 1900, p. 701, pl. 38, fig. 4; Dumitrica, 1975, text-fig. 2.9.

Pseudodictyomitra tiara: O'Dogherty, 1994, p. 109, pl. 8, figs. 9–11.

Pseudodictyomitra nakasekoi: Taketani, 1982, p. 60, pl. 12, figs. 4–6; Kuhnt *et al.*, 1986, fig. 7.S; Erbacher, 1994, pl. 15, figs. 5 and 6; O'Dogherty, 1994, p. 109, pl. 8, figs. 9–11; Salvini and Marcucci Passerini, 1998, fig. 6.n; Tumanda and Sashida, 1988, text-fig. 4.13; Bragin *et al.*, 2000, text-fig. 4.D.

? *Pseudodictyomitra nakasekoi*: Hashimoto and Ishida, 1997, pl. 1, fig. 12.

Non *Pseudodictyomitra nakasekoi*: Vishnevskaya, 2001, pl. 125, fig. 30 (? *Pseudodictyomitra* ex gr. *P. carpatica* (Lozyniak, 1969)).

Pseudodictyomitra carpatica: Marcucci *et al.*, 1991, text-fig. 3k; Wakita and Bambang, 1994, text-fig. 4.1.

Holotype. Tohoku University, Japan, IGPS, no. 97566; Cenomanian, Utafue Formation, Yezo Group, Hokkaido, Japan (Taketani, 1982, pl. 12, fig. 4).

Comparison. *P. nakasekoi* differs from *Pseudodictyomitra pseudomacrocephala* (Squinabol, 1903) in having a conical rather than a club-shaped shell and larger pores piercing right through the shell, in the middle parts of the chambers (between costae).

Occurrence. Albian–Turonian, worldwide; Upper Cenomanian of northern Turkey.

Material. More than ten specimens.

Pseudodictyomitra pseudomacrocephala (Squinabol, 1903)

Plate 7, fig. 4; Plate 32, figs. 9, 14–16

Dictyomitra pseudomacrocephala: Squinabol, 1903, p. 139, pl. 10, fig. 2; Petrushevskaya and Kozlova, 1972, p. 550, pl. 2, fig. 5.

Dictyomitra malleola: Pessagno, 1969b, p. 610, pl. 5, fig. A; Petrushevskaya and Kozlova, 1972, p. 550, pl. 2, fig. 5.

Dictyomitra sp.: Foreman, 1973, p. 264, pl. 14, fig. 16.

Pseudodictyomitra pseudomacrocephala: Pessagno, 1977, p. 51, pl. 8, figs. 10 and 11 (= specimens of Pessagno, 1976, pl. 3, figs. 2, 3); Schmidt-Effing, 1980, fig. 8; Schaaf, 1981, pl. 24, figs. 1a and 1b; Nakaseko and Nishimura, 1981, p. 159, pl. 9, figs. 1–4; pl. 16, figs. 7 and 8; Taketani, 1982, p. 61, pl. 5, figs. 4a and 4b; pl. 12, figs. 7 and 8; Kuhnt *et al.*, 1986, pl. 7.T; Teraoka and Kurimoto, 1986, pl. 4, figs. 10 and 11; Thurow, 1988, p. 405, pl. 1, fig. 13; pl. 3, fig. 16; Thurow and Kuhnt, 1986, fig. 9.11; Erbacher, 1994, pl. 8, figs. 4 and 5; O'Dogherty, 1994, p. 108, pl. 8, figs. 5–8; Hashimoto and Ishida, 1997, pl. 1, fig. 2; Salvini and Marcucci Passerini, 1998, fig. 8.h; Khan *et al.*, 1999, pl. 4, fig. d; Bragin *et al.*, 2000, text-fig. 4.C; Vishnevskaya, 2001, pl. 129, figs. 5 and 9.

Holotype. Northern Italy, southern Venetian Alps, Scaglia Bianca Formation, Teolo Series; upper Lower Cretaceous–lower Upper Cretaceous, Upper Albian–Lower Turonian (Squinabol, 1903, pl. 10, fig. 2).

Remarks. The Early Turonian specimens of the Belaya Mountain section are characterized by a poorly developed club-shaped thickening of the shell.

Occurrence. Upper Albian–Lower Turonian, worldwide; Middle–Upper Cenomanian of northern Turkey; Upper Cenomanian–Lower Turonian of the Crimean Mountains.

Material. More than 30 specimens.

Pseudodictyomitra quasilodogaensis Bragina, sp. nov.

Plate 6, fig. 9

Etymology. From the Latin *quasi* (as if) and *lodogaensis* (species name by Pessagno (1977)).

Holotype. GIN, no. 4871/61; northern Turkey, Tomalar Formation, Tomalar section; Upper Cretaceous, Upper Cenomanian.

Description. The shell is narrowly conical and consists of eight to ten chambers. The cephalis is small, broadly conical, and devoid of pores. The thorax is conical and as high as the cephalis but one-third wider. The abdomen is cylindrical, slightly wider and four times higher than the thorax. The combination of cephalis, thorax, and abdomen forms a structure that resembles a high helmet. This structure possesses only two rows of pores: one row separates the cephalis from the thorax and the other separates the thorax from the abdomen. All the post-abdominal chambers are barrel-shaped, separated by double rows of rounded pores that are enclosed in massive pore frames. and The post-abdominal chambers have longitudinal costae (9 to 12 per half-circle) that are not continuous from one double row of pores on a chamber junction to another. A single row of three pores, frequently blind, occurs between adjacent costae. The costae are hemispherical either distinctly (in the first two post-abdominal chambers) or less distinctly (in the subsequent chambers), because of their fractured and flattened middle parts. The neighboring costae of the middle and distal portions of the shell are connected by weak transverse ridges.

Measurements. Shell length, 550; maximal width, 100; height of each post-abdominal chamber, 70.

Comparison. *P. quasilodogaensis* differs from *P. pentacolaensis* Pessagno, 1977 in that the proximal part of the shell is shaped like a helmet and includes the cephalis and from *P. lodogaensis* Pessagno, 1977 in the shape of the costae in the third and subsequent post-abdominal chambers.

Occurrence. Upper Cenomanian of northern Turkey, Tomalar Formation, Tomalar section.

Material. Three complete and nine incomplete specimens.

Genus *Mita* Pessagno, 1977

Mita (?) cypraea Bragina, sp. nov.

Plate 7, fig. 5

Etymology. From Cyprus, where the species was found for the first time.

Holotype. GIN, no. 4871/66; northern Turkey, Tomalar Formation, Tomalar section; Upper Cretaceous, Upper Cenomanian.

Description. The shell is conical and multichambered. The cephalis is small and has a short apical horn (if any). The first five to seven chambers gradually increase in width, the three distal chambers are equal in width, and the last chamber is slightly narrower than the penultimate one. Outer constrictions between chambers are virtually absent. The costae that extend from the cephalis to the aperture are continuous, moderately thick, and covered by irregularly spaced weakly developed nodes. The adjacent costae on the cephalis, thorax, and abdomen are separated by a double or, occasionally, single row of pores and those on the subsequent post-abdominal chambers are separated by two or, occasionally, three longitudinal rows of pores. The pores are small, rounded to subquadrate in cross section, and arranged in both longitudinal and transverse rows in subquadrate pore frames of irregular outlines. There are minor spines and nodes at the vertices of the pore frames.

Measurements. Shell length, 300–500; maximal width, 180–200; height of each post-abdominal chamber, 25–40.

Plate 7

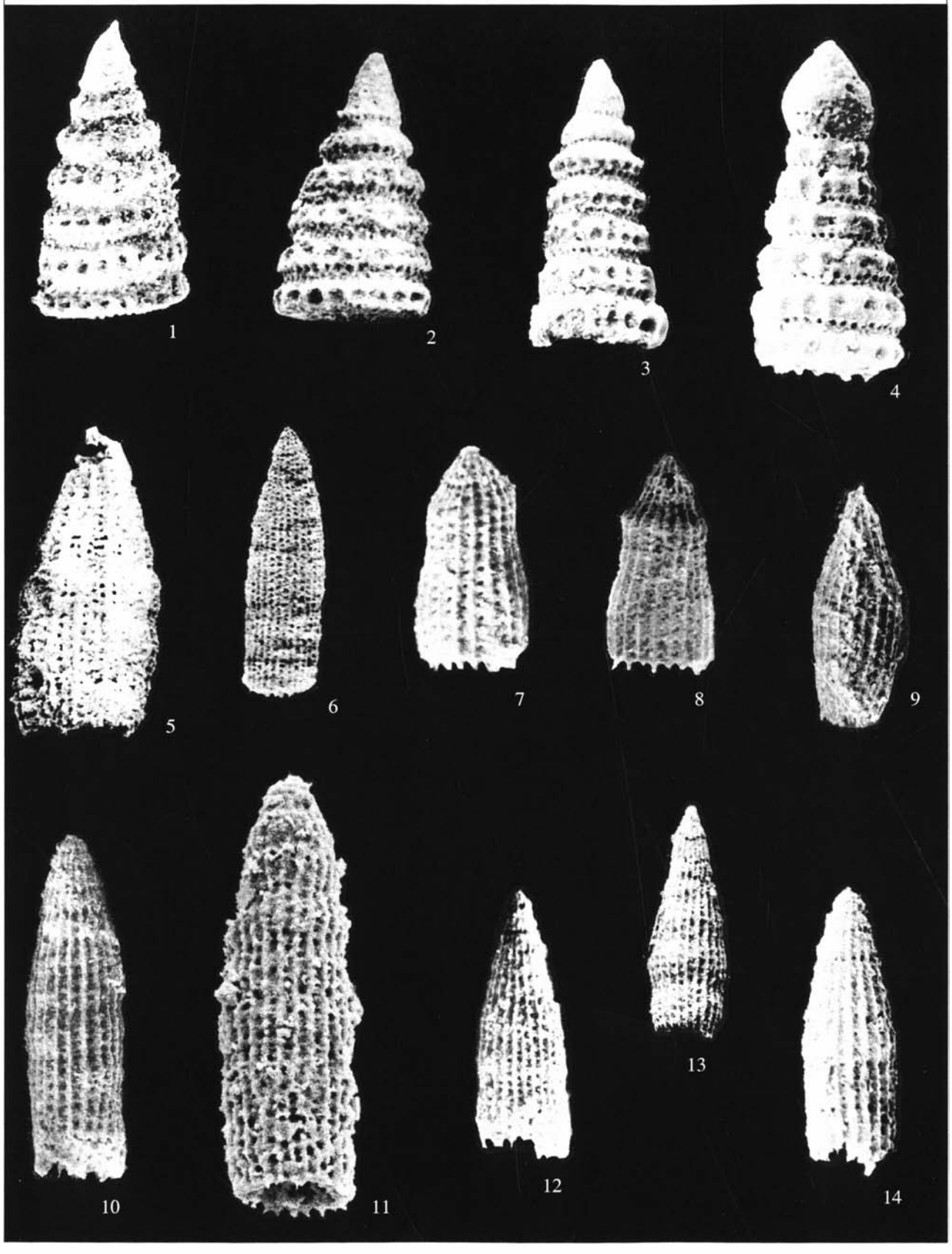

Remarks. This specimen is only tentatively assigned to the genus *Mita*. Unlike *Thanarla* species, typical representatives of *Mita* have no more than a double row of pores between adjacent costae. On the other hand, the representatives of *Thanarla* have shells of regular outline with more distinct costae without nodes.

Occurrence. Northern Turkey, Tomalar Formation, Tomalar and Ürküt sections, Middle–Upper Cenomanian.

Material. More than ten specimens.

Family Archaeodictyomitridae Pessagno, 1976
Genus *Thanarla* Pessagno, 1977

Thanarla: Pessagno, 1977, p. 45.

Type species. *Phormocyrtis veneta* Squinabol, 1903; Upper Albian–Lower Turonian, Teolo Locality, northern Italy.

Diagnosis. Shell multicyrtoid, with costae extending from the proximal part to aperture. Usually no outer constrictions between chambers. Costae continuous throughout the shell length.

Species composition. More than ten species; Cretaceous, worldwide.

Comparison. *Thanarla* differs from *Archaeodictyomitra* Pessagno, 1976, in having no outer constrictions between chambers. Some *Thanarla* species have a single constriction on the shell, which usually serves as a diagnostic feature of these species.

Remarks. Some species are difficult to assign with certainty to either *Thanarla* Pessagno, 1977 or *Archaeodictyomitra* Pessagno, 1976. It seems that this difficulty is due to the fact that their diagnoses rely on characters of the shell exterior. It is quite possible that closer examination of the internal structure of the cephalic chamber in these genera may improve their diagnoses.

Occurrence. Cretaceous, worldwide.

Thanarla gracilis (Squinabol, 1903)

Plate 7, fig. 9

Sethoconus gracilis: Squinabol, 1903, p. 131, pl. 10, fig. 13.

Mita gracilis: Schaaf, 1984, p. 110-111, text-figs. H (= holotype refigured), 1, 3, 4a, and 4b (= specimen of Schaaf, 1981, pl. 24, figs. 13a, 13b), 5a–5c; Thurow, 1988, p. 402, pl. 3, fig. 2; Hashimoto and Ishida, 1997, pl. 1, fig. 5.

? Mita magnifica: Schaaf, 1981, pl. 24, figs. 13a and 13b.

Dictyomitra gracilis: O'Dogherty, 1994, p. 73, pl. 1, figs. 12–25.

Archaeodictyomitra chalilovi: Jud, 1994, p. 63, pl. 1, figs. 13 and 14.

Archaeodictyomitra sp. ex gr. *A. vulgaris*: Bragin *et al.*, 2000, text-fig. 3.I.

Holotype. Northern Italy, southern Venetian Alps, Colli Euganei Formation, Teolo Locality; upper Lower Cretaceous–lower Upper Cretaceous, Upper Albian–Lower Turonian (Squinabol, 1903, pl. 10, fig. 13).

Description. The shell is narrowly conical and has a short apical horn. Proximally narrowly conical, the shell slowly expands into a barrel shape. The costae that begin on the cephalothorax or post-abdominal chambers extend up to the aperture. The cephalis and thorax may be free of costae. Adjacent costae are separated by a single row of rounded to oval pores.

Measurements. Shell length, 280–492; maximal width, 120–183.

Comparison. *Th. gracilis* differs from *T. veneta* (Squinabol, 1903) in the narrowly conical proximal part of the shell.

Occurrence. Albian–Lower Turonian, worldwide; Upper Cenomanian of northern Turkey.

Material. More than ten specimens.

Thanarla veneta (Squinabol, 1903)

Plate 7, figs. 7 and 8; Plate 33, fig. 11

Phormocyrtis veneta: Squinabol, 1903, p. 134, pl. 9, fig. 30.

Dictyomitra veneta: Petrushevskaya and Kozlova, 1972, p. 550, pl. 2, fig. 2.

Phormocyrtis (?) veneta: Pessagno, 1976, p. 55, pl. 3, fig. 10.

Pars *Thanarla praeveneta*: Pessagno, 1977, p. 46, pl. 7, figs. 16, 18, 23, and 27; non fig. 11 (= *T. brouweri ?*).

Thanarla veneta: Pessagno, 1977, p. 46, pl. 7, figs. 5, 12, 17, 19, and 25; pl. 12, fig.8; Schmidt-Effing, 1980, figs. 3 and 23; Nakaseko and Nishimura, 1981, p. 164, pl. 6, figs. 13–15; pl. 15, fig. 15; Taketani, 1982, p. 60, pl. 11, figs. 20 and 21; Thurow, 1988, p. 407, pl. 4, fig. 14; Erbacher, 1994, pl. 20, fig. 4; O'Dogherty, 1994, p. 93, pl. 4, figs. 5 and 6; Salvini and Marcucci Passerini, 1998, text-fig. 8.k; Bragin *et al.*, 2000, text-fig. 3.L.

Non *Thanarla veneta*: Thurow, 1988, p. 407, pl. 4, fig. 13 (= *Thanarla praeveneta* Pessagno, 1977); Vishnevskaya, 2001, pl. 76, fig. 4 (= *Thanarla praeveneta* Pessagno, 1977); pl. 85, figs. 7–10 (= *Thanarla praeveneta* Pessagno, 1977).

Holotype. Northern Italy, southern Venetian Alps, Colli Euganei, Teolo Locality; upper Lower Cretaceous–lower Upper Cretaceous, Upper Albian–Lower Turonian (Squinabol, 1903, pl. 9, fig. 30).

Explanation of Plate 7

Figs. 1–3. *Pseudodictyomitra nakasekoi* Taketani, 1982, specimens: (1) GIN, no. 4871/62, ×200; (2) GIN, no. 4871/63, ×200; and (3) GIN, no. 4871/64, ×170.

Fig. 4. *Pseudodictyomitra pseudomacrocephala* (Squinabol, 1903), GIN, no. 4871/65, ×200.

Fig. 5. *Mita (?) cypraea* sp. nov., holotype GIN, no. 4871/66, ×160.

Figs. 6, 10, and 11. *Archaeodictyomitra sliteri* Pessagno, 1977, specimens: (6) GIN, no. 4871/70, ×150; (10) GIN, no. 4871/71, ×160; and (11) GIN, no. 4871/72, ×350.

Figs. 7 and 8. *Thanarla veneta* (Squinabol, 1903): (7) GIN, no. 4871/67, ×250; (8) GIN, no. 4871/68, ×180.

Fig. 9. *Thanarla gracilis* (Squinabol, 1903), (9) GIN, no. 4871/69, ×160.

Figs. 12 and 14. *Archaeodictyomitra simplex* Pessagno, 1977: (12) GIN, no. 4871/73, ×150; (14) GIN, no. 4871/74, ×160.

Fig. 13. *Archaeodictyomitra delicata* sp. nov., holotype GIN, no. 4871/75, ×120.

Figs. 1–3, 5, 10, and 13. From the Tomalar section; Figs. 4, 6–9, 11, 12, and 14. From the Ürküt section.

Comparison. *T. veneta* differs from *T. praeveneta* Pessagno, 1977 in the shell consisting of a broadly conical proximal part and subcylindrical distal part.

Occurrence. Upper Albian–Santonian, worldwide; Cenomanian of Italy; Upper Cenomanian of northern Turkey; Lower Turonian of the Crimean Mountains.

Material. More than ten specimens.

Genus *Archaeodictyomitra* Pessagno, 1976

Archaeodictyomitra: Pessagno, 1976, p. 49.

Type species. *Archaeodictyomitra squinaboli* Pessagno, 1976; Upper Cretaceous, Turonian, Venado Formation, Great Valley section, California.

Diagnosis. Shell narrowly conical, multicyrtoid, usually without apical horn. Costae continuous along entire length of shell. Outer constrictions between chambers weak or absent. Single row of pores between adjacent costae.

Species composition. More than 15 species, including the type species and a new species, *A. (?) speciosa* sp. nov.; Jurassic–Cretaceous, worldwide.

Comparison. *Archaeodictyomitra* differs from *Dictyomitra* Zittel, 1876 in the continuous costae.

Archaeodictyomitra crebrisulcata (Squinabol, 1904)

Plate 33, fig. 12

Dictyomitra crebrisulcata: Squinabol, 1904, p. 231, pl. 10, fig. 1; O'Dogherty, 1994, p. 75, pl. 2, figs. 12–17.

Holotype. Northern Italy, southern Venetian Alps, Colli Euganei, Teolo Locality; upper Lower Cretaceous–lower Upper Cretaceous, Middle Albian–Cenomanian (Squinabol, 1904, pl. 10, fig. 1).

Description. The shell is narrowly conical and multichambered. The cephalis is small and has a short apical horn (if any). The cephalis, thorax, and abdomen are almost equal in height and width. The post-abdominal chambers only slightly increase in width. The shell may be slightly inflated. The costae that extend from the cephalis to the aperture are very thin and continuous. Some costae begin on post-abdominal chambers. The costae amount to 15 per half-circle. The pores are fine and do not necessarily pierce right through the shell.

Measurements. Shell length, 300–600; maximal width, 90–110.

Comparison. *A. crebrisulcata* differs from *A. vulgaris* Pessagno, 1977 in the narrower and narrowly conical shell.

Occurrence. Middle Albian–Cenomanian of the Tethys; Lower Turonian of the Crimean Mountains.

Material. More than 20 specimens.

Archaeodictyomitra delicata Bragina, sp. nov.

Plate 7, fig. 13; Plate 8, fig. 13

Etymology. From the Latin *delicatus* (delicate).

Holotype GIN, no. 4871/75; northern Turkey, Tomalar Formation, Tomalar section; Upper Cretaceous, Upper Cenomanian.

Description. The shell is small, fusiform, with hardly noticeable outer constrictions between chambers. The cephalis is small, narrowly conical, and not quite as high as the thorax and abdomen. The combination of these three parts forms a high cone. The first post-abdominal chamber is almost cylindrical and slightly narrower than the abdomen. The next three to five post-abdominal chambers are of equal height and increase slightly in width distally. The distal chambers narrow, thus making the shell fusiform. The shell has longitudinal costae from the cephalis to the aperture. The widest chamber bears 11 to 13 costae per half-circle. Pores pierce the shell throughout, almost doubling in diameter from the cephalic chamber to the second post-abdominal chamber. The pores are rounded to polygonal in cross section and positioned in irregular pore frames. The pore frames connecting neighboring longitudinal costae are more clearly defined and only slightly lower in profile than the costae.

Measurements. Shell length, 275–330; width, 103–150.

Comparison. *A. delicata* differs from *A. regina* (Campbell et Clark, 1944) in having irregular rounded–polygonal pores, poorly pronounced outer constrictions, and fusiform shell.

Occurrence. Northern Turkey, Tomalar section, Upper Cenomanian.

Material. Eight complete and 12 incomplete specimens.

Archaeodictyomitra simplex Pessagno, 1977

Plate 7, figs. 12 and 14

Archaeodictyomitra simplex: Pessagno, 1977, p. 43, pl. 6, figs. 1, 24, and 28.

Holotype. USNM-Pessagno, no. 24273; California coast, Great Valley sequence, Locality NSF 860;

Explanation of Plate 8

Figs. 1, 6, and 11. *Archaeodictyomitra squinaboli* Pessagno, 1976, specimens: (1) GIN, no. 4871/76: (a) porosity and costae of cephalothorax, ×350, and (b) general view, ×120; (6) GIN, no. 4871/77, ×150; (11) GIN, no. 4871/78, ×120.

Figs. 2–4, 7, and 14. *Dictyomitra montisserei* (Squinabol, 1903), specimens: (2) GIN, no. 4871/79; (3) GIN, no. 4871/80; (4) GIN, no. 4871/81; (7) GIN, no. 4871/82 (2–4, 7, ×150); and (14) GIN, no. 4871/83, distorted, ×120.

Fig. 5. *Dictyomitra napaensis* Pessagno, 1976, GIN, no. 4871/84, ×120.

Figs. 8–10, and 12. *Archaeodictyomitra sliteri* Pessagno, 1977, specimens: (8) GIN, no. 4871/85, ×120; (9) GIN, no. 4871/85-1, ×120; (10) GIN, no. 4871/85-2, ×120; and (12) GIN, no. 4871/86, ×100.

Fig. 13. *Archaeodictyomitra delicata* sp. nov., paratype GIN, no. 4871/87, ×175.

Figs. 1–3, 6, 11–13. From the Tomalar section; Figs. 4, 5, 7–10, and 14. From the Ürküt section.

Plate 8

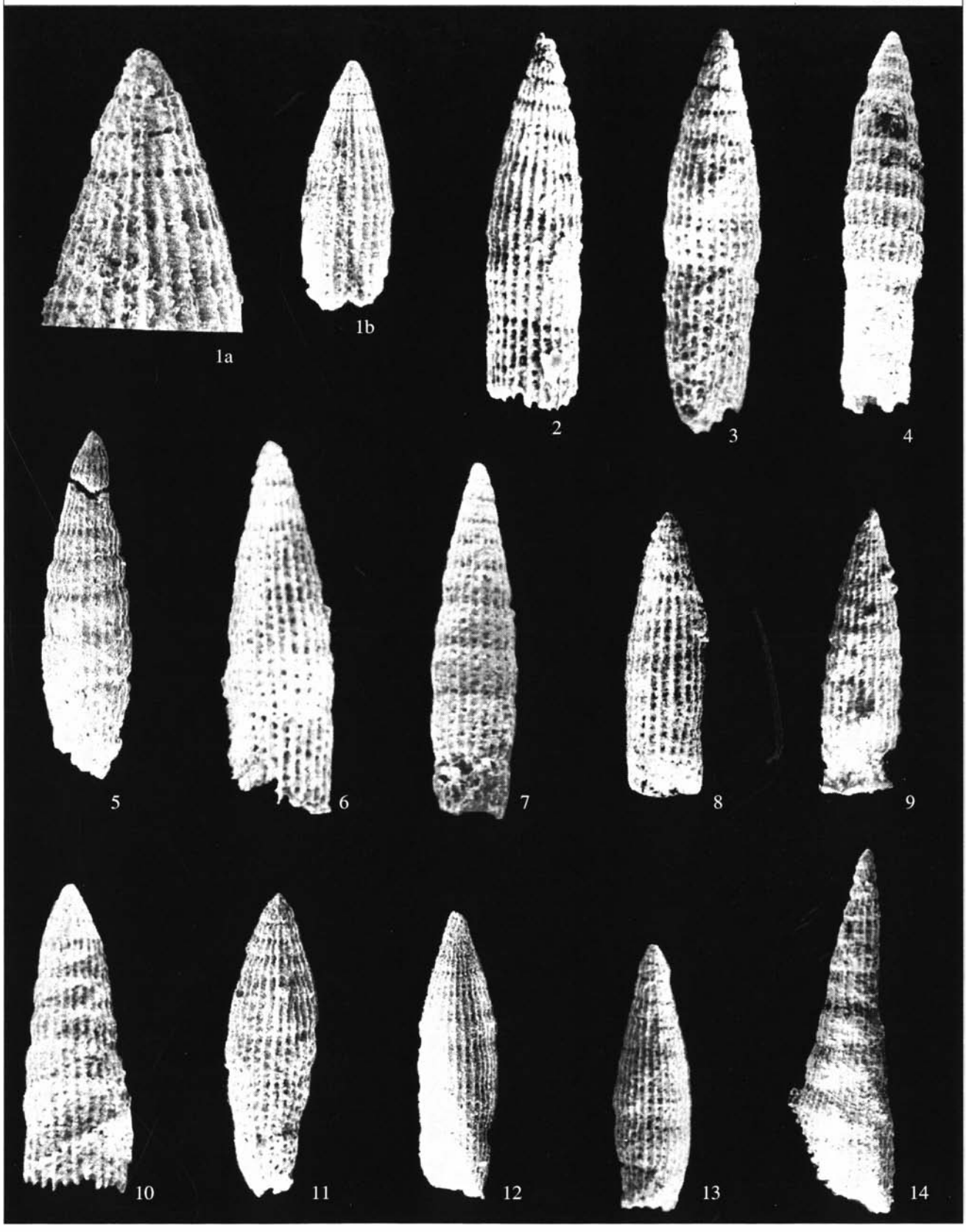

Lower Cretaceous, Upper Albian (Pessagno, 1977, pl. 6, figs. 1, 18, 24).

Occurrence. Albian of California; Middle–Upper Cenomanian of northern Turkey.

Material. More than ten specimens.

Archaeodictyomitra sliteri Pessagno, 1977

Plate 7, figs. 6, 10, and 11; Plate 8, figs. 8–12; Plate 34, fig. 6.

Archaeodictyomitra sliteri: Pessagno, 1977, p. 43, pl. 6, figs. 3, 4, 22, 23, and 27.

Holotype. USNM-Pessagno, no. 242771; California coast, Great Valley sequence, Locality NSF 934; Upper Cretaceous, Lower Cenomanian (Pessagno, 1977, pl. 6, figs. 3, 22).

Comparison. *A. sliteri* differs from *A. vulgaris* Pessagno, 1977 in having a narrowly conical fusiform shell, closely spaced costae, and a subspherical but not conical cephalis.

Occurrence. Cenomanian of California; Middle–Upper Cenomanian of northern Turkey; Lower Turonian of the Crimean Mountains.

Material. More than ten specimens.

Archaeodictyomitra (?) speciosa Bragina, sp. nov.

Plate 9, fig. 1

Etymology. From the Latin *speciosus* (special).

Holotype. GIN, no. 4871/88; Northern Turkey, Tomalar Formation, Ürküt section; Upper Cretaceous, Middle Cenomanian.

Description. The shell is narrowly conical and consists of 17 or more chambers. The cephalis is small, broadly conical, without pores. The combination of the apical horn and vertical spine resembles a short small ridge. The thorax is shaped like a truncated cone and has sparse fine pores. The abdomen and subsequent chambers are cylindrical, virtually invariable in height, and connected without outer constrictions. The pores between adjacent chambers are usually oval and form a single transverse row. There are no pores between the cephalis and the middle part of the shell. The middle part shows irregular, winding striations that vary in length, are oriented along the main shell axis, and somewhat resemble costae. The pores in this part are sparse and do not pierce right through the shell. The pores of the distal part are rounded to polygonal in cross section and arranged in hexagonal to pentagonal patterns. The diameters of the pores are equal to or slightly less than the distance between them. The striations are not developed distally.

Measurements. Shell length, 550; maximal shell width, 100; apical horn height, 15.

Comparison. This species differs from *A. turritum* (Squinabol, 1904) in the absence of well-defined costae on the shell surface and in the presence of a ridgelike structure consisting of the conjoined apical and vertical horns.

Remarks. *A. (?) speciosa* sp. nov. is only tentatively included into *Archaeodictyomitra* because of its lack of characteristic distinct costae on the chambers.

Occurrence. Northern Turkey, Ürküt and Tomalar sections, Middle Cenomanian.

Material. Four complete and seven incomplete specimens.

Archaeodictyomitra squinaboli Pessagno, 1976, emend. herein

Plate 8, figs. 1, 6, and 11; Plate 33, figs. 14, 15, and 17

Archaeodictyomitra squinaboli: Pessagno, 1976, p. 50, pl. 5, figs. 2–8; 1977, p. 50, pl. 5, figs. 2–8.; Kazintsova, 1993, p. 72, pl. VIII, figs. 8–10; pl. X, fig. 8; pl. XI, fig. 6, 8; pl. XV, fig. 8; pl. XXI, fig. 7.

Non *Archaeodictyomitra squinaboli*: Vishnevskaya, 2001, pl. 125, figs. 39 and 40 (=*Mita magnifica* Pessagno, 1977).

Dictyomitra montisserei: O'Dogherty, 1994, p. 77, pl. 3, fig. 11.

Holotype. USNM, no. 186360; California, Great Valley sequence, Locality NSF 432; Upper Cretaceous, Turonian (Pessagno, 1976, pl. 5, figs. 2, 3).

Description. The shell is conical and multichambered, possesses barely visible outer constrictions between chambers, gradually widens toward the penultimate chamber, and then slightly narrows. The cephalis is small and hemispherical. The subsequent chambers increase only slightly in height and width. The shell surface is covered with costae from the cephalis to the aperture. Some costae begin on the thorax or, abdomen, or even on the post-abdominal chambers. The widest part of the shell has 14 to 16 costae per half-circle. The adjacent costae are separated by a single longitudinal

Explanation of Plate 9

Fig. 1. *Archaeodictyomitra (?) speciosa* sp. nov., holotype GIN, no. 4871/88: (a) general view, ×150, and (b) shell wall, ×350.

Figs. 2 and 6. *Stichomitra communis* Squinabol, 1903: (2) GIN, no. 4871/89, ×150; (6) GIN, no. 4871/90, ×120.

Figs. 3–5, and 7. *Stichomitra insignis* (Squinabol, 1904), specimens: (3) GIN, no. 4871/91, ×150; (4) GIN, no. 4871/92, ×120; (5) GIN, no. 4871/93, ×65; and (7) GIN, no. 4871/94, ×110.

Fig. 8. *Eostichomitra warzigita* Empson-Morin, 1981, GIN, no. 4871/95, ×300.

Figs. 9 and 11. *Amphipyndax stocki* (Campbell et Clark, 1944), specimens: (9) GIN, no. 4871/96, ×150; and (11) GIN, no. 4871/97, ×200.

Figs. 10 and 12. *Amphipyndax ellipticus* Nakaseko et Nishimura, 1981, specimens: (10) GIN, no. 4871/98, ×175; and (12) GIN, no. 4871/99, ×100.

Figs. 13 and 14. *Amphipyndax conicus* Nakaseko et Nishimura, 1981, specimens: (13) GIN, no. 4871/100, ×175; and (14) GIN, no. 4871/101, ×150.

Figs. 1–3, 5–8, 10–14. From the Ürküt section; Figs. 4, 9. From the Tomalar section.

Plate 9

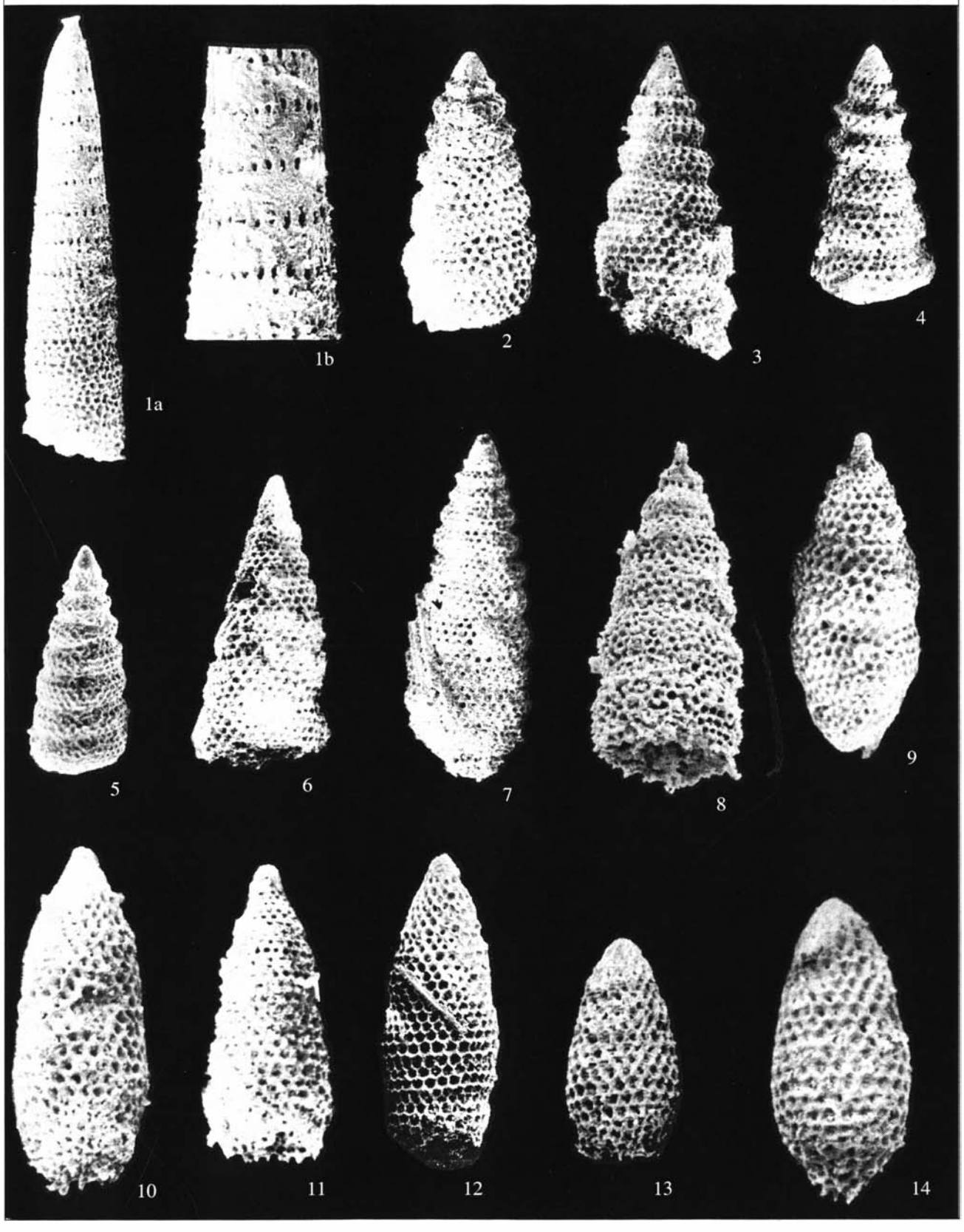

row of rounded pores (three or four pores on each chamber). The pores that pierce right through the shell usually occur from the second chamber onwards. The aperture is small, rounded, open, and occasionally has a short tubular extension.

Measurements. Shell length, 365–455; width, 130–140.

Comparison. *A. squinaboli* differs from *A. regina* (Campbell et Clark, 1944) in having several costae extending from the thorax and post-abdominal segments and a fusiform shell with a narrowly conical proximal part.

Occurrence. Albian–Campanian of California and Japan; Coniacian–Campanian of the Koryak Upland; Lower Cenomanian–Campanian of southwestern Sakhalin; Lower Turonian of the Crimean Mountains; Middle–Upper Cenomanian of northern Turkey.

Material. More than 20 specimens.

Archaeodictyomitra vulgaris Pessagno, 1977

Plate 33, fig. 18

Archaeodictyomitra vulgaris: Pessagno, 1977, p. 44, pl. 6, fig. 15.

Holotype. USNM-Pessagno, no. 2427775; California coast, Great Valley sequence, Locality NSF 940; Lower Cretaceous, Upper Aptian (Pessagno, 1977, pl. 6, fig. 15).

Occurrence. Upper Aptian of California; Lower Turonian of the Crimean Mountains.

Material. Eight specimens.

Genus *Dictyomitra* Zittel, 1876

Dictyomitra montisserei (Squinabol, 1903)

Plate 8, figs. 2–4, 7, and 14

Sichophormis Montis Serei: Squinabol, 1903, p. 137, pl. 8, fig. 38.

Dictyomitra montisserei: O'Dogherty, 1994, p. 77, pl. 3, figs. 1–8, 16–17, 19–21, and 28–29.

Holotype. Northern Italy, southern Venetian Alps, Colli Euganei, locality of Teolo; upper Lower Cretaceous–lower Upper Cretaceous, Upper Albian–Lower Turonian (Squinabol, 1903, pl. 8, fig. 38).

Occurrence. Upper Albian–Lower Turonian of Italy, Middle–Upper Cenomanian of northern Turkey.

Material. More than ten specimens.

Dictyomitra napaensis Pessagno, 1976

Plate 8, fig. 5

Dictyomitra napaensis: Pessagno, 1976, p. 53, pl. 4, fig. 16; pl. 5, figs. 1 and 9.

Holotype. USNM, no. 186366; California coast, Great Valley sequence, Venado Formation, Locality NSF 432; Upper Cretaceous, Turonian (Pessagno, 1977, pl. 4, fig. 16).

Occurrence. Turonian of California; Upper Cenomanian of northern Turkey.

Material. Seven specimens.

Genus *Stichomitra* Cayeux, 1897, emend. herein

Stichomitra: Cayeux, 1897, p. 204; Foreman, 1968, p. 71; O'Dogherty, 1994, p. 138.

Type species. *Stichomitra bertrandi* Cayeux, 1897.

Diagnosis. Shell usually narrowly conical, multichambered. Cephalis subspherical, without pores. No apical horn. Outer constrictions distinct. Pores rounded and hexagonally arranged. Pore frames may be developed. Shell widely open or sacculately closed. Aperture may be tubular.

Species composition. Several tens of species; Berriasian–Maastrichtian.

Comparison. *Stichomitra* differs from *Amphipyndax* Foreman, 1966 in that the cephalis is undivided into lower and upper parts.

Stichomitra communis Squinabol, 1903, emend. herein

Plate 9, figs. 2 and 6; Plate 32, figs. 10–12; Plate 33, fig. 16

Stichomitra communis: Squinabol, 1903, p. 139, pl. 8, fig. 45; Schmidt-Effing, 1980, pl. 8, fig. 10; pl. 19, fig. 11; Nakaseko and Nishimura, 1981, p. 162, pl. 11, fig. 11; Schaaf, 1984, p. 162–163, text-figs. 8a and 8b; Kuhnt *et al.*, 1986, pl. 7, fig. w; Thurow, 1988, p. 406, pl. 4, fig. 10; O'Dogherty, 1994, p. 144, pl. 17, figs. 6–9, 12–16; Hashimoto and Ishida, 1997, pl. 1, fig. 3; Salvini and Marcucci Passerini, 1998, fig. 8.j; Bragin *et al.*, 2000, fig. 4B; Vishnevskaya, 2001, pl. 129, fig. 8.

Non *Stichomitra communis*: Erbacher, 1994, pl. 14, fig. 10 (= *S. magna* Squinabol, 1904); Vishnevskaya, 2001, pl. 79, fig. 3

Parvicingula ? tekschaensis: Schaaf, 1981, p. 436, pl. 3, fig. 12; pl. 20, figs. 3a and 3b.

Holotype. Northern Italy, southern Venetian Alps, Colli Euganei, Teolo Series; upper Lower Cretaceous–lower Upper Cretaceous, Upper Albian–Lower Turonian (Squinabol, 1903, pl. 8, fig. 45).

Description. The shell is narrowly conical and thin-walled and most commonly consists of 8–11 barrel-shaped chambers. The cephalis is small, circular to conical, without pores, and, occasionally, separated from the thorax by an indistinct row of fine pores. The thorax is a little wider and higher than the cephalis, pierced with fine rounded pores, which frequently do not pierce right through the shell. The abdomen is wider and higher than the thorax. The post-abdominal chambers vary only slightly in length and reach their greatest width in the middle or, occasionally, nearer to the aperture. Both the abdomen and all the post-abdominal chambers are covered with small rounded pores of almost equal size, arranged in a hexagonal pattern. Their diameters slightly exceed the distance between them. The pores of all post-abdominal chambers are in poorly defined pentagonal to hexagonal pore frames. The shell narrows slightly toward the aperture.

Measurements. Shell length, 460–363; maximal width, 200–138.

Comparison. *S. communis* differs from *S. insignis* Squinabol, 1904 in having swollen, distinctly barrel-shaped chambers.

Remarks. *S. communis* Squinabol, 1903 is probably an ancestral form of *S. cechena* Foreman, 1968, the earliest examples of which were discovered in the

Coniacian–Santonian of the Russian Plain (Bragina, 1994).

Occurrence. Albian–Turonian, worldwide; Middle–Upper Cenomanian of northern Turkey; Upper Cenomanian–Lower Turonian of the Crimean Mountains.

Material. More than 50 specimens.

Stichomitra insignis (Squinabol, 1904)

Plate 9, figs. 3–5, 7

Dictyomitra insignis: Squinabol, 1904, p. 233, pl. 10, fig. 6.

Stichomitra insignis: Nakaseko and Nishimura, 1981, p. 162, pl. 11, fig. 11.

Dictyomitra communis: O'Dogherty, 1994, p. 144, pl. 17, figs. 10 and 11.

Holotype. Northern Italy, southern Venetian Alps, Teolo Series; upper Lower Cretaceous–lower Upper Cretaceous, Upper Albian–Lower Turonian (Squinabol, 1904, pl. 10, fig. 6).

Occurrence. Albian–Lower Turonian of the Tethys and Pacific oceans; Upper Cenomanian of northern Turkey; Lower Turonian of the Crimean Mountains.

Material. More than 20 specimens.

Stichomitra magna Squinabol, 1904

Plate 32, fig. 13

Stichomitra magna: Squinabol, 1904, p. 234, pl. 10, fig. 8; O'Dogherty, 1994, p. 146, pl. 17, figs. 17–21.

Stichomitra communis: Erbacher, 1994, pl. 14, fig. 10.

Holotype. Northern Italy, southern Venetian Alps, Scaglia Bianca Formation, Teolo Series; upper Lower Cretaceous–lower Upper Cretaceous, Upper Albian–Lower Turonian (Squinabol, 1904, pl. 10, fig. 8).

Description. The shell is narrowly conical and multichambered. The cephalis is small, conical, without an apical horn. The subsequent chambers are trapezoidal. The thorax and abdomen and the first three postabdominal chambers gradually increase in height and width, but the subsequent chambers are unchangeable. The shell surface is densely covered with small pores. Outer constrictions are absent. The aperture is widely open and rounded.

Measurements. Shell length, 750–550; maximal width, 150–140.

Comparison. *S. magna* differs from *S. communis* Squinabol, 1903 in the absence of outer constrictions between chambers.

Occurrence. Cenomanian–Turonian, worldwide; Albian–Lower Turonian of Italy and Spain; Lower Turonian of the Crimean Mountains; Upper Cenomanian of northern Turkey.

Material. More than 20 specimens.

Genus *Eostichomitra* Empson-Morin, 1981

Eostichomitra warzigita Empson-Morin, 1981

Plate 9, fig. 8

Eostichomitra warzigita: Empson-Morin, 1981, p. 280, pl. 13, figs. 1A–1D.

Holotype. USNM, no. 305362; Mid-Pacific Mountains, DSDP Borehole 313 (Empson-Morin, 1981, pl. 13, fig. 1).

Occurrence. Campanian of the Pacific Ocean; Middle Cenomanian of northern Turkey.

Material. Six specimens.

Family Amphipyndacidae Riedel, 1967

Genus *Amphipyndax* Foreman, 1966

Amphipyndax conicus Nakaseko et Nishimura, 1981

Plate 9, figs. 13 and 14; Plate 32, figs. 5 and 6

Amphipyndax conicus: Nakaseko and Nishimura, 1981, p. 143, pl. 12, figs. 1 and 2; pl. 17, fig. 8.

Holotype. Osaka University, Japan, holotype has not been designated, but the specimen illustrated by Nakaseko and Nishimura (1981, pl. 12, fig. 2) may in future be designated as a lectotype; southwestern Japan, Shimanto Group, Borehole 5a; Lower Cretaceous, Albian.

Occurrence. Albian of Japan; Middle Cenomanian of northern Turkey.

Material. Five specimens.

Amphipyndax ellipticus Nakaseko et Nishimura, 1981

Plate 9, figs. 10 and 12

Amphipyndax ellipticus: Nakaseko and Nishimura, 1981, p. 144, pl. 12, figs. 7, 8a, and 8b.

Holotype. Osaka University, southwestern Japan, Shimanto Group; upper Lower Cretaceous–lower Upper Cretaceous, Albian–Cenomanian (Nakaseko and Nishimura, 1981, p. 144, pl. 12, figs. 7, 8a, 8b).

Occurrence. Albian–Cenomanian of the Pacific Ocean; Middle–Upper Cenomanian of northern Turkey.

Material. Six specimens.

Amphipyndax stocki (Campbell et Clark, 1944)

Plate 9, figs. 9 and 11; Plate 32, fig. 8

Stichocapsa (?) stocki: Campbell, Clark, 1944, p. 44, pl. 8, figs. 31–33.

Stichocapsa megalocephalia: Campbell, Clark, 1944, p. 44, pl. 8, figs. 26 and 34.

Dictyomitra pyramidalis: Kozlova in Kozlova, Gorbovets, 1966, p. 116, pl. 6, fig. 1.

Stichocapsa pyramidata: Amon, 2000, pl. 10, fig. 13.

Amphipyndax stocki: Foreman, 1968 p. 78, pl. 8, figs. 12a–12c; Schmidt-Effing, 1980, fig. 6; Taketani, 1982, p. 52, pl. 2, figs. 9a and 9b; pl. 10, figs. 13 and 14; Iwata and Tajika, 1986, pl. 1, fig. 2; Kazintsova, 1993, p. 70, pl. IV, fig. 10; pl. VIII, fig. 4; pl. XI, fig. 7; pl. XVII, fig. 7; pl. XXII, fig. 6; O'Dogherty, 1994, p. 147, pl. 18, figs. 13–15; Sporli and Aita, 1994, pl. 1, fig. 8; Khokhlova *et al.*, 1994, pl. 13.1.12; Ling *et al.*, 1996, pl. 2, fig. 15; Hashimoto and Ishida, 1997, pl. 2, fig. 17; Hollis, 1997, pl. 15, figs. 5, 6, and 8; Vishnevskaya, 2001, pl. 4, figs. 11–13.

Protoamphipyndax stocki: Ling, 1991, pl. 3, fig. 6.

? *Amphipyndax stocki*: Hollis, 1997, pl. 15, figs. 7 and 9.

Non *Amphipyndax stocki*: Petrushevskaya and Kozlova, 1972, p. 545, pl. 8, figs. 16 and 17 (= *A.* ex gr. *A. pseudoconulus* (Pessagno, 1963)).

Non *Stichomitra* sp.: Vishnevskaya, 2001, pl. 4, fig. 5.

Holotype. California, Tesla County, Moreno Formation; Upper Cretaceous, Campanian (Campbell and Clark, 1944, pl. 8, fig. 33).

Description. The shell is multichambered and conical, gradually widening towards the last chamber, which narrows slightly toward the aperture. The cephalis is subspherical and divided into an upper (spherical) and a lower (ellipsoidal) parts. The cephalis lacks pores and an apical horn. The outer constrictions (if present) are poorly defined. The inner septa are incomplete. The chambers gradually increase in height and width. The shell is pierced with rounded pores, which are arranged in two or three rows on each chamber in hexagonal and pentagonal patterns. The pore frames are polygonal but may be absent from some specimens. Some shells have a tubular aperture.

Measurements. Shell length, 330–150; maximal width, 131–75.

Comparison. *A. stocki* differs from *A. pseudoconulus* (Pessagno, 1963) in the absence of nodes on the shell surface.

Occurrence. Albian–Maastrichtian, worldwide; Lower Turonian of the Crimean Mountains; Middle–Upper Cenomanian of northern Turkey.

Material. More than 20 specimens.

Family Williriedellidae Dumitrica, 1970
Genus *Holocryptocanium* Dumitrica, 1970

Holocryptocanium: Dumitrica, 1970, p. 75; Pessagno, 1977, p. 40.

Type species. *Holocryptocanium tuberculatum* Dumitrica, 1970; Upper Cretaceous, Cenomanian, locality of Podu Dûmboviţei, Romania.

Diagnosis. Three-chambered shell with cephalothorax completely encased in abdomen. Abdomen spherical or subspherical, larger in size than cephalis and thorax.

Species composition. *H. astiensis* Pessagno, 1977; *H. barbui* Dumitrica, 1970; *H. geysersensis* Pessagno, 1977; and *H. tuberculatum* Dumitrica, 1970; Albian–Campanian, worldwide.

Comparison. *Holocryptocanium* differs from *Hemicryptocapsa* Dumitrica, 1970 in the completely hidden cephalothorax and occasional absence of the apertural pore.

Holocryptocanium astiensis Pessagno, 1977

Plate 10, fig. 11

Holocryptocanium astiensis: Pessagno, 1977, p. 40, pl. 6, figs. 16 and 21; Non *Holocryptocanium astiensis*: Salvini and Marcucci Passerini, 1998, fig. 6.j. (= *H.* ex gr. *H. geysersensis* Pessagno, 1977).

Holocryptocanium cf. *tuberculatum*: Teraoka, Kurimoto, 1986, pl. 4, fig. 2.

Holotype. USNM-Pessagno, no. 242820; California coast, Great Valley sequence, Locality MG 236, Franciscan Formation; Upper Cretaceous, Lower Cenomanian (Pessagno, 1977, pl. 6, fig. 21).

Comparison. *H. astiensis* differs from *H. tuberculatum* Dumitrica, 1970 in that the tubercles are hemispherical, less abundant, and larger in size.

Occurrence. Albian–Cenomanian, worldwide; Middle–Upper Cenomanian of northern Turkey.

Material. More than ten specimens.

Holocryptocanium barbui Dumitrica, 1970, emend. herein

Plate 10, fig. 12; Plate 31, figs. 1 and 2

Holocryptocanium barbui: Dumitrica, 1970, p. 76, pl. 17, figs. 105–108a; pl. 21, fig. 136; 1975, p. 87–89, text-fig. 2, fig. 1; Pessagno, 1977, p. 40, pl. 6, fig. 18; Nakaseko *et al.*, 1979, p. 23, pl. 5, fig. 6; Schaaf, 1981, pl. 10, figs. 6a and 6b; Teraoka and Kurimoto, 1986, pl. 4, fig. 1; pl. 2, fig. 1; Thurow, 1988, p. 401, pl. 5, figs. 5–8; Erbacher, 1994, pl. 5, fig. 8; pl. 13, fig. 11; Hashimoto and Ishida, 1997, pl. 1, fig. 8; Salvini and Marcucci, 1998, text-fig. 8.a; Bragin *et al.*, 2000, text-fig. 3.G; Vishnevskaya, 2001, pl. 22, figs. 1–3; pl. 84, figs. 1–6.

Holocryptocanium sp.: Erbacher, 1994, pl. 5, fig. 9.

Non *Holocryptocanium barbui*: Amon, 2000, p. 69, pl. 9, fig. 14 (= *H.* cf. *H. tuberculatum* Dumitrica, 1970).

Holocryptocanium barbui barbui: Nakaseko and Nishimura, 1981, p. 153, pl. 3, figs. 1–4.

Holocryptocanium barbui japonicum: Nakaseko and Nishimura, 1981, p. 154, pl. 3, figs. 5–7.

Holotype. Personal collection of Dumitrica, no. 1477-7; Romania, locality of Podu Dûmboviţei; Upper Cretaceous, Cenomanian (Dumitrica, 1970, pl. 17, figs. 108a, 108b).

Description. The shell is spherical. The cephalothorax is completely hidden. The cephalis is spherical and virtually without pores. Its upper part is incorporated into the lower layer of the double-layered wall of the abdomen. The thorax is subspherical, twice as large as the cephalis in diameter, and covered with rounded to polygonal pores. The pore diameter is equal to or greater than the distance between pores. The pore frames are polygonal, with the vertices elevated in lateral view and terminated with triangular spines. The thorax is connected with the abdomen by thin long beams extending from the upper part of the thorax. The lower part of the thorax terminates with a circular open-

Explanation of Plate 10

Figs. 1, 2, 4, and 5. *Diacanthocapsa ancus* (Foreman, 1968), specimens: (1) GIN, no. 4871/102, ×370; (2) GIN, no. 4871/103, ×370; (4) GIN, no. 4871/104, ×250; and (5) GIN, no. 4871/107, ×200.

Figs. 3 and 7. *Diacanthocapsa antiqua* (Squinabol, 1903): specimens: (3) GIN, no. 4871/105, ×500; and (7) GIN, no. 4871/106, ×160.

Fig. 6. *Diacanthocapsa matsumotoi* (Taketani, 1982), GIN, no. 4871/108, ×220.

Fig. 8. *Diacanthocapsa elongata* sp. nov., holotype GIN, no. 4871/109, ×450.

Fig. 9. *Diacanthocapsa euganea* (Squinabol, 1903), GIN, no. 4871/110, ×400.

Fig. 10. *Holocryptocanium geysersensis* Pessagno, 1977, GIN, no. 4871/111, ×200.

Fig. 11. *Holocryptocanium astiensis* Pessagno, 1977, GIN, no. 4871/112, ×300.

Fig. 12. *Holocryptocanium barbui* Dumitrica, 1970, GIN, no. 4871/113, ×250.

Figs. 4 and 9. From the Tomalar section. Others come from the Ürküt section.

Plate 10

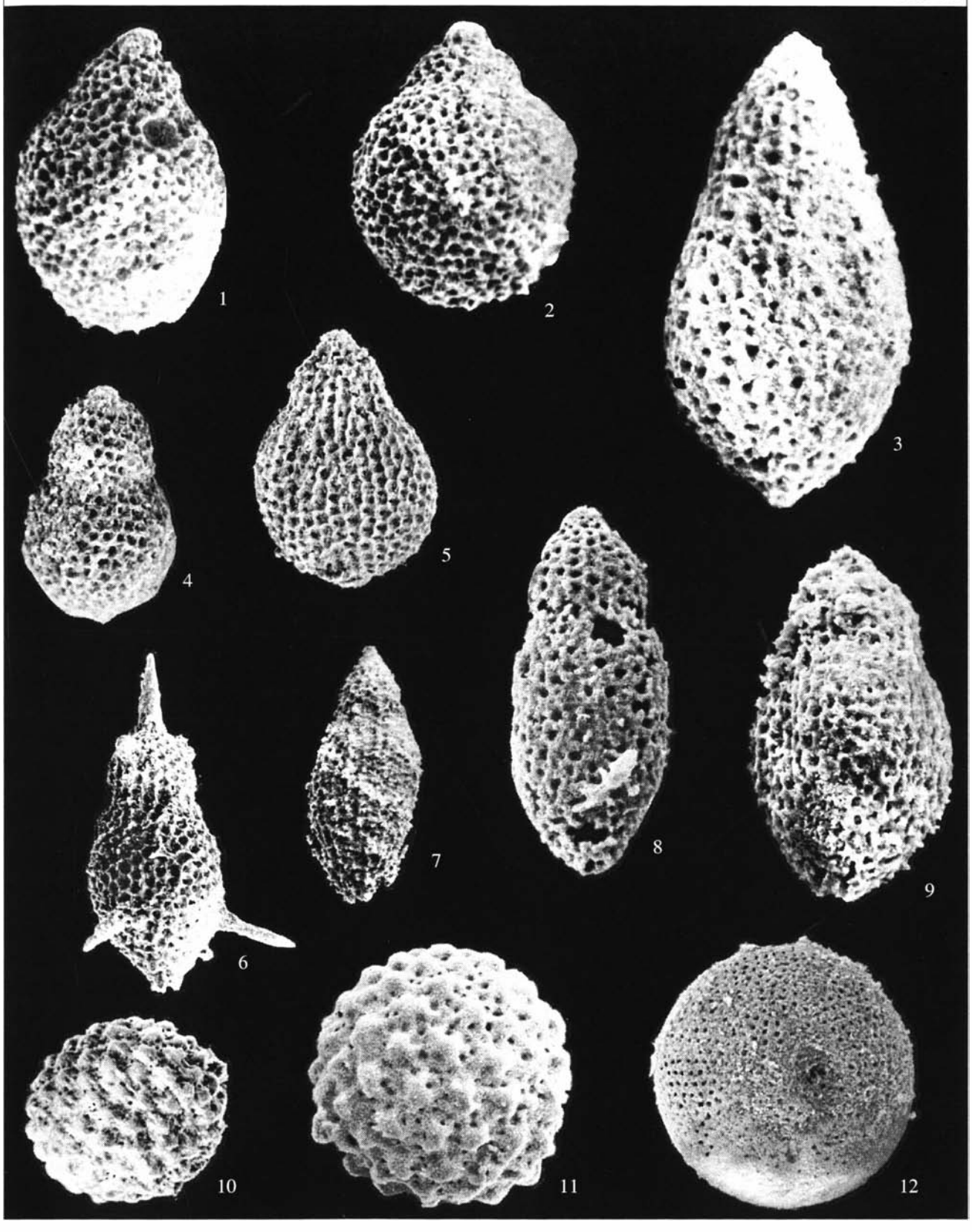

ing and, usually, with three massive spines. The abdomen is spherical, except for a small depression above the cephalis, six to nine times as large as the thorax, with double-layered wall. The abdomen is covered with small rounded pores arranged in hexagonal to pentagonal patterns. The pore diameter is less than the distance between pores. The pore frames resemble honeycombs, with vertices elevated in lateral view. Some specimens lack pore frames. The abdomen terminates with a small circular aperture. Some well-preserved specimens exhibit a thin-walled hemispherical velum closing the depression characteristic of this species.

Measurements. Abdomen diameter, 200–160.

Comparison. *H. barbui* differs from *H. geysersensis* Pessagno, 1977 in the absence of abdominal tubercles.

Remarks. *H. japonicum* Nakaseko et Nishimura, 1981 is a form of the widely variable species *H. barbui* Dumitrica, 1970.

Occurrence. Albian–Turonian, worldwide; Middle–Upper Cenomanian of northern Turkey; Lower Turonian of the Crimean Mountains.

Material. More than ten specimens.

Holocryptocanium geysersensis Pessagno, 1977

Plate 10, fig. 10

Holocryptocanium geysersensis: Pessagno, 1977, p. 41, pl. 6, figs. 19, 25, and 26.

Holotype. USNM-Pessagno, no. 242821; California coast, Great Valley sequence, Locality MG 236, Franciscan Formation; Upper Cretaceous, Lower Cenomanian (Pessagno, 1977, pl. 6, figs. 19, 25).

Comparison. *H. geysersensis* differs from *H. astiensis* Pessagno, 1977 in the conical tubercules and in the greater numbers of tubercles per half-circle.

Occurrence. Lower Cenomanian of California; Middle Cenomanian of northern Turkey.

Material. Six specimens.

Genus *Diacanthocapsa* Squinabol, 1903, emend. herein

Diacanthocapsa: Squinabol, 1903, p. 133; Dumitrica, 1970, p. 61.

Type species. *Diacanthocapsa euganea* Squinabol, 1903; upper Lower Cretaceous–lower Upper Cretaceous, Middle Albian–Cenomanian; Teolo Locality, southern Venetian Alps, northern Italy.

Diagnosis. Shell cryptocephalic, three-chambered. Cephalis small, hemispherical, usually without pores, without apical horn. Cephalis encased partly or completely in thorax. Thorax barrel-shaped with compressed aperture. Abdomen varies in shape from barrel-shaped to tear-shaped and to almost regularly spherical. Abdomen considerably larger than thorax and, sometimes, triangular in cross section. Both thorax and abdomen possess pores. Abdomen sometimes terminates with small narrow aperture.

Species composition. Tens of species, including *D. aksuderensis* sp. nov., *D. elongata* sp. nov., *D. inflata* sp. nov., *D. tavridae* sp. nov., and *D. urkutica* sp. nov.; Cretaceous–Paleogene, worldwide.

Comparison. *Diacanthocapsa* differs from *Turbocapsula* O'Dogherty, 1994 in the absence of costae from the shell surface.

Remarks. In modern practice, morphotypes with a centrally placed apical horn on the cephalis top are attributed to *Diacanthocapsa*.

Diacanthocapsa acuminata Dumitrica, 1970

Plate 11, figs. 11 and 14

Diacanthocapsa acuminata: Dumitrica, 1970, p. 65, pl. VII, figs. 38, 39a, 39b, and 43.

Non *Eustonerius acuminatus*: Pignotti, 1994, pl. 1, fig. 6.

? *Diacanthocapsa acuminata*: Nakaseko and Nishimura, 1981, p. 149, pl. 5, figs. 7 and 8 (= *D.* ex gr. *D. acuminata* Dumitrica, 1970).

Holotype. Personal collection of Dumitrica, no. 1625-10; Romania, locality of Valea Mare; Upper Cretaceous, Lower Campanian (Dumitrica, 1970, pl. VII, fig. 38).

Remarks. *D. acuminata* Dumitrica, 1970 is usually common in Campanian deposits, but in the region under consideration in this paper, some specimens of this species were found in much older deposits.

Occurrence. Lower Campanian of Romania; Middle–Upper Cenomanian of northern Turkey.

Material. Fifteen specimens.

Diacanthocapsa aksuderensis Bragina, sp. nov.

Plate 31, fig. 10

Etymology. From the Aksudere Gully in the Crimean Mountains, where it was first discovered.

Holotype. GIN, no. 4870/12; Crimean Mountains, Aksudere Gully section, Lower Turonian.

Explanation of Plate 11

Figs. 1–5. *Cryptamphorella micropora* sp. nov., specimens: (1) paratype GIN, no. 4871/114, ×275; (2) GIN, no. 4871/115, ×250; (3) holotype GIN, no. 4871/116, ×250; (4) GIN, no. 4871/117, ×250; and (5) GIN, no. 4871/118, ×275.

Figs. 6 and 7. *Diacanthocapsa brevithorax* Dumitrica, 1970, specimens (6) GIN, no. 4871/119, ×200; (7) GIN, no. 4871/120, ×350.

Fig. 8. *Diacanthocapsa betica* O'Dogherty, 1994, GIN, no. 4871/121, ×400.

Figs. 9, 10, and 12. *Immersothorax cyclops* Dumitrica, 1970, specimens: (9) GIN, no. 4871/122, ×300; (10) GIN, no. 4871/123, ×550; and (12) GIN, no. 4871/124, ×400.

Fig. 11, 14. *Diacanthocapsa acuminata* Dumitrica, 1970, specimens: (11) GIN, no. 4871/125, ×350; and (14) GIN, no. 4871/126, incomplete, ×400.

Fig. 13. *Diacanthocapsa urkutica* sp. nov., holotype GIN, no. 4871/127, ×200.

All specimens come from the Ürküt section.

Plate 11

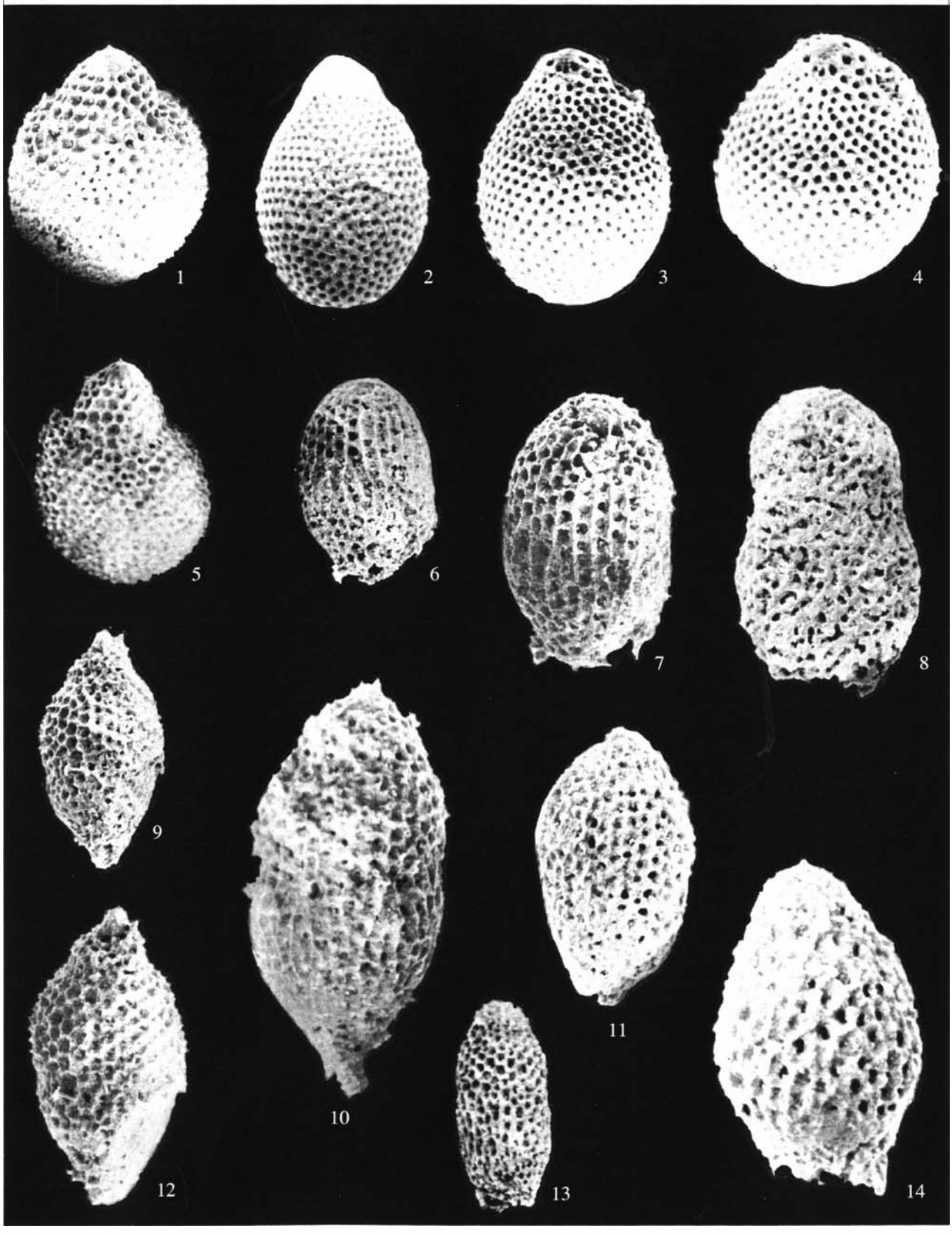

Description. The shell is fusiform. The cephalis is subspherical and bears a short apical horn and fine, frequently blind, randomly arranged pores. The thorax is barrel-shaped, 1.5 times the height and twice the width of the cephalis. The pores are rounded, cover the entire thorax, and are arranged in pentagonal and hexagonal patterns. The pore frames are pentagonal and hexagonal. Their vertices are raised and terminate with spinules. The outer constriction between the thorax and abdomen is indistinct. The distance between pores is less than or equal to the pore diameter. The abdomen is slightly wider than the thorax and less distinctly barrel-shaped. Distally, the abdomen gradually narrows to form a long, wide apertural tube. The apertural pores are sparse and randomly arranged.

Measurements. Shell length, 220; width, 105.

Comparison. *D. aksuderensis* differs from *D. matsumotoi* (Taketani, 1982) in the shorter apical horn, larger cephalis, smaller abdomen, long, wide aperture, and fusiform shell.

Remarks. Like *D. matsumotoi* (Taketani, 1982), it has an apical horn, a feature which is not typical of congeneric species.

Occurrence. Crimean Mountains, Aksudere Gully, Lower Turonian.

Material. Five complete and four incomplete specimens.

Diacanthocapsa ancus (Foreman, 1968)

Plate 10, figs. 1, 2, 4, and 5; Plate 31, figs. 6 and 7

Theocapsomma ancus: Foreman, 1968, p. 32, pl. 4, fig. 3.

Diacanthocapsa cf. *ancus*: Dumitrica, 1970, p. 64, pl. VI, figs. 35a and 35b; pl. VII, fig. 40; pl. XX, fig. 125; Nakaseko and Nishimura, 1981, p. 149, pl. 5, fig. 5; Ishida and Hashimoto, 1996, text-fig. 3.22; Hashimoto and Ishida, 1997, pl. 1, fig. 20; pl. 2, fig. 13.

Diacanthocapsa umbilicata: Hashimoto and Ishida, 1997, pl. 1, fig. 12.

Non *Diacanthocapsa ancus*: Iwata and Tajika, 1986, pl. 4, fig. 8 (= *D. teren* (Foreman, 1968)); Schaaf, 1981, pl. 24, figs. 9a and 9b (= *D. teren* (Foreman, 1968)); Thurow, 1988, pl. 4, fig. 8 (= *D.* ex gr. *D. galeata* Dumitrica, 1970).

Immersothorax marinae: Amon, 2000, p. 64, pl. 9, fig. 5.

Holotype. USNM, no. 159949; California, Moreno Formation, Locality 1144; Upper Cretaceous, Upper Maastrichtian (Foreman, 1968, pl. 4, fig. 3).

Comparison. *D. ancus* differs from *D. teren* (Foreman, 1968) in the arrangement of the pores in hexagonal and pentagonal patterns rather than in longitudinal rows.

Remarks. Unlike *D. ancus* (Foreman, 1968), it shows considerable variation in the shape of the abdomen.

Occurrence. Cenomanian–Maastrichtian, worldwide; Middle–Upper Cenomanian of northern Turkey; Lower Turonian of the Crimean Mountains.

Material. More than 20 specimens.

Diacanthocapsa antiqua (Squinabol, 1903), emend. herein

Plate 10, figs. 3 and 7; Plate 31, figs. 11 and 12; Plate 32, fig. 2

Theocorys antiqua: Squinabol, 1903, p. 135, pl. 8, fig. 25.

Myllocercion cf. *acineton*: Marcucci *et al.*, 1991, text-fig. 4.

Eustonerius acuminatus: Pignotti, 1994, pl. 2, fig. 2.

Diacanthocapsa antiqua: O'Dogherty, 1994, p. 220, pl. 36, figs. 25–28.

Holotype. Northern Italy, southern Venetian Alps, Colli Euganei, Teolo Locality; upper Lower Cretaceous–lower Upper Cretaceous, Upper Albian–Lower Turonian (Squinabol, 1903, pl. 8, fig. 25).

Description. The shell is tear-shaped and has a subspherical cephalis half-hidden in the thorax. The cephalic pores are few, small, rounded, and randomly arranged. The thorax is barrel-shaped, 3 times as wide and 2 to 2.5 times as long as the cephalis, and is covered with rounded pores that are arranged hexagonally and pentagonally in pore frames resembling honeycombs. The abdomen is one-third wider and 2 to 3.5 times as long as the thorax. Owing to barely perceptible surface depressions, the abdomen is irregularly rounded in cross section. The abdominal pores tend to be arranged in indistinct longitudinal rows. The pores are set in barely perceptible irregular frames with fine secondary spines at their vertices. Occasionally the abdomen has weakly developed longitudinal striations. The aperture is rounded, almost completely closed, or indistinctly tubular.

Measurements. Shell length, 210–155, maximal width, 110–89.

Comparison. *D. antiqua* differs from *D. ovoidea* Dumitrica in the incompletely hidden cephalis and abdominal depressions.

Occurrence. Upper Albian–Lower Turonian of Italy and Spain; Upper Cenomanian of northern Turkey; Lower Turonian of the Crimean Mountains.

Material. More than ten specimens.

Diacanthocapsa betica O'Dogherty, 1994, emend. herein

Plate 11, fig. 8; Plate 31, fig. 14

Diacanthocapsa betica: O'Dogherty, 1994, p. 216, pl. 36, figs. 1–7.

Holotype. UL, no. 9967; Spain, Betic Cordillera, Locality Mc-268b, Carbonero Formation; Middle Aptian (O'Dogherty, 1994, pl. 36, fig. 1).

Description. The shell is three-chambered, with a small, partly hidden cephalis. The cephalis is subspherical, without an apical horn or pores. There is no outer constriction between the thorax and the cephalis. The thorax is subspherical, much larger (four to six times) than the cephalis. The outer constriction (if any) between the thorax and the abdomen is poorly defined. Between the thorax and the abdomen there is a sutural pore that is three or four times larger in diameter than the pores on the shell surface. The abdomen is barrel-shaped, equal to or slightly larger in size than the thorax. The lumbar stricture is poorly developed. The thorax and abdomen are porous. The pores are fine, rounded to oval, varying in size, and randomly arranged. The striation on the thorax and abdomen is weak.

Measurements. Shell length, 153–80; maximal width, 90–63.

Comparison. *D. betica* differs from *D. ovoidea* Dumitrica, 1970 in the wider shell and larger sutural pore and from *D. ancus* (Foreman, 1968) in the cephalis completely encased in the thorax and striation between pores.

Remarks. Early Turonian specimens have more widely spaced pores and a less elongated shell.

Occurrence. Lower–Middle Aptian of Italy; Upper Cenomanian of northern Turkey; Lower Turonian of the Crimean Mountains.

Material. Nine specimens.

Diacanthocapsa brevithorax Dumitrica, 1970

Plate 11, figs. 6 and 7

Diacanthocapsa brevithorax: Dumitrica, 1970, p. 62, pl. VII, fig. 41.

Holotype. Collection of Dumitrica, no. 1629-2; Romania, Podu Dâmboviţei; Upper Cretaceous, Cenomanian (Dumitrica, 1970, pl. VII, fig. 41).

Comparison. *D. brevithorax* differs from *D. betica* O'Dogherty (1994) in the longitudinal costae of the thorax and abdomen.

Occurrence. Cenomanian of Romania; Upper Cenomanian of northern Turkey.

Material. Eight specimens.

Diacanthocapsa elongata Bragina, sp. nov.

Plate 10, fig. 8; Plate 32, fig. 1

Etymology. From the Latin *elongatus* (elongate).

Holotype. GIN, no. 4871/109; Northern Turkey, Tomalar Formation, Ürküt section, Middle Cenomanian.

Description. The shell is fusiform and consists of three chambers. The cephalis is hemispherical, without an apical horn, and partly encased in the thorax. The thorax is spherical to barrel-shaped and bears large rounded pores in hexagonal pore frames. The frame vertices are slightly raised. The thorax is more than twice the height and width of the cephalis, but half the height and a quarter of the diameter of the abdomen. The abdomen looks like an extremely elongated ellipse in longitudinal section, and is circular in cross section. It terminates in a small aperture. The thoracic and abdominal pores are equal in size. The abdominal pores are arranged in pentagonal and hexagonal patterns. The pore frames of the abdomen are indistinct in outline.

Measurements. Shell length, 150–300, maximal width, 90–125.

Comparison. *D. elongata* differs from *D. fossilis* (Squinabol, 1904) in the more widely spaced abdominal pores and less inflated, rounded (not nearly triangular) cross section of the abdomen.

Occurrence. Middle Cenomanian of northern Turkey; Lower Turonian of the Crimean Mountains.

Material. Three complete and seven incomplete specimens.

Diacanthocapsa euganea Squinabol, 1903

Plate 10, fig. 9

Diacanthocapsa euganea: Squinabol, 1903, p. 133, pl. 8, fig. 26; Taketani, 1982, p. 68, pl. 8, figs. 2a–3b; pl. 12, fig. 15; Kato and Iwata, 1989, pl. 8, fig. 4; Tumanda, 1989, p. 36, pl. 7, fig. 5; O'Dogherty, 1994, p. 218, pl. 36, figs. 19–21; Salvini and Marcucci Passerini, 1998, text-fig. 6e.

Non *Diacanthocapsa euganea*: Erbacher, 1994, pl. 19, fig. 12 (= *D.* ex gr. *D. amphora* (Campbell et Clark, 1944)).

Holotype. Northern Italy, southern Venetian Alps, Colli Euganei, Teolo Locality; upper Lower Cretaceous–lower Upper Cretaceous, Middle Albian–Cenomanian (Squinabol, 1903, pl. 8, fig. 26).

Comparison. *D. euganea* differs from *D. antiqua* (Squinabol, 1903) in the smaller thorax and less inflated abdomen, which is larger than the thorax.

Occurrence. Middle Albian–Lower Turonian, worldwide; Upper Cenomanian of northern Turkey.

Material. More than ten specimens.

Diacanthocapsa fossilis (Squinabol, 1904)

Plate 31, fig. 13

Dicolocapsa fossilis: Squinabol, 1904, p. 218, pl. 7, fig. 19.

Diacanthocapsa brevithorax: Nakaseko et al., 1979, p. 149, pl. 5, fig. 6.

Diacanthocapsa fossilis: O'Dogherty, 1994, p. 217, pl. 36, figs. 8–11.

Holotype. Northern Italy, southern Venetian Alps, Colli Euganei, Teolo Locality; upper Lower Cretaceous–lower Upper Cretaceous, Middle Albian–Cenomanian (Squinabol, 1904, pl. 7, fig. 19).

Comparison. *D. fossilis* differs from *D. ovoidea* Dumitrica, 1970, in the subtriangular cross section of the abdomen.

Occurrence. Middle Albian–Lower Turonian of Italy and Japan; Lower Turonian of the Crimean Mountains.

Material. More than 20 specimens.

Diacanthocapsa inflata Bragina, sp. nov.

Plate 31, fig. 9

Etymology. From the Latin *inflatus* (inflated).

Holotype. GIN, no. 4870/11; Crimean Mountains, Belaya Mountain section, Lower Turonian.

Description. The shell has a completely hidden cephalis. The thorax is wide, hemispherical. The outer constriction between the thorax and abdomen is poorly defined. The abdomen is shaped like a barrel and rapidly tapers distally. The abdomen terminates in a small aperture. The abdomen slightly exceeds the thorax in width. The thorax and abdomen are covered with small pores arranged in a hexagonal pattern. The pore frames are poorly developed, most commonly hexagonal, with sharp spines at their vertices that make the shell surface thorny. The thorax and abdomen have low indistinct longitudinal costae. The number of costae per half-circle is 15–17 on the thorax and 20 or 21 on the abdomen.

Measurements. Shell length, 230; maximal width, 175.

Comparison. *D. inflata* differs from *D. acuminata* Dumitrica, 1970 in that the thorax and cephalis are

of almost equal height and in the more indistinct and low longitudinal costae.

Remarks. The following phylogenetic lineage is possible: Early Cenomanian *D. acuminata* Dumitrica, 1970–Turonian *D. inflata* sp. nov.–Campanian *D.* sp. Dumitrica, 1970.

Occurrence. Lower Turonian of the Crimean Mountains.

Material. Four complete and four incomplete specimens.

Diacanthocapsa matsumotoi (Taketani, 1982)

Plate 10, fig. 6

Eusyringium (?) matsumotoi: Taketani, 1982, p. 57, pl. 4, figs. 1a–3b; pl. 11, fig. 12.

Diacanthocapsa matsumotoi: O'Dogherty, 1994, p. 219, pl. 36, figs. 22–24.

Holotype. Tohoku University, Japan, IGPS, no. 97538; Japan, Urakawa Formation, Yezo Group; Upper Cretaceous, Coniacian–Santonian (Taketani, 1982, pl. 4, figs. 3a, 3b).

Remarks. *D. matsumotoi* differs from the typical representatives of *Diacanthocapsa* in having a thick apical horn.

Occurrence. Upper Cretaceous of the Pacific and Tethys; Middle–Upper Cenomanian of northern Turkey.

Material. Five specimens.

Diacanthocapsa rara (Squinabol, 1904)

Plate 31, figs. 4 and 5

Diacanthocapsa rara: Squinabol, 1904, p. 218, pl. 7, fig. 17; Salvini and Marcucci Passerini, 1998, text-fig. 9.p.

Holotype. Northern Italy, southern Venetian Alps, Teolo Series, Scaglia Bianca Formation; upper Lower Cretaceous–lower Upper Cretaceous, Middle Albian–Cenomanian (Squinabol, 1904, pl. 7, fig. 17).

Comparison. *D. rara* differs from *D. antiqua* (Squinabol, 1903) in the more inflated and larger abdomen.

Occurrence. Middle Albian–Cenomanian of Italy and Spain; Lower Turonian of the Crimean Mountains.

Material. Twelve specimens.

Diacanthocapsa tavridae Bragina, sp. nov.

Plate 31, fig. 8

Etymology. From Tavrida, the ancient name of the Crimea.

Holotype. GIN, no. 4870/10; Crimean Mountains, Belaya Mountain section, Lower Turonian.

Description. The shell has a subspherical cephalis slightly hidden in the thorax. The cephalic pores are rounded, rare, small, and randomly arranged. The thorax is shaped like a dome and narrows distally to form a cylinder. The thorax is 3.5 times wider and 4 times longer than the cephalis. The thoracic pores are rounded, of variable size, set in pore frames resembling honeycombs, and arranged in hexagonal and pentagonal patterns, with slightly raised vertices. The abdomen is elliptical, one-fourth wider and one-fifth longer than the thorax. The abdominal pores are arranged in pentagonal and hexagonal patterns and tend to form indistinct transverse rows distally. The pore frames resemble irregular honeycombs. The aperture is circular and almost completely closed.

Measurements. Shell length, 250; maximal width, 125.

Comparison. *D. tavridae* differs from *Diacanthocapsa ancus* (Foreman, 1968) in the subcylindrical thorax and narrower abdomen.

Occurrence. Lower Turonian of the Crimean Mountains.

Material. Four complete and seven incomplete specimens.

Diacanthocapsa urkutica Bragina, sp. nov.

Plate 11, fig. 13

Etymology. From the Ürküt section, where it was first discovered.

Holotype. GIN, no. 4871/127; northern Turkey, Tomalar Formation, Ürküt section; Upper Cenomanian.

Description. The shell is fusiform and consists of three chambers. The cephalis is completely encased in the thorax. The thorax is barrel-shaped and has rounded pores in hexagonal pore frames with slightly raised vertices. The outer constriction between the thorax and abdomen is poorly defined. The abdomen is 1.5 times higher than the thorax but is equal in length. The abdomen is circular in cross section. The abdominal pores are slightly smaller than those on the thorax, and are arranged in pentagonal and hexagonal patterns in indistinct pore frames. The abdomen tapers toward the aperture, where the abdominal pores become much smaller.

Measurements. Shell length, 190; maximal width, 75.

Comparison. *D. urkutica* differs from *D. acuminata* Dumitrica, 1970 in the completely hidden cephalis, the absence of costae on the thorax and abdomen, and the narrower shell.

Occurrence. Upper Cenomanian of northern Turkey, Ürküt section.

Material. Four complete and three incomplete specimens.

Genus *Gongylothorax* Foreman, 1968

Gongylothorax verbeeki (Tan Sin Hok, 1927)

Plate 36, fig. 8

Dicolocapsa verbeeki: Tan Sin Hok, 1927, p. 44, pl. 8, figs. 40 and 41.

Gongylothorax verbeeki: Foreman, 1968, p. 20, pl. 2, figs. 8a–8c; Dumitrica, 1970, p. 57, pl. I, figs. 6a and 6b; pl. II, figs. 8a–8c.

Holotype. The specimen shown in figs. 40 and 41 (Tan Sin Hok, 1927, pl. 8, figs. 40, 41).

Comparison. *G. verbeeki* differs from *G. favosus* Dumitrica, 1970 in the more closely spaced pores and smaller diameter of pore frames.

Remarks. *G. verbeeki* is common in the Campanian and Maastrichtian, but scarce in the Lower Turonian of the Crimean Mountains.

Occurrence. Campanian–Maastrichtian of the Pacific and Tethys; Lower Turonian of the Crimean Mountains.

Material. Seven specimens.

Genus *Cryptamphorella* Dumitrica, 1970

Cryptamphorella: Dumitrica, 1970, p. 80.

Type species. *Hemicryptocapsa conara* Foreman, 1968; Upper Cretaceous, Upper Maastrichtian, Locality 1144, Moreno Formation, California.

Diagnosis. Shell with three chambers; thorax hidden in abdomen. Abdomen large, inflated, without aperture.

Species composition. *C. conara* (Foreman, 1968), *C. macropora* Dumitrica, 1970; *C. sphaerica* (White, 1928); and *C. micropora* sp. nov.; Cretaceous, worldwide.

Comparison. *Cryptamphorella* differs from *Hemicryptocapsa* Tan Sin Hok, 1927 in the absence of pores on the thorax.

Cryptamphorella conara (Foreman, 1968)

Plate 12, fig. 9

Hemicryptocapsa conara: Foreman, 1968, p. 35, pl. 4, figs. 11a and 11b; Bragina in: Khokhlova *et al.*, 1994, pl. 13.1.13; Hashimoto and Ishida, 1997, pl. 3, fig. 12.

Cryptamphorella conara: Dumitrica, 1970, p. 80, pl. XI, figs. 66a–66c; Salvini and Marcucci Passerini, 1998, text-fig. 7q.

Holotype. USNM, no. 157953; California, Moreno Formation, Locality 1144; Upper Cretaceous, Upper Maastrichtian (Foreman, 1968, pl. 4, figs. 11a, 11b).

Comparison. *C. conara* differs from *C. sphaerica* (White, 1928) in the greater height-to-width ratio of the abdomen and the absence of costae running from the thorax base to the cephalis top.

Occurrence. Upper Maastrichtian of California; Lower Campanian of Romania; Campanian–Maastrichtian of the Atlantic; Upper Cenomanian of northern Turkey; Lower Turonian of the Crimean Mountains.

Material. More than 20 specimens.

Cryptamphorella micropora Bragina, sp. nov.

Plate 11, figs. 1–5

Etymology. From the Latin *micro* (very small) and *porus* (pore).

Holotype. GIN, no. 4871/116; northern Turkey, Tomalar Formation, Ürküt section; Upper Cretaceous, Middle Cenomanian.

Description. The shell is shaped like a teardrop. The cephalis is hemispherical and has a hyaline wall. The thorax is twice as high and wide as the cephalis. The thoracic pores are rounded and set in penta-, or hexa-, or, occasionally, heptagonal frames. The pore diameter is greater than or equal to the distance between pores. A well-defined depression at the thoracic base indicates the presence of a sutural pore. The thorax gradually passes into the fairly rapidly widening abdomen. The abdomen is two or three times wider and three times higher than the thorax. The abdomen is elliptical to almost spherical and has pores of identical size and arrangement to those of the thorax.

Measurements. Shell length, 160; width, 120.

Comparison. The new species differs from *C. sphaerica* (White, 1928) in the finer pores and the shell with a distinct depression between the thorax base and abdomen.

Occurrence. Middle Cenomanian of northern Turkey.

Material. Eleven specimens.

Cryptamphorella sphaerica (White, 1928)

Plate 12, fig. 7; Plate 31, fig. 3; Plate 32, fig. 4

Baculogypsina (?) sphaerica: White, 1928, p. 306, pl. 41, figs. 12 and 13.

Aulonia sphaerica: Pessagno, 1962, p. 366, pl. 6, fig. 3.

Holocryptocapsa ? sphaerica: Pessagno, 1963, p. 206, pl. 1, fig. 3; pl. 5, figs. 1 and 2.

Cryptamphorella sphaerica: Dumitrica, 1970, p. 82, pl. XII, figs. 73a and 73b, 74a–74c; pl. XX, figs. 133a and 133b.

Holotype. The holotype is lost, but there are paratypes in the personal collection of Dumitrica, no. 1625-14; Romania, Valea Mare sequence; Upper Cretaceous, Lower Campanian (Dumitrica, 1970, pl. XII, figs. 73a, 73b, 74a–74c).

Occurrence. Lower Campanian of Romania; Campanian of California; Upper Cenomanian of northern Turkey; Lower Turonian of the Crimean Mountains.

Material. More than ten specimens.

Family Carpocaniidae Haeckel, 1881

Genus *Immersothorax* Dumitrica, 1970

Immersothorax cyclops Dumitrica, 1970

Plate 11, figs. 9, 10, and 12

Immersothorax cyclops: Dumitrica, 1970, p. 78, pl. XVIII, figs. 112a–112c; pl. XXI, figs. 139a and 139b.

Holotype. Personal collection of Dumitrica, no. 1625-3; Romania, Valea Mare section; Upper Cretaceous, Lower Campanian (Dumitrica, 1970, pl. XVIII, figs. 112a–112c).

Occurrence. Lower Campanian of Romania; Upper Cenomanian of northern Turkey.

Material. Five specimens.

Genus *Squinabollum* Dumitrica, 1970

Squinabollum: Dumitrica, 1970, p. 83.

Type species. *Clistosphaera fossilis* Squinabol, 1903; Middle Albian–Cenomanian, Teolo Series, southern Venetian Alps, northern Italy.

Plate 12

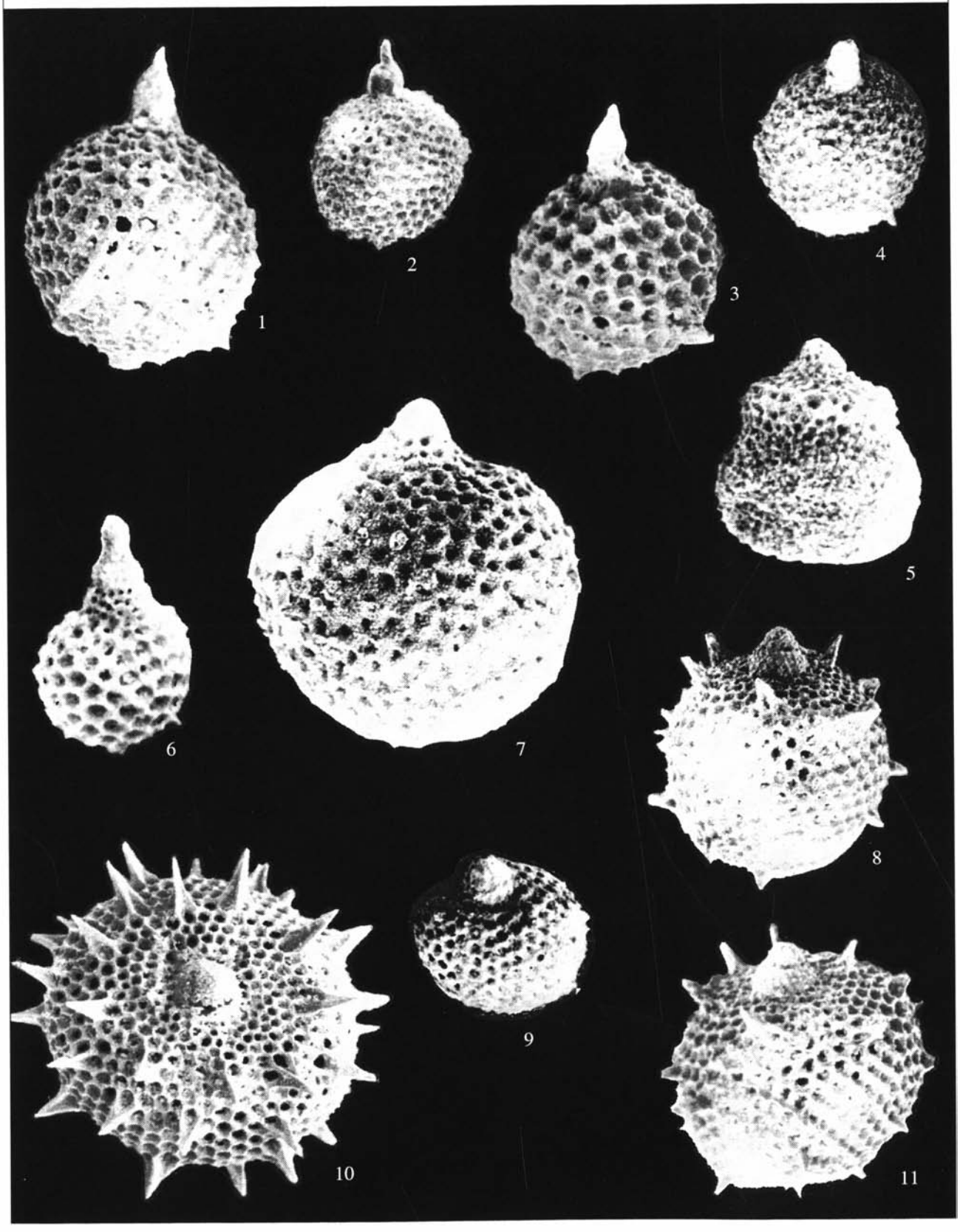

Comparison. *Squinabollum* differs from *Cryptamphorella* Dumitrica,1970 in the cephalis consisting of two (lower and upper) parts divided by an inclined plane and in the well-developed apical horn.

Species composition. The genus is monotypic, represented by *Squinabollum fossile* (Squinabol, 1903).

Squinabollum fossile (Squinabol, 1903), emend. herein

Plate 12, figs. 1–4

Clistosphaera fossilis: Squinabol, 1903, p. 130, pl. 10, fig. 11.

Squinabollum fossilis: Dumitrica, 1970, p. 83, pl. 19, figs. 118a–118c, 119a–119c; Nakaseko and Nishimura, 1981, p. 161, pl. 5, figs. 3 and 4; Taketani, 1982, p. 70, pl. 6, figs. 10a–11b; pl. 13, figs. 10 and 11; Teraoka and Kurimoto, 1986, pl. 4, fig. 4; Salvini and Marcucci Passerini, 1998, text-fig. 6s; Kazintsova, 1993, p. 66, pl. XV, fig. 7.

Squinabollum fossile: O'Dogherty, 1994, p. 203, pl. 32, figs. 4–10.

Non *Squinabollum fossilis*: Thurow, 1988, p. 406, pl. 4, fig. 21.

Non *Squinabollum fossile*: Erbacher, 1994, pl. 5, figs. 14 and 15 (= *Sethocapsa leiostraca* Foreman, 1973); Vishnevskaya, 2001, p. 187, pl. 22, figs. 7–11 (= *Sethocapsa leiostraca* Foreman, 1973).

Holotype. Northern Italy, southern Venetian Alps, Colli Euganei, Teolo Series; upper Lower Cretaceous–lower Upper Cretaceous, Middle Albian–Cenomanian (Squinabol, 1903, pl. 10, fig. 11).

Description. The shell is three-chambered. The cephalis is helmet-shaped, divided into two parts by an inclined plane. The upper part is conical apically. The thorax is cylindrical and half of the height of the cephalis. The lower parts of the cephalis and the thorax together form a cylinder. The lower part of the thorax is encased in the abdominal cavity. The abdomen is large, subspherical, and has a diameter many times greater than that of the thorax. The size of the pores and pattern of the pore frames vary considerably from specimen to specimen. Most commonly the pores are arranged in a hexagonal pattern and set in frames resembling honeycombs with ridgelike spines at the vertices. In some specimens, the pore frames may be poorly developed and the shell surface is smooth rather than thorny. The lower part of the abdomen may bear three to seven long, thin, randomly arranged secondary spines.

Measurements. Shell length, 200–152, maximal width, 150–125, length of apical horn, 40–10, length of cephalothorax, 80–50.

Remarks. Mediterranean representatives of *S. fossile* (Squinabol, 1903) described by O'Dogherty (1994) are characterized by a long apical horn and five to seven long secondary spines randomly arranged on the abdomen surface.

Occurrence. Albian–Santonian, worldwide; Upper Cenomanian of northern Turkey; Lower Turonian of the Crimean Mountains; Upper Santonian of southwestern Sakhalin (Bragina, 2001).

Material. More than 20 specimens.

Genus *Sethocapsa* Haeckel, 1881

Sethocapsa simplex Taketani, 1982

Plate 12, fig. 6

Sethocapsa simplex: Taketani, 1982, p. 63, pl. 5, figs. 8a–8c; pl. 13, fig. 1; Jud, 1994, p. 105, pl. 20, fig. 8; Urquhart and Robertson, 2000, pl. 1, fig. 17.

Siphocampium ? davidi: Schaaf, 1981, pl. 5, fig. 7.

Squinabollum fossilis: Thurow, 1988, p. 406, pl. 4, fig. 21.

Hiscocapsa asseni: O'Dogherty, 1994, p. 200, pl. 31, figs. 7–13.

Holotype. Tohoku University, Japan, IGPS, no. 97583; Cenomanian, Utafue Formation, Yezo Group, Japan (Taketani, 1982, pl. 5, figs. 8a–8c).

Occurrence. Upper Cretaceous, worldwide; Middle Cenomanian of northern Turkey.

Material. Five specimens.

Genus *Trisyringium* Vinassa, 1901

Trisyringium echitonicum (Aliev, 1967)

Plate 12, figs. 8, 10, and 11

Tricolocapsa echitonica: Aliev, 1967, p. 25, text-figs. b and c.

Gen. et sp. indet 6: Thurow, 1988, pl. 4, fig. 24.

Trisyringium echitonicum: O'Dogherty, 1994, p. 209, pl. 34, figs. 5–8.

Sethocapsa leiostraca: Erbacher, 1994, pl. 5, fig. 11.

Holotype. Northeastern Azerbaijan, Kelevudag Mountain; Lower Cretaceous, Middle Albian (Aliev, 1967, text-fig. b).

Comparison. *T. echitonicum* differs from *T. capellinii* Vinassa, 1901, in its lack of abdominal tubercles.

Occurrence. Middle Albian of Azerbaijan; Middle–Upper Albian of Italy; Middle–Upper Cenomanian of northern Turkey.

Material. Five specimens.

Genus *Pogonias* O'Dogherty, 1994

Pogonias: O'Dogherty, 1994, p. 172.

Type species. *Pogonias prodromus* O'Dogherty, 1994; Lower Cretaceous, Upper Albian, Locality Bo-685.20, Umbria-Marche Apennines, central Italy.

Explanation of Plate 12

Figs. 1–4. *Squinabollum fossile* (Squinabol, 1903), specimens: (1) GIN, no. 4871/128, ×350; (2) GIN, no. 4871/129, ×200; (3) GIN, no. 4871/130, ×300; and (4) GIN, no. 4871/131, ×200.

Fig. 5. *Pogonias ? hirsutus* (Squinabol, 1904), GIN, no. 4871/132, ×200.

Fig. 6. *Sethocapsa simplex* Taketani, 1982, GIN, no. 4871/133, ×300.

Fig. 7. *Cryptamphorella sphaerica* (White, 1928), GIN, no. 4871/134, ×350.

Figs. 8, 10, and 11. *Trisyringium echitonicum* (Aliev, 1967), specimens: (8) GIN, no. 4871/135, ×200; (10) GIN, no. 4871/137, ×350; and (11) GIN, no. 4871/136, ×200.

Fig. 9. *Cryptamphorella conara* (Foreman, 1968), GIN, no. 4871/138, ×150.

Fig. 10. From the Tomalar section. Others come from the Ürküt section.

Diagnosis. Shell two-chambered, with small spherical cephalis, usually with apical horn. Thorax subcylindrical to tetrahedral, rapidly drawn out distally into three or more appendages. Aperture closed.. Thorax and appendages porous, thick-walled, occasionally spongy. Pores rounded to hexagonal. Collar stricture between cephalis and thorax weakly developed or absent.

Species composition. *P. incallidus* O'Dogherty, 1994; *P. missilis* O'Dogherty, 1994; *P. prodromus* O'Dogherty, 1994; and *P. harpago* O'Dogherty, 1994; Middle Albian–Lower Turonian of the Tethys.

Comparison. Homeomorphic species belonging to *Sethochytris* Haeckel, 1881 appeared in the Middle Eocene.

Pogonias ? hirsutus (Squinabol, 1904), emend herein

Plate 12, fig. 5

Sethocyrtis ? hirsuta: Squinabol, 1904, p. 215, pl. 7, fig. 11.

Non *Platycryphalus* spp. aff. *P. hirsuta*: Foreman, 1975, p. 616, pl. 2G, fig. 2; pl. 6, figs. 7–9 (= *Rhopalosyringium mosquiense* (Smirnova et Aliev: in Aliev, Smirnova, 1969)).

Pogonias ? hirsutus: O'Dogherty, 1994, p. 175, pl. 25, figs. 9–13.

Holotype. Central Italy, southern Venetian Alps, Colli Euganei, Teolo Series; upper Lower Cretaceous–lower Upper Cretaceous, Upper Albian–Lower Turonian (Squinabol, 1904, pl. 7, fig. 11).

Description. The shell has three chambers. The cephalis is small, subspherical, with apical and vertical horns that are thick and three-bladed at the base and almost equally long. The thorax is barrel-shaped, rapidly inflates proximally, and is slightly higher and three or four times wider than the cephalis. The abdomen is barrel-shaped and 1.5–2 times the height of the thorax. There is a well-defined outer constriction between the thorax and abdomen. The shell is pierced with closely spaced fine pores of irregular outline. The pore frames are penta- to heptagonal, with small spines at the vertices that make the surface thorny. The thoracic pores are almost twice as large as the pores of the cephalis and abdomen, and are in considerably more ridged pore frames with more markedly raised vertices.

Measurements. Shell length, 200; thorax width, 130; abdomen width, 180.

Remarks. O'Dogherty (1994) only tentatively assigned *P. ? hirsutus* (Squinabol, 1904) to *Pogonias*. Correct generic assignment may well be possible after a thorough study of the cephalis structure of both typical forms of this genus and *P. ? hirsutus*.

Occurrence. Upper Albian–Lower Turonian of Italy; Upper Cenomanian of northern Turkey.

Material. More than ten specimens.

Pogonias missilis O'Dogherty, 1994

Plate 33, fig. 5

Pogonias missilis: O'Dogherty, 1994, p. 174, pl. 25, figs. 1–5.

Holotype. UL, no. 3295; central Italy, Umbria-Marche Apennines, Locality no. Bo-685.20; Lower Cretaceous, Upper Albian (O'Dogherty, 1994, pl. 25, fig. 1).

Comparison. *P. missilis* differs from *P. incallidus* O'Dogherty, 1994 in the presence of costae on the abdomen and the absence of arms.

Occurrence. Middle–Upper Albian of Italy and Spain; Lower Turonian of the Crimean Mountains.

Material. More than ten specimens.

Family Artostrobiidae Riedel, 1967

Genus *Siphocampe* Haeckel, 1881, sensu Nigrini, 1977

Siphocampe: Haeckel, 1881, p. 1499; Nigrini, 1977, p. 254.

Type species. *Siphocampe annulosa* Haeckel, 1887.

Diagnosis. Artostrobiidae with five, six, or more segments. No apical horn. Horizontal tubus of vertical spine (V). Post-thoracic part subcylindrical. Shell surface with grooves and small ridges. Aperture slightly narrowed.

Species composition. The type species and more than 20 species, including *S. praevanderhoofi* sp. nov.; Cretaceous–Recent, worldwide.

Comparison. *Siphocampe* differs from *Tricolocampium* Haeckel, 1887 in having more chambers and well-developed grooves and ridges.

Siphocampe altamontensis (Campbell et Clark, 1944)

Plate 13, fig. 1

Tricolocampe (Tricolocamptra) altamontensis: Campbell, Clark, 1944, p. 33, pl. 7, figs. 24 and 26.

Explanation of Plate 13

Fig. 1. *Siphocampe altamontensis* (Campbell et Clark, 1944), GIN, no. 4871/139, ×275.

Fig. 2. *Siphocampe praevanderhoofi* sp. nov., holotype GIN, no. 4871/140, ×250.

Fig. 3. *Siphocampe bassilis* (Foreman, 1968), GIN, no. 4871/141, ×400.

Figs. 4–6. *Pseudoeucyrtis spinosa* (Squinabol, 1903), specimens: (4) GIN, no. 4871/142, ×200; (5) GIN, no. 4871/143, ×100; and (6) GIN, no. 4871/144, ×100.

Fig. 7. *Tubilustrium transmontanum* O'Dogherty, 1994, GIN, no. 4871/145, ×120.

Fig. 8. *Tubilustrium guttaeformis* (Bragina, 1991), GIN, no. 4871/146, ×100.

Figs. 9–11. *Spongostichomitra phalanga* O'Dogherty, 1994, specimens: (9) GIN, no. 4871/147, ×100; (10) GIN, no. 4871/148, ×120; and (11) GIN, no. 4871/149, ×70.

Figs. 12 and 13. *Cornutella californica* Campbell et Clark, 1944, specimens: (12) GIN, no. 4871/150, ×200; and (13) GIN, no. 4871/151, ×300.

Fig. 14. *Afens liriodes* Riedel et Sanfilippo, 1974, GIN, no. 4871/152, ×80.

Fig. 14. From the Tomalar section. Others come from the Ürküt section.

Plate 13

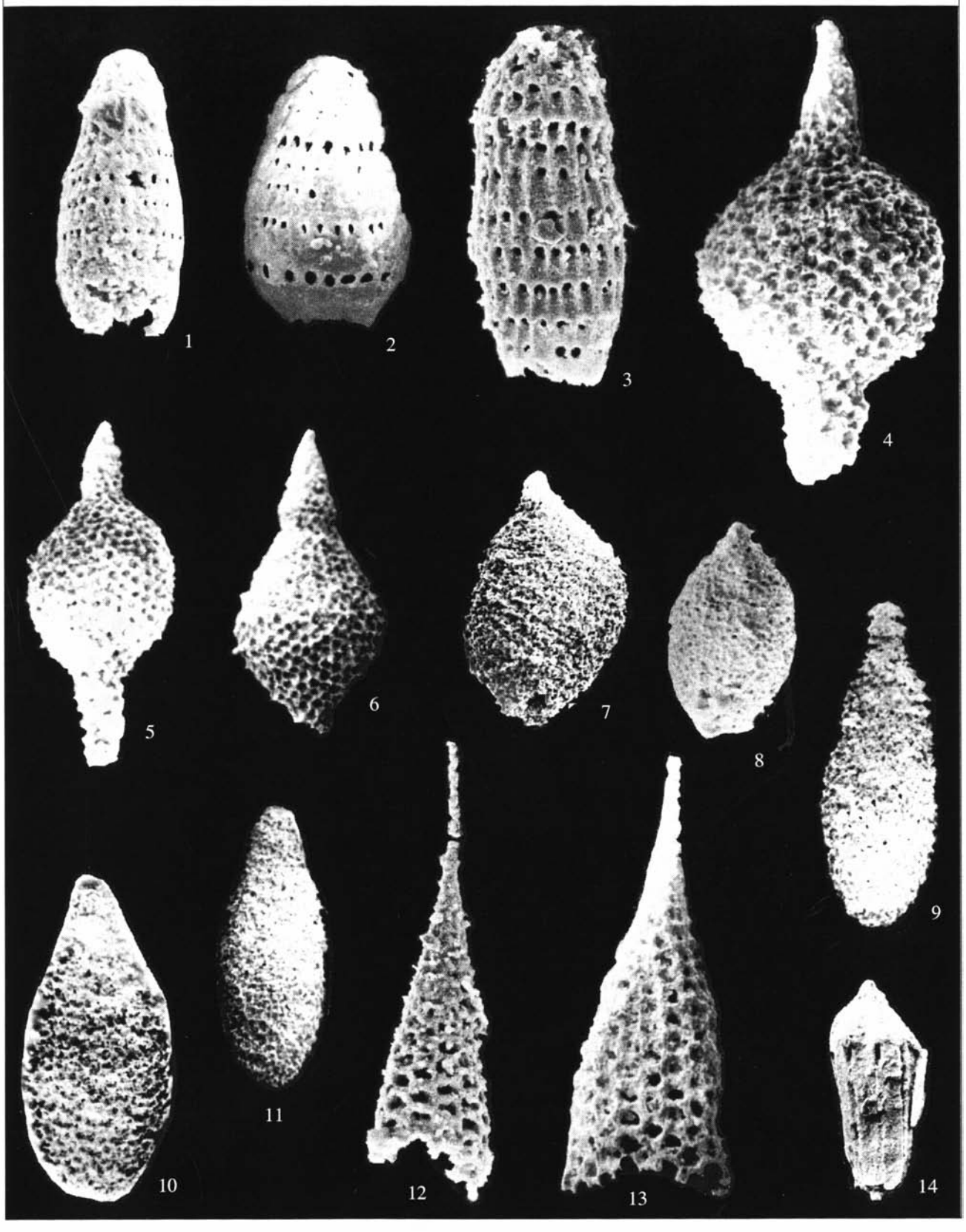

Theocampe altamontensis: Foreman, 1968, p. 53, pl. 6, figs. 14a and 14b; 1978, p. 745, pl. 5, fig. 27; Empson-Morin, 1981, p. 262, pl. 6, figs. 1A–1D; Taketani, 1982, p. 53, text-fig. 1; Vishnevskaya, 2001, p. 191, pl. 126, fig. 42.

Siphocampe altamontensis: Ling, 1991, p. 320, pl. 1, fig. 12.

Holotype. USNM, no. 34523; California, Moreno Formation, Tesla County; Upper Cretaceous, Campanian (Campbell and Clark, 1944, pl. 7, figs. 24, 26).

Remarks. This work illustrates the earliest representatives of *S. altamontensis* (Campbell et Clack, 1944), which was widespread in the Campanian and Maastrichtian. The Cenomanian specimens have characteristic features, such as a slightly wider abdomen and weakly developed striation on the cephalothorax.

Occurrence. Campanian–Maastrichtian of California, Japan, the Pacific; Upper Cenomanian of northern Turkey.

Material. Five specimens.

Siphocampe bassilis (Foreman, 1968)

Plate 13, fig. 3

Theocampe bassilis: Foreman, 1968, p. 51, pl. 6, fig. 12.

Non *Theocampe bassilis*: Ling, Lazarus, 1990, pl. 3, fig. 19 (= *Siphocampe* ex gr. *S. altamontensis* (Campbell et Clark, 1944)).

Holotype. USNM, no. 157983; California, Moreno Formation, locality of Marsha Shale; Upper Cretaceous, Upper Maastrichtian (Foreman, 1968, pl. 6, fig. 12).

Remarks. The occurrence of *S. bassilis* (Foreman, 1968) at such a low stratigraphic level (the Upper Cenomanian of northern Turkey) is unusual. It is common in the Campanian and Maastrichtian.

Occurrence. Maastrichtian of California; Upper Cenomanian of northern Turkey.

Material. Five specimens.

Siphocampe praevanderhoofi Bragina, sp. nov.

Plate 13, fig. 2

Etymology. From the Latin *prae* (pre, before) and the species name *vanderhoofi* (Campbell and Clark, 1944).

Holotype. GIN, no. 4871/140; northern Turkey, Tomalar Formation, Ürküt section, Upper Cenomanian.

Description. The shell looks like a wide cap with an inflated lower part. The cephalis is subspherical, without an apical horn. The tubus of the vertical spine is well-defined and oriented perpendicular to the main axis of the shell. The thorax is conical. The pores on the cephalis and thorax are fine, irregular in outline, and randomly arranged. The outer constriction between the thorax and abdomen is barely visible. The thorax and abdomen are separated by a transverse row of oval pores. The abdomen is inflated, barrel-shaped (with its greatest width below the middle), and gradually narrowing distally and tapering to form a wide aperture. The cephalis, thorax, and the proximal part of the abdomen have indistinct striations directed toward the main axis of the shell. The abdominal pores form distinct transverse rows. Usually there are no more than four rows. The largest pores occur at the junction of the thorax and abdomen and in the distal row.

Measurements. Shell length, 190; maximal width, 115.

Comparison. The new species differs from the typical representatives of *S. vanderhoofi* (Campbell et Clark, 1944) in the narrower abdomen and poorly pronounced striations on the shell surface.

Occurrence. Northern Turkey, Ürküt section, Upper Cenomanian.

Material. Four complete and five incomplete specimens.

Family incertae sedis

Genus *Tubilustrium* O'Dogherty, 1994

Tubilustrium guttaeformis (Bragina, 1991)

Plate 13, fig. 8; Plate 33, fig. 7

Non *Theocampe subtilis*: Squinabol, 1903, p. 135, pl. VIII, fig. 43; Kazintsova, 1987, p. 194, pl. XXXV, fig. 12; Kazintsova, 1993, p. 67, pl. XXI, figs. 2 and 3.

Theocampe (?) guttaeformis: Bragina, 1991b, p. 135, pl. 1, fig. 6, text-fig. 1d.

Etymology. From the Latin *guttaeformis* (tear-shaped).

Holotype. GIN, no. 4823/50; northwestern Kamchatka, Talovka River section, Bystraya Formation, Santonian–Lower Campanian (Bragina, 1991b, pl. I, fig. 6).

Description. The shell is relatively large, tear-shaped, and three-chambered. The cephalis is almost spherical and, usually, smooth and without pores. The thorax is conical, with a slight constriction separating it from the cephalis. The abdomen is large, oval to rounded, strongly inflated, with a small compressed aperture and, occasionally, a short apertural tube. The shell wall gradually thins from the cephalis to the abdomen. The post-cephalic pores are small, rounded to angular, irregular in outline, and randomly arranged. Pore frames strongly vary in form (trigonal to pentagonal) and size. Ridges of pore frames are variable in height, with triangular spines at vertices, which makes the thoracic and abdominal surface thorny.

Measurements. Shell length, 500–320, maximal width, 250–170.

Comparison. *T. guttaeformis* differs from *T. transmontanum* O'Dogherty, 1994 in the symmetrical shell. The cephalothorax of the latter species deviates from the main shell axis.

Occurrence. Middle–Upper Cenomanian of northern Turkey; Lower Turonian of the Crimean Mountains; Coniacian–Campanian of Cyprus; Santonian–Campanian of the Bystraya Formation of northwestern Kamchatka.

Material. More than ten specimens.

Tubilustrium transmontanum O'Dogherty 1994

Plate 13, fig. 7; Plate 33, figs. 6 and 8

Tubilustrium transmontanum: O'Dogherty, 1994, p. 137, pl. 15, figs. 9–19.

Non *Tubilustrium transmontanum*: Khan *et al.*, 1999, pl. 1, fig. j.

Holotype. UL, no. 3280; central Italy, Umbria-Marche Apennines, Locality Bo-685.20; Lower Cretaceous, Upper Albian (O'Dogherty, 1994, pl. 15, fig. 16).

Occurrence. Middle Albian–Middle Cenomanian of Italy; Lower Turonian of the Crimean Mountains; Middle–Upper Cenomanian of northern Turkey.

Material. More than 30 specimens.

Family Syringocapsidae Foreman, 1973

Genus *Pseudoeucyrtis* Pessagno, 1977

Pseudoeucyrtis: Pessagno, 1977, p. 58.

Type species. *Eucyrtis (?) zhamoidai* Foreman, 1973; Borehole 196, Upper Cretaceous beds, the Pacific.

Diagnosis. Shell multicyrtoid, elongated, fusiform, with long apertural tube. Cephalis with or without pores, frequently with massive apical horn. Shell usually double-layered, with double row of pores in polygonal frames. Shell surface frequently thorny. Shell gradually narrowing toward aperture.

Species composition. Tens of species, including *P. tavricus* sp. nov.; Mesozoic, tropical and temperate latitudes.

Comparison. *Pseudoeucyrtis* differs from *Distylocapsa* Squinabol, 1904 in the long conical apertural tube.

Pseudoeucyrtis pulchra (Squinabol), 1904, emend. herein

Plate 33, fig. 13

Theosyringium pulchrum: Squinabol, 1904, p. 222, pl. 8, fig. 7.

Pseudoeucyrtis pulchra: O'Dogherty, 1994, p. 184, pl. 27, figs. 9–13; Salvini and Marcucci Passerini, 1998, text-fig. 10j.

Holotype. Northern Italy, southern Venetian Alps, Colli Euganei, Teolo Series; upper Lower Cretaceous–lower Upper Cretaceous, Upper Albian–Lower Turonian (Squinabol, 1904, pl. 8, fig. 7).

Description. The shell is long, fusiform, delicate and usually consists of four or five chambers. The proximal part, which comprises the cephalis, thorax, abdomen, and, occasionally, the first post-abdominal chamber, is narrowly conical in longitudinal section. The cephalis is small, conical, without pores, with a well-developed apical horn. The next chamber of the cone is porous, slightly increasing in width, and almost constant in height. The first post-abdominal chamber is slightly inflated, and the last chamber is considerably swollen. This part of the shell is the widest. The pore frames slightly increase in size from the proximal to the distal part and are arranged irregularly. The apertural tube is long (frequently more than half of the shell length), narrows toward the margin, and consists of large rounded to polygonal pores oriented longitudinally and surrounded by polygonal (tetragonal to heptagonal) pore frames. Some specimens show pentagonal and hexagonal patterns of pores.

Measurements. Maximal length of shell, 630–462; maximal width, 100–146; length of apertural tube, 285–192.

Comparison. *P. pulchra* differs from *P. spinosa* (Squinabol, 1903) in (1) the more delicate shell, (2) the absence of nodes and spines on the post-abdominal chamber, and (3) the longer apertural tube.

Occurrence. Upper Albian–Lower Turonian of Italy; Lower Turonian of the Crimean Mountains.

Material. More than 20 specimens.

Pseudoeucyrtis spinosa (Squinabol, 1903)

Plate 13, figs. 4–6; Plate 34, fig. 10

Eusyringium spinosum: Squinabol, 1903, p. 141, pl. 8, fig. 42; Thurow, 1988, p. 401, pl. 4, fig. 18; Tumanda and Sashida, 1988, text-fig. 4.8.

Eucyrtis bulbosa: Foreman, 1975, p. 615, pl. 2K, fig. 3.

Eucyrtis spinosus: Dumitrica, 1975, text-fig. 2.25.

Cyrtocapsa grutterinki: Nakaseko and Nishimura, 1981, p. 149, pl. 13, fig. 9.

Eusyringium (?) foremanae: Taketani, 1982, p. 64, pl. 6, figs. 1a and 1b; Thurow, 1988, p. 401, pl. 4, fig. 19; Taketani and Kanie, 1992, text-fig. 3.14.

Pseudoeucyrtis spinosa: O'Dogherty, 1994, p. 183, pl. 27, figs. 1–8.

Holotype. Central Italy, southern Venetian Alps, Colli Euganei, Teolo Series; upper Lower Cretaceous–lower Upper Cretaceous, Upper Albian–Lower Turonian (Squinabol, 1903, pl. 8, fig. 42).

Comparison. *P. spinosa* differs from *P. pulchra* (Squinabol, 1904), in the larger shell with an inflated spherical central part covered by nodes terminating in spinules.

Occurrence. Albian–Turonian, worldwide; Middle–Upper Cenomanian of northern Turkey.

Material. Five specimens.

Pseudoeucyrtis tavricus Bragina, sp. nov.

Plate 34, figs. 1 and 2

Etymology. From Tavrida, the ancient name of the Crimea.

Holotype. GIN, no. 4870/57; Crimean Mountains, Belaya Mountain section, Lower Turonian.

Description. The shell is of fusiform shape (characteristic of this genus) and has seven to nine post-abdominal chambers. The cephalis is subspherical, without pores, and with a long massive cylindrical apical horn. The horn terminates in a short ridgelike structure of irregular outline. The thorax and abdomen are trapezoidal in the main section. Fine rounded pores form a transverse row at the base of the thorax. The abdomen has pores arranged in transverse rows throughout, and small spines thorns at the vertices of several pores. Locally, abdominal pores may be covered by expanded tissue. The cephalothorax, abdomen, and the first two or three post-abdominal segments form a high cone. The subsequent chambers form an almost spherical swelling the diameter of which is twice that of the widest conical portion of the shell. The swelling bears xitoid nodes that are occasionally arranged in transverse rows. The pores on the swelling are larger than those on the conical part. Distally the

shell narrows to form a long cylindrical apertural tubus. The tubus shows fairly distinct longitudinal rows of larger subspherical pores the longest diameters of which are aligned parallel to the main axis of the shell.

Measurements. Shell length, 490–450, maximal width, 150—120, tubus length, 150–100, length of apical horn, 30–20.

Comparison. *P. tavricus* differs from *P. spinosa* (Squinabol, 1903) in having an almost regular narrowly conical shape in front of the spherical swelling, and from *Ps. apochrypha* O'Dogherty, 1994 in the distinct constriction between the conical and subspherical parts, the lesser number and different shape of nodes, and the clearly defined longitudinal orientation of pores on the apertural tube. It differs from all known Late Cretaceous species in having a fairly long tubular apical horn that becomes thicker and ridgelike at the apex.

Occurrence. Lower Turonian of the Crimean Mountains.

Material. Four complete and seven incomplete specimens.

Genus *Spongostichomitra* O'Dogherty, 1994

Spongostichomitra elatica (Aliev, 1968)

Plate 33, fig. 24

Dictyomitra elatica: Aliev, 1968, p. 26, pl. 1, figs. 1 and 2.

Spongostichomitra elatica: O'Dogherty, 1994, p. 152, pl. 18, figs. 25–28.

Holotype. Azerbaijan, Greater Caucasus; Lower Cretaceous, Middle Albian (Aliev, 1968, pl. 1, fig. 1).

Comparison. *S. elatica* differs from *S. phalanga* O'Dogherty, 1994 in having a considerably shorter conical to fusiform shell.

Occurrence. Middle Albian of Azerbaijan; Lower Albian–Middle Cenomanian of Italy; Lower Turonian of the Crimean Mountains.

Material. Nine specimens.

Spongostichomitra phalanga O'Dogherty, 1994

Plate 13, figs. 9–11

Spongostichomitra phalanga: O'Dogherty, 1994, p. 153, pl. 19, figs. 1–11.

Holotype. UL, no. 5213; central Italy, Umbria-Marche Apennines, Locality Gb-84.40; Upper Cretaceous, Lower Cenomanian (O'Dogherty, 1994, pl. 19, fig. 1).

Remarks. There is some doubt in assigning *S. phalanga* O'Dogherty, 1994 to the order Nassellaria because of its outward appearance, which is uncharacteristic of Nassellaria. The internal structure (particularly the cephalis) has not been described by O'Dogherty. This species resembles representatives of the order Spumellaria, e.g., those of the genus *Spongopyle*.

Occurrence. Middle Albian–Lower Cenomanian of Italy and Spain; Middle–Upper Cenomanian of northern Turkey.

Material. Four specimens.

Family Lampromitridae Haeckel, 1881

Genus *Cornutella* Ehrenberg, 1838, sensu Petrushevskaya, 1967

Cornutella californica Campbell et Clark, 1944

Plate 13, figs. 12 and 13

Cornutella (*Cornutissa*) *californica*: Campbell and Clark, 1944, p. 22, pl. 7, fig. 42.

Cornutella (*Cornutissa*) *californica* var. *brevis*: Campbell and Clark, 1944, p. 23, pl. 7, figs. 33, 34, and 43.

Cornutella californica: Iwata and Tajika, 1986, pl. 3, fig. 6; Ling and Lazarus, 1990, pl. 3, fig. 17; Ling, 1991, pl. 1, fig. 14; Hollis, 1997, pl. 17, fig. 13; Takahashi, 1999, text-fig. 2M; Vishnevskaya, 2001, pl. 8, figs. 4 and 5; pl. 126, figs. 43 and 44.

? *Cornutella californica*: Hashimoto and Ishida, 1997, pl. 2, fig. 19; Hollis, 1997, pl. 17, figs. 14 and 15.

Non *Cornutella californica*: Salvini and Marcucci Passerini, 1998, text-fig. 9j.

Holotype. USNM, no. 34520; California, Moreno Formation, Tesla County; Upper Cretaceous, Campanian (Campbell and Clark, 1944, pl. 7, fig. 42).

Occurrence. Cenomanian–Maastrichtian, worldwide; Upper Cenomanian of northern Turkey.

Material. Less than ten specimens.

Order incertae sedis

Genus *Afens* Riedel et Sanfilippo, 1974

Afens liriodes Riedel et Sanfilippo, 1974

Plate 13, fig. 14

Incertae sedis sp. *A*: Moore, 1973, p. 830, pl. 13, figs. 1–3.

Afens liriodes: Riedel and Sanfilippo, 1974, p. 23, pl. 11, fig. 11; pl. 13, figs. 14–16; Foreman, 1978b, p. 750, pl.5, fig. 24; Kling, 1981, p. 548, pl. 1, figs. 23 and 24; pl. 3, figs. 5 and 6; Sanfilippo and Riedel, 1985, p. 624, text-fig. 13. 3a–3c; Thurow, 1988, pl. 2, fig. 1; Osozawa and Okamura, 1993, text-fig. 5. A2; Bragina and Bragin, 1995, pl. III, fig. 17.

Holotype. Scripps Institution of Oceanography, California; 146-15-5, 15-25 cm, S1.2, V32/3; Maastrichtian, southern Indian Ocean; DSDP Leg 26, Borehole 146.

Remarks. The shell varies considerably in shape from subcylindrical to campaniform.

Occurrence. Cenomanian–Maastrichtian, worldwide; Upper Cenomanian of northern Turkey.

Material. More than ten specimens.

Order Spumellaria Ehrenberg, 1875

Suborder Sphaerellaria Haeckel, 1881

Superfamily Actinommoidea Haeckel, 1862

Family Actinommidae Haeckel, 1862, emend. Riedel, 1967

Genus *Archaeocenosphaera* Pessagno et Yang, 1989

Archaeocenosphaera ? mellifera O'Dogherty, 1994

Plate 14, fig. 3; Plate 36, fig. 14

? *Cenosphaera* ? sp. *A*: Empson-Morin, 1984, pl. 1, fig. 6.

? *Hemicryptocapsa* (?) sp.: Teraoka and Kurimoto, 1986, pl. 3, fig. 3.

Hemicryptocapsa polyhedra: Thurow and Kuhnt, 1986, text-fig. 9.21; Thurow, 1988, p. 401, pl. 1, fig. 1; Erbacher, 1994, pl. 17, fig. 11.

Hemicryptocapsa sp. cf. *H. polyhedra*: Thurow, 1988, p. 401, pl. 5, fig. 2.

Hemicryptocapsa sp. *A*: Marcucci and Gardin, 1992, text-fig. 3.1.

Archaeocenosphaera ? mellifera: O'Dogherty, 1994, p. 375, pl. 74, figs. 1–5; Salvini and Marcucci Passerini, 1998, text-fig. 7.o; Khan *et al.*, 1999, pl. 2, fig. o.

Holotype. UL, no. 138; central Italy, Umbria-Marche Apennines, Locality Ap2 (-7,78); Lower Cretaceous, Upper Albian (O'Dogherty, 1994, pl. 74, fig. 4).

Comparison. *A. ? mellifera* differs from its congeners (Pessagno *et al.*, 1989) in the presence of polygonal areas on the shell surface that are separated by acute winglike ridges.

Occurrence. Cenomanian–Campanian, worldwide; Middle Albian–Lower Turonian of Italy and Spain; Middle–Upper Cenomanian of northern Turkey; Upper Cenomanian–Lower Turonian of the Crimean Mountains; Coniacian–Lower Campanian of the Russian Plain.

Material. Less than 50 specimens.

Genus *Cenosphaera* Ehrenberg, 1854

"Cenosphaera" boria Pessagno, 1977

Plate 14, fig. 4; Plate 36, fig. 7

"Cenosphaera" boria: Pessagno, 1977, p. 36, pl. 3, figs. 13 and 19.

Holotype. USNM-Pessagno, no. 242815; California coast, Great Valley sequence, Locality NSF 810; Lower Cretaceous, Berriasian (Pessagno, 1977, pl. 3, figs. 13, 16).

Remarks. Pessagno (1977) tentatively included it in *Cenosphaera*.

Occurrence. Berriasian of California; Upper Cenomanian of northern Turkey; Lower Turonian of the Crimean Mountains.

Material. Five specimens.

Genus *Praeconocaryomma* Pessagno, 1976

Praeconocaryomma californiaensis Pessagno, 1976

Plate 14, fig. 2; Plate 36, figs. 12, 13, and 16

Praeconocaryomma californiaensis: Pessagno, 1976, p. 41, pl. 7, figs. 1–8; Taketani, 1982, p. 47, pl. 9, figs. 1.

Praeconocaryomma universa: Iwata and Tajika, 1986, pl. 5, fig. 9; Thurow and Kuhnt, 1986, text-fig. 9.22.

Non *Praeconocaryomma californiaensis*: Taketani, 1982, p. 47, pl. 9, fig. 2.

Holotype. USNM-Pessagno, no. 165563; California coast, Great Valley sequence, Fiske Creek Formation, Locality NSF 327-C; Upper Cretaceous, Coniacian (Pessagno, 1976, pl. 7, fig. 1).

Comparison. *P. californiaensis* differs from *P. lipmanae* Pessagno, 1976, in having fewer nodes of larger size, polygonal pores, and well-developed ridges extending from the tops of nodes.

Occurrence. Coniacian–Campanian, worldwide; Upper Cenomanian of northern Turkey; Lower Turonian of the Crimean Mountains.

Material. More than 20 specimens.

Praeconocaryomma lipmanae Pessagno, 1976

Plate 14, fig. 1; Plate 41, fig. 17

Praeconocaryomma lipmanae: Pessagno, 1976, p. 41, pl. 4, figs. 12 and 13; Kazintsova, 1993, p. 44, pl. VII, fig. 3; Salvini and Marcucci Passerini, 1998, text-fig. 8c; Vishnevskaya, 2001, pl. 127, fig. 1c.

Non *Praeconocaryomma lipmanae*: Kazintsova, 2002, pl. 1, fig. 2 (= *Acaeniotyle* sp.).

Holotype. USNM-Pessagno, no. 165665; California coast, Great Valley sequence, Upper Fiske Creek Formation, Locality NSF 591; Upper Cretaceous, Lower Turonian (Pessagno, 1976, pl. 4, fig. 13).

Comparison. *P. lipmanae* differs from *P. universa* Pessagno, 1976 in the absence of ridges running from the nodes.

Occurrence. Upper Cenomanian–Santonian, worldwide; Middle–Upper Cenomanian of northern Turkey.

Material. More than 20 specimens.

Praeconocaryomma universa Pessagno, 1976

Plate 36, fig. 15

Praeconocaryomma universa: Pessagno, 1976, p. 42, pl. 6, figs. 14–16; Vishnevskaya, 2001, pl. 21, fig. 3; pl. 126, fig. 1.

Praeconocaryomma cf. *universa*: Schmidt-Effing, 1980, text-figs. 5, 9–11.

Non *Praeconocaryomma universa*: Iwata and Tajika, 1986, pl. 5, fig. 9 (= *P. californiaensis* Pessagno, 1976); Thurow and Kuhnt, 1986, text-fig. 9.22 (= *P. californiaensis* Pessagno, 1976).

Praeconocaryomma californiaensis: Taketani, 1982, p. 47, pl. 9, fig. 2.

Conocaryomma universum: De Wever *et al.*, 1988, pl. 3, fig. 7.

Holotype. USNM-Pessagno, no. 165667; California coast, Great Valley sequence, Upper Yolo Formation, Locality NSF 483; Upper Cretaceous, Coniacian (Pessagno, 1976, pl. 6, fig. 14).

Comparison. *P. universa* differs from *P. californiaensis* Pessagno, 1976 in the more rounded tubercles and the lesser number of tubercles on the semicircumference of the shell.

Occurrence. Coniacian–Santonian, worldwide; Lower Turonian of the Crimean Mountains.

Material. More than 30 specimens

Family Quinquecapsulariidae Dumitrica, 1995

Genus *Quinquecapsularia* Pessagno, 1971

Quinquecapsularia grandiloqua O'Dogherty, 1994

Plate 15, figs. 3 and 4

Quinquecapsularia grandiloqua: O'Dogherty, 1994, p. 270, pl. 48, figs. 1–5.

Holotype. UL, no. 5831; central Italy, Umbria-Marche Apennines, locality no. Asv-5-43; Lower Cretaceous, Upper Albian (O'Dogherty, 1994, pl. 48, fig. 1).

Comparison. *Q. grandiloqua* differs from *Q. panacea* O'Dogherty, 1994 in the number (9–10) and stoutness of spines.

Occurrence. Upper Albian–Lower Turonian of Italy; Middle–Upper Cenomanian of northern Turkey.

Material. More than 30 specimens.

Quinquecapsularia ombonii (Squinabol, 1903)

Plate 14, fig. 8

Hexastylus Ombonii: Squinabol, 1903, p. 113, pl. 8, fig. 10.

Quinquecapsularia ombonii: O'Dogherty, 1994, p. 268, pl. 47, figs. 21–24.

Holotype. Northern Italy, southern Venetian Alps, Colli Euganei, Teolo locality; upper Lower Cre-

Plate 14

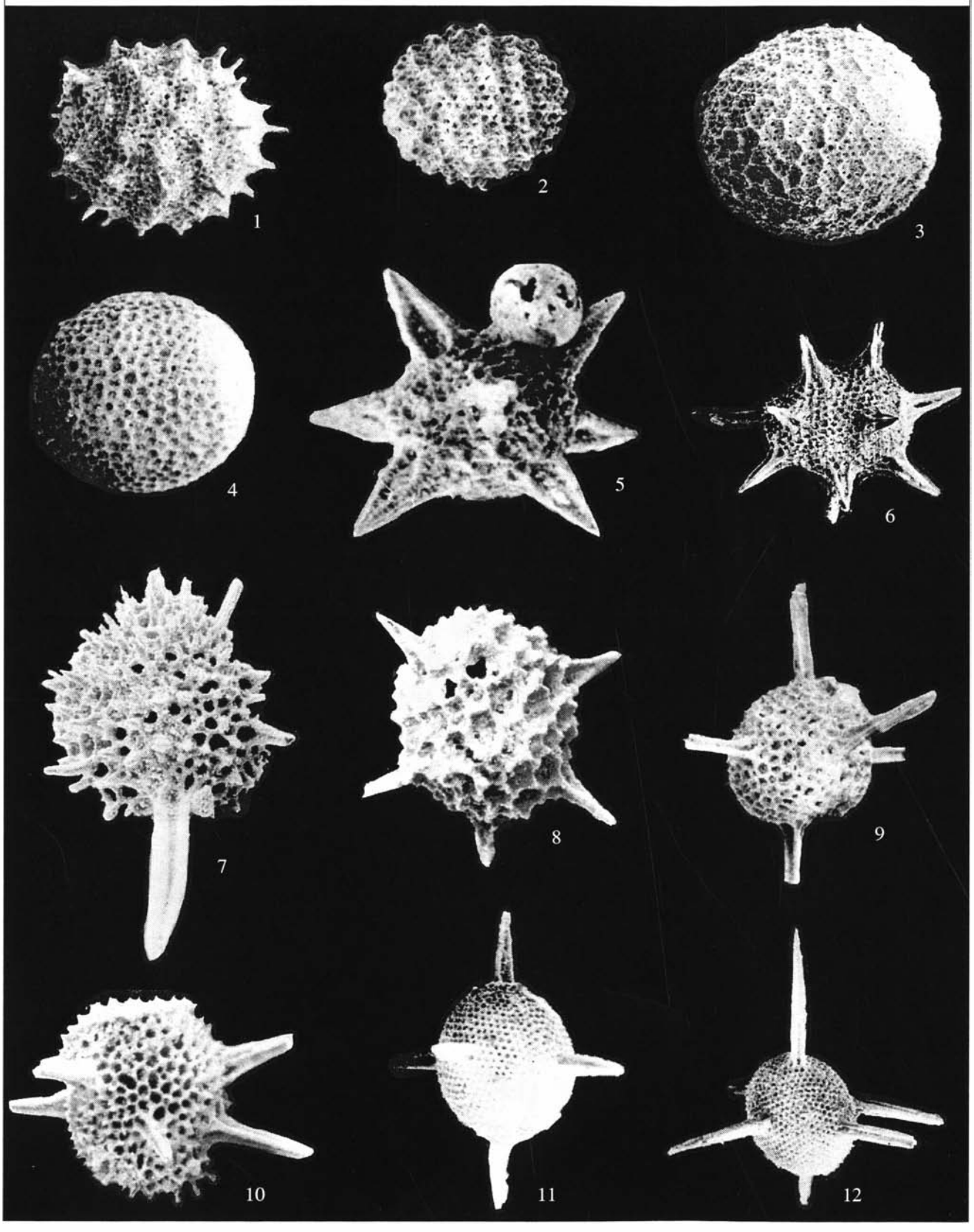

taceous–lower Upper Cretaceous, Upper Albian–Lower Turonian (Squinabol, 1903, pl. 8, fig. 10).

Comparison. *Q. umbonii* is distinguished from *Q. panacea* O'Dogherty, 1994 by its larger cortical shell, larger pores of greater size variability, and much shorter, acutely conical, spines.

Occurrence. Middle Albian–Lower Turonian of Italy; Middle–Upper Cenomanian of northern Turkey.

Material. More than 20 specimens.

Quinquecapsularia panacea O'Dogherty, 1994

Plate 15, figs. 5 and 6

Quinquecapsularia panacea: O'Dogherty, 1994, p. 270, pl. 48, figs. 6–10.

Acanthosphaera ? wisniowskii: Vishnevskaya, 2001, pl. 21, fig. 10.

Holotype. UL, no. 6288; central Italy, Umbria-Marche Apennines, locality no. Asv-5-43; Upper Cretaceous, Lower Turonian (O'Dogherty, 1994, pl. 48, fig. 9).

Occurrence. Lower Turonian of Italy; Upper Cenomanian of northern Turkey.

Material. More than ten specimens.

Quinquecapsularia parvipora (Squinabol, 1903)

Plate 35, fig. 3

Acanthosphaera parvipora: Squinabol, 1903, p. 115, pl. 8, fig. 5.

Quinquecapsularia parvipora: O'Dogherty, 1994, p. 269, pl. 47, figs. 25–28.

Holotype. Northern Italy, southern Venetian Alps, Teolo or Brustolo locality (indicated imprecisely); upper Lower Cretaceous–lower Upper Cretaceous, Albian–Turonian, Scaglia Bianca Formation (Squinabol, 1903, pl. 8, fig. 5).

Comparison. *Q. parvipora* differs from *Q. panacea* O'Dogherty, 1994 by the well-developed thorns at the pore frame junctions.

Occurrence. Albian–Turonian of Italy; Upper Cenomanian of northern Turkey; Lower Turonian of the Crimean Mountains.

Material. More than ten specimens.

Family *incertae sedis*

Genus *Falsocromyodrimus* O'Dogherty, 1994

Remarks. O'Dogherty (1994) established the genus *Falsocromyodrimus* and described several new species, which he ascribed to it. O'Dogherty included *Falsocromyodrimus* in the family Quinquecapsulariidae Dumitrica, 1994. The main diagnostic character of this family is the internal pentagonal prism. However, O'Dogherty did not study the internal morphology of *Falsocromyodrimus*. An incomplete specimen of *F. mirabilis* (Squinabol, 1903), shown in Pl. 15, fig. 7, demonstrates a connection between the spines in the center. This character is typical of the order Entactinaria. In spite of many features in common with *F. ? fragosus* O'Dogherty (order Spumellaria), 1994, the recently described species of *Cuboctostylus* (Bragina, 1999b) are referred to the order Entactinaria.

Falsocromyodrimus mirabilis (Squinabol, 1903)

Plate 15, fig. 7; Plate 35, figs. 9 and 16

Cromyodrimus mirabilis: Squinabol, 1903, p. 116, pl. 10, fig. 15.

Falsocromyodrimus mirabilis: O'Dogherty, 1994, p. 272, pl. 48, figs. 11–15.

Falsocromyodrimus cardulus: O'Dogherty, 1994, p. 274, pl. 49, figs. 1–8.

Holotype. Northern Italy, southern Venetian Alps, Teolo locality; upper Lower Cretaceous–lower Upper Cretaceous, Upper Albian–Lower Turonian (Squinabol, 1903, pl. 10, fig. 15).

Occurrence. Albian–Lower Turonian of the Tethys; Cenomanian of the Pacific Ocean; Upper Cenomanian of northern Turkey; Lower Turonian of the Crimean Mountains.

Material. Fewer than ten specimens.

Family Xiphostylidae Haeckel, 1881

Genus *Pseudoacanthosphaera* O'Dogherty, 1994

Pseudoacanthosphaera: O'Dogherty, 1994, p. 296.

Type species. *Staurosphaera magnifica* Squinabol, 1904; upper Lower Cretaceous–lower Upper Cretaceous, Upper Albian–Lower Turonian; Teolo locality, Colli Euganei, southern Venetian Alps, northern Italy.

Explanation of Plate 14

Fig. 1. *Praeconocaryomma lipmanae* Pessagno, 1976, GIN, no. 4871/153, ×180.

Fig. 2. *Praeconocaryomma universa* Pessagno, 1976, GIN, no. 4871/154, ×160.

Fig. 3. *Archaeocenosphaera ? mellifera* O'Dogherty, 1994, GIN, no. 4871/155, ×120.

Fig. 4. *"Cenosphaera" boria* Pessagno, 1977, GIN, no. 4871/156, ×150.

Figs. 5 and 6. *Staurosphaeretta wisniowskii* (Squinabol, 1903), specimens (5) GIN, no. 4871/157, ×240; and (6) GIN, no. 4871/158, ×120.

Fig. 7. *Pseudoacanthosphaera galeata* O'Dogherty, 1994, GIN, no. 4871/159, ×170.

Fig. 8. *Quinquecapsularia ombonii* (Squinabol, 1903), GIN, no. 4871/160, ×200.

Figs. 9 and 10. *Staurosphaeretta grandipora* (Squinabol, 1903): specimens: (9) GIN, no. 4871/161, ×100; and (10) GIN, no. 4871/162, ×120.

Figs. 11 and 12. *Staurosphaeretta micropora* sp. nov.: (11) holotype GIN, no. 4871/163, ×100); and (12) paratype GIN, no. 4871/164, ×60.

All specimens come from the Ürküt section.

Plate 15

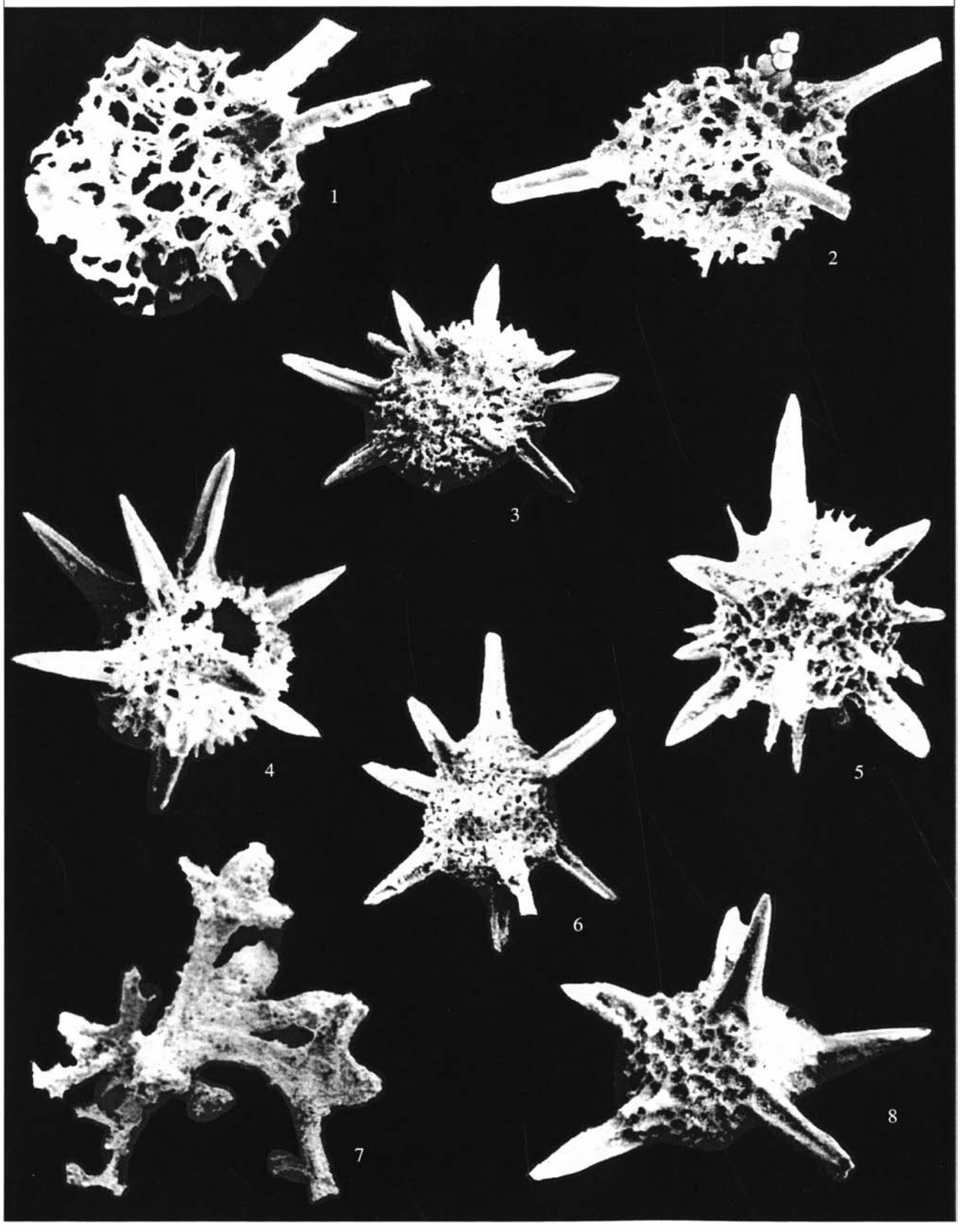

Diagnosis. Cortical shell sometimes large, with very variable number (two to twelve) of primary spines, usually long, strongly bladed. Pores of cortical shell round or pentagonal to heptagonal; pore frames irregular in outline. Secondary spines variable in form and size.

Species composition. *P. magnifica* (Squinabol, 1904), *P. galeata* O'Dogherty, 1994, *P. superba* (Squinabol, 1904), *P. spinosissima* (Squinabol, 1904); Middle Albian–Lower Maastrichtian?; geographical ranges have not been determined.

Comparison. The genus is distinguished from *Staurosphaeretta* Squinabol, 1904 by the presence of thorns on the surface of the cortical shell.

Pseudoacanthosphaera galeata O'Dogherty, 1994, emend. herein

Plate 35, fig. 5

Pseudoacanthosphaera galeata: O'Dogherty, 1994, p. 297, pl. 53, figs. 16–19.

Holotype. UL, no. 3302; central Italy, Umbria-Marche Apennines, locality no. Bo-685.20; Lower Cretaceous, Upper Albian (O'Dogherty, 1994, pl. 53, fig. 18).

Description. The cortical shell is subspherical, as is typical of the genus. It has 8–12 long primary spines regularly spaced over the entire surface of the cortical shell. The distal parts of the spines are slightly inflated and may exhibit torsion. Distally, they are sharply pointed. Small rounded angular pores are variable in size and set in pentagonal or hexagonal frames of irregular outline. The highest frames enclose two or three pores, making the shell surface polygonal. Well-pronounced thorns of nonuniform length and outline are observed at the points of contact between several pores.

Measurements. Cortical shell diameter, 293–250; length of primary spines, 410–160.

Comparison. *P. galeata* is distinguished from *P. magnifica* (Squinabol, 1904) by the number, form, and location of spines as well as the mode of porosity of the cortical shell.

Occurrence. Upper Albian–Lower Cenomanian of Italy; Lower Turonian of the Crimean Mountains.

Material. Fewer than 50 specimens.

Pseudoacanthosphaera magnifica (Squinabol, 1904)

Plate 38, fig. 1

Staurosphaera magnifica: Squinabol, 1904, p. 191, pl. 3, fig. 1.

Non *Hexastylus magnificus*: Schaaf, 1981, pl. 7, fig. 2.

Pseudoacanthosphaera magnifica: O'Dogherty, 1994, p. 297, pl. 54, figs. 1, 3, and 4.

Non *Pseudoacanthosphaera magnifica*: O'Dogherty, 1994, p. 297, pl. =54, fig. 2 (= *Staurosphaeretta euganea* (Squinabol, 1903)).

Holotype. Northern Italy, southern Venetian Alps, Colli Euganei, Teolo locality; upper Lower Cretaceous–lower Upper Cretaceous, Upper Albian–Lower Turonian (Squinabol, 1904, pl. 3, fig. 1).

Comparison. *P. magnifica* is distinguished from *P. galeata* O'Dogherty, 1994 by its less numerous primary spines that gradually taper distally.

Occurrence. Albian–Lower Turonian of Italy and Spain; Upper Cenomanian of northern Turkey; Lower Turonian of the Crimean Mountains.

Material. More than 50 specimens.

Pseudoacanthosphaera spinosissima (Squinabol, 1904)

Plate 35, figs. 17 and 18

Xiphosphaera spinosissima: Squinabol, 1904, p. 188, pl. 2, fig. 9.

Pseudoacanthosphaera spinosissima: O'Dogherty, 1994, p. 299, pl. 54, figs. 11–15.

Holotype. Northern Italy, southern Venetian Alps, Colli Euganei, Teolo locality; upper Lower Cretaceous–lower Upper Cretaceous, Upper Albian–Lower Turonian (Squinabol, 1904, pl. 2, fig. 9).

Comparison. Unlike the congeneric species, *P. spinosissima* has only two primary spines.

Occurrence. Upper Albian–Lower Turonian of Italy; Upper Cenomanian of northern Turkey; Lower Turonian of the Crimean Mountains.

Material. Fewer than ten specimens.

Pseudoacanthosphaera superba (Squinabol, 1904)

Plate 35, figs. 6 and 7

Trisphaera superba: Squinabol, 1904, p. 190, pl. 2, fig. 13.

Pseudoacanthosphaera superba: O'Dogherty, 1994, p. 298, pl. 54, figs. 5–10.

Holotype. Northern Italy, southern Venetian Alps, Colli Euganei, Teolo locality; upper Lower Cretaceous–lower Upper Cretaceous, Upper Albian–Lower Turonian (Squinabol, 1904, pl. 2, fig. 13).

Comparison. *P. superba* is distinguished from *P. magnifica* (Squinabol, 1904) by long branching sec-

Explanation of Plate 15

Figs. 1 and 2. *Pseudoacanthosphaera galeata* O'Dogherty, 1994; specimens: (1) GIN, no. 4871/165, ×150; and (2) GIN, no. 4871/166, ×120.

Figs. 3 and 4. *Quinquecapsularia grandiloqua* O'Dogherty, 1994, specimens: (3) GIN, no. 4871/167, ×80; and (4) GIN, no. 4871/168, ×90.

Figs. 5 and 6. *Quinquecapsularia panacea* O'Dogherty, 1994, specimens: (5) GIN, no. 4871/169, ×120; and (6) GIN, no. 4871/170, ×100.

Fig. 7. *Falsocromyodrimus mirabilis* (Squinabol, 1903), GIN, no. 4871/171, ×300.

Fig. 8. *Quinquecapsularia ombonii* (Squinabol, 1903), GIN, no. 4871/172, ×150.

All specimens come from the Ürküt section.

ondary spines on the cortical shell and by a variable number of primary spines.

Occurrence. Upper Albian–Lower Turonian of Italy and Spain; Lower Turonian of the Crimean Mountains.

Material. More than 20 specimens.

Genus *Staurosphaeretta* Squinabol, 1904

Staurosphaeretta: Squinabol, 1904.

Type species. *Staurosphaera longispina* Squinabol, 1903; upper Lower Cretaceous–lower Upper Cretaceous, Upper Albian–Lower Turonian; Teolo locality, Colli Euganei, southern Venetian Alps, northern Italy.

Diagnosis. Large shell with 4–6 or more primary spines radiating symmetrically. Cortical shell usually large, spherical, with regularly spaced pores in polygonal pore frames.

Species composition. *S. euganea* (Squinabol, 1903), *S. grandipora* (Squinabol, 1903), *S. longispina* (Squinabol, 1903), *S. micropora* sp. nov., *S. wisniowskii* (Squinabol, 1903); Upper Albian–Lower Turonian.

Comparison. This genus is distinguished from *Tetracanthellipis* Squinabol, 1903 by its larger number of primary spines and its spongy cortical shell.

Staurosphaeretta euganea (Squinabol, 1903)

Plate 16, figs. 1 and 3

Staurosphaera euganea: Squinabol, 1903, p. 112, pl. 10, fig. 18.
Staurosphaera veneta: Squinabol, 1904, p. 191, pl. 3, fig. 2.
Staurosphaera amplissima: Foreman, 1973, p. 259, pl. 3, fig. 6.
Staurosphaeretta euganea: O'Dogherty, 1994, pp. 292–293, pl. 52, figs. 1–5.

Holotype. Northern Italy, southern Venetian Alps, Teolo locality; upper Lower Cretaceous–lower Upper Cretaceous, Upper Albian–Lower Turonian (Squinabol, 1903, pl. 10, fig. 18).

Remarks. Occasionally, one spine is longer than the other three.

Occurrence. Middle Albian–Lower Turonian of Italy; Middle–Upper Cenomanian of northern Turkey; Lower Turonian of the Crimean Mountains.

Material. More than ten species.

Staurosphaeretta grandipora (Squinabol, 1903)

Plate 14, figs. 9 and 10

Hexastylus grandiporus: Squinabol, 1903, p. 113, pl. 10, fig. 17.
Staurosphaeretta grandipora: O'Dogherty, 1994, p. 293, pl. 52, fig. 15–18.

Holotype. Northern Italy, southern Venetian Alps, Teolo locality; upper Lower Cretaceous–lower Upper Cretaceous, Upper Albian–Lower Turonian (Squinabol, 1903, pl. 10, fig. 17).

Comparison. *S. grandipora* is distinguished from *S. euganea* (Squinabol, 1904) by the presence of two extra spines, in addition to the four spines radiating in a single plane toward the corners of a rectangle. The two additional spines are located in the opposite poles of the shell in a plane perpendicular to that of the four spines.

Occurrence. Upper Albian–Lower Turonian of Italy and Spain; Middle–Upper Cenomanian of northern Turkey; Lower Turonian of the Crimean Mountains.

Material. Five specimens.

Staurosphaeretta micropora Bragina, sp. nov.

Plate 14, figs. 11 and 12

Etymology. From the Latin *micropora* (finely porous).

Holotype. GIN, no. 4871/163; northern Turkey, Ürküt section; Upper Cretaceous, Middle Cenomanian.

Description. The spherical cortical shell possesses six primary spines. Two spines are polar and four are in a plane perpendicular to that of the two polar spines. The spines are approximately equal in length to one another, and to the shell diameter. The spines are three-bladed from the base to the distal end and taper to become acutely conical distally. The small pores of the cortical shell are uniform in size and arranged in a hexagonal pattern. The pore diameter is less than, or equal to, the distance between pores. The pore frames are hexagonal, with poorly developed thorns.

Measurements. Cortical shell diameter, 280; spine length, 400.

Comparison. *S. micropora* differs from *S. grandipora* (Squinabol, 1903) in the smaller pores and acutely conical spines.

Occurrence. Middle Cenomanian of northern Turkey.

Material. Ten complete and six incomplete specimens.

Staurosphaeretta longispina (Squinabol, 1903)

Plate 16, figs. 2, 4, and 5; Plate 37, fig. 14; Plate 38, fig. 2

Staurosphaera longispina: Squinabol, 1903, p. 112, pl. 9, fig. 1.

Explanation of Plate 16

Figs. 1 and 3. *Staurosphaeretta euganea* (Squinabol, 1903), specimens: (1) GIN, no. 4871/173, ×120; and (3) GIN, no. 4871/174, ×100.

Figs. 2, 4, and 5. *Staurosphaeretta longispina* (Squinabol, 1903), specimens: (2) GIN, no. 4871/175, ×90; (4) GIN, no. 4871/176, ×100; and (5) GIN, no. 4871/177, ×120.

Fig. 6. *Tetracanthellipsis euganeus* Squinabol, 1903, GIN, no. 4871/178, ×130.

Figs. 7–10. *Hexapyramis pantanellii* Squinabol, 1903, specimens: (7) GIN, no. 4871/179, ×200; (8) GIN, no. 4871/180, ×100; (9) GIN, no. 4871/181, ×150; and (10) GIN, no. 4871/182, ×120.

Fig. 8. From the Tomalar section. The others come from the Ürküt section.

Plate 16

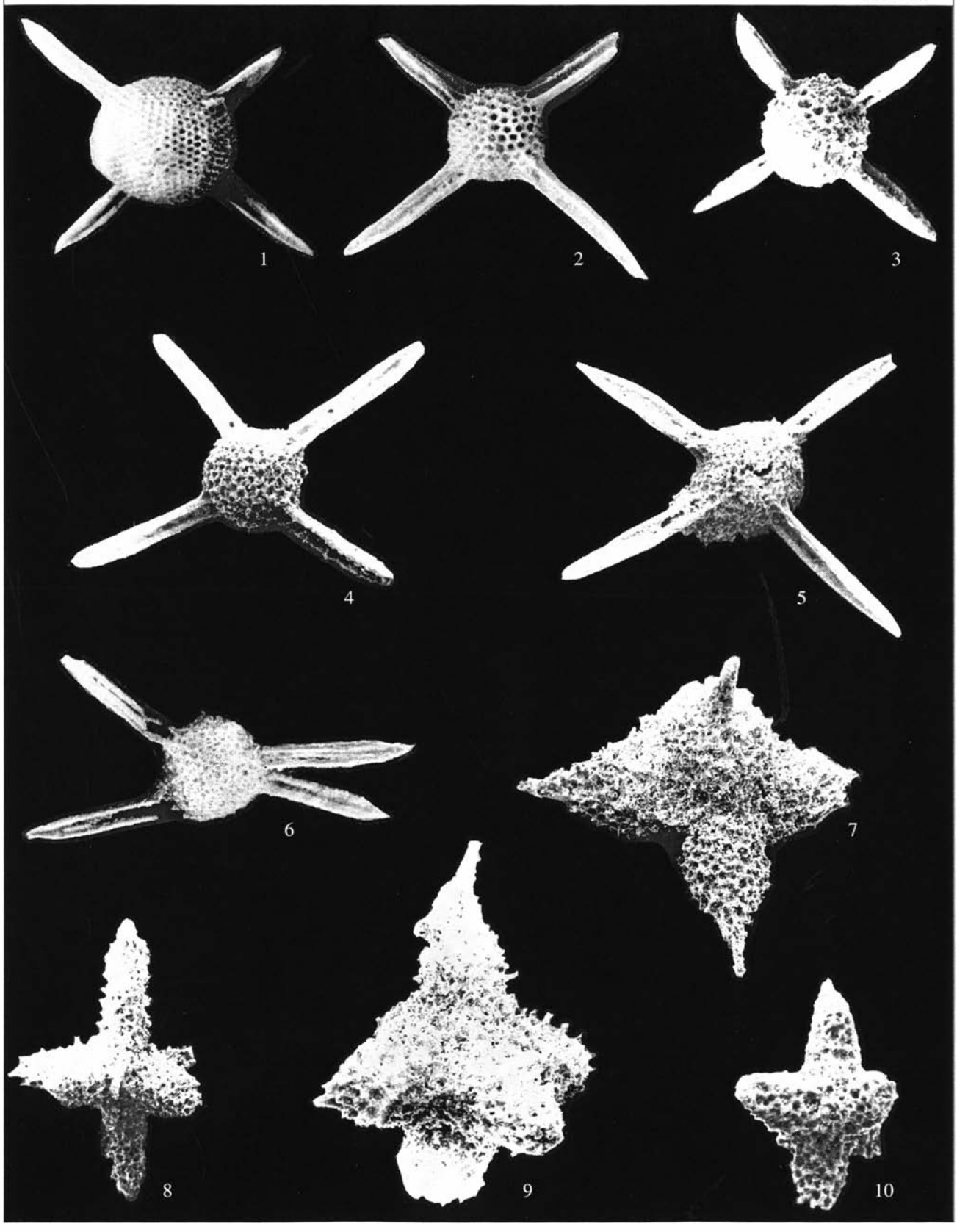

Staurosphaeretta hindei: Squinabol, 1904.
Staurosphaeretta longispina: O'Dogherty, 1994, p. 292, pl. 52, figs. 6–10.

Holotype. Northern Italy, southern Venetian Alps, Colli Euganei, Teolo locality; upper Lower Cretaceous–lower Upper Cretaceous, Upper Albian–Lower Turonian (Squinabol, 1903, pl. 9, fig. 1).

Comparison. *S. longispina* is distinguished from *S. euganea* (Squinabol, 1903) by the smaller diameter of the cortical shell and by its markedly longer spines.

Occurrence. Middle Albian–Lower Turonian of Italy; Middle–Upper Cenomanian of northern Turkey; Lower Turonian of the Crimean Mountains.

Material. More than ten specimens.

Staurosphaeretta wisniowskii (Squinabol, 1903)

Plate 14, figs. 5 and 6; Plate 36, fig. 17

Acanthosphaera Wisniowskii: Squinabol, 1903, p. 114, pl. 8, fig. 6.
Staurosphaeretta wisniowskii: O'Dogherty, 1994, p. 294, pl. 53, figs. 1–6.

Holotype. Northern Italy, southern Venetian Alps, Colli Euganei, Teolo locality; upper Lower Cretaceous–lower Upper Cretaceous, Upper Albian–Lower Turonian (Squinabol, 1903, pl. 8, fig. 6).

Comparison. This species is distinguished from *S. longispina* (Squinabol, 1903) by its greater number of spines (more than eight) whose length does not exceed the cortical shell diameter.

Occurrence. Middle Albian–Lower Turonian of Italy; Middle–Upper Cenomanian of northern Turkey; Lower Turonian of the Crimean Mountains.

Material. More than 50 specimens.

Genus *Tetracanthellipsis* Squinabol, 1903

Tetracanthellipsis euganeus Squinabol, 1903

Plate 16, fig. 6

Tetracanthellipsis euganeus: Squinabol, 1903, p. 177, pl. 8, fig. 9; O'Dogherty, 1994, p. 295, pl. 53, figs. 8–10.

Holotype. Northern Italy, southern Venetian Alps, Teolo locality; upper Lower Cretaceous–lower Upper Cretaceous, Middle Albian–Lower Turonian (Squinabol, 1903, pl. 8, fig. 9).

Comparison. *T. euganeus* differs from *T. gregalis* O'Dogherty, 1994 in the longer spines of a different shape (without thorns).

Occurrence. Upper Albian–Lower Turonian of Italy; Middle–Upper Cenomanian of northern Turkey.

Material. Fewer than 20 specimens.

Genus *Hexapyramis* Squinabol, 1903

Hexapyramis pantanellii Squinabol, 1903

Plate 16, figs. 7–10

Hexapyramis pantanellii: Squinabol, 1903, p. 114, pl. 10, fig. 5; Kuhnt *et al.*, 1986, pl. 7, fig. B; Thurow, 1988, p. 401, pl. 6, fig. 5; Erbacher, 1994, pl. 5, figs. 2 and 3; O'Dogherty, 1994, p. 283, pl. 50, figs. 3–7.

Holotype. Northern Italy, southern Venetian Alps, Colli Euganei, Teolo locality; upper Lower Cretaceous–lower Upper Cretaceous, Upper Albian–Lower Turonian (Squinabol, 1903, pl. 10, fig. 5).

Comparison. *H. pantanellii* differs from *H. precedis* Jud, 1994 in the longer rays and in the absence of smooth, high costae extending from one pore frame to another.

Occurrence. Albian–Turonian of Italy, Spain, and the Atlantic Region; Middle–Upper Cenomanian of northern Turkey; Lower Turonian of the Crimean Mountains.

Material. More than 50 specimens.

Family Leugeonidae Yang et Wang, 1990

Genus *Acaeniotyle* Foreman, 1973

Acaeniotyle diaphorogona Foreman, 1973

Plate 17, fig. 4; Plate 41, figs. 7 and 16

Acaeniotyle diaphorogona: Foreman, 1973, p. 258, pl. 2, figs. 2–5; 1975, p. 607, pl. 3, figs. 1 and 2; Nakaseko and Nishimura, 1981, p. 141, pl. 1, fig. 12; Schaaf, 1981, p. 431, pl. 15, fig. 2; Thurow, 1988, p. 396, pl. 9, fig. 8; Taketani and Kanie, 1992, fig. 3.1; Erbacher, 1994, pl. 5, fig. 1; O'Dogherty, 1994, p. 284, pl. 50, figs. 8–11; Urquhart and Robertson, 2000, pl. 1, fig. 21.
Acaeniotyle diaphorogona gr.: Jud, 1994, p. 57, pl. 1, fig. 4.
Acaeniotyle vitalis: Khan *et al.*, 1999, pl. 2, fig. e.
Acaeniotyle ex gr. *diaphorogona*: Vishnevskaya, 2001, pl. 21, fig. 12.

Holotype. USNM, no. 189032; northwestern Pacific, DSDP Leg 20; Lower Cretaceous (Foreman, 1973, pl. 2, fig. 3).

Comparison. *A. diaphorogona* is distinguished from *A. umbilicata* (Rust, 1898) by having three instead of two primary spines.

Occurrence. Hauterivian–Turonian worldwide; Middle–Upper Cenomanian of northern Turkey; Upper Cenomanian–Lower Turonian of the Crimean Mountains.

Material. More than 50 specimens.

Acaeniotyle longispina (Squinabol, 1903)

Plate 35, fig. 19; Plate 38, fig. 16

Xiphosphaera fossilis: Squinabol, 1903, p. 110, pl. 8, fig. 14.
Xiphosphaera longispina: Squinabol, 1903, p. 110, pl. 8, fig. 13.

Explanation of Plate 17

Figs. 1 and 2. *Acaeniotyle macrospina* (Squinabol, 1903), specimens: (1) GIN, no. 4871/183, ×200; and (2) GIN, no. 4871/184, ×200.

Figs. 3 and 7. *Acaeniotyle umbilicata* (Rust, 1898), (3) GIN, no. 4871/185, ×200); and (7) GIN, no. 4871/186, ×110.

Fig. 4. *Acaeniotyle diaphorogona* Foreman, 1973, GIN, no. 4871/187, ×120.

Figs. 5 and 6. *Triactoma cellulosa* Foreman, 1973, specimens: (5) GIN, no. 4871/188, ×120; and (6) GIN, no. 4871/189, ×130.

Fig. 8. *Triactoma compressa* (Squinabol, 1904), GIN, no. 4871/190, ×180.

Figs. 9 and 10. *Triactoma micropora* sp. nov., (9) paratype GIN, no. 4871/191, ×150; and (10) holotype GIN, no. 4871/192, ×100.
All specimens come from the Ürküt section.

Plate 17

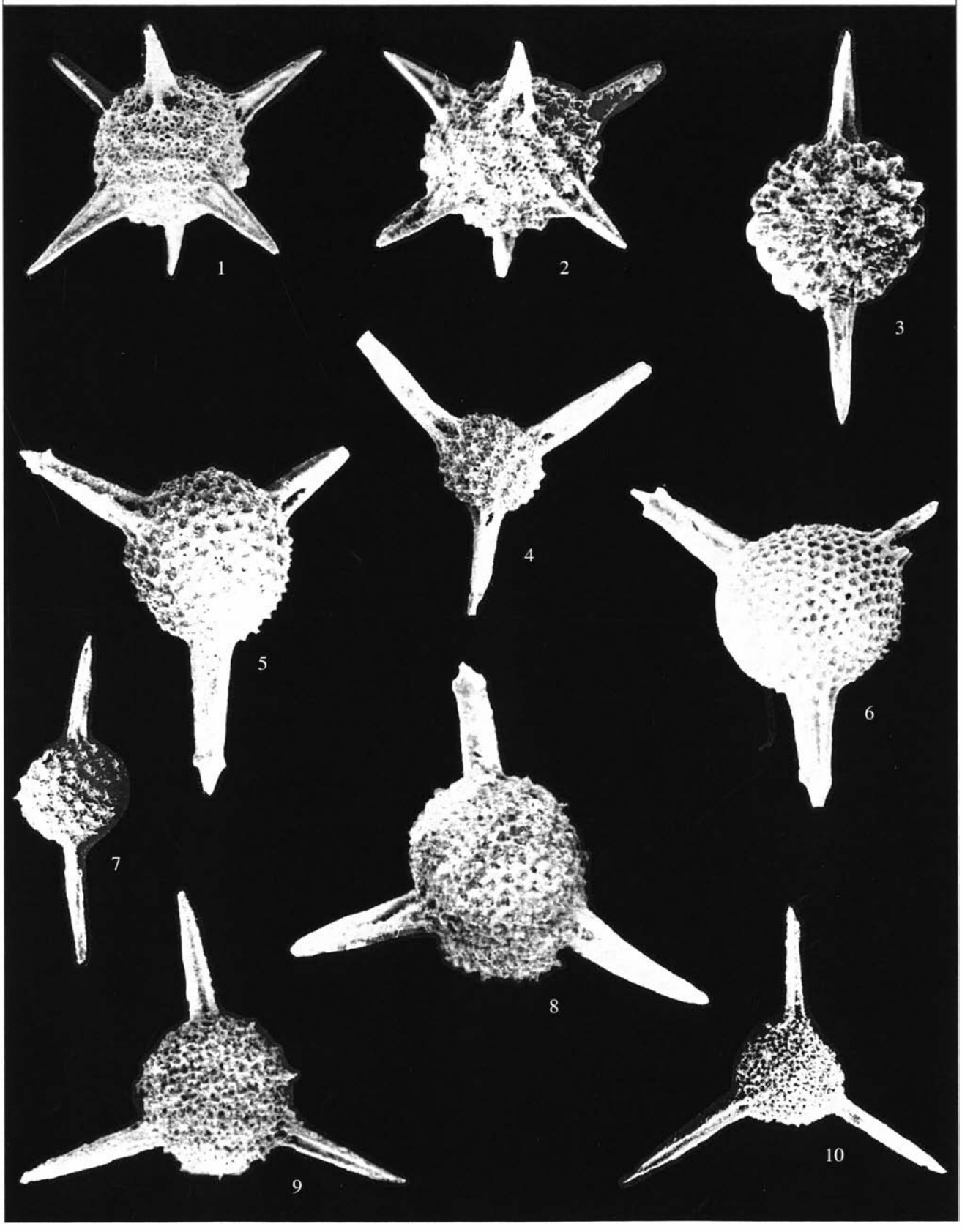

Plate 18

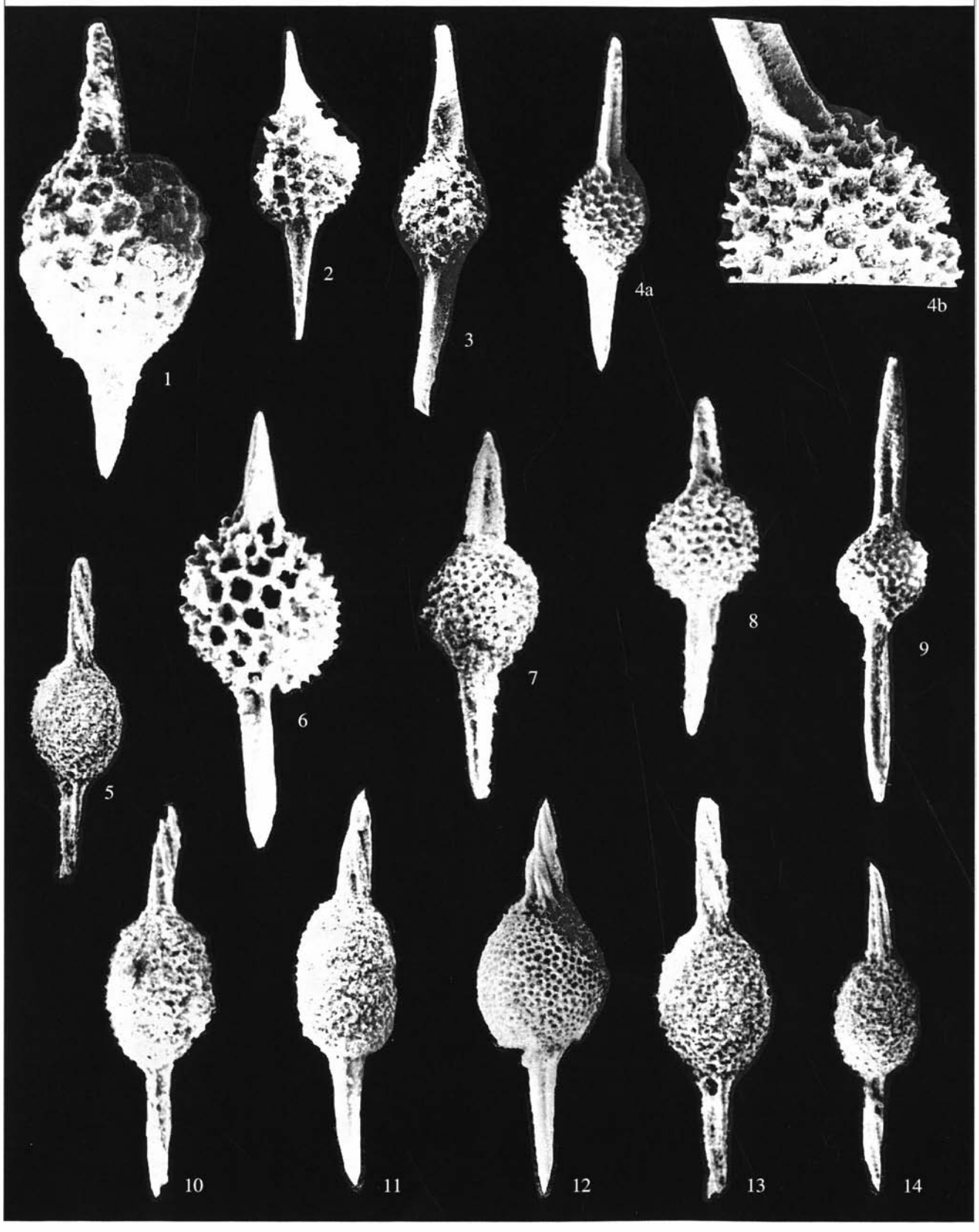

Acaeniotyle sp. aff. *A. umbilicata* sensu lato: Foreman, 1973, pl. 1, fig. 15; 1975, p. 609, pl. 2E, fig. 8; Li and Wu, 1985, pl. 1, fig. 8.

Acaeniotyle longispina: O'Dogherty, 1994, p. 290, pl. 51, figs. 21–25.

Non *Acaeniotyle longispina*: Vishnevskaya, 2001, pl. 21, fig. 8.

Holotype. Northern Italy, southern Venetian Alps, Colli Euganei, Teolo locality; upper Lower Cretaceous–lower Upper Cretaceous, Upper Albian–Lower Turonian (Squinabol, 1903, pl. 8, fig. 14).

Occurrence. Albian–Turonian worldwide; Lower Turonian of the Crimean Mountains.

Material. Fewer than 40 specimens.

Acaeniotyle macrospina (Squinabol, 1903)

Plate 17, figs. 1 and 2

Hexastylus macrospina: Squinabol, 1903, p. 112, pl. 8, fig. 7.

Actinomma (?) tuberculatum: Li and Wu, 1985, p. 73, pl. 2, fig. 17.

Acaeniotyle macrospina: O'Dogherty, 1994, p. 289, pl. 51, figs. 15–18.

Holotype. Northern Italy, southern Venetian Alps, Colli Euganei, Teolo locality; upper Lower Cretaceous–lower Upper Cretaceous; Upper Albian–Lower Turonian (Squinabol, 1903, pl. 8, fig. 7).

Comparison. *A. macrospina* differs from *A. umbilicata* (Rust, 1898) in having four spines in the plane perpendicular to that of the two polar spines. The apices of the four spines form the shape of a rectangle.

Occurrence. Upper Albian–Lower Turonian of Italy, Spain, and Tibet; Middle–Upper Cenomanian of northern Turkey.

Material. Fewer than 20 specimens.

Acaeniotyle umbilicata (Rüst, 1898)

Plate 17, figs. 3 and 7; Plate 41, fig. 8

Xiphosphaera umbilicata: Rüst, 1898, p. 7, pl. 1, fig. 9; Dumitrica, 1972, p. 832, pl. 1, fig. 1.

Xiphosphaera tuberosa: Tan, 1927, p. 35, pl. 5, fig. 1.

Acaeniotyle umbilicata: Foreman, 1973, p. 258, pl. 1, figs. 12–14, 16; 1975, p. 607, pl. 2E, figs. 14–17, pl. 3, fig. 3; Nakaseko and Nishimura, 1981, p. 141, pl. 1, fig. 7 (= specimen of Nakaseko *et al.*, 1979, pl. 4, fig. 7); pl. 14, fig. 2; Schaaf, 1981, pl. 6, fig. 11; Thurow, 1988, p. 396, pl. 9, fig. 7; pl. 15, figs. 3a and 3b; O'Dogherty, 1994, p. 289, pl. 51, figs. 19 and 20; Taketani and Kanie, 1992, Fig. 3.2; Bragin *et al.*, 2000, fig. 3.B; Urquhart and Robertson, 2000, pl. 1, fig. 19.

Non *Acaeniotyle umbilicata*: Foreman, 1975, p. 609, pl. 2E, fig. 8 (= *A. longispina* (Squinabol, 1903)); Erbacher, 1994, pl. 1, fig. 2 (= *A. starka* Empson-Morin, 1981).

Holotype. Northern Italy, southern Alps, Cittiglio locality; Neocomian, Maiolica Formation (Rust, 1898, pl. 1, fig. 9).

Occurrence. Upper Oxfordian–Turonian worldwide; Middle–Upper Cenomanian of northern Turkey; Lower Turonian of the Crimean Mountains.

Material. Fewer than 50 specimens.

Genus *Triactoma* Rüst, 1885

Triactoma: Rüst, 1885, p. 289.

Tripocyclia: Pessagno in Pessagno *et al.*, 1989, p. 212.

Type species. *Triactoma tithonianum* Rust, 1885; Jurassic, Tithonian; Beds with aptychi; Germany.

Diagnosis. Shell spherical, compressed, with three long spines, their apices arranged in a triangle shape.

Species composition. The type species and more than 15 species, including *T. micropora* sp. nov.; Pliensbachian–Coniacian worldwide.

Comparison. *Triactoma* differs from *Staurosphaeretta* Squinabol, 1904 in having only three spines.

Triactoma cellulosa Foreman, 1973

Plate 17, figs. 5 and 6; Plate 41, fig. 15

Triactoma cellulosa: Foreman, 1973, p. 259, pl. 2, figs. 9 and 10; pl. 16, fig. 9; O'Dogherty, 1994, p. 300, pl. 54, figs. 19–23.

Holotype. USNM, no. 189039; northwestern Pacific region, DSDP Leg 20; Lower Cretaceous, Aptian?–Upper Albian (Foreman, 1973, pl. 2, fig. 9).

Comparison. *T. cellulosa* is distinguished from *T. hexeris* O'Dogherty (1994) by its spherical shell and arrow-shaped spines.

Occurrence. Aptian?–Upper Albian of the northwestern Pacific Ocean; Middle Albian–Lower Turonian of Italy; Middle–Upper Cenomanian of northern Turkey; Lower Turonian of the Crimean Mountains.

Material. Fewer than 20 specimens.

Triactoma compressa (Squinabol, 1904), emend. herein

Plate 17, fig. 8; Plate 37, figs. 15 and 16; Plate 38, figs. 3 and 12

Spongotripus compressus: Squinabol, 1904, p. 206, pl. 6, fig. 7.

Triactoma compressa: O'Dogherty, 1994, p. 302, pl. 55, figs. 9–13.

Holotype. Northern Italy, southern Venetian Alps, Colli Euganei, Teolo locality; upper Lower Cretaceous–lower Upper Cretaceous, Upper Albian–Lower Turonian (Squinabol, 1904, pl. 6, fig. 7).

Explanation of Plate 18

Fig. 1. *Protoxiphotractus ventosus* O'Dogherty, 1994, GIN, no. 4871/193, ×500.

Figs. 2–4, and 6. *Dicroa rara* (Squinabol, 1904), specimens: (2) GIN, no. 4871/194, ×150; (3) GIN, no. 4871/195, ×140; (4) GIN, no. 4871/196: (a) general view, ×120, and (b) shell; porosity and ridged base of spine, ×450.

Figs. 5, 10, 11, 13, and 14. *Archaeospongoprunum cortinaensis* Pessagno, 1973, specimens: (5) GIN, no. 4871/197, ×120; (10) GIN, no. 4871/198; (11) GIN, no. 4871/199; (13) GIN, no. 4871/200; and (14) GIN, no. 4871/201 (10, 11, 13, 14, ×150).

Figs. 7 and 8. *Archaeospongoprunum pontidum* sp. nov.: (7) holotype GIN, no. 4871/202, ×200; and (8) paratype GIN, no. 4871/203, ×160.

Fig. 9. *Stylosphaera anatolica* sp. nov., holotype GIN, no. 4871/204, ×180.

Fig. 12. *Archaeospongoprunum klingi*, Pessagno, 1977, GIN, no. 4871/205, ×120.

All specimens come from the Ürküt section.

Plate 19

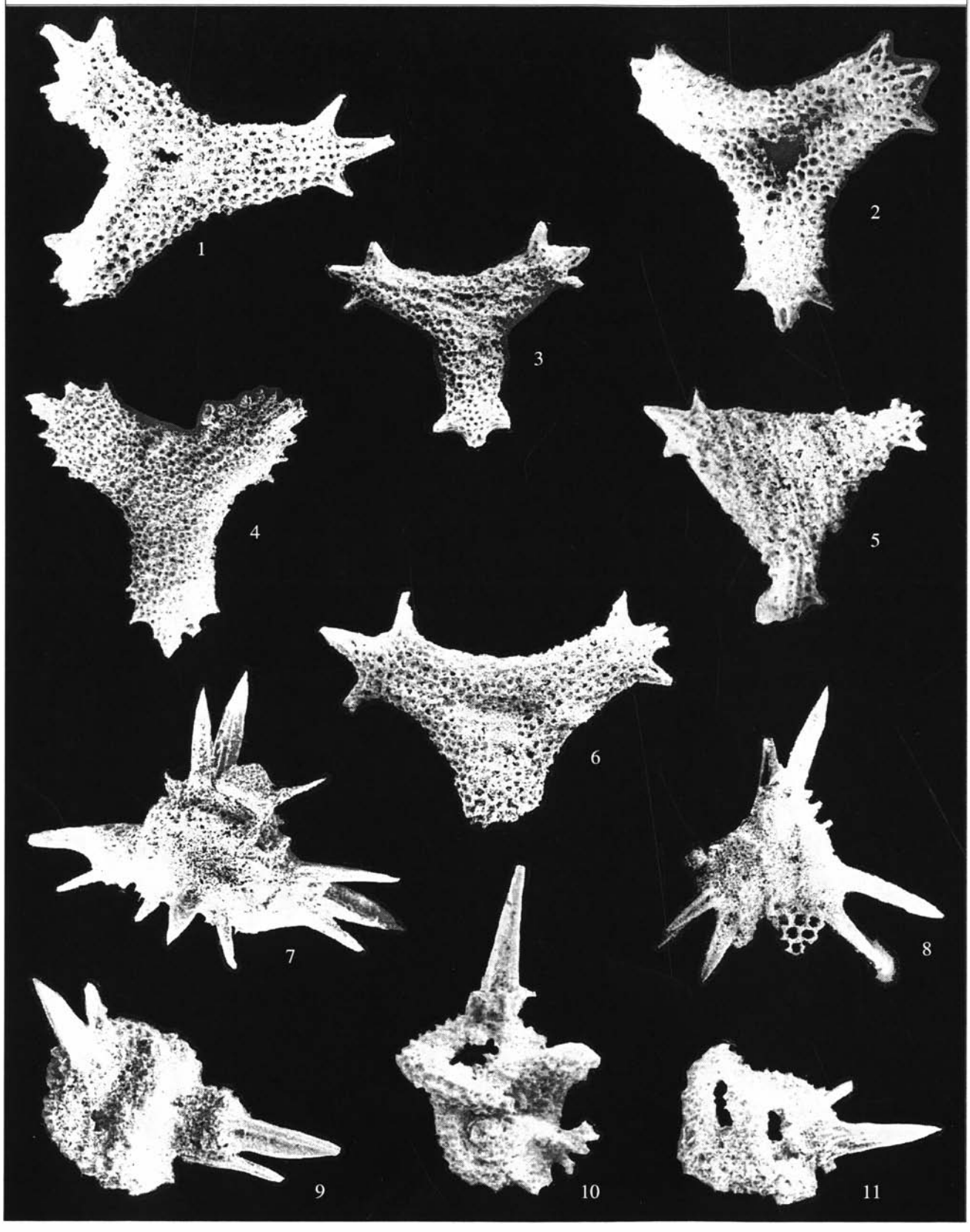

Description. The slightly flattened shell is rounded in outline. Three primary spines, almost equal in length, are arranged with their apices forming the shape of an isosceles triangle. The spines are massive, three-bladed, and slightly tapering. The edges of the blades are rounded–inflated. The cortical shell is covered by small round pores arranged in a hexagonal-pentagonal pattern. The patagium may be developed over the cortical shell.

Measurements. Cortical shell diameter, 260–100; primary spine length, 220–150.

Comparison. *T. compressa* is distinguished from *T. paronai* (Squinabol, 1903) by its slightly flattened (to lens-shaped) cortical shell and shorter spines, with their apices arranged in the shape of an isosceles triangle.

Occurrence. Upper Albian–Lower Turonian of Italy; Middle–Upper Cenomanian of northern Turkey; Lower Turonian of the Crimean Mountains.

Material. Fewer than 20 specimens.

Triactoma fragilis Bragina, 1996

Plate 41, figs. 1 and 6

Etymology. From the Latin *fragilis* (fragile).

Holotype. GIN, no. 4840/2; Cyprus; Upper Santonian–Lower Campanian, Perapedhi Formation.

Description. The spherical shell has a thin latticed wall and round pores. The hexagonal and pentagonal pore frames show small smooth nodes at the vertices. From 10 to 12 pore frames occur on the shell surface along the axis of the primary spines. The spines are short, narrow, at most one-fourth the diameter of the cortical shell. The base of each spine has three large oval pores. The pores are contiguous, with minor grooves thinning out in the middle of each spine. The spines abruptly taper distally.

Measurements. Cortical shell diameter, 120; spine length, up to 40.

Comparison. *T. fragilis* is distinguished from *T. parva* O'Dogherty, 1994 by its smoother shell surface, finer cortical pores, and three instead of four primary spines.

Occurrence. Upper Santonian–Lower Campanian of Cyprus; Lower Turonian of the Crimean Mountains.

Material. 15 specimens.

Triactoma micropora Bragina, sp. nov.

Plate 17, figs. 9 and 10

Triactoma sp. *A*: Khan *et al.*, 1999, pl. 1, fig. 1.

Etymology. From the Latin *micropora* (tiny pore).

Holotype. GIN, no. 4871/192; northern Turkey, Ürküt section; Upper Cretaceous, Middle Cenomanian, Tomalar Formation.

Description. The shell is subtriangular to rounded in outline, with three spines arranged in the shape of an isosceles triangle. The shell is regular to irregular (flattened centrally), lenticular in cross section. The spines are massive, three-bladed, acutely conical distally. The spine length is equal to, or slightly more than, the shell diameter. The shell is densely pierced by small polygonal pores nonuniform in size and irregularly arranged. Pore frames are irregular and polygonal, with pointed thorns, which vary substantially in size and shape. This makes the shell surface distinctly rough.

Measurements. Shell diameter in outline, 200; spine length, 150.

Comparison. *T. micropora* differs from *T. cellulosa* Foreman, 1973 in the irregular arrangement of the pores and the variable form of the cortical shell as well as the acutely conical apices of the spines.

Remarks. *T. micropora* is a second species of *Triactoma*, in addition to *T. compressa* (Squinabol, 1904), that possesses a nonspherical cortical shell and occurs in the Upper Cretaceous.

Occurrence. Cenomanian–Turonian of Spain; northern Turkey, Tomalar Formation, Ürküt section, Middle–Upper Cenomanian.

Material. Five complete and 11 incomplete specimens.

Triactoma parva (Squinabol, 1903)

Plate 41, fig. 2

Theodiscus parvus: Squinabol, 1903, p. 119, pl. 8, fig. 20.

Triactoma parva: O'Dogherty, 1994, p. 303, pl. 54, figs. 24–27.

Holotype. Northern Italy, southern Venetian Alps, Colli Euganei, Teolo locality; upper Lower Cretaceous–lower Upper Cretaceous, Upper Albian–Lower Turonian (Squinabol, 1903, pl. 8, fig. 20).

Comparison. Unlike the other species of *Triactoma* Rust, 1885, *T. parva* has four (as opposed to three) primary spines.

Explanation of Plate 19

Figs. 1–3, 5, and 6. *Paronaella spica* sp. nov., specimens: (1) GIN, no. 4871/206, ×130; (2) GIN, no. 4871/207, ×130; (3) GIN, no. 4871/208, ×100; (5) GIN, no. 4871/209, ×120; and (6) GIN, no. 4871/210, ×160.

Fig. 4. *Patulibracchium obesum* Pessagno, 1977, GIN, no. 4871/211, ×120.

Figs. 7–11. *Pyramispongia glascockensis* Pessagno, 1973, specimens: (7) GIN, no. 4871/212, ×130; (8) GIN, no. 4871/213, ×130; (9) GIN, no. 4871/214, ×160; (10) GIN, no. 4871/215, ×150); and (11) GIN, no. 4871/216, ×120; (10, 11) skeletal fragments.

Fig. 11. From the Tomalar section; others come from the Ürküt section.

Plate 20

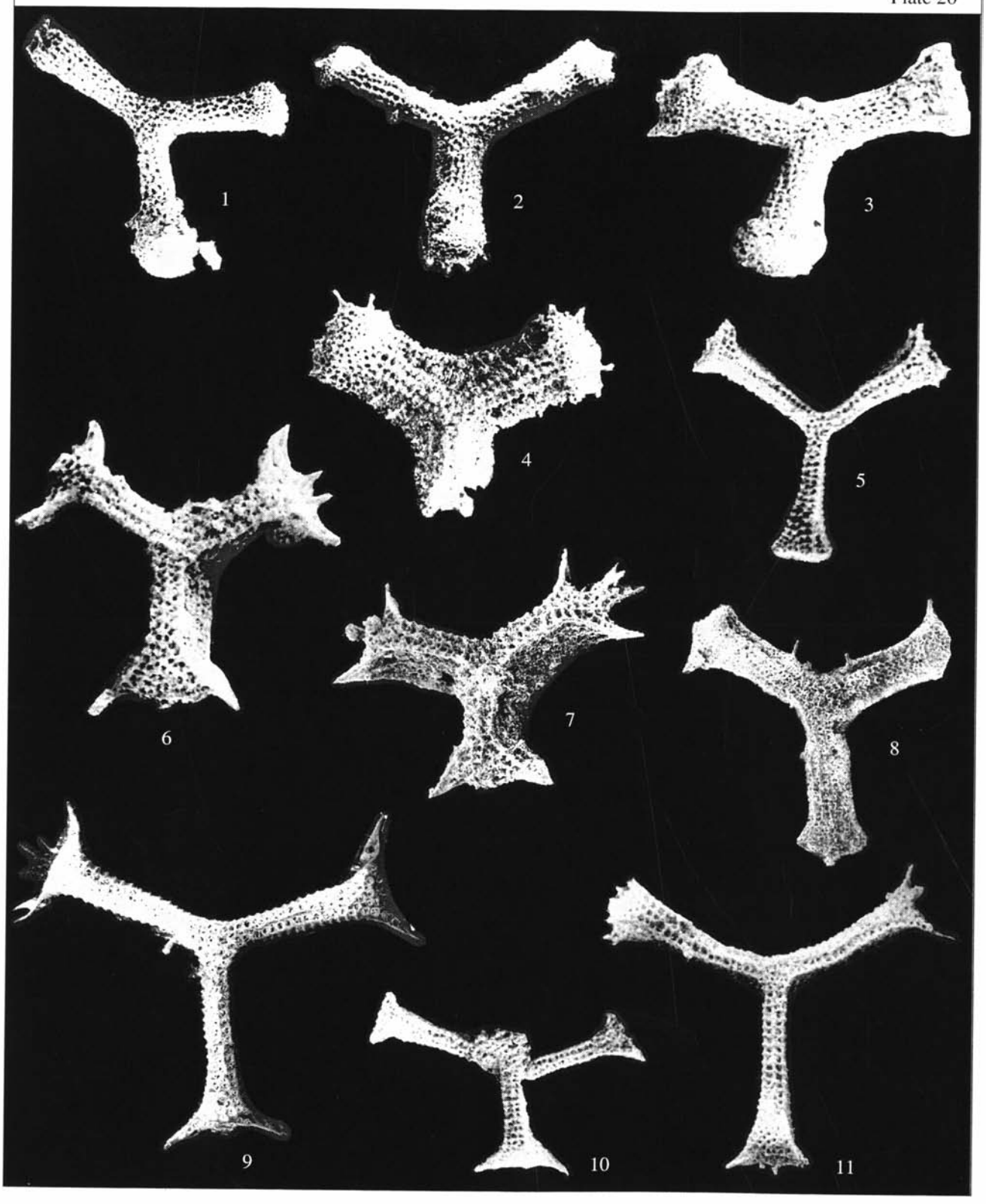

Occurrence. Upper Albian–Lower Turonian of Italy; Upper Cenomanian–Lower Turonian of the Crimean Mountains.

Material. Fewer than 20 specimens.

Family Pantanelliidae Pessagno, 1977
Genus *Dicroa* Foreman, 1975
Dicroa rara (Squinabol, 1904)

Plate 18, figs. 2–4, 6

Xiphosphaera rara: Squinabol, 1904, p. 189, pl. 2, fig. 10.
Dicroa rara: O'Dogherty, 1994, p. 281, pl. 49, figs. 26–30.

Holotype. Northern Italy, southern Venetian Alps, Colli Euganei, Teolo locality; upper Lower Cretaceous–lower Upper Cretaceous, Upper Albian–Lower Turonian (Squinabol, 1904, pl. 2, fig. 10).

Comparison. *D. rara* is distinguished from *D. periosa* Foreman, 1975 by the nonbifurcating polar spines.

Occurrence. Middle Albian–Lower Turonian of Italy; Middle–Upper Cenomanian of northern Turkey.

Material. Fewer than ten specimens.

Genus *Protoxiphotractus* Pessagno, 1973
Protoxiphotractus ventosus O'Dogherty, 1994

Plate 18, fig. 1

Protoxiphotractus ventosus: O'Dogherty, 1994, p. 277, pl. 49, figs. 17–20.

Holotype. UL, no. 5880; central Italy, Umbria-Marche Apennines, locality no. Asv-5-43; Upper Cretaceous, Lower Turonian (O'Dogherty, 1994, pl. 49, fig. 18).

Comparison. *P. ventosus* is distinguished from *P. machinosus* O'Dogherty, 1994 by the presence of only two primary spines, situated at the polar ends.

Occurrence. Lower Turonian of Italy and Spain; Middle–Upper Cenomanian of northern Turkey.

Material. Fewer than ten specimens.

Family Sponguridae Haeckel, 1887
Genus *Archaeospongoprunum* Pessagno, 1973

Archaeospongoprunum: Pessagno, 1973, p. 57.

Type species. *Archaeospongoprunum venadoensis* Pessagno, 1973; Middle–Upper Turonian, Venado Formation; California.

Diagnosis. Shell cylindrical, elliptical, or ellipsoidal, subdivided into two or three parts. Two polar spines three- or four-bladed in cross section. Spines usually with longitudinal grooves between the blades. Blades sometimes with spiral torsion.

Species composition. Several dozen species, including *A. archaeobipartitum* sp. nov., *A. pontidum* sp. nov., *A. sphaericum* sp. nov.; Cretaceous worldwide.

Comparison. *Archaeospongoprunum* differs from *Spongoprunum* Haeckel in having polar spines with longitudinal grooves alternating with the ridges.

Archaeospongoprunum archaeobipartitum Bragina, sp. nov.

Plate 35, fig. 14

Etymology. From the Latin *archaeo* (ancient) and the species name *bipartitum* established by Pessagno (1973).

Holotype. GIN, no. 4870/88; Crimean Mountains, Belaya Mountain section; Lower Turonian.

Description. The main axis divides the shell into two subspherical swollen parts, which are closely spaced and have two polar spines. The spines are very massive, three-bladed, and abruptly taper distally. One spine shows strong torsion. The spines are approximately as long as the diameter of the cortical shell in the section perpendicular to the main axis. The cortical shell is covered with large, rounded polygonal pores, set in 6- or 7-angled frames with triangular thorns at their elevated vertices. The pore diameter is equal to, or 1.5 time greater than, the distance between the neighboring pores.

Measurements. Cortical shell length, 270; greatest width, 150; spine length, 150.

Comparison. The new species is distinguished from *A. bipartitum* Pessagno, 1973 by the more massive pore frames of the cortical shell and by the fact that one spine is twisted strongly.

Remarks. Pessagno (1973) noted that some specimens of *A. bipartitum* have slightly coiling spine ends. This feature, and the similarity of their cortical shells, suggest that *A. archaeobipartitum* sp. nov. could be ancestral to *A. bipartitum* Pessagno, 1973.

Occurrence. Lower Turonian of the Crimean Mountains.

Material. Five complete and nine incomplete specimens.

Explanation of Plate 20

Figs. 1 and 2. *Patulibracchium woodlandensis* Pessagno, 1971, specimens: (1) GIN, no. 4871/217, ×120; and (2) GIN, no. 4871/218, ×150.

Fig. 3. *Pessagnobrachia fabianii* (Squinabol, 1914); GIN, no. 4871/219, ×100.

Figs. 4, 5, 8–11. *Halesium quadratum* Pessagno, 1971, specimens: (4) GIN, no. 4871/220, incomplete, ray terminations covered by patagium, ×170; (5) GIN, no. 4871/221, ×100; (8) GIN, no. 4871/222, ×120; (9) GIN, no. 4871/223, ×130; (10) GIN, no. 4871/224, ×80; and (11) GIN, no. 4871/225, ×100.

Figs. 6 and 7. *Halesium sexangulum* Pessagno, 1971, specimens: (6) GIN, no. 4871/226, ×120; and (7) GIN, no. 4871/227, ×130.

Figs. 9 and 11. From the Tomalar section. Other specimens come from the Ürküt section.

Plate 21

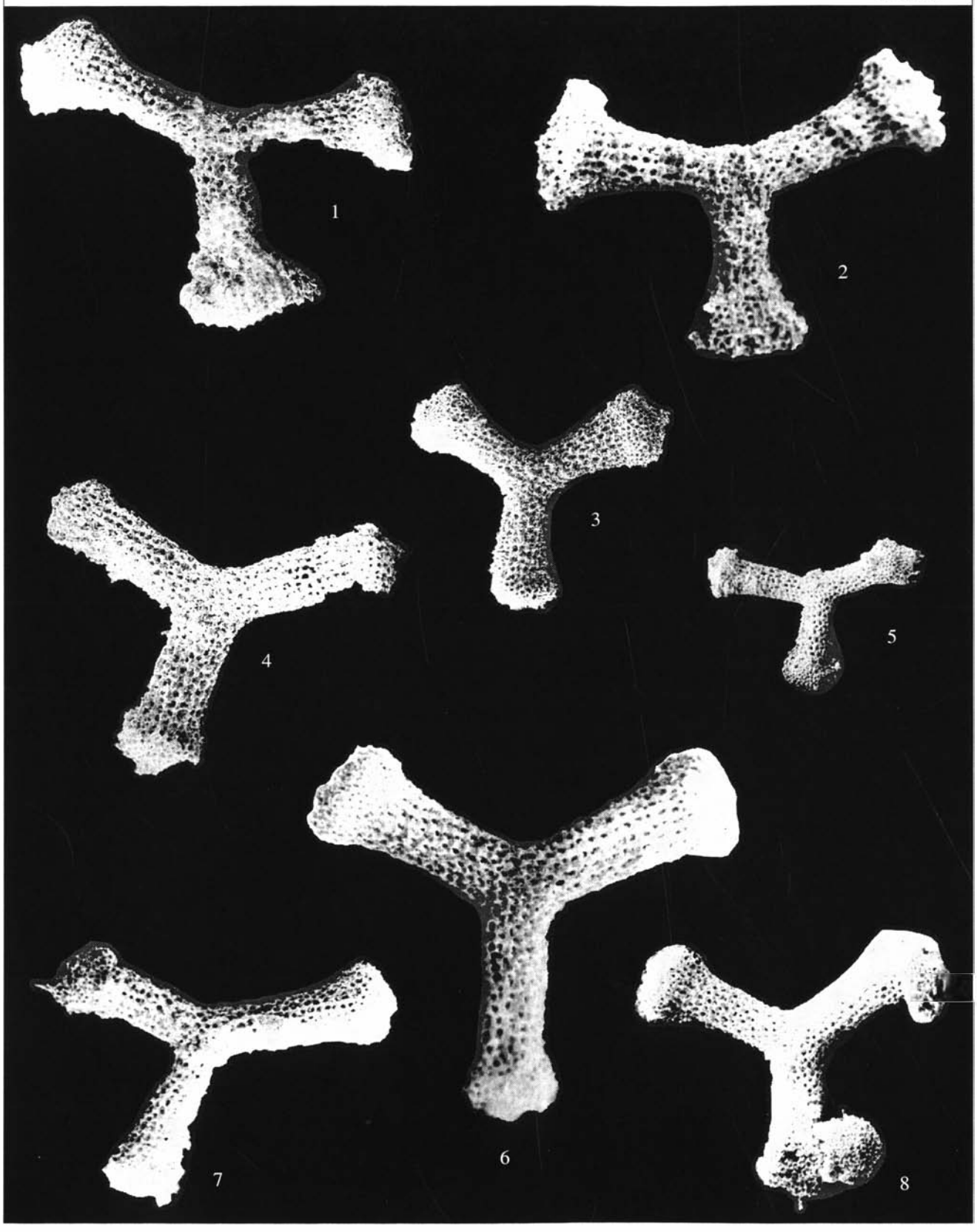

***Archaeospongoprunum cortinaensis* Pessagno, 1973**

Plate 18, figs. 5, 10, 11, 13, and 14; Plate 35, figs. 11, 12, 15, and 20

Archaeospongoprunum cortinaensis: Pessagno, 1973, p. 60, pl. 9, figs. 4–6; 1976, pl. 1, fig. 3; 1977, pl. 1, fig. 8; Schmidt-Effing, 1980, fig. 15; Nakaseko and Nishimura, 1981, p. 147, pl. 1, fig. 9; Schaaf, 1981, pl. 7, fig. 11; Thurow, 1988, p. 398, pl. 9, fig. 19; Salvini and Marcucci Passerini, 1998, fig. 9.b.

Holotype. USNM-Pessagno, no. 165602; California coast, Great Valley sequence, locality NSF 350; Upper Cretaceous, Lower Cenomanian, lower part of the Fiske Creek Formation (Pessagno, 1973, pl. 9, fig. 4).

Occurrence. Cenomanian–Coniacian worldwide; Upper Cenomanian–Lower Turonian of the Crimean Mountains; Upper Turonian of southwestern Sakhalin; Middle–Upper Cenomanian of northern Turkey.

Material. More than 30 specimens.

***Archaeospongoprunum klingi* Pessagno, 1977**

Plate 18, fig. 12

Archaeospongoprunum klingi: Pessagno, 1977, p. 29, figs. 1, 21, 23, and 24.

Holotype. USNM-Pessagno, no. 242803; California coast, Great Valley sequence, locality NSF 884; Lower Cretaceous, Upper Albian (Pessagno, 1977, pl. 2, figs. 1, 21, 23, and 24).

Comparison. *A. klingi* differs from *A. cortinaensis* Pessagno, 1973 in the structure of the twisted spine: (1) its base is more massive and (2) its blades may have a single deep groove at the base, which curved in the same direction as the twisting of the spine.

Occurrence. Upper Albian of California; Middle–Upper Cenomanian of northern Turkey.

Material. More than ten specimens.

***Archaeospongoprunum pontidum* Bragina, sp. nov.**

Plate 18, figs. 7 and 8

Etymology. From the Latin *pontidum*, based on the name of the area.

Holotype. GIN, no. 4871/202; northern Turkey, Ürküt section; Upper Cretaceous, Upper Cenomanian.

Description. The shell ranges from subspherical to regularly spherical, with two polar spines. The spines are very massive, three-bladed, and substantially narrowed at the end. One spine is slightly shorter and often more massive than the other. The blades of one spine are different in spatial orientation from those of the other. The length of the longest spine exceeds the cortical shell diameter. The pores of the cortical shell are rounded polygonal, set in 6- or 7-angled frames with triangular thorns at their elevated vertices.

Measurements. Long spine, 150; short spine, 100; shell diameter, 130.

Comparison. The new species is distinguished from *A. cortinaensis* Pessagno, 1973 by the spherical cortical shell and the absence of spine torsion.

Occurrence. Middle–Upper Cenomanian of northern Turkey.

Material. Eight complete and four incomplete specimens.

***Archaeospongoprunum sphaericum* Bragina, sp. nov.**

Plate 35, fig. 10

Etymology. From the Latin *sphaericus* (spherical).

Holotype. GIN, no. 4870/82; Crimean Mountains, Belaya Mountain section, Lower Turonian.

Description. The shell is nearly regularly spherical, with two three-bladed polar spines. The cortical shell is spongy. One polar spine is slightly shorter than the other and strongly twisted.

Measurements. Cortical shell diameter, 140–150; length of spines, 135 and 80.

Comparison. The new species is distinguished from *A. cortinaensis* Pessagno, 1973 by the spherical cortical shell.

Occurrence. Lower Turonian of the Crimean Mountains.

Material. Five complete and eight incomplete specimens.

***Archaeospongoprunum triplum* Pessagno, 1973**

Plate 35, fig. 13

Archaeospongoprunum triplum: Pessagno, 1973, p. 66, pl. 10, figs. 5 and 6; pl. 11, figs. 1–3; 1976, p. 33, pl. 6, fig. 2; Salvini and Marcucci Passerini, 1998, fig. 9.c; Vishnevskaya, 2001, pl. 125, figs. 14 and 15.

Holotype. USNM-Pessagno, no. 165606; California coast, Great Valley sequence, locality NSF 483; Upper Cretaceous, Coniacian, Yolo Formation (Pessagno, 1973, pl. 10, fig. 5).

Comparison. *A. triplum* differs from *A. bipartitum* Pessagno, 1973, in having a tripartite (instead of bipartite) shell.

Occurrence. Coniacian of California, Turonian–Coniacian of the Pacific region; Coniacian–Santonian of the Russian Plate; Lower Turonian of the Crimean Mountains; Middle–Upper Cenomanian of southwestern Sakhalin.

Material. More than ten specimens.

Explanation of Plate 21

Figs. 1, 2, 4, and 7. *Pessagnobrachia fabianii* (Squinabol, 1914), specimens: (1) GIN, no. 4871/228, ×130; (2) GIN, no. 4871/229, ×130; (4) GIN, no. 4871/230, ×130; and (7) GIN, no. 4871/231, ×100.

Figs. 3, 5, 6, and 8. *Patulibracchium woodlandensis* Pessagno, 1971, specimens: (3) GIN, no. 4871/232, ×100; (5) GIN, no. 4871/233, ×65; (6) GIN, no. 4871/234, ×140; and (8) GIN, no. 4871/235, ×100.

All specimens come from the Ürküt section.

Plate 22

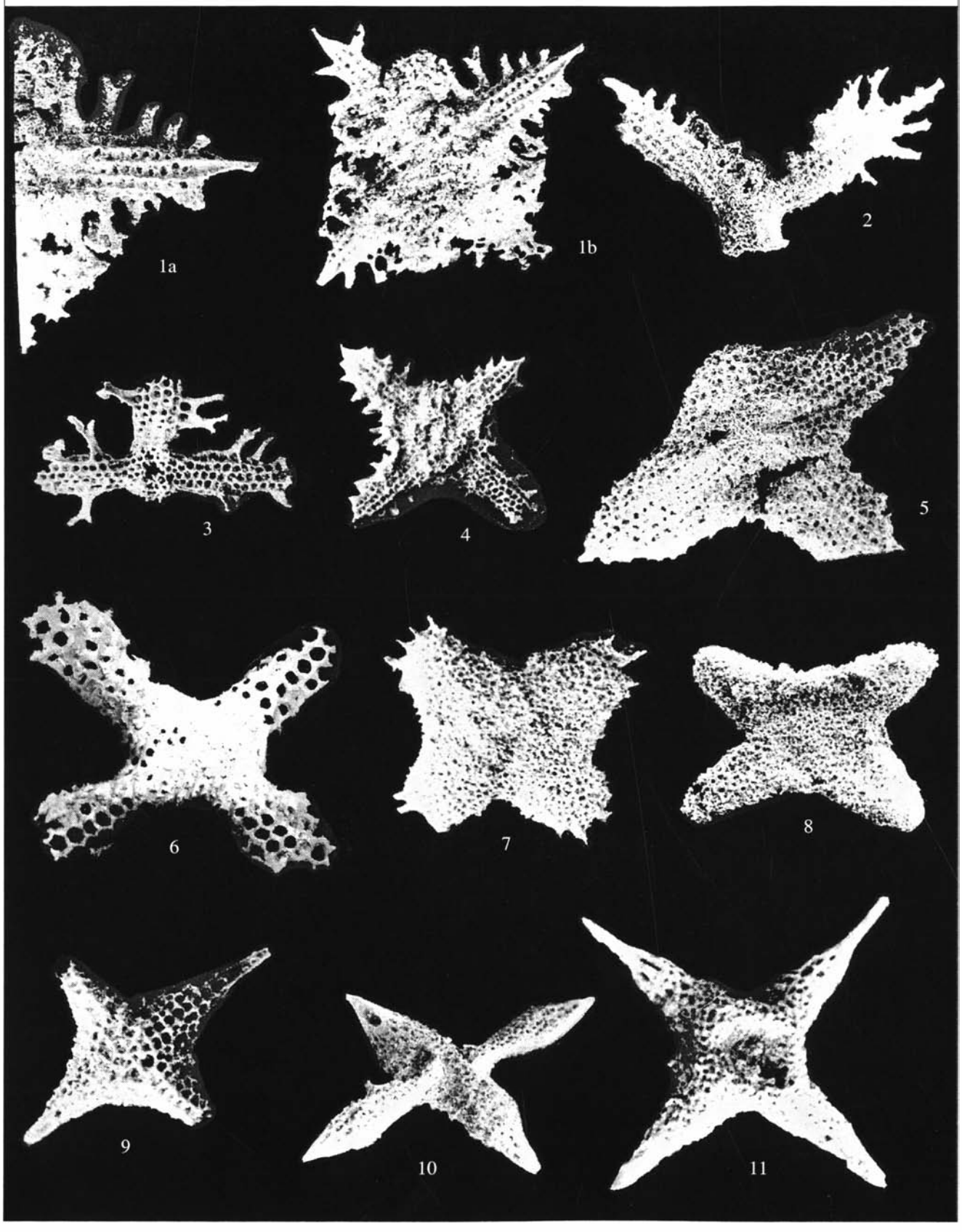

***Archaeospongoprunum* sp. *A.* sensu Pessagno, 1977**

Plate 38, fig. 15

Archaeospongoprunum sp. *A.*: Pessagno, 1977, p. 30, pl. 2, fig. 2.

Remarks. This morphotype from the Upper Albian beds of the Great Valley sequence was recorded without a description, probably because of the scarcity of specimens.

Occurrence. Upper Albian of California; Lower Turonian of the Crimean Mountains.

Material. Fewer than ten specimens.

Genus *Stylosphaera* Ehrenberg, 1847

Stylosphaera: Ehrenberg, 1847, p. 54.

Type species. *Stylosphaera hispida* Ehrenberg, 1854; Eocene; Barbados.

Diagnosis. Cortical shell subspherical to elliptical, with 10 to 20 pores in semiequator. Two polar primary spines. One spine longer than main axis of cortical shell. Single medullary shell inside cortical shell.

Species composition. Several dozen species, including *S. anatolica* sp. nov.; Upper Mesozoic–Recent.

Comparison. *Stylosphaera* is distinguished from *Amphisphaera* Haeckel, 1881 by having one (instead of two) medullar shells.

***Stylosphaera anatolica* Bragina, sp. nov.**

Plate 18, fig. 9

Etymology. From the Latin *anatolica* from Anatolia, where this species was collected for the first time.

Holotype. GIN, no. 4871/204; northern Turkey, Ürküt section; Upper Cretaceous, Middle Cenomanian.

Description. The shell is subspherical and has two long and massive polar spines. It is pierced by fine polygonal pores in polygonal frames with elevated vertices that make the shell surface rough. The three-bladed spines are constant in width throughout most of their length, but sharply narrow distally. The blades of one spine are similar in spatial orientation to those of the other. The termination of one spine may show slight torsion (40°). The spine length is 1.5–2 times greater than the cortical shell diameter.

Measurements. Spine length, 220; shell diameter, 120.

Comparison. The new species is distinguished from *S. ? macroxiphus* Rust, 1898 by the spatial orientation of the spine edges (the blades of one spine are similar in spatial orientation to those of the other); the smaller pores, and the only very slight variation in the size and shape of the pores.

Occurrence. Middle Cenomanian of northern Turkey.

Material. Four complete and three incomplete specimens.

Family Hagiastridae Riedel, 1967, emend. Pessagno, 1971

Genus *Paronaella* Pessagno, 1971

Paronaella: Pessagno, 1971a, p. 46.

Type species. *Paronaella solanoensis* Pessagno, 1971; Upper Cretaceous, Upper Turonian–Coniacian, Yolo Formation; locality NSF 483, California coast.

Diagnosis. Shell three-rayed in plan, without bracchiopyle. Rays may be different or equal in length, round or oval in cross section, and porous. Rays may bear small nodes. Terminations of rays variable in shape (ranging from swollen to smooth and pointed), sometimes with spines.

Species composition. More than ten species, including *P. spica* sp. nov. Stratigraphic and geographical ranges have not been determined.

Comparison. *Paronaella* differs from *Patulibracchium* Pessagno, 1971 in the absence of a bracchiopyle.

***Paronaella pseudoaulophacoides* O'Dogherty, 1994**

Plate 37, fig. 1

Paronaella pseudoaulophacoides: O'Dogherty, 1994, p. 356, pl. 67, figs. 8 and 9.

Holotype. UL, no. 6627; central Italy, Umbria-Marche Apennines, locality no. Asv-5-43; Upper Cretaceous, Lower Turonian (O'Dogherty, 1994, pl. 67, fig. 8).

Comparison. *P. pseudoaulophacoides* differs from *P. californiaensis* Pessagno, 1971 in the high tholus, completely fused rays, and in the shell shape, which is distinctly triangular in outline.

Occurrence. Lower Turonian of Italy and the Crimean Mountains.

Material. More than 20 specimens.

Explanation of Plate 22

Figs. 1–7. *Savaryella quadra* (Foreman, 1978), specimens: (1) GIN, no. 4871/236, (a) shell fragment to show porosity and patagium, ×180, and (b) general view, ×120; (2) GIN, no. 4871/237, ×120 and (3) GIN, no. 4871/238, ×90, shell fragments to show branching thorns of rays; (4) GIN, no. 4871/239, ×90; (5) GIN, no. 4871/240, ×120; (6) GIN, no. 4871/241, ×350; and (7) GIN, no. 4871/242, shell covered entirely with patagium, ×100.

Fig. 8. *Crucella aster* (Lipman, 1952), GIN, no. 4871/243, ×130.

Fig. 9. *Crucella euganea* (Squinabol, 1903), GIN, no. 4871/244, ×150.

Fig. 10. *Crucella hispana* O'Dogherty, 1994, GIN, no. 4871/245, ×80.

Fig. 11. *Crucella cachensis* Pessagno, 1971: GIN, no. 4871/246, ×130.

Fig. 2. From the Tomalar section; other specimens come from the Ürküt section.

Plate 23

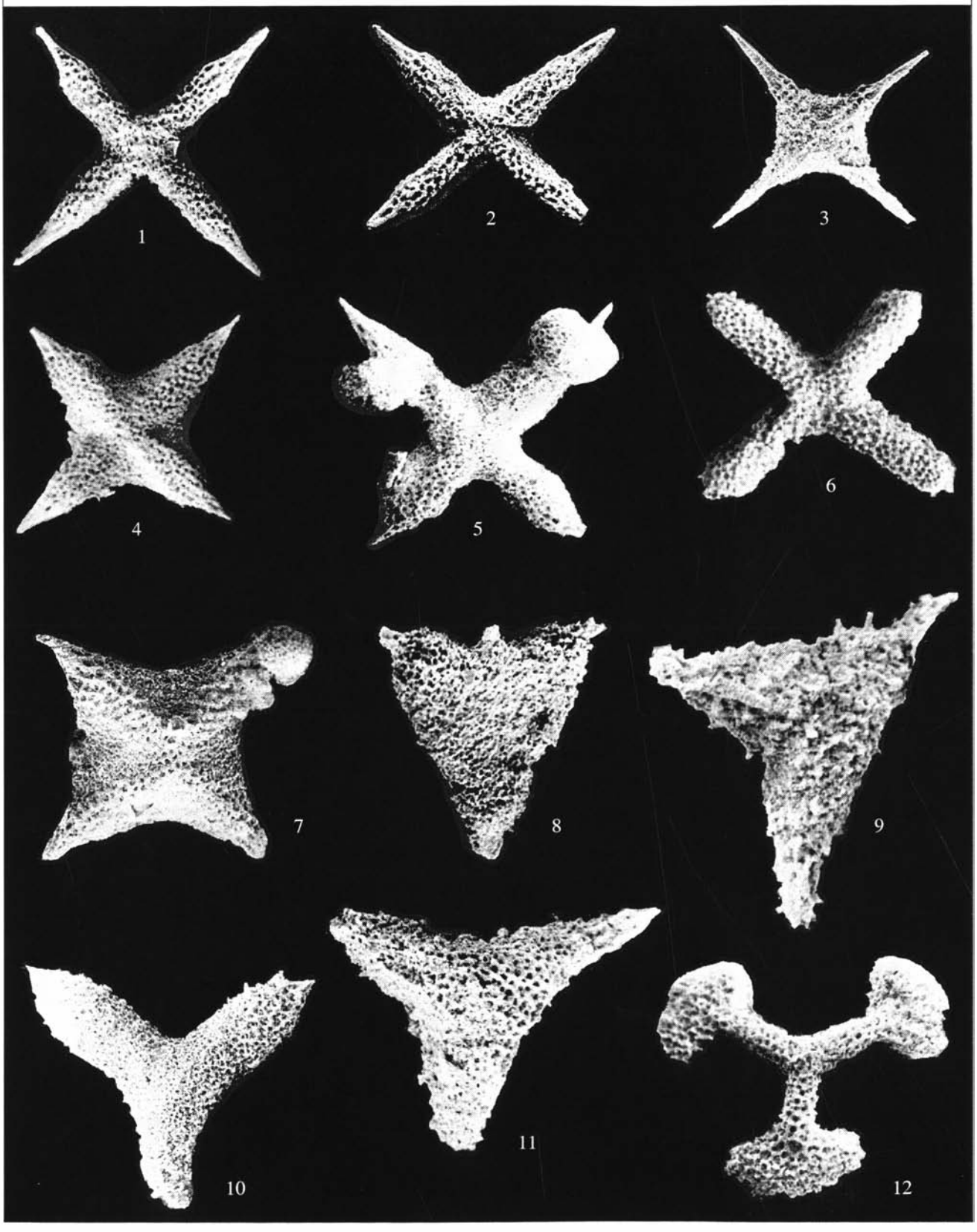

Paronaella solanoensis Pessagno, 1971

Plate 39, fig. 12

Paronaella solanoensis: Pessagno, 1971a, p. 48, pl. 10, figs. 2 and 3; Thurow and Kuhnt, 1986, text-fig. 9.18; Erbacher, 1994, pl. 17, fig. 15; Khan *et al.*, 1999, pl. 1.n.

Halesium sp.: Vishnevskaya, 2001, pl. 129, fig. 6.

Holotype. USNM-Pessagno, no. 165550; California coast, Great Valley sequence, locality NSF 483; Upper Cretaceous, Upper Turonian–Coniacian, Yolo Formation (Pessagno, 1971a, pl. 10, fig. 2).

Comparison. *P. solanoensis* is distinguished from *P. venadoensis* Pessagno, 1971 by the rays, which terminate in three massive spines almost equal in length.

Occurrence. Turonian–Coniacian of California, Spain, and Italy; Middle–Upper Cenomanian of northern Turkey; Upper Cenomanian–Lower Turonian of the Crimean Mountains.

Material. More than 20 specimens.

Paronaella spica Bragina, sp. nov.

Plate 19, figs. 1–3, 5, and 6; Plate 37, figs. 5, 6, 8, and 9; Plate 40, figs. 13 and 16

Spongodiscid gen. et sp. indet.: Foreman, 1971, pl. 5, fig. 4.

Paronaella sp.: Erbacher, 1994, pl. 12, fig. 7.

Paronaella grapevinensis: O'Dogherty, 1994, p. 352, pl. 1–8.

Etymology. From the Latin *spica* (spiny).

Holotype. GIN, no. 4870/114; Crimean Mountains, Sel'-Bukhra Mountain section; Lower Turonian.

Description. The shell is three-rayed in outline. The small central part is not elevated, and its diameter is equal to the width of its rays. The rays are rectangular in cross section, arranged in the shape of an equilateral or isosceles triangle and constant in width throughout most of their length, becoming wedge-shaped distally. Each ray terminates in a short spine with two shorter rays on either side. Several additional spines are present along the entire extent of the lateral edges of the rays. All the spines are bladed and abruptly taper distally, so that their ends become circular in cross section. The rays are covered by pores forming three or four rows, which extend from the base to the distal end. The pores are small, rounded polygonal, in low pore frames irregular in outline but predominantly tetragonal or pentagonal. The shell is often almost completely covered by the patagium, which makes it subtriangular. Only the apices of the rays usually remain uncovered.

Measurements. Ray length, 140–70; ray width, 70–30; pore diameter, 10–5.

Comparison. *P. spica* is distinguished from *P. solanoensis* Pessagno, 1971 by thinner rays constant in width, the nonpseudoaulophacoid structure of the shell, the less massive spines on the ray ends, and the well-developed patagium, which may cover up to 80% of the shell surface.

Occurrence. Middle Albian–Lower Turonian of Italy and the Pacific; Middle–Upper Cenomanian of Turkey; Lower Turonian of the Crimean Mountains.

Material. More than ten complete and several tens of incomplete specimens.

Genus *Halesium* Pessagno, 1971

Halesium: Pessagno, 1971a, p. 23.

Type species. *Halesium sexangulum* Pessagno, 1971; Upper Cretaceous, Lower Cenomanian, Fiske Creek Formation, upper part of Antelope Shale Beds; California, Great Valley section, locality NSF 350.

Diagnosis. Shell consisting of three long, narrow rays forming isosceles triangle shape. Rays rectangular in cross section, with lateral spines directed away from ray center. Weakly developed spine placed centrally on ray termination. Bracchiopyle sometimes located in place of one spine. Rays with three beams extending from their proximal part to end and with regular transverse and longitudinal rows of nodes alternating with round pores.

Species composition. *H. crassum* (Ozwoldova, 1979), *H. diacanthum* (Squinabol, 1914), *H. nevianii* (Squinabol, 1903), *H. quadratum* Pessagno, 1971, and *H. sexangulum* Pessagno, 1971; Cretaceous worldwide.

Comparison. *Halesium* differs from *Paronaella* Pessagno, 1971 in the presence of two to four beams on the rays, with regular transverse and longitudinal rows of nodes between these beams.

Explanation of Plate 23

Figs. 1 and 2. *Crucella messinae* Pessagno, 1971, specimens: (1) GIN, no. 4871/247, ×120; and (2) GIN, no. 4871/248, ×150.

Fig. 3. *Crucella euganea* (Squinabol, 1903), GIN, no. 4871/252, ×100.

Figs. 4, 5, and 7. *Crucella irwini* Pessagno, 1971, specimens: (4) GIN, no. 4871/249, ×140; (5) GIN, no. 4871/250, ×100; and (7) GIN, no. 4871/251, ×120.

Fig. 6. *Savaryella novalensis* (Squinabol, 1914), GIN, no. 4871/253, ×150.

Figs. 8 and 10. *Cavaspongia californiaensis* Pessagno, 1973, specimens: (8) GIN, no. 4871/254, ×120; and (10) GIN, no. 4871/255, ×160.

Figs. 9 and 11. *Cavaspongia antelopensis* Pessagno, 1973, specimens: (9) GIN, no. 4871/256, ×180; and (11) GIN, no. 4871/257, ×160.

Fig. 12. *Pessagnobrachia macphersoni* O'Dogherty, 1994, GIN, no. 4871/258, ×120.

All specimens come from the Ürküt section.

Halesium diacanthum (Squinabol, 1914)

Plate 40, fig. 10

Dictyastrum diacanthos: Squinabol, 1914, p. 274, pl. 21, fig. 3.

Halesium diacanthum: O'Dogherty, 1994, p. 349, pl. 65, figs. 1–8.

Holotype. Northern Italy, Venetian Alps, Vicentino Province, Novale locality; upper Lower Cretaceous–lower Upper Cretaceous, Upper Albian–Lower Turonian (Squinabol, 1914, pl. 21, fig. 3).

Comparison. *Halesium diacanthum* is distinguished from *H. quadratum* Pessagno, 1971 by the somewhat curved rays and less regular arrangement of pores on the rays.

Occurrence. Upper Albian–Lower Turonian of Italy and Spain; Lower Turonian of the Crimean Mountains.

Material. More than 30 specimens.

Halesium quadratum Pessagno, 1971, emend. herein

Plate 20, figs. 4, 5, 8–11; Plate 40, fig. 9

(?) *Distyastrum triacantos*: Squinabol, 1903, p. 121, pl. 9, fig. 28.

Halesium quadratum: Pessagno, 1971a, p. 23, pl. 3, figs. 1–6; pl. 4, figs. 1 and 2; Thurow and Kuhnt, 1986, text-fig. 9.16; Erbacher, 1994, pl. 16, fig. 8; pl. 17, fig. 14.

Halesium triacantos: O'Dogherty, 1994, p. 350, pl. 65, figs. 9–14.

Holotype. USNM-Pessagno, no. 165547; California, Great Valley sequence, locality NSF 350; Lower Cenomanian, Fiske Creek Formation (Pessagno, 1971a, pl. 3, figs. 1, 2).

Description. The shell shape is typical of the genus. The rays are narrow, long, and constant in width from the center to the base of the terminal spines and, distally, sharply widen in outline and framed by the marginal spines, which are directed away from the center of rays. The distal parts of the rays are inflated and higher in relief than their bases. A weakly developed spine is placed centrally on the ray end. A well-developed bracchiopyle may be in place of one of these spines. Three beams extend along the rays from their proximal part to the inflated end, the two lateral beams being slightly higher in relief than the intermediate one. The rays have both transverse and longitudinal rows of nodes alternating with rounded pores.

Measurements. Ray length, 350–250; width of the ray base, 75–34; greatest width of the ray end, 100–50.

Comparison. *H. quadratum* is distinguished from *H. sexangulum* Pessagno, 1971 in the form of the rays, which are longer, narrower and lower in relief, with the distal spines directed away from the ray center, and the rounded pores forming both transverse and longitudinal rows (in contrast, the pores of *H. sexangulum* are subtriangular and positioned between small beams connecting intermittently spaced nodes).

Occurrence. Lower Cenomanian–Turonian of California; Campanian of Cyprus; Upper Cenomanian–Lower Turonian of Italy and Spain; Lower Turonian of the Crimean Mountains; Middle–Upper Cenomanian of northern Turkey.

Material. More than 20 specimens.

Halesium sexangulum Pessagno, 1971

Plate 20, figs. 6 and 7; Plate 39, figs. 7 and 10

(?) *Distyastrum amissum*: Squinabol, 1914, p. 273, pl. 21 (2), fig. 2.

Halesium sexangulum: Pessagno, 1971a, p. 25, pl. 1, figs. 5 and 6; pl. 2, figs. 1–6; 1976, p. 29, pl. 1, fig. 6; Thurow and Kuhnt, 1986, text-fig. 9.15; Erbacher, 1994, pl. 16, fig. 9; pl. 17, fig. 13; Salvini and Marcucci Passerini, 1998, text-fig. 7.c.

Halesium cf. *sexangulum*: Kuhnt *et al.*, 1986, pl. 7, fig. e.

(?) *Halesium sexangulum*: Thurow, 1988, p. 401, pl. 6, fig. 3.

Halesium amissum: O'Dogherty, 1994, p. 351, pl. 65, figs. 15–23.

Holotype. USNM-Pessagno, no. 165544; California, Great Valley sequence, locality NSF 350; Upper Cretaceous, Lower Cenomanian, Fiske Creek Formation, upper part of Antelope Shale Beds (Pessagno, 1971a, pl. 1, figs. 5 and 6).

Occurrence. Lower Cenomanian of California; Upper Cenomanian–Lower Turonian of the Crimean Mountains, Italy, and Spain; Middle–Upper Cenomanian of northern Turkey; Campanian of Cyprus.

Material. More than 20 specimens.

Genus *Patulibracchium* Pessagno, 1971

Patulibracchium: Pessagno, 1971a, p. 26.

Type species. *Patulibracchium davisi* Pessagno, 1971; Upper Cretaceous, Lower Cenomanian, Fiske Creek Formation, Antelope Shale Beds, Franciscan Complex; California.

Diagnosis. Shell three-rayed in plan. Bracchiopyle present on one ray and occasionally bordered by secondary spines. Rays equal in size or slightly differing in length and circular, oval, or rectangular in cross section. Ray ends usually inflated, becoming arrow-shaped in outline. Each ray with one middle apical spine and, occasionally, with two additional spines. Pores in triangular to hexagonal or pentagonal pore frames.

Species composition. More than 20 species. Cretaceous worldwide.

Comparison. *Patulibracchium* differs from *Paronaella* Pessagno, 1971 in the presence of the bracchiopyle.

Patulibracchium ingens (Lipman, 1952), emend. Bragina (in Bragina and Bragin, in press)

Plate 40, figs. 12 and 14

Rhopalastrum ingens:-Lipman, 1952, p. 35, pl. XI, fig. 6.

Patulibracchium teslaensis: Salvini and Marcucci Passerini, 1998, fig. 8.b.

Non *Patulibracchium* cf. *ingens*: Vishnevskaya, 2001, p. 176, pl. 122, fig. 14 [*Pessagnobracchia rara* (Squinabol, 1914)].

Patulibracchium inaequalum: Pessagno, 1971a, p. 33, pl. 4, figs. 3–6; pl. 5, fig. 1.

Holotype. Chernyshev Central Geological Museum (TsGM), collection 6999, no. 26/28; Russian Plate, Penza Region, near the town of Kuznetsk; Upper Cretaceous, Santonian (Lipman, 1952, pl. XI, fig. 6).

Description. The shell is large and composed of three rays of different lengths. Two longer rays are slightly curved in opposite directions and positioned in almost the same line. The third ray is the shortest, and

is positioned almost at right angles to the others. The middle part of the shell is almost equal in diameter to the ray base and is slightly raised in relief. The ray bases are similar in width and, in some specimens, the ray width remains constant up to the arrow-shaped termination. In some specimens, the wide arrow-shaped termination characterizes either the two longer rays or the short one. The widest part of the arrow-shaped termination is raised in relief. Distally, the rays taper considerably and lower in relief and occasionally have a short spine at the end. The bracchiopyle commonly occurs in the short ray. The shell has rounded subrectangular pores, which usually form rows extending from the proximal part to the distal. Pore frames may bear small and low subspherical or conical nodes at vertices. The pores on the arrow-shaped terminations are in a hexagonal–pentagonal arrangement.

Measurements. Length of the short ray, 200–180; length of the long ray, 600–500.

Comparison. In distinction from *P. teslaensis* Pessagno, 1971, the rays of *P. ingens* differ in length and its long rays are positioned almost in line.

Occurrence. Nonstratified Coniacian–Campanian of the Russian Plate; Campanian of California; Lower Turonian of Italy; Upper Cenomanian of northern Turkey; Upper Cenomanian–Lower Turonian of the Crimean Mountains.

Material. More than 30 specimens.

Patulibracchium obesum Pessagno, 1977

Plate 19, fig. 4

Patulibracchium obesum: Pessagno, 1977, p. 27, pl. 1, figs. 17 and 18.

Holotype. USNM-Pessagno, no. 242797; California coast, Great Valley sequence, locality NSF 854; Lower Cretaceous, Lower Albian (Pessagno, 1977, pl. 1, figs. 17, 18).

Comparison. *P. obesum* differs from *P. venadoensis* Pessagno, 1971 in the wider rays with the round ends.

Occurrence. Lower Albian of California and Italy; Middle–Upper Cenomanian of northern Turkey; Upper Cenomanian–Lower Turonian of the Crimean Mountains; Upper Turonian of southwestern Sakhalin.

Material. More than 20 specimens.

Patulibracchium woodlandensis Pessagno, 1971, emend. herein

Plate 20, figs. 1 and 2; Plate 21, figs. 3, 5, 6, and 8; Plate 40, figs. 4, 7, and 15

Patulibracchium woodlandensis: Pessagno, 1971a, p. 45, pl. 5, figs. 2–6; Erbacher, 1994, pl. 16, fig. 11; pl. 18, fig. 2.

Non *Patulibracchium woodlandensis*: Erbacher, 1994, pl. 12, fig. 8 (= *P.* sp. aff. *P. woodlandensis* Pessagno, 1971).

Holotype. USNM-Pessagno, no. 165505; California coast, Great Valley sequence, locality NSF 350; Lower Cenomanian, upper Antelope Shale Formation and lower Fiske Creek Formation (Pessagno, 1971a, pl. 5, figs. 2, 3).

Description. The shell possesses three rays with the apices arranged in the shape of an equilateral triangle. Its central part is small, with the diameter not exceeding the width of the ray base. The rays gradually increase in width up to the raised bulbous termination, which is two times wider than the ray base. Distally, the terminations have short, variously developed spines. The bracchiopyle is commonly well-developed. The rays may have one or two short, narrow lateral spinules. The shell pores are fine, rounded polygonal, set in ridged irregularly polygonal frames, which bear small and relatively low hemispherical and conical nodes at their vertices. The patagium is relatively weakly developed.

Measurements. Ray length, 250–150; ray width, 80–60.

Occurrence. Lower Cenomanian of California; Middle-Upper Cenomanian of northern Turkey; Lower Turonian of the Crimean Mountains; Upper Cenomanian of southwestern Sakhalin, beds with *Cuboctostylus trifurcatus–Cassideus yoloensis* (Bragina, 2001).

Material. More than 50 specimens.

Patulibracchium (?) quadroastrum Bragina, 2003

Plate 39, fig. 11

Hagiastrum sp.: Bragina in Zinkevich *et al.*, 1988, pl. I, fig. 9.

(?) *Hagiastridae* gen. et sp. indet.: Bragina, Vituchin, 1997, pl. I, fig. 1.

Patulibracchium (?) quadroastrum: Bragina, 2003, p. 29, pl. III, figs. 3 and 6.

Etymology. From the Latin *quadroastrum* (four-rayed star).

Holotype. GIN, no. 4850/12; southern Sakhalin, Naiba River Basin; Upper Turonian, Unit VI of the Bykov Formation, beds with *Orbiculiforma monticelloensis–Cavaspongia contracta.*

Description. The shell is large and has four rays. The tholus is not raised in relief. Its diameter is one-third the ray length and equal to the width of the basal and middle parts of the rays. The ray terminations are acute and irregular in outline. One ray has a tubular bracchiopyle with small peripheral spinules, which is characteristic of the genus. The thorns and polygonal pores are set in irregular pore frames and are randomly distributed over the shell. The pore diameter is equal to, or lesser than, the distance between pores.

Measurements. Holotype no. 4850/12: ray length, 100; ray width, 35; pore size, 3–6.

Comparison. This species is distinguished from *P. inaequalum* Pessagno, 1971 by the presence of four rays of equal length, and from all other members of the genus *Patulibracchium* Pessagno, 1971 by the presence of the fourth ray.

Remarks. *P.* ? *quadroastrum* Bragina, 2003 was tentatively ascribed to *Patulibracchium* Pessagno, 1971 because of the presence of the fourth ray.

Occurrence. Maastrichtian of Kamchatka; Upper Turonian of southwestern Sakhalin; Lower Turonian of the Crimean Mountains.

Material. Six specimens.

Plate 24

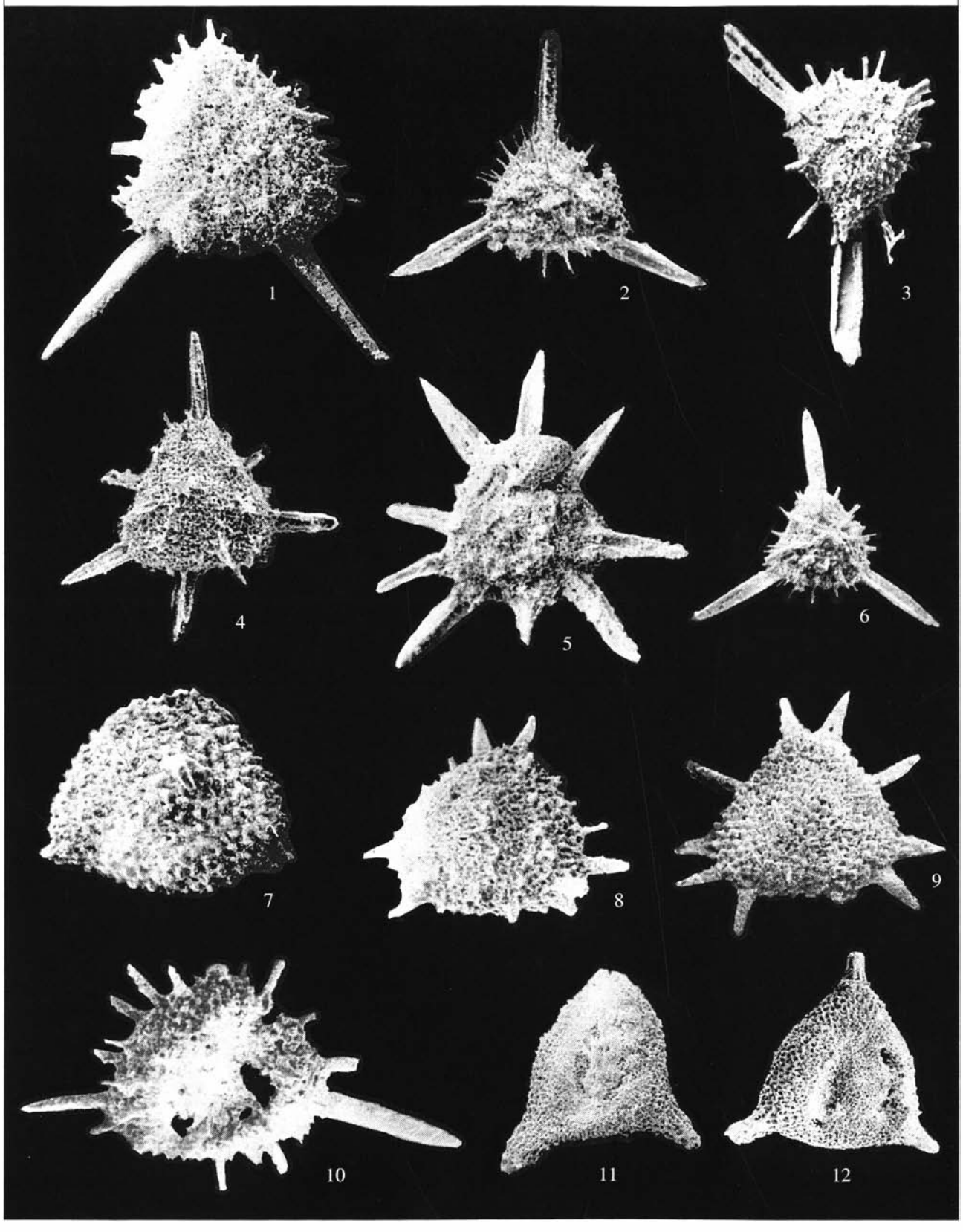

Genus *Savaryella* Jud, 1994

Savaryella quadra (Foreman, 1978)

Plate 22, figs. 1–7

Crucella quadra: Foreman, 1978a, p. 841, pl. 1, fig. 10.

Savaryella quadra: O'Dogherty, 1994, p. 372, pl. 72, figs. 1–7.

Holotype. Southeastern Atlantic, Leg 40, Site 364, depth interval 26–6, 56–58; uppermost Albian–Cenomanian (Foreman, 1978a, pl. 1, fig. 10).

Comparison. *S. quadra* differs from *S. spinosa* O'Dogherty, 1994 in the constant width of the rays throughout their length, and the orientation of the pores along the ray length.

Occurrence. Upper Albian–Cenomanian of the southeastern Atlantic; Upper Albian–Middle Cenomanian of Italy and Spain; Middle–Upper Cenomanian of northern Turkey; Lower Turonian of the Crimean Mountains.

Material. More than 15 specimens.

Savaryella novalensis (Squinabol, 1914)

Plate 23, fig. 6; Plate 39, figs. 1, 2, and 4

X-Astrum novalensis: Squinabol, 1914, p. 278, pl. 20, fig. 7.

Savaryella novalensis: O'Dogherty, 1994, p. 372, pl. 72, figs. 12–19.

Holotype. Northern Italy, Venetian Alps, Vicentino Province, Novale locality; upper Lower Cretaceous–lower Upper Cretaceous, Upper Albian–Lower Turonian (Squinabol, 1914, pl. 20, fig. 7).

Comparison. *S. novalensis* differs from the closely allied *S. spinosa* O'Dogherty, 1994 in the weakly differentiated central part and apices of rays arranged strictly in the shape of a regular rectangle and from *S. stella* O'Dogherty, 1994 by its much smaller, less strongly raised central area, and by having four (instead of five) rays.

Occurrence. Middle Albian–Lower Cenomanian of Italy; Upper Cenomanian of northern Turkey; Lower Turonian of the Crimean Mountains.

Material. More than 10 specimens.

Genus *Crucella* Pessagno, 1971

Crucella aster (Lipman, 1952) emend. Bragina (in Bragina and Bragin, in press)

Plate 22, fig. 8; Plate 38, fig. 14

Histiastrum aster: Lipman, 1952, p. 35, pl. 2, figs. 6 and 7; 1962, p. 300, pl. II, fig. 5; Kozlova and Gorbovets, 1966, p. 84, pl. III, fig. 9; Schaaf, 1981, pl. 8, fig. 1; Amon, 2000, pl. 6, figs. 14 and 15.

Crucella aster: Nakaseko and Nishimura, 1981, p. 148, pl. 2, fig. 10 (nomen nudum); Bragina and Bragin, in press

Non *Crucella aster*: Nakaseko and Nishimura, 1981, p. 148, pl. 2, fig. 9 (= *C. robusta* Bragina in Bragina and Bragin 1995); Urquhart and Banner, 1994, fig. 4.y; Gorbatchik and Kazintsova, 1998, pl. 1, fig. 10; Kazintsova, 2002, pl. 1, fig. 4.

Crucella cf. *aster*: Iwata and Tajika, 1986, pl. 5, fig. 4.

Holotype. TsGM, collection 6999, no. 16/28; Russian Plate, Penza Region, near the town of Kuznetsk; Santonian.

Description. The shell is medium-sized, with the apices of the rays arranged to form a square. The central part is small and is not raised in relief. Rays are wide at the base and gradually narrow distally to terminate with a massive spine. The shell is pierced with densely and irregularly spaced fine, rounded polygonal pores.

Measurements. Space between two adjacent ray apices, 247–437; ray length, 152–57; greatest ray width, 95–65; spine length, 60–20.

Comparison. *C. aster* is distinguished from *C. espartoensis* Pessagno, 1971 by the absence of distinct pore frames of regular outline and by the ray shape: the rays are not very conical in outline.

Occurrence. Uppermost Albian–Campanian worldwide; Upper Cenomanian–Lower Turonian of the Crimean Mountains; Upper Cenomanian of northern Turkey.

Material. More than 15 specimens.

Crucella cachensis Pessagno, 1971

Plate 22, fig. 11; Plate 38, figs. 8, 10, and 11; Plate 39, figs. 5, 6, and 9

Crucella cachensis: Pessagno, 1971a, p. 53, pl. 9, figs. 1–3; Foreman, 1971, p. 612, pl. 5, fig. 6; 1975, p. 612, pl. 5, fig. 6; Pessagno, 1976, p. 31, pl. 3, figs. 14 and 15; Taketani, 1982, p. 50, pl. 9, fig. 16; Kuhnt *et al.*, 1986, pl. 7, fig. J; Thurow and Kuhnt, 1986, text-figs. 9.5 and 9.6; Thurow, 1988, p. 399, pl. 2, fig. 13; Marcucci *et al.*, 1991, text-figs. 4j–4l; Marcucci and Gardin, 1992, text-fig. 4.m; O'Dogherty, 1994, p. 370, pl. 71, figs. 15–22; Salvini and Marcucci Passerini, 1998, fig. 9.k; Khan *et al.*, 1999, pl. 4, fig. h.

Non *Crucella cachensis*: Gorka, 1991, p. 42, pl. 2, figs. 7 and 8 (= *C.* ex gr. *C. bossoensis* Jud, 1994); p. 42, pl. 2, fig. 10 (= *C.* ex gr. *remanei* Jud, 1994); Vishnevskaya, 1993, pl. 10, fig. 4 (= *C.* ex gr. *C. espartoensis* Pessagno, 1971).

Crucella cachensis tolfaensis: Marcucci and Gardin, 1992, p. 563, text-figs. 4l and 4n; Pignotti, 1994, pl. 1, fig. 5; pl. 3, figs. 6 and 7.

Holotype. USNM-Pessagno, no. 165562; California coast, Great Valley sequence, locality NSF 697; Upper Cretaceous, Middle Turonian, Venado Formation (Pessagno, 1971a, pl. 9, figs. 5 and 6).

Explanation of Plate 24

Figs. 1 and 10. *Becus regius* O'Dogherty, 1994, specimens: (1) GIN, no. 4871/259, ×180; and (10) GIN, no. 4871/260, ×160.

Figs. 2, 3, and 6. *Becus horridus* (Squinabol, 1903), specimens: (2) GIN, no. 4871/261, ×120; (3) GIN, no. 4871/262, ×130; and (6) GIN, no. 4871/263, ×100.

Figs. 4 and 5. *Dispongotripus triangularis* (Squinabol, 1904), specimens: (4) GIN, no. 4871/264, ×140; and (5) GIN, no. 4871/265, ×180.

Fig. 7. *Pseudoaulophacus praefloresensis* Pessagno, 1972, GIN, no. 4871/266, ×100.

Figs. 8 and 9. *Pseudoaulophacus turcensis* sp. nov.: (8) GIN, no. 4871/267, ×140; and (9) holotype GIN, no. 4871/268, ×120.

Figs. 11 and 12. *Cavaspongia euganea* (Squinabol, 1904), specimens: (11) GIN, no. 4871/269, ×80; and (12) GIN, no. 4871/270, ×100.

Fig. 7. From the Tomalar section; all other specimens come from the Ürküt section.

Plate 25

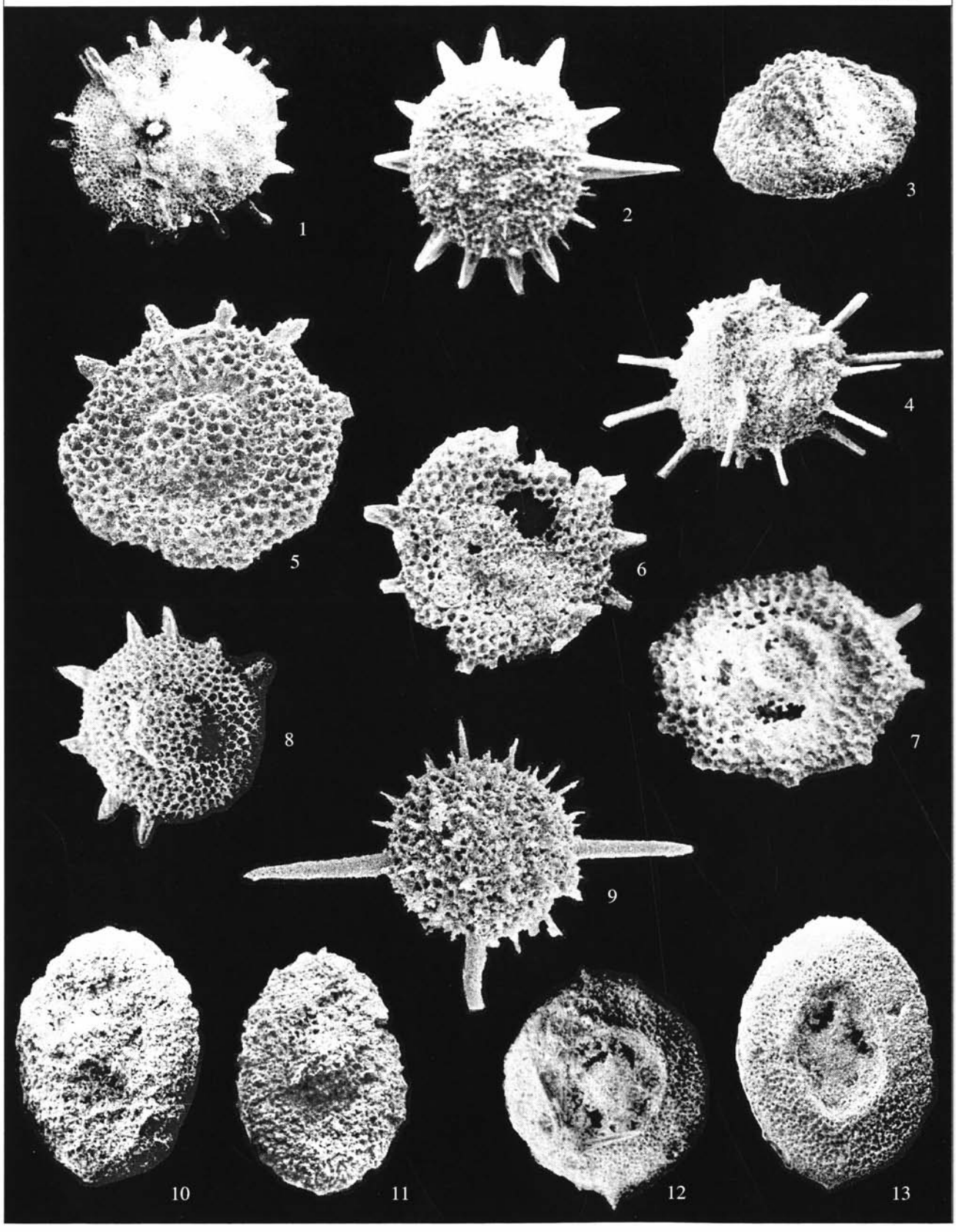

Comparison. *C. cachensis* differs from *C. irwini* Pessagno, 1971 in the high cylindrical tholus and the considerably lowered central part.

Remarks. The exterior of the holotype of *C. cachensis tolfaensis* Marcucci (Salvini and Marcucci Passerini, 1998) corresponds exactly to the diagnosis of *C. cachensis* Pessagno, 1971.

Occurrence. Turonian of California and the Atlantic; Lower Turonian of Italy, Spain, and Turkey; Lower Turonian of the Pacific; Upper Cenomanian–Lower Turonian of the Crimean Mountains; Upper Cenomanian of northern Turkey.

Material. More than 20 specimens.

Crucella euganea (Squinabol, 1903)

Plate 22, fig. 9; Plate 23, fig. 3

Stauralastrum euganeum: Squinabol, 1903, p. 123, p. 9, fig. 19.

Non *Hagiastrum ? euganeum*: Schaaf, 1981, p. 434, pl. 11, figs. 1a and 1b.

Pseudocrucella (?) sp.: Kuhnt *et al.*, 1986, pl. 7, fig. 1.

Crucella sp. *D*: Thurow, 1988, p. 399, pl. 5, fig. 23.

Crucella (?) sp.: Erbacher, 1994, pl. 18, fig. 3.

Crucella euganea: O'Dogherty, 1994, p. 367, pl. 70, figs. 10–20; Khan *et al.*, 1999, pl. 4, fig. i.

Holotype. Northern Italy, southern Venetian Alps, locality within Colli Euganei; upper Lower Cretaceous–lower Upper Cretaceous, Upper Albian–Lower Turonian (Squinabol, 1903, pl. 9, fig. 19).

Comparison. *C. euganea* differs from *C. aster* (Lipman, 1960) in the tholus rising above the shell, the larger subquadrate pores, and the longitudinal pore rows along the lengths of the rays.

Occurrence. Cenomanian–Lower Turonian of Italy, Spain, and the Atlantic; Middle–Upper Cenomanian of northern Turkey.

Material. Fewer than ten specimens.

Crucella hispana O'Dogherty, 1994

Plate 22, fig. 10

Crucella hispana: O'Dogherty, 1994, p. 365, pl. 70, figs. 1–5.

Holotype. UL, no. 5831; central Italy, Umbria-Marche Apennines, locality no. Asv-5-43; Lower Cretaceous, Upper Albian (O'Dogherty, 1994, pl. 48, fig. 1).

Occurrence. Upper Aptian of Italy and Spain; Upper Cenomanian of northern Turkey.

Material. Fewer than ten specimens.

Crucella irwini Pessagno, 1971

Plate 23, figs. 4, 5, and 7; Plate 39, figs. 3 and 8

Crucella irwini: Pessagno, 1971a, p. 54, pl. 9, figs. 4–6; O'Dogherty, 1994, p. 369, pl. 71, figs. 7–14.

Holotype. USNM-Pessagno, no. 165582; California coast, Great Valley sequence, locality NSF 705B; Upper Cretaceous, Middle Turonian, Marsh Creek Formation (Pessagno, 1971a, pl. 9, fig. 4).

Occurrence. Cenomanian–Campanian worldwide; Lower Turonian of the Crimean Mountains; Middle–Upper Cenomanian of northern Turkey.

Material. More than 15 specimens.

Crucella latum (Lipman, 1960), emend. Bragina (in Bragina and Bragin, in press)

Plate 37, fig. 12; Plate 38, fig. 13

Histiastrum latum: Lipman, 1960, p. 130, pl. XXIX, figs. 7 and 8; Amon, 2000, pl. 6, fig. 17.

Spongostaurus (?) hokkaidoensis: Iwata and Tajika, 1986, pl. 9, fig. 9.

Holotype. TsGM, collection 7767, no. 56/3; Western Siberia, lowermost radiolarian sequence, Borehole 1-R; Santonian–Campanian (Lipman, 1960, p. 130, pl. XXIX, figs. 7, 8).

Description. The shell is medium-sized, square in outline. Pores are small rounded polygonal, densely and irregularly spaced. The long, massive spines are commonly rounded in cross section and project from the corners of the square. The spines are occasionally hidden under the patagium, which may cover the shell.

Measurements. Shell length, 300–180; spine length, 70–30.

Occurrence. Uppermost Albian–Campanian worldwide; Lower Turonian of the Crimean Mountains.

Material. More than 20 specimens.

Crucella messinae Pessagno, 1971

Plate 23, figs. 1 and 2; Plate 38, fig. 5

Crucella messinae: Pessagno, 1971a, p. 56, pl. 6, figs. 1–3; 1976, p. 32, pl. 1, fig. 4 (= holotype refigured); 1977, p. 27, pl. 1, figs. 3, 4, and 13; Kuhnt *et al.*, 1986, pl. 7, fig. D; Thurow, 1988, p. 399, pl. 5, fig. 22; Erbacher, 1994, pl. 2, fig. 10; pl. 12, fig. 3; O'Dogherty, 1994, p. 368, pl. 70, figs. 21–24; Salvini and Marcucci Passerini, 1998, fig. 7p; Khan *et al.*, 1999, pl. 4, fig. j.

Explanation of Plate 25

Figs. 1 and 2. *Dactyliodiscus lenticulatus* (Jud, 1994), specimens: (1) GIN, no. 4871/271, ×100; and (2) GIN, no. 4871/272, ×90.

Fig. 3. *Patellula verteroensis* (Pessagno, 1963), GIN, no. 4871/273, ×160.

Fig. 4. *Patellula cognata* O'Dogherty, 1994, GIN, no. 4871/274, ×120.

Figs. 5–8. *Dactyliosphaera silviae* Squinabol, 1904, specimens: (5) GIN, no. 4871/275, ×150; (6) GIN, no. 4871/276, ×120; (7) GIN, no. 4871/277, ×130; and (8) GIN, no. 4871/278, ×130.

Fig. 9. *Dactyliodiscus spinosus* sp. nov., holotype GIN, no. 4871/279, ×200.

Figs. 10 and 11. *Orbiculiforma ovoidea* sp. nov.: (10) paratype GIN, no. 4871/280, ×110; and (11) holotype GIN, no. 4871/281, ×120.

Fig. 12. *Godia concava* (Li et Wu, 1985), GIN, no. 4871/282, ×70.

Fig. 13. *Godia tomalarea* sp. nov., holotype GIN, no. 4871/283, ×80.

Figs. 8–11. The Tomalar section; all other specimens come from the Ürküt section.

Plate 26

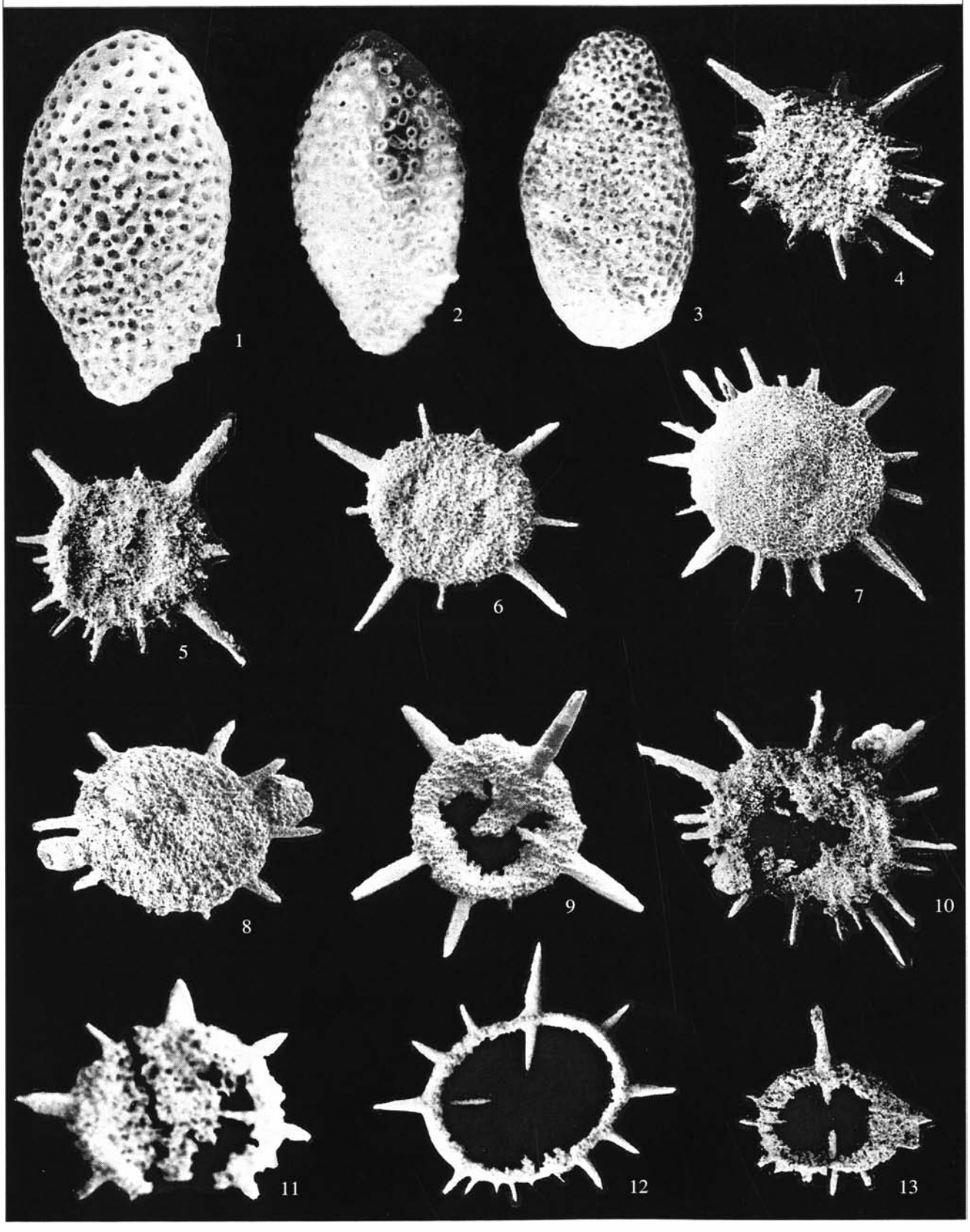

Non *Crucella messinae*: Taketani, 1982, p. 50, pl. 9, fig. 17 (= *C. irwini* Pessagno, 1971).

Holotype. USNM-Pessagno, no. 165569; California coast, Great Valley sequence, locality NSF 350; Upper Cretaceous, Lower Cenomanian, Fiske Creek Formation (Pessagno, 1971a, pl. 6, fig. 1).

Comparison. *C. messinae* is distinguished from *C. aster* (Lipman, 1952) by its more inflated rays and the pentagonal–hexagonal arrangement of the pores.

Occurrence. Lower Cenomanian of California; Albian–Cenomanian of Italy and the Atlantic; Middle–Upper Cenomanian of northern Turkey; Upper Cenomanian–Lower Turonian of the Crimean Mountains; undivided Coniacian–Campanian of the Russian Plate.

Material. More than 20 specimens.

Genus *Pessagnobrachia* Kozur et Mostler, 1978

Pessagnobrachia: Kozur et Mostler, 1978, p. 142.

Type species. *Patulibracchium teslaensis* Pessagno, 1971; Upper Cretaceous, Campanian, Upper Panoche Group; California.

Diagnosis. Spongy discoidal shell with three rays, largely covered by patagium.

Species composition. About ten species, including *P. fabianii* (Squinabol, 1914) and *P. macphersoni* O'Dogherty, 1994; Berriasian–Coniacian of the Tethys and Atlantic.

Comparison. *Pessagnobrachia* is distinguished from *Paronaella* Pessagno, 1971 by the presence of the bracchiopyle and more spongy skeleton. In distinction from *Halesium* Pessagno, 1971, it lacks beams on the upper and lower parts of the shell and pores arranged in parallel rows on the rays.

Pessagnobrachia macphersoni O'Dogherty, 1994, emend. herein

Plate 23, fig. 12

Pessagnobrachia macphersoni: O'Dogherty, 1994, p. 361, pl. 68, figs. 14–20.

Holotype. UL, no. 3767; central Italy, Umbria-Marche Apennines, locality Gc-1073-94; Middle Cenomanian (O'Dogherty, 1994, pl. 68, fig. 18).

Description. The shell is three-rayed. The ray width is almost constant in outline from the base to the wide club-shaped termination. In relief, the shell gradually lowers from the central part to the ray terminations. The ray pores are small, variable in size, in a hexagonal-pentagonal arrangement and in irregular pore frames. Being densely covered by the patagium, some shells are subtriangular in outline.

Measurements. Ray length, 220–200; ray width at the base, 90–45; greatest width of terminations, 225–160.

Comparison. *P. macphersoni* is distinguished from *P. dalpiazii* (Squinabol, 1914) by the high relief of the central part.

Occurrence. Middle Cenomanian of Italy and Spain; Upper Cenomanian of northern Turkey.

Material. Fewer than ten specimens.

Pessagnobrachia fabianii (Squinabol, 1914)

Plate 21, figs. 1, 2, 4, and 7

Rhopalastrum Fabianii: Squinabol, 1914, p. 274, pl. 21, fig. 4.

Pessagnobrachia fabianii: O'Dogherty, 1994, p. 359, pl. 67, figs. 17–25.

Holotype. Northern Italy, Venetian Alps, Vicentino Province, Novale locality, Teolo locality; upper Lower Cretaceous–lower Upper Cretaceous, Upper Albian–Lower Turonian (Squinabol, 1914, pl. 21, fig. 4).

Occurrence. Upper Albian–Lower Turonian of Italy and Spain; Middle–Upper Cenomanian of northern Turkey.

Material. Fewer than ten specimens.

Family Cavaspongiidae Pessagno, 1973
Genus *Cavaspongia* Pessagno, 1973
Synonym: *Dumitricaia* Pessagno, 1976.

Cavaspongia: Pessagno, 1973, p. 76.

Type species. *Cavaspongia antelopensis* Pessagno, 1973; Upper Cretaceous, Lower Turonian, Antelope Shale Beds, Fiske Creek Formation; California.

Diagnosis. Cortical shell biconvex and three-rayed. Rays constant in length to termination. Terminations with short lateral spinules (variable in number) on both sides of massive central spine (frequently broken). Cortical shell connected with medullary shell by three massive spongy beams extending from central spines or ray terminations. Medullary shell connected to internal part of cortical shell by narrow radiating spines of variable number.

Species composition. *C. antelopensis* Pessagno, 1973, *C. californiaensis* Pessagno, 1973, *C. cylindrica* O'Dogherty, 1994, *C. contracta* O'Dogherty, 1994, *C. euganea* (Squinabol, 1904), *C. helice* O'Dogherty, 1994, *C. robusta* sp. nov., *C. sphaerica* O'Dogherty, 1994, *C. tavrica* sp. nov., *C. tricornis*

Explanation of Plate 26

Figs. 1 and 2. *Phaseliforma laxa* Pessagno, 1972, specimens: (1) GIN, no. 4871/284, ×200; and (2) GIN, no. 4871/285, ×160.

Fig. 3. *Phaseliforma carinata* Pessagno, 1972, GIN, no. 4871/286, ×160.

Figs. 4–13. *Dactyliodiscus longispinus* (Squinabol, 1904), specimens: (4) GIN, no. 4871/287, ×80; (5) GIN, no. 4871/288, ×100; (6) GIN, no. 4871/289, ×90; (7) GIN, no. 4871/290, ×100; (8) GIN, no. 4871/291, ×120; (9) GIN, no. 4871/292, ×120; (10) GIN, no. 4871/293, ×120; (11) GIN, no. 4871/294, ×120; (12) GIN, no. 4871/295, ×120; and (13) GIN, no. 4871/296, ×60. (9–13) incomplete specimens showing internal structure of shell.

Fig. 8. From the Tomalar section; all other specimens come from the Ürküt section.

Plate 27

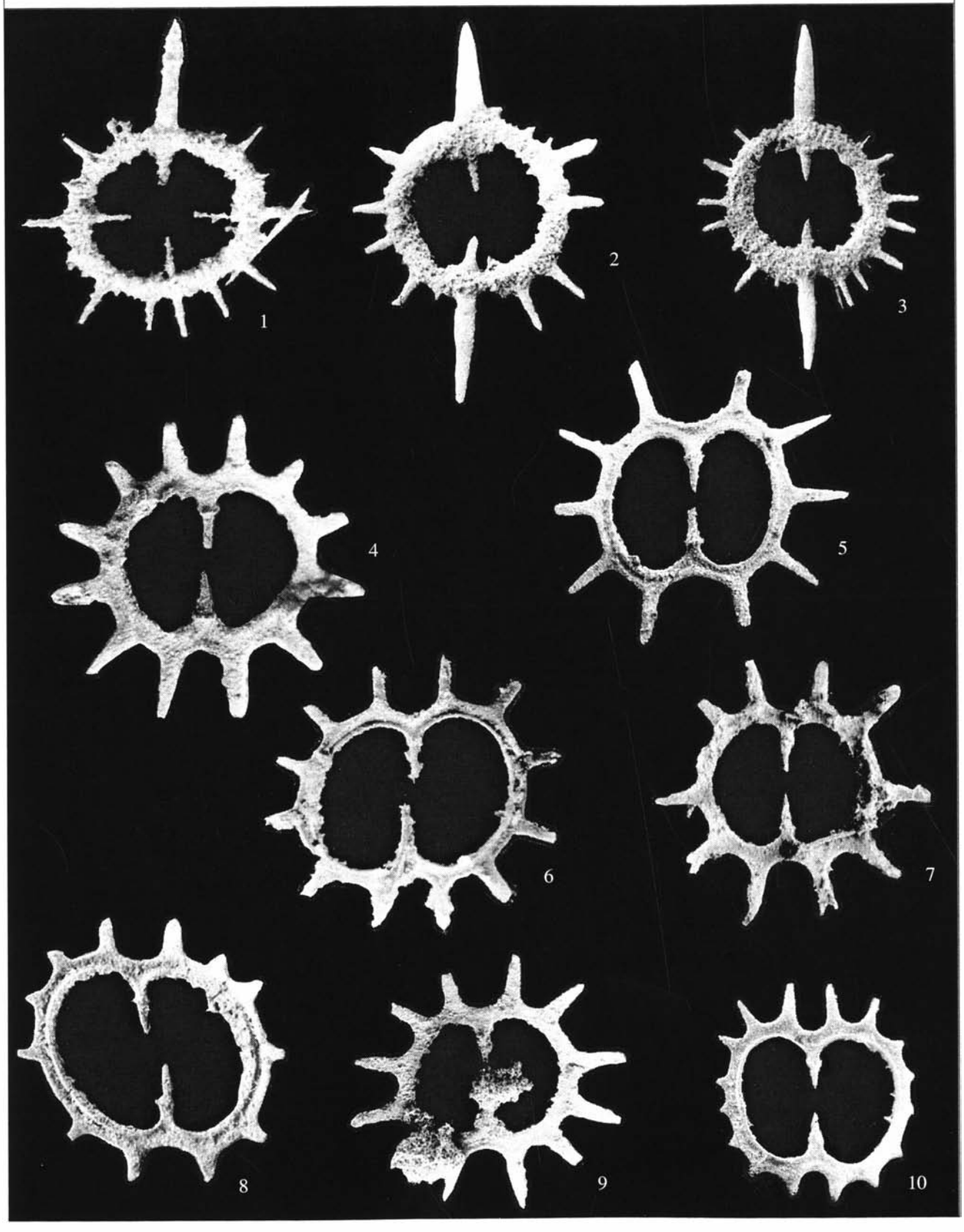

O'Dogherty, 1994; Middle Albian–Campanian, geographical range has not been determined.

Comparison. *Cavaspongia* differs from *Cyclastrum* Rust, 1898 in the distinctly three-rayed shell and the better developed patagium.

Cavaspongia antelopensis Pessagno, 1973

Plate 23, figs. 9 and 11; Plate 37, fig. 7

Cavaspongia antelopensis: Pessagno, 1973, p. 76, pl. 18, figs. 4–6; pl. 19, fig. 1; Erbacher, 1994, pl. 18, fig. 10; Salvini and Marcucci Passerini, 1998, fig. 9.g; Thurow and Kuhnt, 1986, text-fig. 9.3; Vishnevskaya, 2001, pl. 115, fig. 9; pl. 129, figs. 2 and 7.

Holotype. USNM-Pessagno, no. 165636; California coast, Great Valley sequence, locality NSF 591; Upper Cretaceous, Lower Turonian, Fiske Creek Formation (Pessagno, 1973, pl. 18, figs. 4 and 5).

Occurrence. Cenomanian–Turonian worldwide; Middle–Upper Cenomanian of northern Turkey; Lower Turonian of the Crimean Mountains.

Material. Fewer than ten specimens.

Cavaspongia californiaensis Pessagno, 1973

Plate 23, figs. 8 and 10

Cavaspongia californiaensis: Pessagno, 1973, p. 77, pl. 19, figs. 2–4.

Holotype. USNM-Pessagno, no. 165638; California coast, Great Valley sequence, locality NSF 591; Upper Cretaceous, Lower Turonian, Fiske Creek Formation (Pessagno, 1973, pl. 19, figs. 2, 3).

Occurrence. Lower Turonian of California; Middle–Upper Cenomanian of northern Turkey; Lower Turonian of the Crimean Mountains.

Material. Fewer than ten specimens.

Cavaspongia contracta O'Dogherty, 1994, emend. herein

Plate 40, fig. 11

Cavaspongia contracta: O'Dogherty, 1994, p. 311, pl. 57, figs. 8–11.

Holotype. UL, no. 5710; central Italy, Umbria-Marche Apennines, locality Gb-84.40; Upper Cretaceous, Lower Cenomanian (O'Dogherty, 1994, pl. 57, fig. 10).

Description. The shell has three narrow rays with the apices forming the shape of an equilateral triangle. The tholus is small, subtriangular, and slightly raised in relief. Rays are oval in cross section, taper distally, and gradually become lower in relief. Shell pores are small and irregular in outline and arrangement.

Measurements. Diameter of the cortical shell, 108, length of the main rays, 2–10.

Comparison. *C. contracta* is distinguished from the type species *C. antelopensis* Pessagno, 1973 by weaker developed, very small central part and narrower rays.

Occurrence. Cenomanian–Lower Turonian of Italy and Spain; Upper Cenomanian of northern Turkey; Upper Cenomanian–Lower Turonian of the Crimean Mountains; Upper Turonian of southwestern Sakhalin.

Material. More than ten specimens.

Cavaspongia euganea (Squinabol, 1904)

Plate 24, figs. 11 and 12; Plate 40, figs. 1 and 8

Euchitonia euganea: Squinabol, 1904, p. 204, pl. 6, fig. 1.

Dumitricaia maxwellensis: Pessagno, 1976, p. 38, pl. 4, figs. 10–11; Thurow and Anderson, 1986, pl. 5, fig. 3; Thurow and Kuhnt, 1986, figs. 9 and 23; Thurow, 1988, p. 400, pl. 2, fig. 22; Erbacher, 1994, pl. 18, fig. 6; Salvini and Marcucci Passerini, 1998, fig. 9.r.

Dumitricaia sp.: Erbacher, 1994, pl. 12, figs. 5 and 6.

Cavaspongia euganea: O'Dogherty, 1994, p. 309, pl. 56, figs. 8–14.

Holotype. Northern Italy, southern Venetian Alps, Colli Euganei, Teolo locality; upper Lower Cretaceous–lower Upper Cretaceous, Upper Albian–Lower Turonian (Squinabol, 1904, pl. 6, fig. 1).

Comparison. *C. euganea* differs from *C. contracta* O'Dogherty (1994) in having poorly pronounced longitudinal pore rows on rays with terminal spines and a well-developed patagium, which entirely covers the shell, except for the ray terminations.

Occurrence. Upper Albian–Lower Turonian of Italy, Spain, and the Atlantic; Middle–Upper Cenomanian of northern Turkey; Lower Turonian of the Crimean Mountains; Upper Cenomanian of southwestern Sakhalin.

Material. More than 30 specimens.

Cavaspongia robusta Bragina, sp. nov.

Plate 37, figs. 2 and 3

Etymology. From the Latin *robustus* (rough, coarse).

Holotype. GIN, no. 4870/110; northern Turkey, Ürküt section; Upper Cretaceous, Upper Cenomanian, Tomalar Formation.

Description. The shell is large, discoidal, triangular with truncate apices. The tholus is triangular and

Explanation of Plate 27

Fig. 1. *Dactyliodiscus longispinus* (Squinabol, 1904), GIN, no. 4871/297, ×100.

Figs. 2 and 3. *Dactyliodiscus (?) longispinus* Squinabol, 1903, incomplete specimens showing an internal structure atypical of the species: (2) GIN, no. 4871/298, ×100; and (3) GIN, no. 4871/299, ×80.

Figs. 4 and 9. *Acanthocircus horridus* Squinabol, 1903, specimens: (4) GIN, no. 4871/305, ×130; and (9) GIN, no. 4871/306, ×120.

Figs. 5–7. *Acanthocircus hueyi* (Pessagno, 1976), specimens: (5) GIN, no. 4871/300, ×110; (6) GIN, no. 4871/301, ×100; and (7) GIN, no. 4871/302, ×120.

Figs. 8 and 10. *Acanthocircus polymorphus* (Squinabol, 1914), specimens: (8) GIN, no. 4871/303, ×130; and (10) GIN, no. 4871/304, ×100.

All specimens come from the Ürküt section.

Plate 28

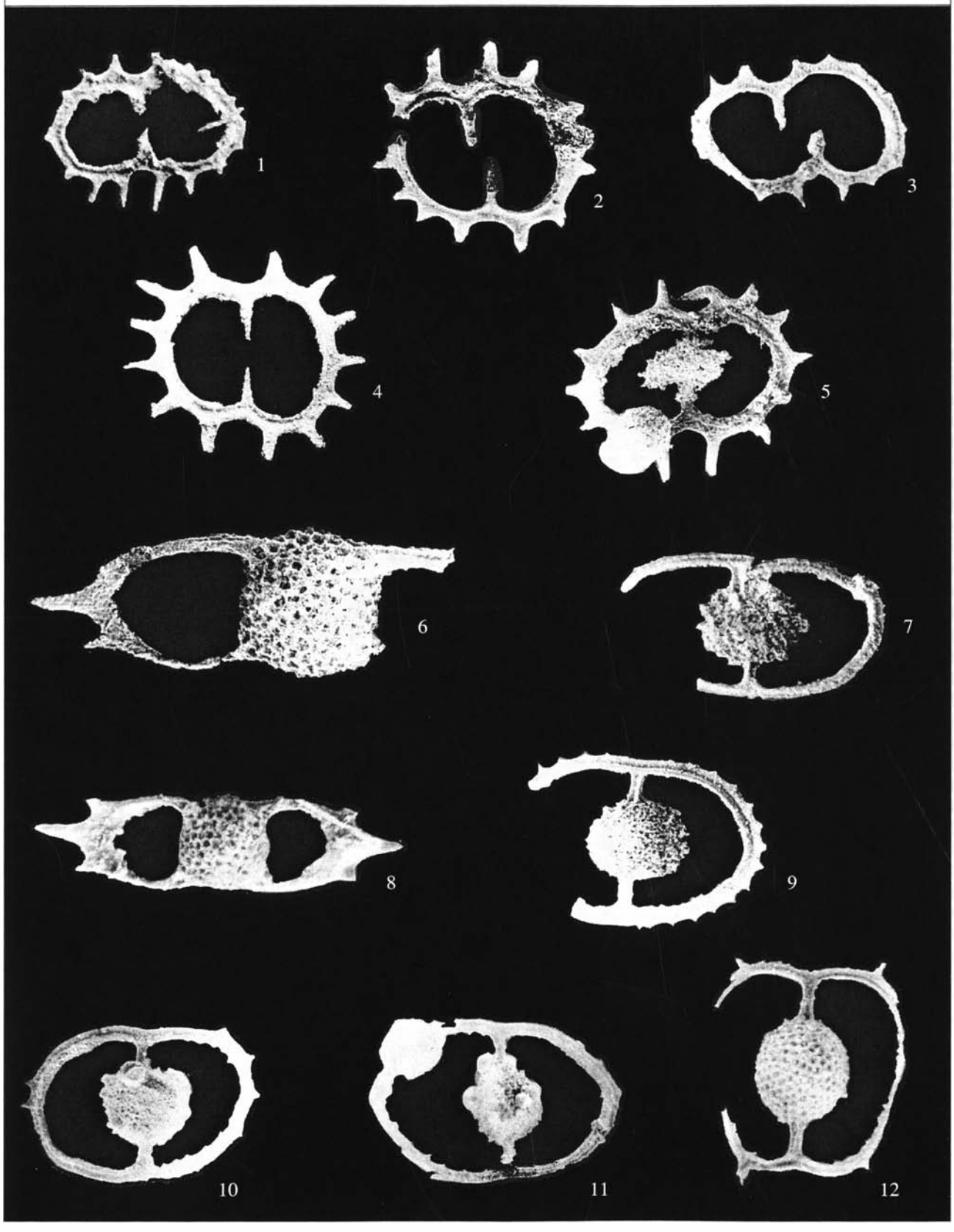

high in relief. In disposition, the tholus resembles miniature projection of the shell (that is, the tholus angles are oriented to the shell angles). The tholus pores are irregular, densely spaced, considerably variable in size, and positioned in polygonal frames, which vary in height in relief. The rest of the shell surface is spongy and covered by the patagium. When the patagium is particularly well-developed, the shell is almost circular in outline (Pl. 17, fig. 2). The patagium almost entirely covers three rays, so that only their terminal spines are visible.

Measurements. Distance between the bases of neighboring rays, 350; length of terminal spines, 30; length of the tholus side, 120; pore diameter, 2.5.

Comparison. The new species differs from *C. contracta* O'Dogherty, 1994 in the well-pronounced tholus, which is high in relief and triangular in shape, and in the patagium covering the larger part of the rays.

Occurrence. Northern Turkey, central Pontic Mountains; Upper Cretaceous, Upper Cenomanian, Tomalar Formation.

Material. Seven complete and five incomplete specimens.

Cavaspongia tavrica Bragina, sp. nov.

Plate 40, figs. 2 and 3

Etymology. From the Latin *tavrica* (from Tavrida, the former name of the Crimea).

Holotype. GIN, no. 4870/156; Crimean Mountains, Belaya Mountain section; Upper Cretaceous, Lower Turonian.

Description. The large disk is oval in plan and has three rays, one of which extends from the apex of the long axis. The apices of the rays form the shape of an isosceles triangle. The shell is spongy and covered by the patagium, which may conceal the larger part of the rays. The rays are often covered by small oval pores, with their long axes directed distally.

Measurements. Shell length along the long axis, 350; shell length along the short axis, 250; width of the ray base, 100; greatest ray length, 200.

Occurrence. Lower Turonian of the Crimean Mountains, Belaya Mountain section.

Material. Three complete and eight incomplete specimens.

Genus *Pyramispongia* Pessagno, 1973

Pyramispongia glascockensis Pessagno, 1973

Plate 19, fig. 7–11; Plate 37; fig. 13

Pyramispongia glascockensis: Pessagno, 1973, p. 79, pl. 21, figs. 2–5; 1976, pl. 1, fig. 9; Thurow and Kuhnt, 1986, text-fig. 9.4; Thurow, 1988, p. 405, pl. 2, fig. 23; Marcucci and Gardin, 1992, text-fig. 3.o; O'Dogherty, 1994, p. 305, pl. 56, figs. 1–5.

Holotype. USNM-Pessagno, no. 165642; California coast, Great Valley sequence, locality NSF 350; Upper Cretaceous, Lower Cenomanian, Fiske Creek Formation (Pessagno, 1973, pl. 21, figs. 2–5).

Occurrence. Cenomanian–Campanian worldwide; Middle–Upper Cenomanian of northern Turkey; Upper Cenomanian–Lower Turonian of the Crimean Mountains.

Material. More than 50 specimens.

Family Pseudoaulophacidae Riedel, 1967

Genus *Pseudoaulophacus* Pessagno, 1963

Pseudoaulophacus: Pessagno, 1963, p. 200.

Type species. *Pseudoaulophacus floresensis* Pessagno, 1963; Upper Cretaceous, Lower Campanian, Cariblanco Formation; Parguera Limestones, Puerto Rico.

Diagnosis. Shell subtriangular in plan and lenticular in cross section. Each shell apex with spine. Tholus higher in relief than rest of shell. Tholus ranging in shape from round to subtriangular and consisting of beams, which combined radially and equatorially in groups of six. Shell surface beyond tholus porous; pores round in outline and arranged in hexagonal or, occasionally, hexagonal–pentagonal patterns. Pores of tholus usually somewhat larger than those of rest of shell. Pore frames hexagonal or polygonal.

Species composition. *P. floresensis* Pessagno, 1963, *P. circularis* sp. nov., *P. parguerensis* Pessagno, 1972, *P. turcensis* sp. nov., more than 10 additional species; Cenomanian–Maastrichtian? worldwide.

Comparison. *Pseudoaulophacus* differs from *Alievium* Pessagno, 1972 in the presence of the tholus and the less regular pattern of the pore frames.

Explanation of Plate 28

Magnification is 120.

Figs. 1–3, and 5. *Acanthocircus imperfectus* sp. nov., specimens: (1) GIN, no. 4871/307; (2) holotype GIN, no. 4871/308; (3) GIN, no. 4871/309; and (5) GIN, no. 4871/310.

Fig. 4. *Acanthocircus hueyi* (Pessagno, 1976), GIN, no. 4871/311.

Figs. 6 and 8. *Vitorfus brustolensis* (Squinabol, 1903), specimens: (6) GIN, no. 4871/312; and (8) GIN, no. 4871/313.

Figs. 7, 9–11. *Acanthocircus impolitus* O'Dogherty, 1994, specimens: (7) GIN, no. 4871/314; (9) GIN, no. 4871/315; (10) GIN, no. 4871/316; and (11) GIN, no. 4871/317.

Fig. 12. *Acanthocircus moorei* (Foreman, 1975), GIN, no. 4871/318.

All specimens come from the Ürküt section.

Plate 29

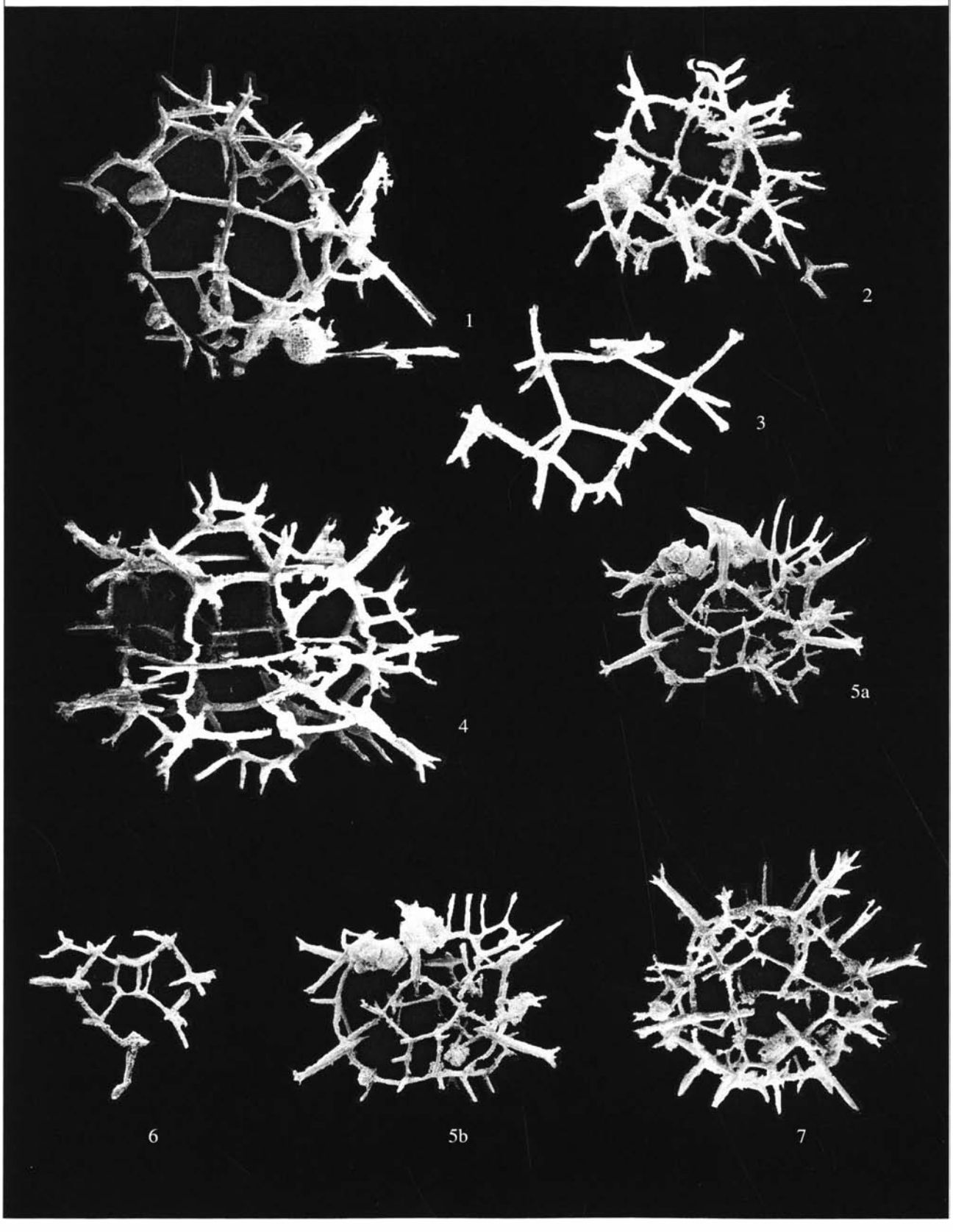

Pseudoaulophacus circularis Bragina, sp. nov.

Plate 36, figs. 6 and 9

Pseudoaulophacus sp. *A*: Pessagno, 1972, p. 312, pl. 30, fig. 6

Non *Pseudoaulophacus putahensis*: O'Dogherty, 1994, p. 320, pl. 59, figs. 1–8, 12, 13.

Etymology. From the Latin *circularis* (circular).

Holotype. GIN, no. 4870/97; Crimean Mountains, Belaya Mountain; Lower Turonian.

Description. The shell is circular in outline, with three spines forming the shape of an equilateral triangle and a poorly pronounced carina. The tholus is low in relief and almost circular in plan. The tholus diameter is one-third of that of the shell. The shell surface is pseudoaulophacoid, pores of the tholus are larger than all others. The spines are relatively massive, three-bladed, and tapering. The spine length is one-quarter to one-third of the shell diameter.

Measurements. Shell diameter, 200; tholus diameter, 50; spine length, 65.

Comparison. The new species is distinguished from *P. floresensis* Pessagno, 1963 by its circular shell.

Occurrence. Middle Cenomanian–Lower Turonian of Italy; Coniacian of California; Lower Turonian of the Crimean Mountains.

Material. 23 specimens.

Pseudoaulophacus parguerаensis Pessagno, 1972

Plate 38, fig. 9

Pseudoaulophacus parguerаensis: Pessagno, 1972, p. 309, pl. 30, fig. 4.

Holotype. USNM-Pessagno, no. 165544; Puerto Rico, Parguera Limestones; Upper Cretaceous, Lower Campanian, Cariblanco Formation (Pessagno, 1972, pl. 30, fig. 4).

Remarks. The poorly preserved specimens of *P. parguerаensis* Pessagno, 1972 look like that shown in Pl. 38, fig. 9. It is evident that it lacks a tholus.

Occurrence. Turonian–Campanian worldwide; Upper Cenomanian–Lower Turonian of the Crimean Mountains.

Material. More than 20 specimens.

Pseudoaulophacus praefloresensis Pessagno, 1972, emend. herein

Plate 24, fig. 7; Plate 36, fig. 2; Plate 39, fig. 13

Pseudoaulophacus praefloresensis: Pessagno, 1972, p. 309, pl. 27, figs. 2–6.

Pseudoaulophacus murphy: Ling *et al.*, 1996, pl. 2, fig. 3.

Holotype. USNM-Pessagno, no. 165593; California, Great Valley sequence, locality NSF 483; Upper Cretaceous, Upper Turonian–Lower Coniacian (Pessagno, 1972, pl. 29, figs. 3, 4).

Description. The shell is discoid, subtriangular in outline, with three spines at the corners. The tholus is distinctly delineated and raised in relief. Its diameter is about one-third of that of the shell. The pseudoaulophacoid surface structure is relatively well-pronounced, and the pores on the tholus are relatively large. The rest of the shell displays a less pronounced pseudoaulophacoid structure.

Measurements. Shell diameter, 230–140; tholus diameter, 100–70; spine length, 70–35.

Comparison. *Pseudoaulophacus praefloresensis* is distinguished from *P. floresensis* Pessagno, 1972 by its less pronounced pseudoaulophacoid surface beyond the tholus, which is not distinctly differentiated from the rest of the shell.

Occurrence. Coniacian–Santonian worldwide; Upper Cenomanian of northern Turkey; Lower Turonian of the Crimean Mountains.

Material. More than 20 specimens.

Pseudoaulophacus putahensis Pessagno, 1972, emend. herein

Plate 36, fig. 3

Pseudoaulophacus putahensis: Pessagno, 1972, p. 310, pl. 27, fig. 1; Thurow and Kuhnt, 1986, text-fig. 9.8; De Wever *et al.*, 1988, p. 169, pl. 1, fig. 2; Salvini and Marcucci Passerini, 1998, fig. 8.e.

Holotype. USNM-Pessagno, no. 165599; California, locality NSF 432-B; Upper Cretaceous, Turonian, Venado Formation (Pessagno, 1972, pl. 27, fig. 1).

Description. The shell is subtriangular in plan, with three massive three-bladed spines extending from the three corners. The carina is virtually absent. Relatively long, narrow secondary spines (two or three on each side of the triangle) may occur between the primary spines in the peripheral part of the shell. The pseudoaulophacoid structure is well-pronounced on the tholus and indistinct on the rest of shell. The tholus is weakly developed and low in relief. Its pores are larger than those on the rest of shell. At the joints between six pores, the pore frames bear semispherical nodes.

Measurements. Shell diameter, 210; tholus diameter, 110; spine length, up to 75.

Comparison. *P. putahensis* differs from *P. lenticulatus* (White, 1928) in the subtriangular shell and the absence of abundant equatorial spinules.

Occurrence. Cenomanian–Turonian worldwide; Middle Cenomanian–Lower Turonian of Italy; Lower Turonian of the Crimean Mountains.

Material. More than 20 specimens.

Explanation of Plate 29

Figs. 1–7. *Archaeoplegma pontidae* gen. et sp. nov., specimens: (1) GIN, no. 4871/319, ×75; (2) GIN, no. 4871/320, ×75; (3) GIN, no. 4871/321, ×75; (4) holotype GIN, no. 4871/322, ×75; (5) GIN, no. 4871/323, ×50, (a) and (b) different views; (6) GIN, no. 4871/324, ×50; and (7) GIN, no. 4871/325, ×50.

All specimens come from the Ürküt section.

Plate 30

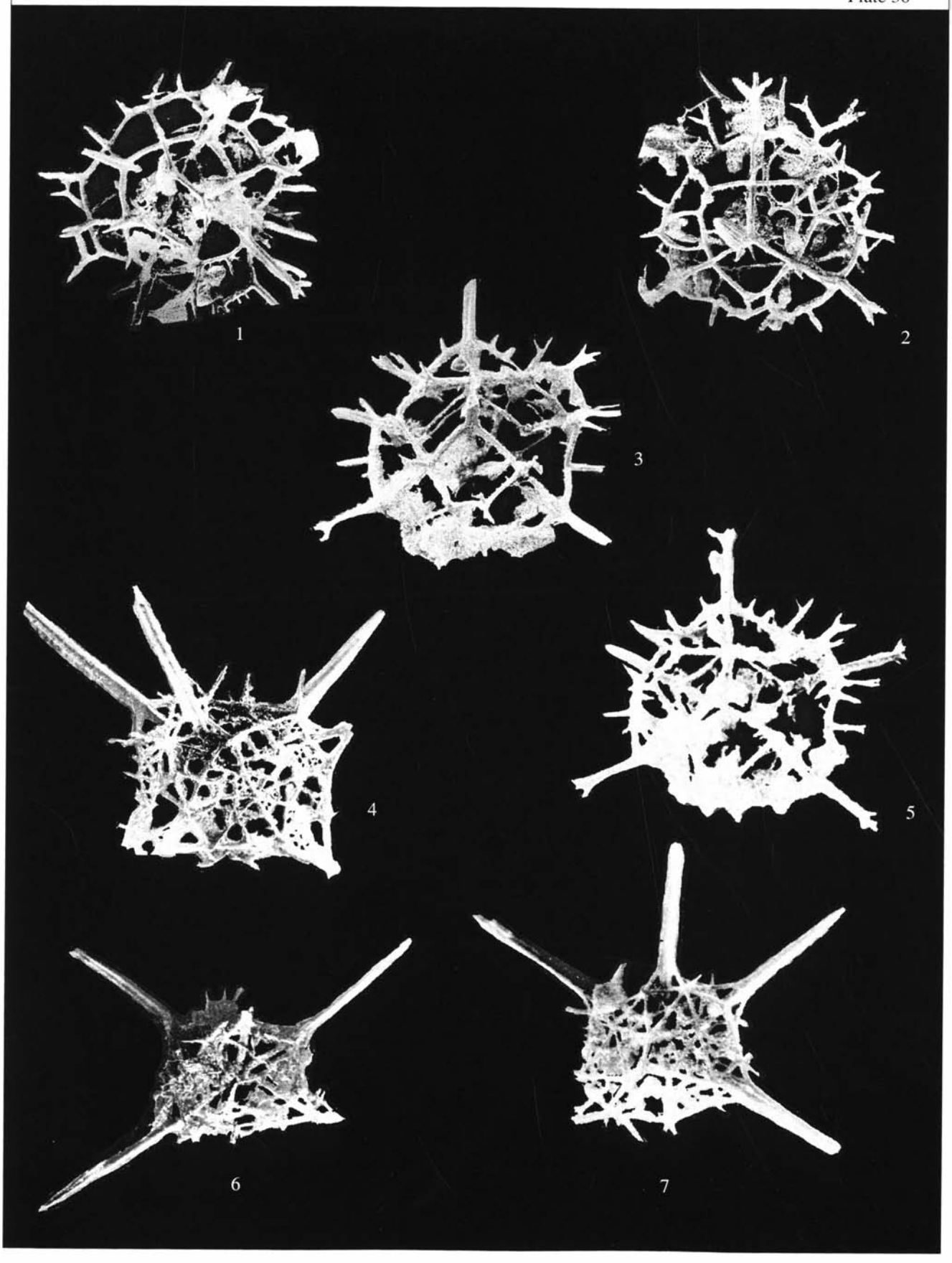

Pseudoaulophacus turcensis Bragina, sp. nov.

Plate 24, figs. 8 and 9

Etymology. From the Latin *turcensis* (Turkish).

Holotype. GIN, no. 4871/268; northern Turkey, Ürküt section; Upper Cretaceous, Middle Cenomanian, Tomalar Formation.

Description. The shell is distinctly triangular in outline. The tholus is circular and low, its diameter at most one-third of that of the shell. The pseudoaulophacoid pores, which are characteristic of *Pseudoaulophacus*, cover the shell, including the tholus. One apex of the shell has three spines, while the other two apices have two spines each. There may be an additional spine in the middle of each side of the shell. The spines are massive and three-bladed at the base. The greatest part is rounded in cross section. The spines have a uniform length equal to the diameter of the tholus.

Measurements. Length of the shell side, 250; spine length; 170; tholus diameter, 90.

Comparison. The new species is distinguished from *P. praefloresensis* Pessagno, 1972 by having two or three spines at the apices of the subtriangular shell.

Occurrence. Northern Turkey; Middle–Upper Cenomanian, Tomalar Formation.

Material. Eight complete and six incomplete specimens.

Genus *Alievium* Pessagno, 1972

Alievium: Pessagno, 1972, p. 297.

Type species. *Theodiscus superbus* Squinabol, 1914; Upper Cretaceous, Novale Group; Vicentino Province, Venetian Alps, northern Italy.

Diagnosis. Shell subtriangular to triangular in plan and lenticular in cross section. Tholus undeveloped. Cortical shell composed of beams; beams in groups of six, extending radially from one center, other end of each beam connected to equatorial beams forming a honeycomb-like structure. Beam joints usually with nodes terminating in thorns. Every shell apex with a spine.

Species composition. *A. gallowayi* (White, 1928), *A. praegallowayi* Pessagno, 1972, *A. superbum* (Squinabol, 1914), and some other species; Cretaceous worldwide.

Comparison. *Alievium* differs from *Dispongotripus* Squinabol, 1903 in the presence of spines on the apices of the triangular shell, and in the cortical shell composed of radial and equatorial structures composed of six beams each.

Alievium sculptus (Squinabol, 1904)

Plate 36, figs. 4 and 5

Theodiscus sculptus: Squinabol, 1904, p. 200, pl. 4, fig. 9.

Pseudoaulophacus sculptus: O'Dogherty, 1994, p. 319, pl. 59, figs. 1–4; Salvini and Marcucci Passerini, 1998, fig. 8.f.

Holotype. Northern Italy, southern Venetian Alps, Colli Euganei, Teolo locality; upper Lower Cretaceous–lower Upper Cretaceous, Upper Albian–Lower Turonian (Squinabol, 1904, pl. 4, fig. 9).

Description. The discoid shell is subtriangular in plan, lenticular in cross section, and has spines extending from the apices. The tholus is undeveloped. The cortical shell is porous, with small pores, ranging in shape from rounded to triangular. The pore frames have indistinct outlines. The points of fusion between pores are usually equipped with a node, which often has a thorn.

Measurements. The longest spine, 155–54; diameter of the cortical shell, 214–158.

Comparison. *A. sculptus* differs from *A. superbum* (Squinabol, 1914) in the greater number and smaller size of the pores on the shell surface.

Occurrence. Middle Albian–Lower Turonian of Italy; Upper Cenomanian of northern Turkey; Lower Turonian of the Crimean Mountains.

Material. More than 20 specimens.

Alievium superbum (Squinabol, 1914), emend. herein

Plate 36, fig. 1

Theodiscus superbus: Squinabol, 1914, p. 271, pl. 20, fig. 4.

Alievium superbum: Pessagno, 1972, p. 302, pl. 24, figs. 3, 5, and 6; pl. 25, fig. 1; Petrushevskaya and Kozlova, 1972, p. 527, pl. 3, figs. 1 and 2; Dumitrica, 1975, text-fig. 2.42; Pessagno, 1976, p. 27, pl. 3, fig. 12; Nakaseko and Nishimura, 1981, p. 142, pl. 2, fig. 2; Taketani, 1982, p. 51, pl. 10, fig. 8; Sanfilippo and Riedel, 1985, p. 594, text-fig. 6.2 (= specimen of Pessagno, 1972, pl. 25, fig. 1); Thurow and Kuhnt, 1986, text-fig. 9.7; De Wever *et al.*, 1988, p. 167, pl. 1, fig. 4; Thurow, 1988, p. 397, pl. 2, fig. 2; Marcucci *et al.*, 1991, text-figs. 4g and 4h; Erbacher, 1994, pl. 18, fig. 11; O'Dogherty, 1994, p. 322, pl. 59, figs. 14–18; Salvini and Marcucci Passerini, 1998, fig. 8.s; Urquhart and Robertson, 2000, pl. 1, fig. 14.

(?) *Pseudoaulophacus superbus*: Moore, 1973, p. 825, pl. 12, figs. 4 and 5; Riedel and Sanfilippo, 1974, p. 780, pl. 3, figs. 1–3.

Alievium praegallowayi: Foreman, 1975, p. 613, pl. 1D, figs. 4 (?) and 5; pl. 5, fig. 9; Pessagno, 1976, p. 27, pl. 5, fig. 10 (= specimen of Pessagno, 1972, pl. 25, fig. 2); Taketani, 1982, p. 51, pl. 10, fig. 4; Kuhnt *et al.*, 1986, pl. 7, fig. m.

(?) *Alievium* sp. cf. *A. superbum*: Nakaseko *et al.*, 1979, p. 21, pl. 5, fig. 3.

Alievium sp.: Teraoka, Kurimoto, 1986, pl. 5, fig. 1.

Non *Alievium superbum*: Nakaseko and Nishimura, 1981, p. 142, pl. 2; Schmidt-Effing, 1980, p. 245, text-fig. 14; Schaaf, 1984, p. 162–163, text-figs. 4a and 4b; Thurow, 1988, p. 397, pl. 5, fig. 11 [= *A. sculptus* (Squinabol, 1904)]; Vishnevskaya, 2001, pl. 125, fig. 23 (= *A. praegallowayi* Pessagno, 1972).

Holotype. Northern Italy, Venetian Alps, Vicentino Province; Upper Cretaceous, Novale Group (Squinabol, 1914, pl. 20, fig. 4).

Explanation of Plate 30

Figs. 1–3, 5. *Archaeoplegma pontidae*, gen. et sp. nov., specimens: (1) GIN, no. 4871/327, ×50; (2) GIN, no. 4871/328, ×50; (3) GIN, no. 4871/329, ×50; and (5) GIN, no. 4871/330, ×50.

Figs. 4, 6, and 7. *Cuboctostylus pontidus*, sp. nov.: (4) paratype GIN, no. 4871/331, ×100; (6) GIN, no. 4871/332, ×75; and (7) holotype GIN, no. 4871/333, ×75.

All specimens come from the Ürküt section.

Plate 31

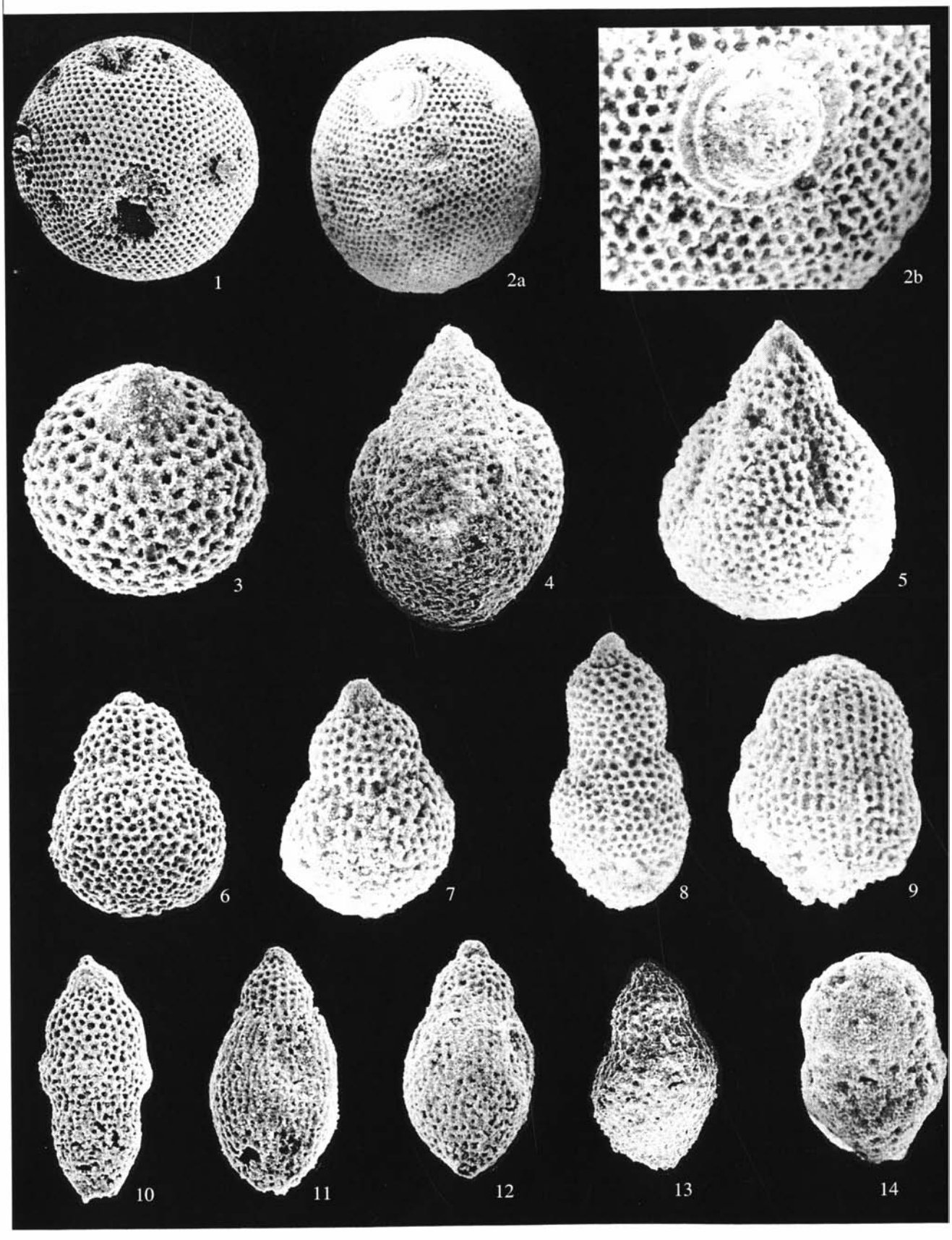

Description. The discoid shell is subtriangular to triangular in outline and lenticular in cross section, with massive spines extending from the corners. The tholus is not pronounced. The cortical shell is composed of beams in groups of six extending radially from a single center. Each beam is attached to an equatorial beam, forming a honeycomb-like structure. The points of fusion between beams are usually equipped with nodes terminating in thorns. Each corner of the shell bears a spine.

Measurements. Shell diameter, 170–230; spine length, 40–140.

Comparison. *A. superbum* is distinguished from *Alievium gallowayi* (White, 1928) by the pore rows, which are not strictly parallel to every side of the triangular shell, and by the presence of relatively high thorns at the points of contact between several pores.

Remarks. *A. praegallowayi* Pessagno, 1972 and *A. sculptus* (Squinabol, 1904) are often mistakenly identified as *A. superbum* (Squinabol, 1914). There may be a continuous lineage that includes *A. sculptus* (Squinabol, 1904)—*A. superbum*—*A. praegallowayi Pessagno*—*A. gallowayi.*

Occurrence. Turonian worldwide; Lower Turonian of the Crimean Mountains.

Material. More than ten specimens.

Family Dactyliosphaeridae Squinabol, 1904

Genus *Quadrigastrum* O'Dogherty, 1994

Quadrigastrum: O'Dogherty, 1994, p. 341.

Type species. *Quadrigastrum oculus* O'Dogherty, 1994; Upper Cretaceous, Middle Cenomanian; Umbria-Marche Apennines, central Italy.

Diagnosis. Shell discoid, round to square in outline, with four massive primary spines, their apices arranged in the shape of a rectangle. Spines four-bladed in cross section. Peripheral edge occasionally with additional spines. Shell surface spongy or, occasionally, with thorns.

Species composition. *Q. oculus* O'Dogherty, 1994, *Q. lapideum* O'Dogherty, 1994, *Q. insulsum* O'Dogherty, 1994; Middle Albian–Lower Coniacian of the Tethys.

Comparison. *Quadrigastrum* is distinguished from *Dactyliosphaera* Squinabol, 1904 by the long, well-developed primary spines.

Quadrigastrum insulsum O'Dogherty, 1994, emend. herein

Plate 36, fig. 11

Quadrigastrum insulsum: O'Dogherty, 1994, p. 343, pl. 64, figs. 11–13.

Holotype. UL, no. 3692; central Italy, Umbria-Marche Apennines, locality Gc-1073.94; Middle Cenomanian (O'Dogherty, 1994, pl. 64, fig. 13).

Description. The discoid shell is square to almost circular in outline. Four primary spines are long, massive, and trihedral and oriented towards the corners of the square. Peripheral secondary spines vary considerably in size. The small rounded polygonal pores of the shell are randomly arranged. The pore frames are irregular in outline and noticeably variable in relief. The frame costae bear numerous thorns varying considerably in size and shape. This makes the shell surface rough.

Measurements. Diameter of cortical shell, 270–230; length of primary spines, 160–130.

Comparison. Unlike *Q. oculus* O'Dogherty, 1994, *Q. insulsum* is not subdivided into a central part and four rays diverging from it.

Occurrence. Lower Cenomanian–Lower Turonian of Italy; Upper Turonian of southwestern Sakhalin; Lower Turonian of the Crimean Mountains.

Material. More than ten specimens.

Genus *Dactyliosphaera* Squinabol, 1904

Dactyliosphaera silviae Squinabol, 1904

Plate 25, figs. 5–8

Gen. et sp. nov.: Squinabol, 1903, p. 121, pl. 9, fig. 21.

Dactyliosphaera Silviae: Squinabol, 1904, p. 196, pl. 4, fig. 3.

Pseudoaulophacus sp. *D.*: Thurow, 1988, pl. 12, fig. 13.

Dactyliosphaera silviae: Dumitrica, 1975, text-fig. 2.14; O'Dogherty, 1994, p. 341, pl. 63, figs. 22–26.

Holotype. Northern Italy, southern Venetian Alps, Colli Euganei, Teolo locality; upper Lower Cretaceous–lower Upper Cretaceous, Upper Albian–Lower Turonian (Squinabol, 1904, pl. 4, fig. 3).

Explanation of Plate 31

Plates 31–41 show radiolarians from the Crimea.

Figs. 1 and 2. *Holocryptocanium barbui* Dumitrica, 1970, specimens: (1) GIN, no. 4870/2, ×200, and (2) GIN, no. 4870/3: (a) general view, ×200, and (b) shell fragment (supposed velum), ×500.

Fig. 3. *Cryptamphorella sphaerica* (White, 1928), GIN, no. 4870/4, ×300.

Figs. 4 and 5. *Diacanthocapsa rara* (Squinabol, 1904), ×250, specimens: (4) GIN, no. 4870/5; and (5) GIN, no. 4870/6.

Figs. 6 and 7. *Diacanthocapsa ancus* (Foreman, 1968), ×300, specimens: (6) GIN, no. 4870/7; and (7) GIN, no. 4870/8.

Fig. 8. *Diacanthocapsa tavridae* sp. nov.: holotype GIN, no. 4870/10, ×200.

Fig. 9. *Diacanthocapsa inflata* sp. nov.: holotype GIN, no. 4870/11, ×200.

Fig. 10. *Diacanthocapsa aksuderensis* sp. nov.: holotype GIN, no. 4870/12, ×200.

Figs. 11 and 12. *Diacanthocapsa antiqua* (Squinabol, 1903), ×200, specimens: (11) GIN, no. 4870/13; and (12) GIN, no. 4870/14.

Fig. 13. *Diacanthocapsa fossilis* (Squinabol, 1904), GIN, no. 4870/9, ×200.

Fig. 14. *Diacanthocapsa betica* O'Dogherty, 1994, GIN, no. 4870/15, ×200.

Plate 32

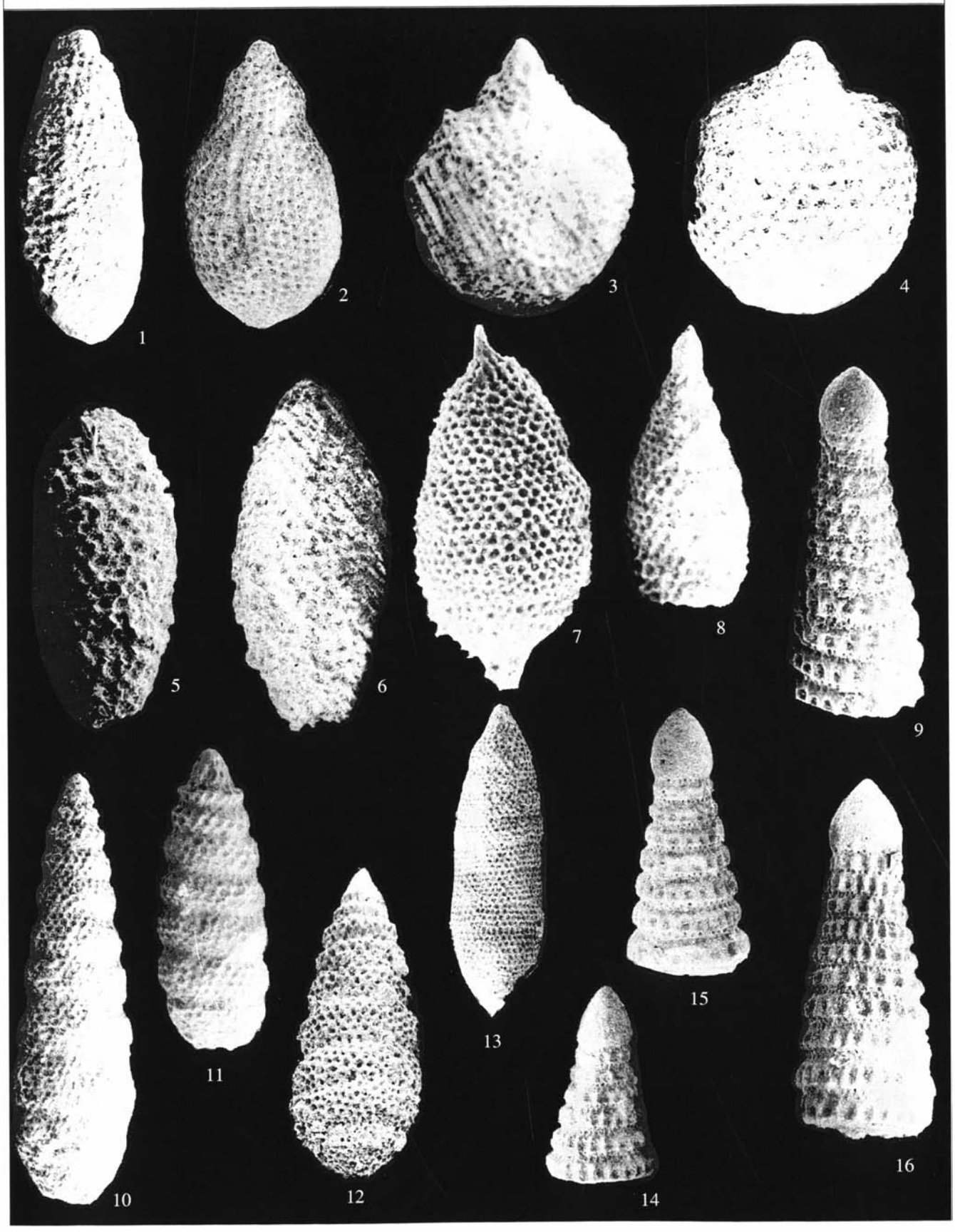

Occurrence. Upper Albian–Lower Turonian of Italy, Spain, and the Atlantic; Middle–Upper Cenomanian of northern Turkey.

Material. More than 20 specimens.

Family Spongodiscidae Haeckel, 1882
Genus *Dactyliodiscus* Squinabol, 1903

Dactyliodiscus: Squinabol, 1903, p. 120.

Type species. *Dactyliodiscus cayeuxi* Squinabol, 1903; upper Lower Cretaceous–lower Upper Cretaceous, Upper Albian–Lower Turonian; Teolo locality, Colli Euganei, southern Venetian Alps, northern Italy.

Diagnosis. Shell discoid, circular in outline, with variable number of equatorial spines. Shell surface spongy, with irregularly arranged polygonal spines and, occasionally, with numerous irregularly arranged nodes. Tholus weakly developed.

Species composition. *D. cayeuxi* Squinabol, 1903, *D. lenticulatus* (Jud, 1994), *D. longispinus* Squinabol, 1903, *D. rubus* O'Dogherty, 1994, and *D. spinosus* sp. nov.; Upper Berriasian–Turonian of the Tethys.

Comparison. *Dactyliodiscus* differs from *Godia* Tumanda, 1986 in the absence of a groove along the peripheral edge of the tholus and in having nodes not only on the upper shell surface but also on and the lower one.

Dactyliodiscus lenticulatus (Jud, 1994), emend. herein

Plate 25, figs. 1 and 2; Plate 41, fig. 11

Godia sp. *C.*: Thurow, 1988, p. 401, pl. 5, fig. 15.

Godia lenticulata: Jud, 1994, p. 78, pl. 10, figs. 10 and 11; Salvini and Marcucci Passerini, 1998, fig. 9.u.

Dactyliodiscus lenticulatus: O'Dogherty, 1994, p. 331, pl. 61, figs. 12–15.

Holotype. UL, no. Bo-556.5; central Italy, Umbria-Marche Apennines, locality Bo.566.50:454; Lower Cretaceous, Lower Barremian (Jud, 1994, pl. 10, fig. 11).

Description. The shell is large, discoid in plan, and, occasionally, biconvex lenticular in cross section. The convexity is weakly pronounced. The carina is undeveloped. Pores are small, rounded polygonal, and irregularly spaced. Pore frames are tetragonal to pentagonal, irregular in outline. The shell surface is rough owing to small narrow thorns at the vertices and sparse low nodes in the central part of the shell. The nodes vary in shape from semispherical to conical. The nodes sometimes bear spines, the length of which is three or four times the node height. Relatively short secondary spines, developed to varying degrees, radiate in the equatorial part.

Measurements. Diameter of cortical shell, 480–241; the longest spines, 93–26.

Comparison. *D. lenticulatus* is distinguished from *D. cayeuxi* Squinabol, 1903 by equatorial spines only slightly varying in thickness and length.

Remarks. *D. cayeuxi* Squinabol, 1903 and *D. lenticulatus* (Jud, 1994) are evidently members of the same continuous lineage. This is corroborated by rare specimens of *D. lenticulatus* with much longer equatorial spines (Pl. 25, fig. 2).

Occurrence. Barremian–Middle Cenomanian of Italy; Middle–Upper Cenomanian of northern Turkey; Upper Cenomanian–Lower Turonian of the Crimean Mountains.

Material. More than 20 specimens.

Dactyliodiscus longispinus (Squinabol, 1904)

Plate 26, figs. 4–13; Plate 27, fig. 1; Plate 38, figs. 4 and 7; Plate 41, fig. 10

Stylotrochus longispina: Squinabol, 1904, p. 207, pl. 6, fig. 8.

Dactyliodiscus longispinus: O'Dogherty, 1994, p. 333, pl. 62, figs. 6–11.

Holotype. Northern Italy, southern Venetian Alps, Colli Euganei; upper Lower Cretaceous–lower Upper Cretaceous, Upper Albian–Lower Turonian (Squinabol, 1904, pl. 6, fig. 8).

Remarks. Incomplete specimens that are rather similar in internal structure to members of *Spongosaturnalis* are shown in Pl. 26, figs. 9–13 and Pl. 27, fig. 1.

Occurrence. Upper Albian–Lower Turonian of Italy; Middle–Upper Cenomanian of northern Turkey; Lower Turonian of the Crimean Mountains.

Material. More than 20 specimens.

Dactyliodiscus spinosus Bragina, sp. nov.

Plate 25, fig. 9

Etymology. From the Latin *spinosus* (spiny).

Explanation of Plate 32

Fig. 1. *Diacanthocapsa elongata* sp. nov., GIN, no. 4870/16, ×200.

Fig. 2. *Diacanthocapsa antiqua* (Squinabol, 1903), GIN, no. 4870/17, ×200).

Fig. 3. *Nassellaria* gen. et sp. indet., GIN, no. 4870/18, ×200.

Fig. 4. *Cryptamphorella sphaerica* (White, 1928), GIN, no. 4870/19, ×200.

Figs. 5 and 6. *Amphipyndax conicus* Nakaseko and Nishimura, 1981, ×200, specimens: (5) GIN, no. 4870/20; and (6) GIN, no. 4870/21.

Fig. 7. *Distylocapsa veneta* (Squinabol, 1904), GIN, no. 4870/22, ×250.

Fig. 8. *Amphipyndax stocki* (Campbell et Clark, 1944), GIN, no. 4870/23, ×200.

Figs. 9, 14–16. *Pseudodictyomitra pseudomacrocephala* (Squinabol, 1903), ×150, specimens: (9) GIN, no. 4870/24; (14) GIN, no. 4870/25; (15) GIN, no. 4870/26; and (16) GIN, no. 4870/27.

Figs. 10–12. *Stichomitra communis* Squinabol, 1903, specimens: (10) GIN, no. 4870/28, ×100; (11) GIN, no. 4870/29, ×150; and (12) GIN, no. 4870/30, ×120.

Fig. 13. *Stichomitra magna* Squinabol, 1904, GIN, no. 4870/31, ×150.

Plate 33

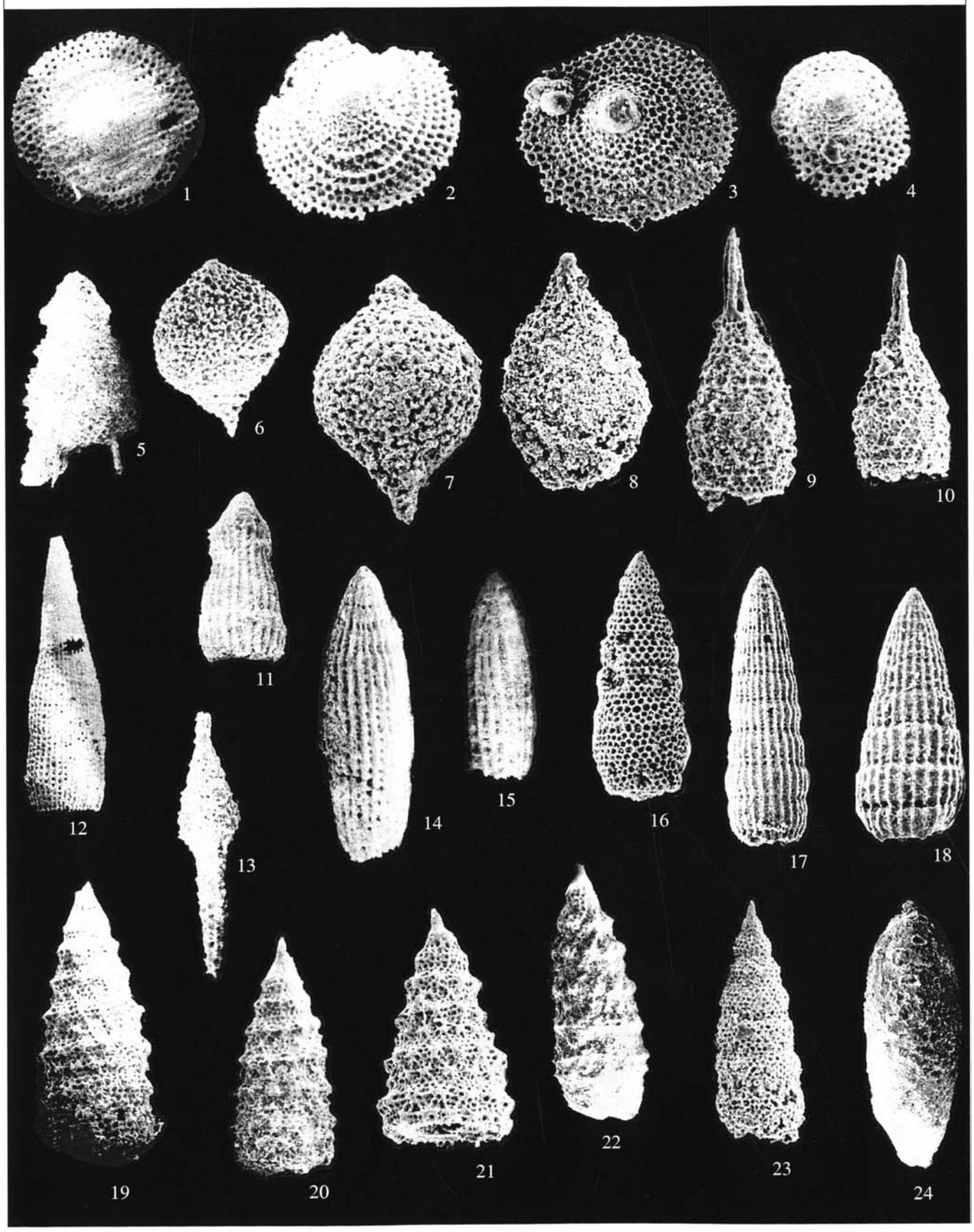

Holotype. GIN, no. 4871/279; northern Turkey, Tomalar section; Upper Cenomanian.

Description. The shell is large and discoid in plan. The keel is undeveloped. The rounded polygonal pores are arranged irregularly. The pore frames are tetragonal to heptagonal, and irregular in outline. Sharply conical small nodes are occasionally present at pore vertices. The nodes bear spines, the length of which is three or four times greater than the node height. Short secondary spines and three long massive spines radiate irregularly in the equatorial part. The three massive spines are rounded in cross section and their apices are arranged in the pattern of three of the four corners of a visualized rectangle.

Measurements. Diameter of the cortical shell, 175; length of the primary spines, 130–135.

Comparison. The new species is distinguished from *D. cayeuxi* Squinabol, 1903 by the orientation of the three long spines to the three apices of a rectangle and the shape of these spines, which are rounded in cross section and slightly tapering.

Remarks. The new species differs from *D. longispinus* Squinabol, 1903 in having larger pores on the cortical shell, pore frames with conical nodes at the vertices, long and narrow spinules on the nodes, and delicate secondary spines in the equatorial part.

Occurrence. Upper Cenomanian of northern Turkey.

Material. Four complete and three incomplete specimens.

Genus *Godia* Wu, 1986

Godia: Wu, 1986.

Type species. *Godia floreusa* Wu, 1986; Upper Cretaceous, Cenomanian; southern Tibet.

Diagnosis. Shell very large, rounded or polygonal in plan, with short equatorial spines. Central area somewhat depressed or raised. Depression of central part encircled by small nodes. Most of shell surface covered by pores in pentagonal–tetragonal frames.

Species composition. About ten species, including *G. tomalarea* sp. nov.; Lower Valanginian–Lower Turonian, geographical ranges have not been defined.

Comparison. *Godia* differs from *Dactyliodiscus* Squinabol, 1903 in having the central depression encircled by nodes.

Godia concava (Li et Wu, 1985)

Plate 25, fig. 12

Orbiculiforma concave: Li and Wu, 1985, p. 73, pl. 2, figs. 22 and 23.
Godia concava: O'Dogherty, 1994, p. 334, pl. 62, figs. 12–15.

Holotype. southern Tibet; Upper Cretaceous, Lower Cenomanian (Li and Wu, 1985, pl. 2, fig. 22).

Occurrence. Lower Cenomanian of Tibet; Aptian–Lower Cenomanian of Italy; Middle–Upper Cenomanian of northern Turkey.

Material. More than ten specimens.

Godia tomalarea Bragina, sp. nov.

Plate 25, fig. 13

Etymology. From the Latin *tomalarea* from the area of the first find in the Tomalar section (northern Turkey).

Holotype. GIN, no. 4871/283; northern Turkey, Tomalar section; Upper Cenomanian.

Description. The shell is large and oval in plan. The central area is oval; its long axis is in line with the long axis of the shell. The central area is noticeably lower in relief than the peripheral one. It is encircled by

Explanation of Plate 33

Figs. 1–3. *Petasiforma glascockensis* Pessagno, 1969, specimens: (1) GIN, no. 4870/32, ×100; (2) GIN, no. 4870/33, ×150; and (3) GIN, no. 4870/34, ×150.

Fig. 4. *Petasiforma tavridae* sp. nov., holotype 4870/35, ×150.

Fig. 5. *Pogonias missilis* O'Dogherty, 1994, GIN, no. 4870/36, ×100.

Figs. 6 and 8. *Tubilustrium transmontanum* O'Dogherty, 1994, specimens: (6) GIN, no. 4870/37, ×100; and (8) GIN, no. 4870/38, ×150.

Fig. 7. *Tubilustrium guttaeformis* (Bragina, 1991), GIN, no. 4870/39, ×100.

Figs. 9 and 10. *Phalangites hastatus* O'Dogherty, 1994, ×100, specimens: (9) GIN, no. 4870/40; and (10) GIN, no. 4870/41.

Fig. 11. *Thanarla veneta* (Squinabol, 1903), GIN, no. 4870/42, ×100.

Fig. 12. *Archaeodictyomitra crebrisulcata* (Squinabol, 1904), GIN, no. 4870/43, ×100.

Fig. 13. *Pseudoeucyrtis pulchra* (Squinabol, 1904), GIN, no. 4870/44, ×100.

Figs. 14, 15, and 17. *Archaeodictyomitra squinaboli* Pessagno, 1976, specimens: (14) GIN, no. 4870/45, ×100; (15) GIN, no. 4870/46, ×100; and (17) GIN, no. 4870/47, ×150.

Fig. 16. *Stichomitra communis* Squinabol, 1903, GIN, no. 4870/48, ×100.

Fig. 18. *Archaeodictyomitra vulgaris* Pessagno, 1977, GIN, no. 4870/49, ×150.

Figs. 19, 20, and 22. *Xitus spicularius* (Aliev, 1965), ×100, specimens: (19) GIN, no. 4870/50; (20) GIN, no. 4870/51; and (22) GIN, no. 4870/52.

Fig. 21. *Xitus asymbatos* (Foreman, 1968), GIN, no. 4870/53, ×100.

Fig. 23. *Xitus spineus* Pessagno, 1977, GIN, no. 4870/54, ×100.

Fig. 24. *Spongostichomitra elatica* (Aliev, 1968), GIN, no. 4870/55, ×100.

Plate 34

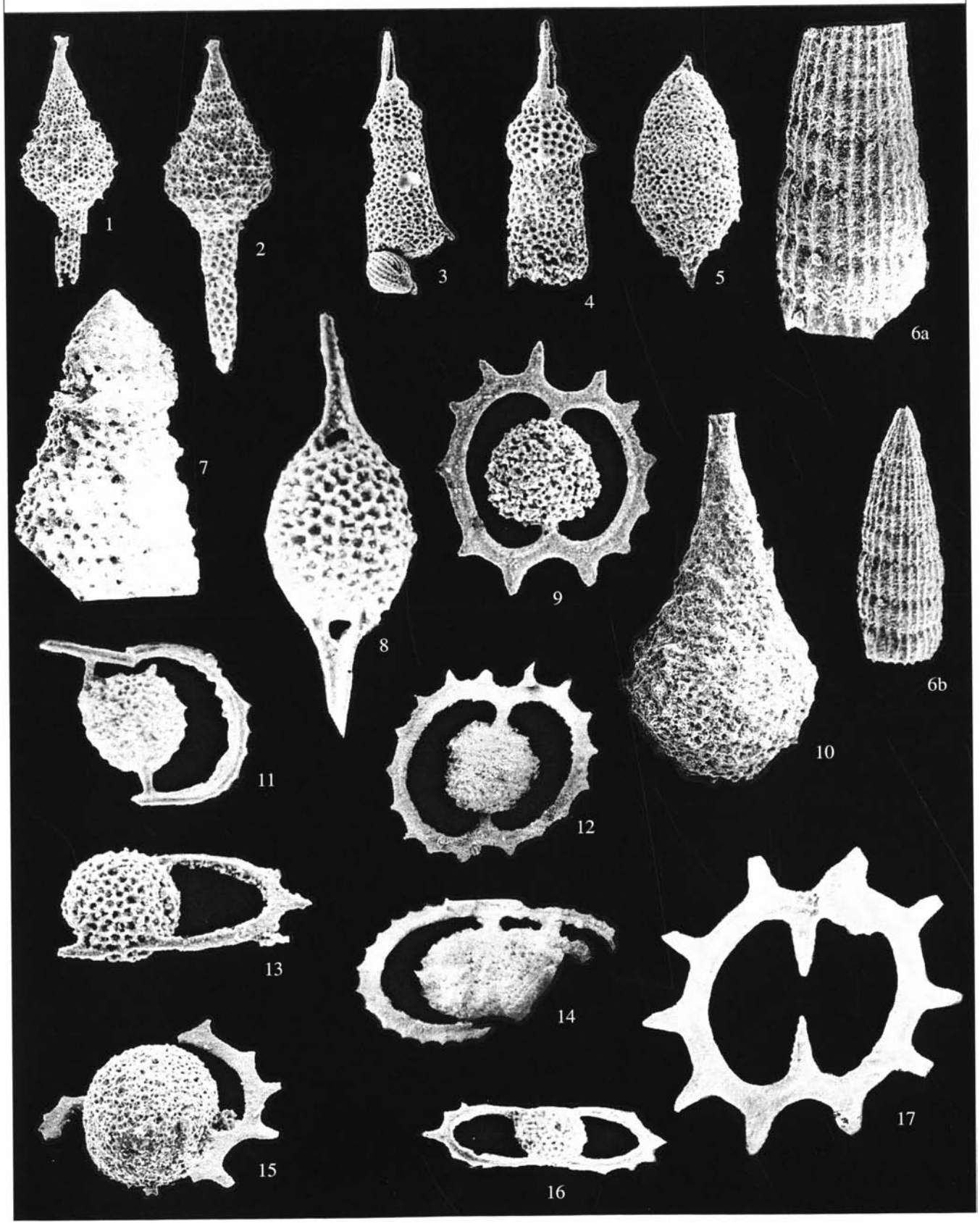

a ridge that is higher in relief than the equatorial part of the shell. The keel is weakly developed. The shell is spongy.

Measurements. Long axis of the cortical shell, 280–200; short axis of the cortical shell, 180–100.

Comparison. The new species differs from *G. concava* (Li et Wu, 1985) in the oval shell outline.

Occurrence. Upper Cenomanian of northern Turkey.

Material. More than 30 specimens.

Family Orbiculiformidae Pessagno, 1973

Genus *Orbiculiforma* Pessagno, 1973

Orbiculiforma: Pessagno, 1973, p. 71.

Type species. *Orbiculiforma quadrata* Pessagno, 1973; Upper Cretaceous, Coniacian–Santonian, Yolo Formation; California, Great Valley sequence.

Diagnosis. Shell large, discoid, circular to oval or square in outline. Central depression with tholus. Equatorial spines and openwork patagium over spongy shell sometimes present.

Species composition. *O. quadrata* Pessagno, 1973, *O. maxima* Pessagno, 1977, *O. ornata* sp. nov., *O. ovoidea* sp. nov., and more than 20 other species; Middle Jurassic–Cretaceous worldwide.

Comparison. *Orbiculiforma* differs from *Godia* Tumanda, 1986 in having a depression in the central part of the shell that is not encircled by nodes.

Orbiculiforma ornata Bragina, sp. nov.

Plate 41, figs. 4 and 5

Etymology. From the Latin *ornata* (ornamented).

Holotype. GIN, no. 4870/173; Crimean Mountains, Aksudere gully; Upper Cretaceous, Lower Turonian.

Description. The shell is discoid and oval in outline. The tholus is undeveloped. The shell surface is covered by small conical tubercles of variable size, scattered randomly (10 to 25 tubercles are present on either side of the shell in outline). The peripheral keel tubercles are somewhat larger, and vary in number from 14 to 22. The shell surface is pierced with fine pores in a pentagonal–hexagonal pattern.

Measurements. Holotype GIN, no. 4870/173: shell length along the long axis, 250, and along the short axis, 100; height of the peripheral processes, 10.

Comparison. The new species is distinguished from *O. maxima* Pessagno, 1977 by its oval shell outline and by the presence of tubercles positioned radially on the equatorial edge of the shell and the absence of spinules on the equatorial edge.

Remarks. Specimens of this new species have also been discovered among the Campanian radiolarian association from the Volga Region near Volgograd.

Occurrence. Lower Turonian of the Crimean Mountains.

Material. Eight specimens.

Orbiculiforma ovoidea Bragina, sp. nov.

Plate 25, figs. 10 and 11

Etymology. From the Latin *ovoidea* (oval).

Holotype. GIN, no. 4871/281; northern Turkey, Tomalar section; Upper Cenomanian, Tomalar Formation.

Description. The shell is discoid and oval in outline. The keel is undeveloped. The tholus is low, semispherical, bordered by a shallow and relatively narrow depression in the peripheral part. The shell is spongy and has a barrel-shaped cross section of peripheral parts.

Measurements. Shell length along the long axis, 400, and along the short axis 300; tholus diameter, 150.

Comparison. The new species differs from *O. maxima* Pessagno, 1977 in the oval shell outline.

Occurrence. Upper Cenomanian of northern Turkey.

Material. Ten specimens.

Explanation of Plate 34

Figs. 1 and 2. *Pseudoeucyrtis tavricus* sp. nov., ×100: (1) GIN, no. 4870/56; and (2) holotype GIN, no. 4870/57.

Figs. 3 and 4. *Rhopalosyringium euganeum* (Squinabol, 1903), ×100, specimens: (3) GIN, no. 4870/1; and (4) GIN, no. 4870/58.

Fig. 5. *Distylocapsa veneta* (Squinabol, 1904), GIN, no. 4870/59, ×200.

Fig. 6. *Archaeodictyomitra sliteri* Pessagno, 1977, GIN, no. 4870/60: (a) a shell fragment ×500, (b) general view ×200.

Fig. 7. *Novixitus costatus* sp. nov., GIN, no. 4870/61, ×500.

Fig. 8. *Vitorfus morini* Empson-Morin, 1981, GIN, no. 4870/62, ×500.

Figs. 9 and 12. *Acanthocircus multidentatus* (Squinabol, 1914), ×100, specimens: (9) GIN, no. 4870/63; and (12) GIN, no. 4870/64.

Fig. 10. *Pseudoeucyrtis spinosa* (Squinabol, 1903), GIN, no. 4870/65, ×250.

Figs. 11 and 14. *Acanthocircus impolitus* O'Dogherty, 1994, ×100, specimens: (11) GIN, no. 4870/66; and (14) GIN, no. 4870/67.

Fig. 13. *Vitorfus brustolensis* (Squinabol, 1903), GIN, no. 4870/68, ×250.

Fig. 15. *Acanthocircus tympanum* O'Dogherty, 1994; GIN, no. 4870/69, incomplete shell, ×200.

Fig. 16. *Vitorfus campbelli* Pessagno, 1977, GIN, no. 4870/70, ×100.

Fig. 17. *Acanthocircus hueyi* (Pessagno, 1976); GIN, no. 4870/71, ×200.

Plate 35

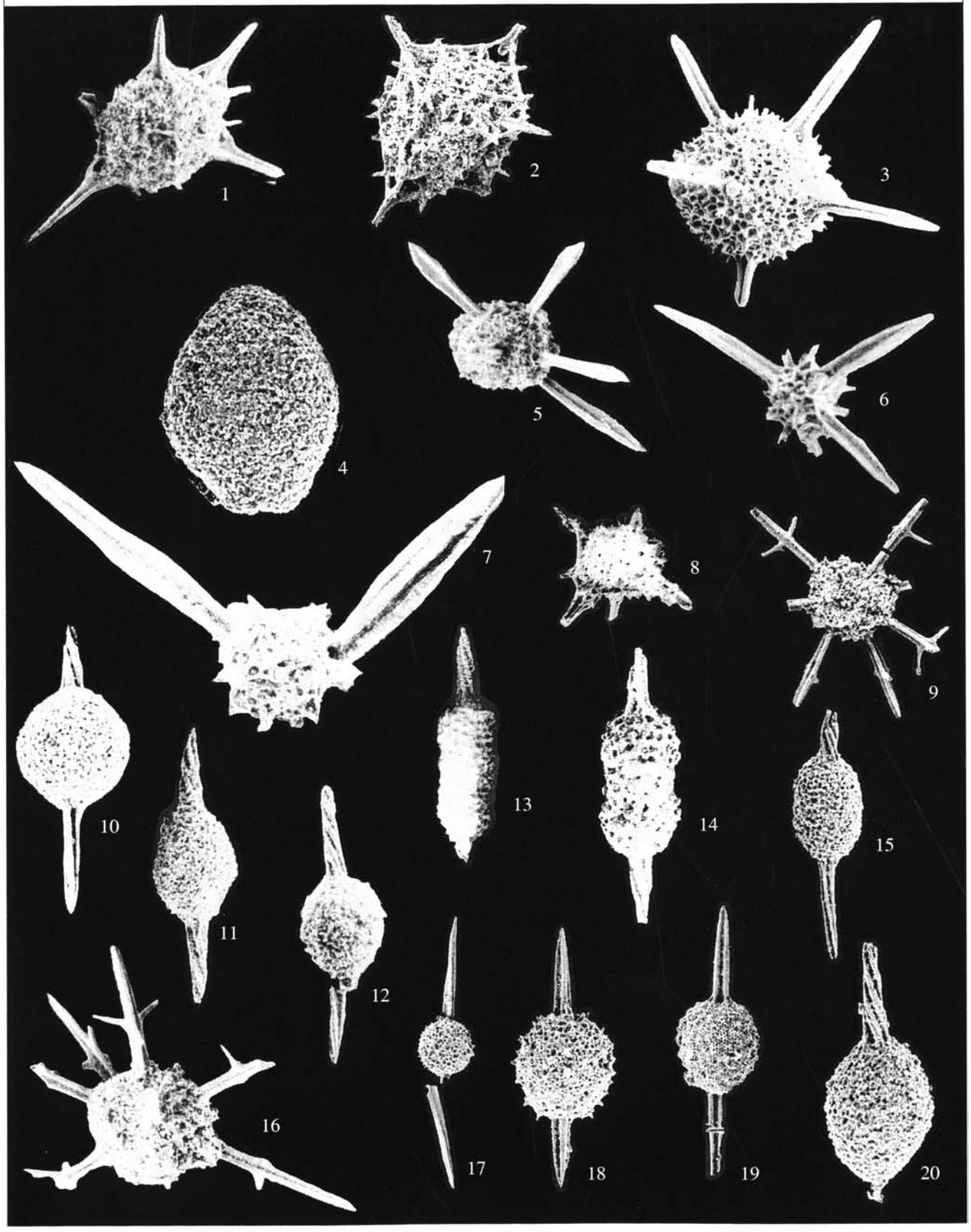

Genus *Patellula* Kozlova, 1972

Patellula: Kozlova in Petrushevskaya and Kozlova, 1972, p. 527.

Type species. *Stylospongia planoconvexa* Pessagno, 1963; Upper Cretaceous, Lower Campanian, Franciscan Complex; Puerto-Rico.

Diagnosis. Shell discoid, with tholus on one side and equatorial spinules. Surface spongy, occasionally resembling pseudoaulophacoid structure.

Species composition. More than ten species, including *P. cognata* O'Dogherty, 1994, *P. coronata* (Tumanda, 1989), *P. helios* (Squinabol, 1903); Cenomanian–Campanian worldwide.

Comparison. *Patellula* differs from *Pseudoaulophacus* Pessagno, 1972 in having a unilaterally convex tholus.

Patellula cognata O'Dogherty, 1994, emend. herein

Plate 25, fig. 4; Plate 37, fig. 17

Patellula cognata: O'Dogherty, 1994, p. 326, pl. 60, figs. 6–12.

Holotype. UL, no. 5482; central Italy, Umbria-Marche Apennines, locality Gb-84.40; Upper Cretaceous, Lower Cenomanian (O'Dogherty, 1994, pl. 60, fig. 6).

Description. The shell is spongy, discoid, and medium-sized. The upper surface of the shell has a high semispherical tholus. The tholus wall is pseudoaulophacoid and occasionally irregular in structure, i.e., the pores are rounded angular and set in hexagonal–pentagonal pore frames. The pores on the area surrounding the tholus are smaller and range in shape from round to polygonal. The lower shell surface is semispherical in cross section, with the radius longer than in the tholus. The keel is poorly pronounced and bordered by secondary spines (from 11 to 30 in number), which vary considerably in length and are oval to lenticular in cross section. Some spines may occur above and below the supposed keel line.

Measurements. Diameter of the cortical shell, 280; spine length, up to 60.

Comparison. *P. cognata* differs from *P. verteroensis* (Pessagno, 1963) in the higher tholus, weakly developed keel with radially arranged secondary spines, and the presence of spines both above and below the keel line.

Occurrence. Cenomanian of Italy; Middle–Upper Cenomanian of northern Turkey; Upper Cenomanian–Lower Turonian of the Crimean Mountains.

Material. More than 20 specimens.

Patellula coronata (Tumanda, 1989)

Plate 37, figs. 4 and 11

Godia (?) sp. *A*: Thurow, 1988, p. 401, pl. 5, fig. 20.

Godia (?) sp. *B*: Thurow, 1988, p. 401, pl. 5, fig. 17.

Godia (?) sp. *C*: Thurow, 1988, p. 401, pl. 9, fig. 15.

Godia (?) sp. *D*: Thurow, 1988, p. 401, pl. 9, fig. 23.

Orbiculiforma coronata: Tumanda, 1989, p. 29, pl. 5, figs. 12–14; pl. 10, fig. 2.

Godia coronata: O'Dogherty, 1994, p. 335, pl. 62, figs. 16–18.

Patellula verteroensis: Khan *et al.*, 1999, pl. 3, fig. c.

Holotype. Japan, northern Hokkaido, Usotan section; Lower Cretaceous, Hauterivian–Barremian, Furebura Formation (Tumanda, 1989, pl. 5, fig. 14).

Description. The shell is medium-sized, discoid, and spongy. The upper surface bears a relatively high hemispherical tholus. The structure of its wall approaches the pseudoaulophacoid pattern. The tholus diameter is approximates one-fifth of the shell diameter. The tholus is bordered by a narrow ridge composed of nodes or spongy meshwork. The ridge diameter is slightly less than one-third of the shell diameter. So, the ridge is not contiguous with the tholus periphery.

Measurements. Shell diameter, 250–413; tholus diameter, 110–187.

Comparison. *P. coronata* is distinguished from *P. verteroensis* (Pessagno, 1963) by the presence of the ridge bordering the tholus, the absence of pseudoaulophacoid porosity on this ridge, and by the development of peripheral spines.

Explanation of Plate 35

Figs. 1, 2, and 8. *Cuboctostylus pontidus* sp. nov., specimens: (1) GIN, no. 4870/72, ×100; (2) GIN, no. 4870/73, ×100; and (8) GIN, no. 4870/74, ×50.

Fig. 3. *Quinquecapsularia parvipora* (Squinabol, 1903), GIN, no. 4870/75, ×200.

Fig. 4. *Phaseliforma inflata* sp. nov., GIN, no. 4870/76, ×350.

Fig. 5. *Pseudoacanthosphaera galeata* O'Dogherty, 1994, GIN, no. 4870/77, ×50.

Figs. 6 and 7. *Pseudoacanthosphaera superba* (Squinabol, 1904), specimens: (6) GIN, no. 4870/78, ×100; and (7) GIN, no. 4870/79, ×200.

Figs. 9 and 16. *Falsocromyodrimus mirabilis* (Squinabol, 1903), specimens: (9) GIN, no. 4870/80, ×50; and (16) GIN, no. 4870/81, ×100.

Fig. 10. *Archaeospongoprunum sphaericum* sp. nov., holotype 4870/82, ×150.

Figs. 11, 12, 15, and 20. *Archaeospongoprunum cortinaensis* Pessagno, 1973, ×100, specimens: (11) GIN, no. 4870/83; (12) GIN, no. 4870/84; (15) GIN, no. 4870/85; and (20) GIN, no. 4870/86.

Fig. 13. *Archaeospongoprunum triplum* Pessagno, 1973, GIN, no. 4870/87, ×150.

Fig. 14. *Archaeospongoprunum archaeobipartitum* sp. nov., holotype GIN, no. 4870/88, ×100.

Figs. 17 and 18. *Pseudoacanthosphaera spinosissima* (Squinabol, 1904), specimens: (17) GIN, no. 4870/89, ×50; and (18) GIN, no. 4870/90, ×100.

Fig. 19. *Acaeniotyle longispina* (Squinabol, 1903), GIN, no. 4870/91, ×100.

Plate 36

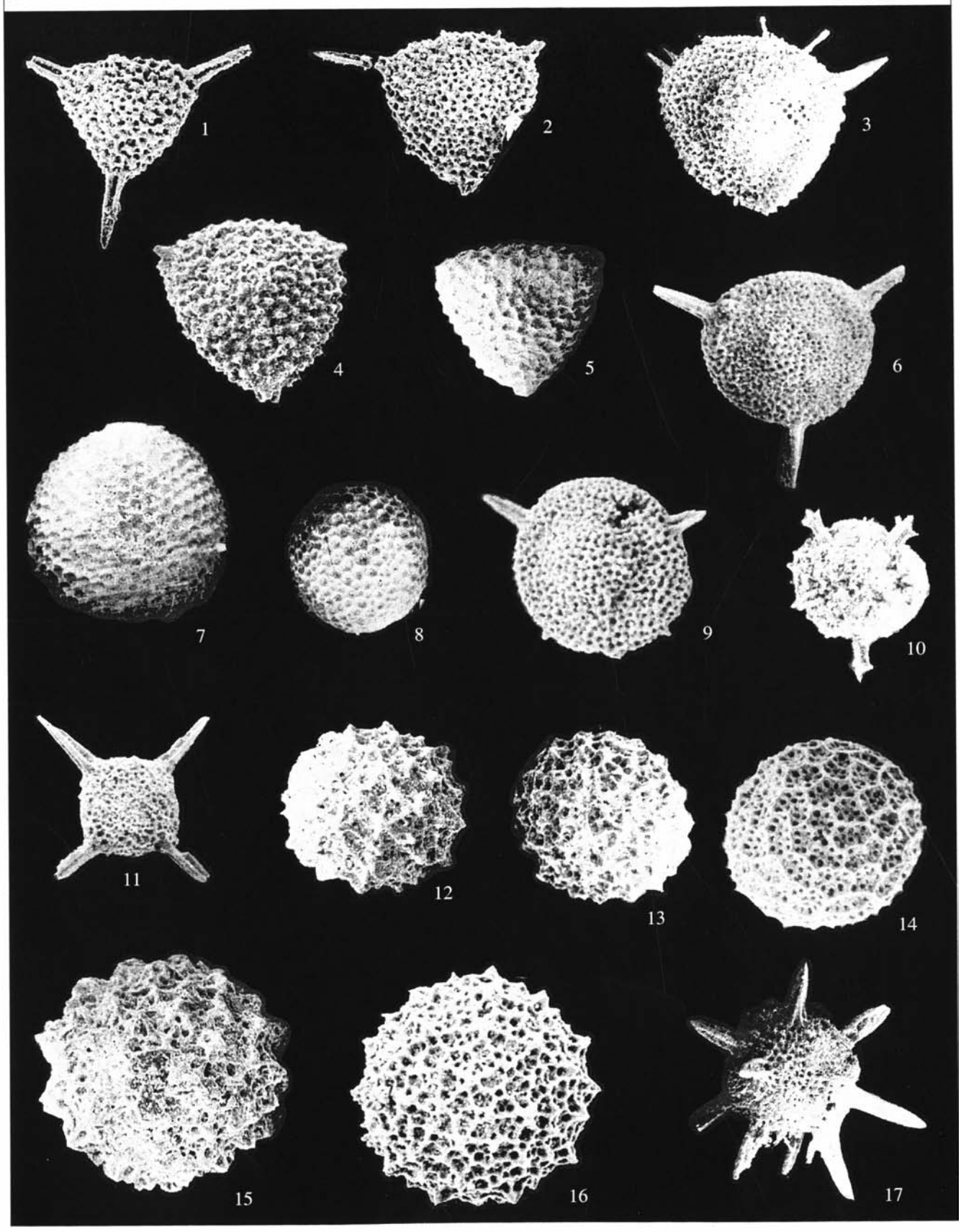

Remarks. *Orbiculiforma coronata* Tumanda, 1989 is here transferred to the genus *Patellula* Kozlova, 1972 on the basis of external features, such as the presence of a well-developed tholus on the upper surface and a poorly pronounced tholus on the lower surface. This species is closely similar to *P. planoconvexa* (Pessagno, 1963) but differs from in the absence of distinct nodes of the pseudoaulophacoid type on the ridge bordering the tholus, and in the presence of peripheral spines.

Occurrence. Hauterivian–Turonian of Japan; Middle Albian–Upper Cenomanian of Italy and Spain; Albian–Turonian of the Atlantic; Lower Turonian of the Crimean Mountains.

Material. More than 20 specimens.

Patellula helios (Squinabol, 1903), emend. herein

Plate 41, fig. 9

Stylotrochus helios: Squinabol, 1903, p. 124, pl. 10, figs. 23 and 23a.

Patellula helios: O'Dogherty, 1994, p. 327, pl. 60, figs. 19–21, 23, and 24.

Non *Patellula helios*: O'Dogherty, 1994, p. 327, pl. 60, fig. 22; Khan *et al.*, 1999, pl. 3, fig. h.

Pseudoaulophacus (?) sp.: Erbacher, 1994, pl. 16, fig. 13.

Pseudoaulophacus ex gr. *pargueraensis*: Vishnevskaya, 2001, pl. 81, figs. 4–7.

Holotype. Northern Italy, southern Venetian Alps, Colli Euganei, Teolo locality; upper Lower Cretaceous–lower Upper Cretaceous, Upper Albian–Lower Turonian (Squinabol, 1903, pl. 10, figs. 23, 23a).

Description. The shell is large, round in outline, and lens-shaped in cross section. The dome-shaped tholus may have a small central depression. The lower surface of the shell varies in shape from strongly convex to flat. Many (16 to 20) massive spines, circular to ellipsoid in cross section, radiate from the peripheral area of the shell. The spines are arranged irregularly and are not strictly confined to the keel line, being positioned both above and below it. The shell surface is covered with small rounded pores in rounded polygonal pore frames. The nodes on the pore borders are extremely weakly developed.

Measurements. Diameter of the cortical shell, 300; diameter of the central part, 87; length of the longest spine, 46.

Remarks. *P. cognata* O'Dogherty, 1994 may be found to fall within the intraspecific variation of *P. helios* (Squinabol, 1903).

Occurrence. Upper Albian–Lower Turonian of Italy and Spain; Cenomanian of the Pacific Ocean (Eastern Mariana Trench); Lower Turonian of the Crimean Mountains.

Material. Twelve specimens.

Patellula verteroensis (Pessagno, 1963)

Plate 25, fig. 3; Plate 37, fig. 10

Stylospongia (S.) verteroensis: Pessagno, 1963, p. 199, pl. 3, figs. 1–6; pl. 6, figs. 2 and 3; pl. 7, figs. 3–6

Patellula verteroensis: Petrushevskaya and Kozlova, 1972, p. 527, pl. 3, figs. 8 and 9; Empson-Morin, 1981, p. 257, pl. 2, figs. 1–5; Thurow, 1988, p. 403, pl. 2, figs. 19 and 20; Tumanda, 1989, p. 34, pl. 9, figs. 15 and 16; O'Dogherty, 1994, p. 328, pl. 60, figs. 25 and 26; Urquhart and Banner, 1994, fig. 4.x.

Non *Patellula verteroensis*: Khan *et al.*, 1999, pl. 3, fig. c.

Holotype. USNM; Puerto-Rico, Parguera limestones, locality PR2503; Upper Cretaceous, Lower Campanian (Pessagno, 1963, pl. 3, figs. 1–3).

Comparison. *P. verteroensis* differs from *P. planoconvexa* (Pessagno, 1963) in the higher tholus and the absence of a ridge surrounding it.

Occurrence. Cenomanian–Campanian worldwide; Middle–Upper Cenomanian of northern Turkey; Upper Cenomanian–Lower Turonian of the Crimean Mountains.

Material. More than 30 specimens.

Genus *Becus* Wu, 1986

Becus regius O'Dogherty, 1994

Plate 24, figs. 1 and 10

Orbiculiforma aff. *O. multangula*: Erbacher, 1994, pl. 17, fig. 1.

Becus regius: O'Dogherty, 1994, p. 318, pl. 58, figs. 19–24.

Non *Becus regius*: O'Dogherty, 1994, p. 318, pl. 58, figs. 18, 25, and 26 (= *Becus* sp. ?).

Holotype. UL, no. 3676; central Italy, Umbria-Marche Apennines, locality Gc-1073.94; Upper Creta-

Explanation of Plate 36

Fig. 1. *Alievium superbum* (Squinabol, 1914), GIN, no. 4870/92, ×100.

Fig. 2. *Pseudoaulophacus praefloresensis* Pessagno, 1972, GIN, no. 4870/93, ×150.

Fig. 3. *Pseudoaulophacus putahensis* Pessagno, 1972, GIN, no. 4870/94, ×150.

Figs. 4 and 5. *Alievium sculptus* (Squinabol, 1904), specimens: (4) GIN, no. 4870/95, ×150; and (5) GIN, no. 4870/96, ×100.

Figs. 6 and 9. *Pseudoaulophacus circularis* sp. nov., ×150 : (6) holotype GIN, no. 4870/97; and (9) GIN, no. 4870/98.

Fig. 7. *"Cenosphaera" boria* Pessagno, 1977, GIN, no. 4870/99, ×200.

Fig. 8. *Gongylothorax verbeeki* (Tan Sin Hok, 1927), GIN, no. 4870/100, ×100.

Fig. 10. *Falsocromyodrimus mirabilis* (Squinabol, 1904), GIN, no. 4870/100-1, ×75.

Fig. 11. *Quadrigastrum insulsum* O'Dogherty, 1994, GIN, no. 4870/101, ×75.

Figs. 12, 13, and 16. *Praeconocaryomma californiaensis* Pessagno, 1976, specimens: (12) GIN, no. 4870/102, ×100; (13) GIN, no. 4870/103, ×100; and (16) GIN, no. 4870/104, (×200.

Fig. 14. *Archaeocenosphaera ? mellifera* O'Dogherty, 1994, GIN, no. 4870/105, ×200.

Fig. 15. *Praeconocaryomma universa* Pessagno, 1976, GIN, no. 4870/106, ×200.

Fig. 17. *Staurosphaeretta wisniowskii* (Squinabol, 1903), GIN, no. 4870/107, ×100.

Plate 37

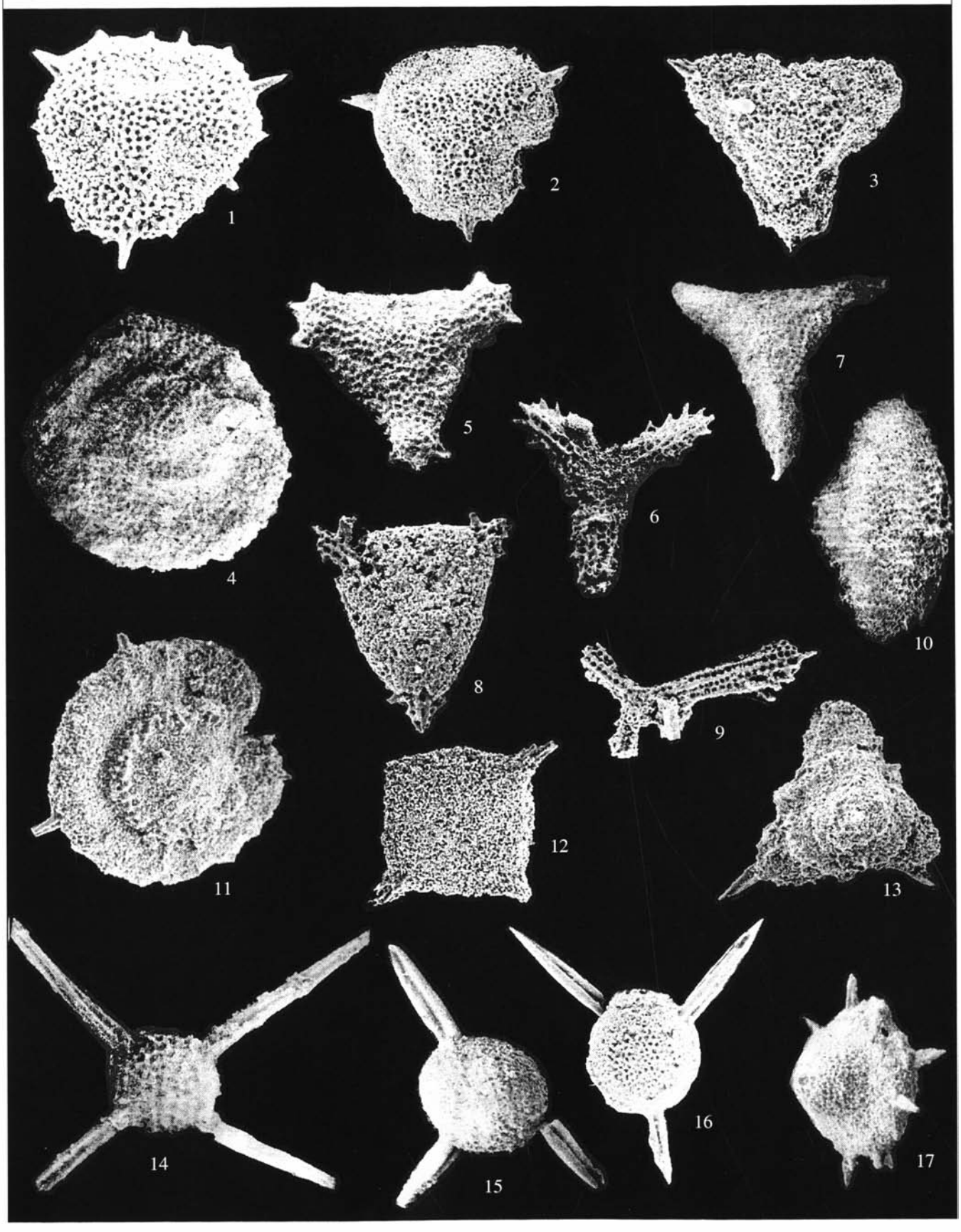

ceous, Middle Cenomanian (O'Dogherty, 1994, pl. 58, fig. 20).

Occurrence. Cenomanian of Italy; Upper Cenomanian of northern Turkey; Lower Turonian of the Crimean Mountains.

Material. More than 20 specimens.

Becus horridus (Squinabol, 1903)

Plate 24, figs. 2, 3, and 6

Theodiscus horridus: Squinabol, 1903, p. 119, pl. 8, fig. 18.

Becus horridus: O'Dogherty, 1994, p. 318, pl. 58, figs. 9, 11–17.

Non *Becus horridus*: O'Dogherty, 1994, p. 318, pl. 58, fig. 10 [= *Becus* ex gr. *B. horridus* (Squinabol, 1903)].

Holotype. Northern Italy, southern Venetian Alps, Colli Euganei, Teolo locality; upper Lower Cretaceous–lower Upper Cretaceous, Upper Albian–Lower Turonian (Squinabol, 1903, pl. 8, fig. 18).

Comparison. *B. horridus* is distinguished from *B. regius* O'Dogherty, 1994 by its lenticular to spherical shell, and by the fact that it always has three three-bladed primary spines.

Occurrence. Upper Aptian–Lower Turonian of Italy; Middle–Upper Cenomanian of northern Turkey.

Material. More than 30 specimens.

Genus *Dispongotripus* Squinabol, 1903

Dispongotripus triangularis (Squinabol, 1904)

Plate 24, figs. 4 and 5

Trochodiscus triangularis: Squinabol, 1904, p. 200, pl. 5, fig. 2.

Dispongotripus triangularis: O'Dogherty, 1994, p. 324, pl. 59, figs. 19–24.

Holotype. Northern Italy, southern Venetian Alps, Colli Euganei, Teolo locality; upper Lower Cretaceous–lower Upper Cretaceous, Upper Albian–Lower Turonian (Squinabol, 1904, pl. 5, fig. 2).

Occurrence. Upper Albian–Lower Turonian of Italy and Spain; Upper Cenomanian of northern Turkey.

Material. Eight specimens.

Family Phaseliformidae Pessagno, 1972

Genus *Phaseliforma* Pessagno, 1972

Phaseliforma: Pessagno, 1972, p. 274.

Type species. *Phaseliforma carinata* Pessagno, 1972; Upper Cretaceous, Campanian, Marsh Creek Formation; California, Great Valley sequence.

Diagnosis. Shell ellipsoid, typically for the family, and perforate. Pores small, rounded -polygonal, in polygonal pore frames of irregular outline. Shell variable in width, often with keel, and sometimes with polar parts slightly compressed.

Species composition. *Phaseliforma carinata* Pessagno, 1972, *P. laxa* Pessagno, 1972, *P. ovum* Jud, 1994, *P. subcarinata* Pessagno 1975, and *P. inflata* sp. nov.; Cretaceous worldwide.

Comparison. *Phaseliforma* is distinguished from *Cromyodruppa* Haeckel, 1887 by the absence of internal concentric ellipsoidal porous shells.

Phaseliforma carinata Pessagno, 1972

Plate 26, fig. 3

Phaseliforma carinata: Pessagno, 1972, p. 274, pl. 22, figs. 1–3.

Holotype. USNM-Pessagno, no. 165575; California, Great Valley sequence, locality NSF 568-B; Upper Cretaceous, Upper Campanian, Marsh Creek Formation (Pessagno, 1972, pl. 22, fig. 1).

Occurrence. Coniacian–Campanian worldwide; Middle–Upper Cenomanian of northern Turkey.

Material. Twelve specimens.

Phaseliforma inflata Bragina, sp. nov.

Plate 35, fig. 4; Plate 40, fig. 5

Etymology. From the Latin *inflata* (inflated).

Holotype. GIN, no. 4870/160; Crimean Mountains, Belaya Mountain section; Lower Turonian.

Description. The shell is large and oval. The cap-shaped polar parts are equal in size and lenticular in cross section, whereas the central part is almost spherical. The keel is absent. In outline, one half of

Explanation of Plate 37

Fig. 1. *Paronaella pseudoaulophacoides* O'Dogherty, 1994, GIN, no. 4870/108, ×200.

Figs. 2 and 3. *Cavaspongia robusta* sp. nov., ×200: (2) paratype GIN, no. 4870/109; and (3) holotype 4870/110.

Figs. 4 and 11. *Patellula coronata* (Tumanda, 1989), ×200, specimens: (4) GIN, no. 4870/111, upper side of the shell; and (11) GIN, no. 4870/112, lower side of the shell.

Figs. 5, 6, 8, and 9. *Paronaella spica* sp. nov., specimens: (5) GIN, no. 4870/113, ×100; (6) holotype GIN, no. 4870/114, ×100; (8) GIN, no. 4870/115, ×100; and (9) GIN, no. 4870/116, porous shell devoid of patagium, ×150.

Fig. 7. *Cavaspongia antelopensis* Pessagno, 1973, GIN, no. 4870/117, ×100.

Fig. 10. *Patellula verteroensis* (Pessagno, 1963), GIN, no. 4870/118, ×100.

Fig. 12. *Crucella latum* (Lipman, 1960), GIN, no. 4870/119, ×200.

Fig. 13. *Pyramispongia glascockensis* Pessagno, 1973, GIN, no. 4870/120, ×100.

Fig. 14. *Staurosphaeretta longispina* (Squinabol, 1903), GIN, no. 4870/121, ×100.

Figs. 15 and 16. *Triactoma compressa* (Squinabol, 1904), specimens: (15) GIN, no. 4870/122, ×150; and (16) GIN, no. 4870/123, ×100.

Fig. 17. *Patellula cognata* O'Dogherty, 1994, GIN, no. 4870/124, ×100.

Plate 38

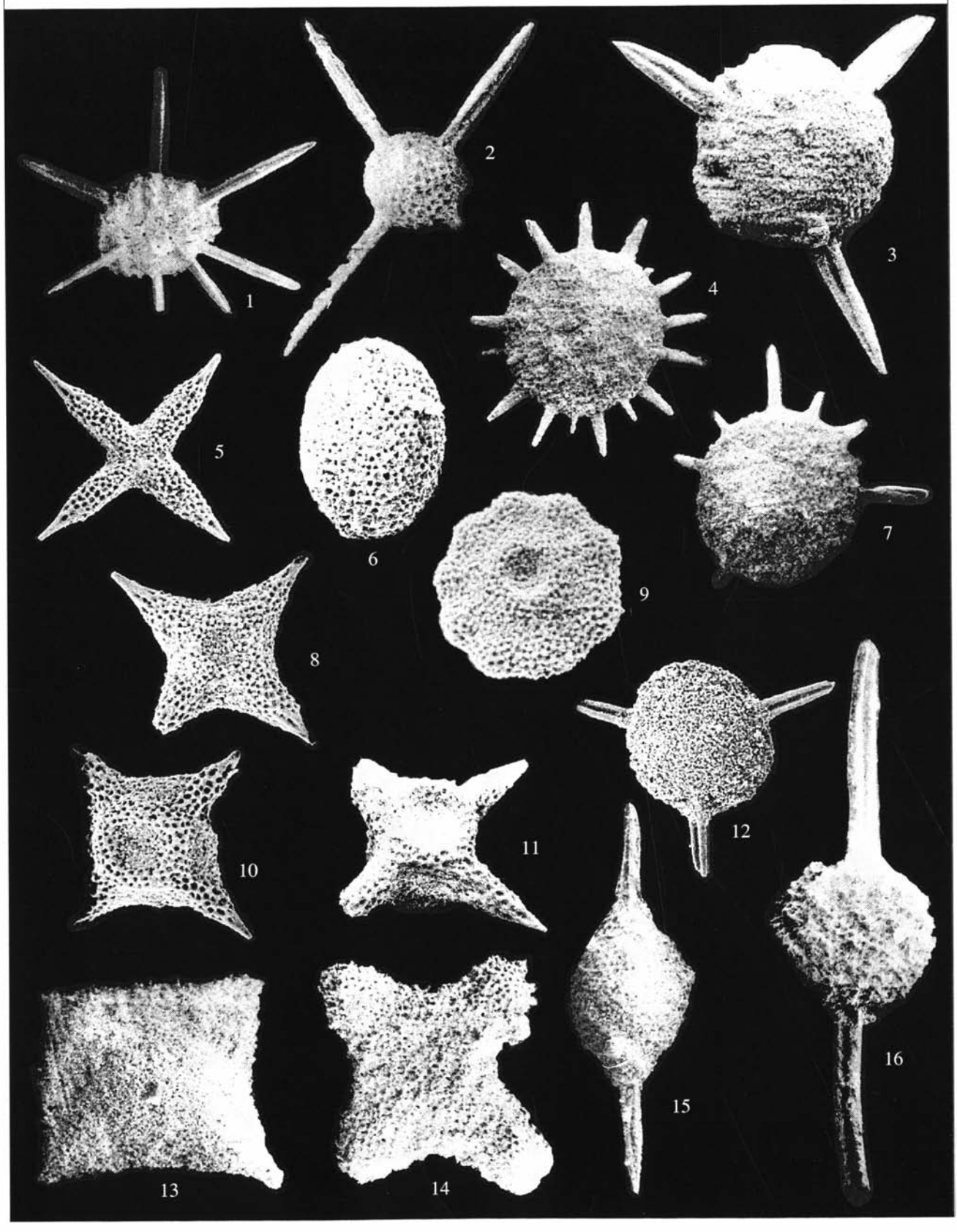

the shell is more convex in the central part than the other. The shell surface is spongy.

Measurements. Shell length, 310; shell width, 200.

Comparison. The new species differs from *P. ovum* Jud, 1994 in the significantly inflated shell, which is somewhat distorted in outline.

Remarks. *P. inflata* sp. nov. is probably a missing member of the lineage *P. ovum* Jud, 1994—*P. inflata* sp. nov.—*P. subcarinata* Pessagno, 1975.

Occurrence. Lower Turonian of the Crimean Mountains.

Material. More than 30 specimens.

Phaseliforma laxa Pessagno, 1972

Plate 26, figs. 1 and 2

Phaseliforma laxa Pessagno, 1972, p. 276, pl. 23, figs. 7–9; Urquhart and Banner, 1994, fig. 4.v; Hollis, 1997, pl. 8, fig. 5.

Phaseliforma cf. *laxa*: Iwata and Tajika, 1986, pl. 4, fig. 7.

Phaseliforma sp.: Iwata and Tajika, 1986, pl. 4, fig. 5.

Non *Phaseliforma laxa*: Hollis, 1997, pl. 8, fig. 1 (= *P.* ex gr. *laxa* Pessagno, 1972)

Phaseliforma carinata: Vishnevskaya, 2001, pl. 4, fig. 3.

Phaseliforma subcarinata: Vishnevskaya, 2001, pl. 6, figs. 3 and 4.

Holotype. USNM-Pessagno, no. 165578; California, Great Valley sequence, locality NSF 572; Upper Cretaceous, Upper Campanian, Marsh Creek Formation (Pessagno, 1972, pl. 23, fig. 7).

Comparison. *P. laxa* is distinguished from *P. carinata* Pessagno, 1972 by its unusually smooth surface and by the absence of a carina.

Occurrence. Coniacian–Campanian worldwide; Middle Cenomanian of northern Turkey.

Material. Nine specimens.

Phaseliforma ovum Jud, 1994

Plate 38, fig. 6

Phaseliforma ovum: Jud, 1994, p. 78, pl. 10, figs. 10 and 11.

Holotype. UL, no. Bo. 566.50:83; Italy, Umbria-Marche Apennines, Fiume Bosso; Lower Cretaceous, Upper Hauterivian–Upper Barremian (Jud, 1994, pl. 10, fig. 10).

Comparison. *P. ovum* is distinguished from *P. laxa* Pessagno, 1972 by the uneven surface of the cortical shell and the smaller, more angular pores.

Occurrence. Upper Hauterivian–Upper Barremian of Italy; Upper Cenomanian of northern Turkey; Lower Turonian of the Crimean Mountains.

Material. Five specimens.

Family Saturnalidae Deflandre, 1953

Genus *Acanthocircus* Squinabol, 1903

Acanthocircus: Squinabol, 1903, p. 124.

Type species. *Acanthocircus irregularis* Squinabol, 1903; upper Lower Cretaceous–lower Upper Cretaceous, Upper Albian–Lower Turonian; central Italy, southern Venetian Alps, Colli Euganei, Teolo locality.

Diagnosis. Saturnalidae with or without border on saturnal ring, varying in shape from circular to broadly ellipsoidal and from subquadrate to subrectangular at species level. Ring bears numerous external rays, with two rays on right and left of every polar spine. Cortical shell spongy.

Species composition. Several dozen species, including *A. imperfectus* sp. nov.; worldwide distribution; stratigraphic ranges have not been established.

Comparison. *Acanthocircus* is distinguished from *Vitorfus* Pessagno, 1977 by its spongy cortical shell, a broader and almost circular saturnal ring, and longer polar spines, which are clearly visible between the cortical shell and the saturnal ring.

Acanthocircus imperfectus Bragina, sp. nov.

Plate 28, figs. 1–3 and 5

Etymology. From the Latin *imperfectus* (imperfect).

Holotype. GIN, no. 4871/308; northern Turkey, Ürküt section; Upper Cretaceous, Upper Cenomanian, Tomalar Formation.

Explanation of Plate 38

Fig. 1. *Pseudoacanthosphaera magnifica* (Squinabol, 1904), GIN, no. 4870/125, ×75.

Fig. 2. *Staurosphaeretta longispina* (Squinabol, 1903), GIN, no. 4870/126, ×150.

Figs. 3 and 12. *Triactoma compressa* (Squinabol, 1904), specimens: (3) GIN, no. 4870/127, ×200; and (12) GIN, no. 4870/128, ×150.

Figs. 4 and 7. *Dactyliodiscus longispinus* (Squinabol, 1904), ×100, specimens: (4) GIN, no. 4870/129; and (7) GIN, no. 4870/130.

Fig. 5. *Crucella messinae* Pessagno, 1971, GIN, no. 4870/131, ×200.

Fig. 6. *Phaseliforma ovum* Jud, 1994, GIN, no. 4870/132, ×100.

Figs. 8, 10, and 11. *Crucella cachensis* Pessagno, 1971, specimens: (8) GIN, no. 4870/133, ×100; (10) GIN, no. 4870/134, ×150; and (11) GIN, no. 4870/135, ×150.

Fig. 9. *Pseudoaulophacus parqueraensis* Pessagno, 1972, GIN, no. 4870/136, ×100.

Fig. 13. *Crucella latum* (Lipman, 1960), GIN, no. 4870/137, ×100.

Fig. 14. *Crucella aster* (Lipman, 1952), GIN, no. 4870/138, ×150.

Fig. 15. *Archaeospongoprunum* sp. *A.* sensu Pessagno, 1977, GIN, no. 4870/139, ×150.

Fig. 16. *Acaeniotyle longispina* (Squinabol, 1903), GIN, no. 4870/140, ×250.

Plate 39

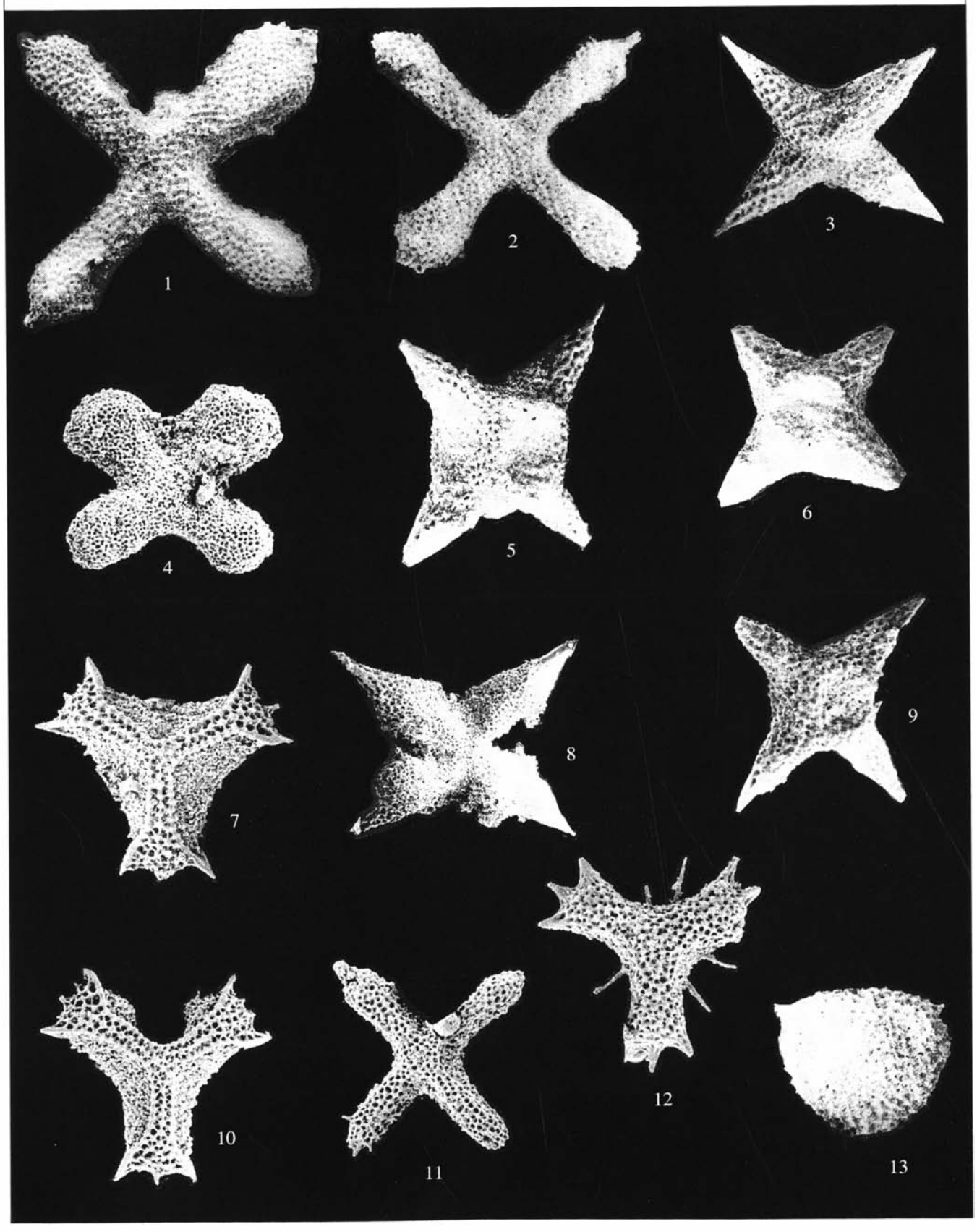

Description. The shell has a flat ellipsoidal ring with two polar spines, not exactly opposite one another. The shortest diameter of the ring lies in the plane of the polar spines. A rim is developed on the internal surface of the ring and at the bases of the external rays. Numerous (12 to 16) external rays vary in shape from moderately to very narrow at the base. The auxiliary rays become shorter as the distance from the polar spines increases: closely positioned rays are longer, whereas the rays located far from the polar spines are extremely short or almost indiscernible. The cortical shell is completely spongy and irregular in outline.

Measurements. Ring diameter (excluding rays), 280–320; spine length, 50–60; length of external rays, 40–50.

Comparison. The new species differs from *A. hueyi* (Pessagno, 1976) in (a) the elliptical saturnal ring, with the shortest diameter in the plane of the polar spines, (b) the position of the polar spines not exactly opposite one another, (c) the narrower and shorter auxiliary rays, which are usually rather numerous, and (d) the poor development of external rays that are far from the primary spines.

Occurrence. Upper Cenomanian of northern Turkey.

Material. Seven complete and eight incomplete specimens.

Acanthocircus impolitus O'Dogherty 1994, emend. herein

Plate 28, figs. 7, 9–11; Plate 34, figs. 11 and 14

Acanthocircus sp. *A:* Pessagno, 1977, p. 32, pl. 2, figs. 16 and 22.

Acanthocircus impolitus: O'Dogherty, 1994, p. 261, pl. 46, figs. 6–9.

Holotype. UL, no. 583; central Italy, Umbria-Marche Apennines, locality Ap2; Lower Cretaceous, Middle Albian (O'Dogherty, 1994, pl. 46, fig. 7).

Description. The shell has a flat ellipsoidal ring with two polar spines. The shortest diameter of the ring lies in the plane of the polar spines. A carina is developed on the inner margin of the ring and on the bases of the external spines. The numerous (14 to 16) auxiliary rays are wide at the base, but very short and hardly discernible in some specimens. The cortical shell is spherical and completely spongy.

Measurements. Diameter of the cortical shell, 158–58; diameter of ring, 375–258; length of the longest spine, 42–33.

Comparison. *A. impolitus* differs from *A. ellipticus* (Squinabol, 1903) in the wider ring and the greater number of auxiliary rays.

Occurrence. Middle Albian–Lower Turonian of Italy, Spain, and California; Middle–Upper Cenomanian of northern Turkey; Lower Turonian of the Crimean Mountains.

Material. Fourteen specimens.

Acanthocircus horridus Squinabol, 1903

Plate 27, figs. 4 and 9

Acanthocircus horridus: Squinabol, 1903, p. 125, pl. 9, fig. 3; O'Dogherty, 1994, p. 253, pl. 44, figs. 4 and 5.

Spongosaturnalis horridus: Schaaf, 1981, pl. 16, fig. 4; Bragin *et al.*, 2000, fig. 3.C.

(?) *Acanthocircus horridus*: O'Dogherty, 1994, p. 253, pl. 44, figs. 1–3, 6.

Holotype. Northern Italy, southern Venetian Alps, Colli Euganei, Teolo locality; upper Lower Cretaceous–lower Upper Cretaceous, Upper Albian–Lower Turonian (Squinabol, 1903, pl. 9, fig. 3).

Comparison. *A. horridus* is distinguished from *A. hueyi* (Pessagno, 1976) by the absence of a rim on the internal surface of the saturnal ring and by the greater number of auxiliary rays.

Occurrence. Upper Albian–Lower Turonian of Italy and Spain; Upper Cretaceous of the Atlantic and Cyprus; Middle–Upper Cenomanian of northern Turkey.

Material. More than 20 specimens.

Acanthocircus hueyi (Pessagno, 1976)

Plate 27, figs. 5–7; Plate 28, fig. 4; Plate 34, fig. 17

Spongosaturninus hueyi: Pessagno, 1976, p. 39, pl. 12, fig. 1; Foreman, 1978b, p. 744, pl. 3, fig. 8.

Acanthocircus hueyi: Foreman, 1975, p. 611, pl. 1A, fig. 6; pl. 4, fig. 10; O'Dogherty, 1994, p. 260, pl. 46, figs. 2, 3, and 5.

(?) *Acanthocircus hueyi:* O'Dogherty, 1994, p. 260, pl. 46, figs. 1 and 4.

Acanthocircus sp.: Salvini and Marcucci Passerini, 1998, fig. 8.o.

Holotype. USNM-Pessagno, no. 165664; California, Great Valley sequence, locality NSF 451; Upper Cretaceous, Upper Campanian, Del Valle Formation (Pessagno, 1976, pl. 12, fig. 1).

Comparison. *A. hueyi* is distinguished from *A. venetus* (Squinabol, 1914) by the presence of a rim on the internal surface of the saturnal ring and the longer auxiliary rays that are located close to the polar spines.

Explanation of Plate 39

Figs. 1, 2, and 4. *Savaryella novalensis* (Squinabol, 1914), specimens: (1) GIN, no. 4870/141, ×150; (2) GIN, no. 4870/142, ×150; and (4) GIN, no. 4870/143, ×100.

Figs. 3 and 8. *Crucella irwini* Pessagno, 1971, specimens: (3) GIN, no. 4870/144, ×100; and (8) GIN, no. 4870/145, ×120.

Figs. 5, 6, and 9. *Crucella cachensis* Pessagno, 1971, specimens: (5) GIN, no. 4870/146, ×120; (6) GIN, no. 4870/147, ×100; and (9) GIN, no. 4870/148, ×100.

Figs. 7 and 10. *Halesium sexangulum* Pessagno, 1971, ×100, specimens: (7) GIN, no. 4870/149; and (10) GIN, no. 4870/150.

Fig. 11. *Patulibracchium (?) quadroastrum* Bragina, 2003, GIN, no. 4870/151, ×150.

Fig. 12. *Paronaella solanoensis* Pessagno, 1971, GIN, no. 4870/152, ×100.

Fig. 13. *Pseudoaulophacus praefloresensis* Pessagno, 1972, GIN, no. 4870/153, ×100.

Plate 40

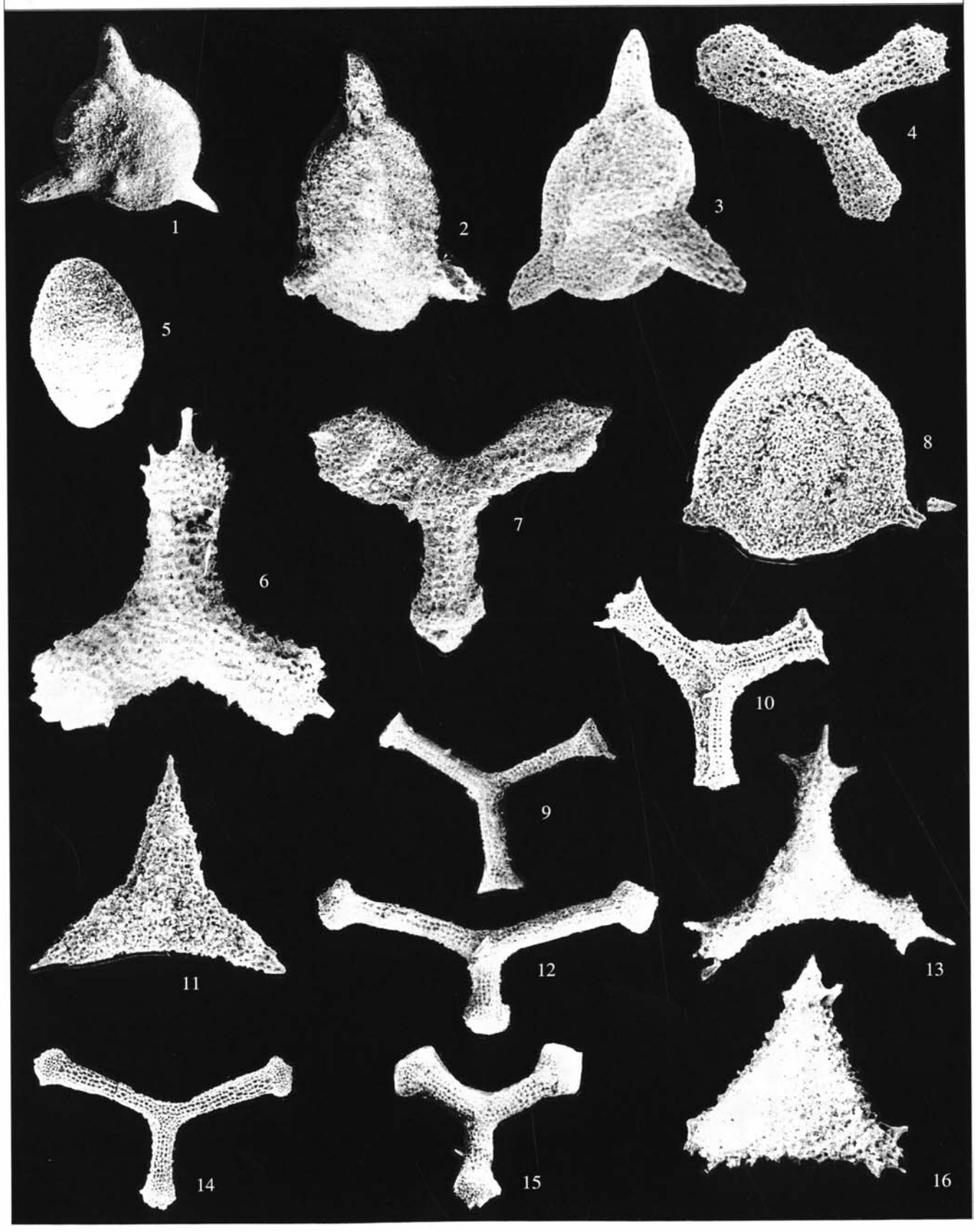

Occurrence. Turonian–Campanian worldwide; Middle–Upper Turonian of northern Turkey; Lower Turonian of the Crimean Mountains.

Material. More than ten specimens.

Acanthocircus moorei (Foreman, 1975)

Plate 28, fig. 12

Spongosaturnalis ? moorei: Foreman, 1975, p. 611, pl. 1B, fig. 11; pl. 4, fig. 9.

Holotype. USNM, no. 219347; North Pacific, DSDP Leg 32, borehole 310; Lower Cretaceous, Albian (Foreman, 1975, pl. 4, fig. 9).

Occurrence. Albian of the North Pacific; Middle–Upper Cenomanian of northern Turkey.

Material. Five specimens.

Acanthocircus multidentatus (Squinabol, 1914)

Plate 34, figs. 9 and 12

Saturnalis multidentatus: Squinabol, 1914, p. 298, pl. 23, figs. 11 and 12.

Acanthocircus multidentatus: O'Dogherty, 1994, p. 255, pl. 44, figs. 7–10.

Holotype. Northern Italy, southern Venetian Alps, Vicentino Province,; Middle Cretaceous Novale Group (Squinabol, 1914, pl. 23, fig. 11).

Comparison. *A. multidentatus* is distinguished from *A. hueyi* (Pessagno, 1976) by a narrow ring, and shorter wedge-shaped auxiliary rays.

Occurrence. Middle Cretaceous of Italy; Lower Turonian of the Crimean Mountains.

Material. More than 30 specimens.

Acanthocircus polymorphus (Squinabol, 1914)

Plate 27, figs. 8 and 10

Saturnalis polymorphus: Squinabol, 1914, pl. 24, figs. 2–7.

Holotype. Northern Italy, southern Venetian Alps, Colli Euganei, Teolo locality; upper Lower Cretaceous–lower Upper Cretaceous, Upper Albian–Lower Turonian (Squinabol, 1914, pl. 24, fig. 2, the specimen illustrated is taken to be the holotype).

Occurrence. Upper Albian–Lower Turonian of Italy; Middle–Upper Cenomanian of northern Turkey.

Material. Eight specimens.

Acanthocircus tympanum O'Dogherty, 1994, emend. herein

Plate 34, fig. 15

Acanthocircus sp. *D.*: Kuhnt *et al.*, 1986, pl. 8, fig. q.

Acanthocircus sp. nov.: Kuhnt *et al.*, 1986, pl. 8, fig. m.; Thurow and Kuhnt, 1986, text-figs. 9.1 and 9.2.

Mesosaturnalis sp.: Erbacher, 1994, pl. 19, figs. 6 and 7.

Acanthocircus tympanum: O'Dogherty, 1994, p. 259, pl. 45, figs. 17–24; Salvini and Marcucci Passerini, 1998, fig. 8.p; Khan *et al.*, 1999, pl. 2, fig. m.

Holotype. UL, no. 6769; central Italy, Umbria-Marche Apennines, locality Asv-5-43; Lower Turonian (O'Dogherty, 1994, pl. 45, fig. 17).

Description. The shell is large and has a narrow subquadrate ring. The ring is slightly concave at the points from which the polar spines diverge. No rim is developed. The auxiliary rays, which are wide at the base and sharply taper, are variously developed. The longest rays are those adjacent to the polar spines. Four to eight auxiliary rays occur on each half of the ring. In total, there are 4 to 15 flat auxiliary rays varying slightly from short and pointed to relatively long with rounded or pointed apices. The auxiliary rays are arranged more or less symmetrically relative to the axis formed by the polar spines. The large cortical shell is centrally convex and rising noticeably above the ring surface. It is cylindrical in the plane perpendicular to the plane of the ring. In the transverse plane, the cylinder is slightly compressed in the center.

Measurements. Diameter of the cortical shell, 195–140; ring diameter, 270–195; maximal spine length, 95–65.

Comparison. *A. tympanum* is distinguished from other species of the genus *Acanthocircus* by the cylindrical shape of the cortical shell.

Occurrence. Cenomanian–Lower Turonian of Italy and Spain; Lower Turonian of the Crimean Mountains.

Material. More than 20 specimens.

Genus *Vitorfus* Pessagno, 1977

Vitorfus brustolensis (Squinabol, 1903)

Plate 28, figs. 6 and 8; Plate 34, fig. 13

Saturnalis brustolensis: Squinabol, 1903, p. 112, pl. 10, fig. 4.

Acanthocircus brustolensis: Donofrio and Mostler, 1978, p. 27, pl. 6, fig. 14.

Explanation of Plate 40

Figs. 1 and 8. *Cavaspongia euganea* (Squinabol, 1904), specimens: (1) GIN, no. 4870/154, ×100; and (8) GIN, no. 4870/154-a, ×120.

Figs. 2 and 3. *Cavaspongia tavrica* sp. nov.: (2) paratype GIN, no. 4870/155, ×100; and (3) holotype GIN, no. 4870/156, ×100.

Figs. 4, 7, and 15. *Patulibracchium woodlandensis* Pessagno, 1971, ×100, specimens: (4) GIN, no. 4870/157; (7) GIN, no. 4870/158; and (15) GIN, no. 4870/159.

Fig. 5. *Phaseliforma inflata* sp. nov., holotype GIN, no. 4870/160, ×100.

Fig. 6. *Paronaella solanoensis* Pessagno, 1971, GIN, no. 4870/161, ×200.

Fig. 9. *Halesium quadratum* Pessagno, 1971, GIN, no. 4870/162, ×100.

Fig. 10. *Halesium diacanthum* (Squinabol, 1914), 4870/163, ×75.

Fig. 11. *Cavaspongia contracta* O'Dogherty, 1994, GIN, no. 4870/164, ×100.

Figs. 12 and 14. *Patulibracchium ingens* (Lipman, 1952), ×75, specimens: (12) GIN, no. 4870/165; and (14) GIN, no. 4870/166.

Figs. 13 and 16. *Paronaella spica* sp. nov., ×100, spec

Plate 41

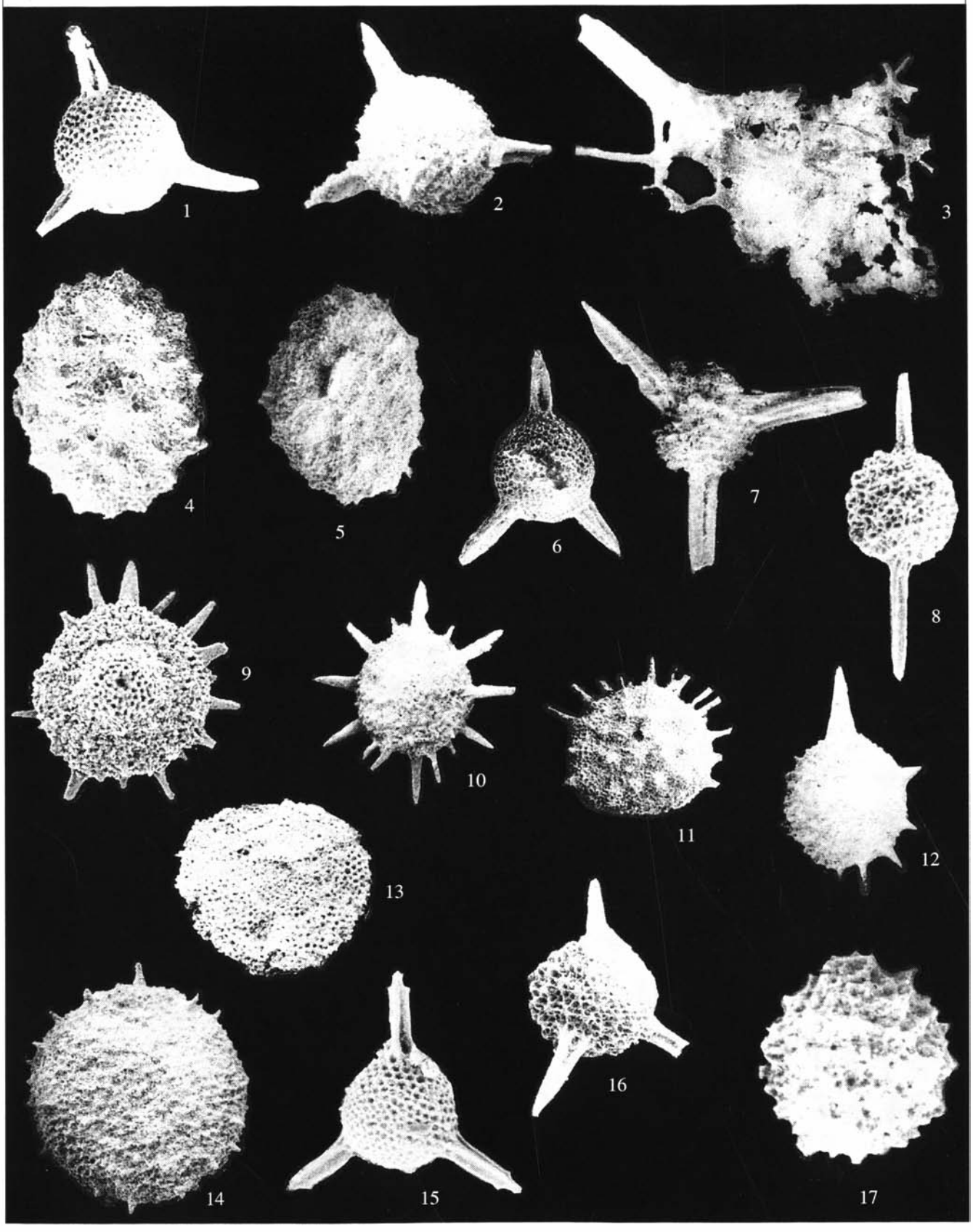

Vitorfus brustolensis: Schmidt-Effing, 1980, pl. 13, fig. 1; Dumitrica, 1985, pl. 2, fig. 3; pl. 3, figs. 1, 2, 9, and 10; Erbacher, 1994, pl. 13, fig. 1; O'Dogherty, 1994, p. 266, pl. 47, figs. 8–11; Aita *et al.*, 1997, pl. 1, fig. 3; Khan *et al.*, 1999, pl. 2, fig. j.

Vitorfus minimus: O'Dogherty, 1994, p. 266, pl. 47, figs. 4–7.

Holotype. Northern Italy, southern Venetian Alps, Colli Euganei, Teolo locality; upper Lower Cretaceous–lower Upper Cretaceous, Upper Albian–Lower Turonian (Squinabol, 1903, pl. 10, fig. 4).

Comparison. *V. brustolensis* differs from *V. campbelli* Pessagno (1977) in the narrower saturnal ring, the presence of only two auxiliary rays near each long external ray, and in the absence of distinct constriction of the ring at the joint with the cortical shell.

Occurrence. Albian–Campanian worldwide; Middle Cenomanian of northern Turkey; Lower Turonian of the Crimean Mountains.

Material. Seven specimens.

Vitorfus campbelli Pessagno, 1977

Plate 34, fig. 16

Vitorfus campbelli: Pessagno, 1977, p. 35, pl. 3, figs. 1, 2, and 7; Li and Wu, 1985, pl. 1, fig. 19; Thurow, 1988, p. 408, pl. 10, fig. 5; Erbacher, 1994, pl. 2, fig. 1; pl. 13, fig. 2; O'Dogherty, 1994, p. 265, pl. 47, figs. 16–20; Salvini and Marcucci Passerini, 1998, fig. 10.s.

Vitorfus sp.: Dumitrica, 1985, pl. 3, fig. 12.

Holotype. USNM-Pessagno, no. 242793; California, Great Valley section, locality NSF 884; Lower Cretaceous, Upper Albian (Pessagno, 1977, pl. 3, fig. 1).

Comparison. *V. campbelli* is distinguished from *V. morini* Empson-Morin, 1981 by having numerous peripheral auxiliary rays and by small dimensions of the ellipsoidal saturnal ring.

Occurrence. Upper Albian of California; Albian–Turonian worldwide; Upper Cenomanian of northern Turkey; Lower Turonian of the Crimean Mountains.

Material. Four specimens.

Vitorfus morini Empson-Morin, 1981

Plate 34, fig. 8

Vitorfus morini: Empson-Morin, 1981, p. 261, pl. 4, figs. 7a–8d; Dumitrica, 1985, pl. 1, figs. 7 and 9; pl. 3, fig. 4; O'Dogherty, 1994, p. 267, pl. 47, figs. 12–15; Salvini and Marcucci Passerini, 1998, fig. 10.t.

Holotype. USNM, no. 305331; Mid-Pacific Mountains, DSDP 32, Site 313; Upper Campanian (Empson-Morin, 1981, p. 4, figs. 8a–8d).

Description. The shell has a typical constricted ellipsoidal ring. The rim on the internal side of the ring may or may not be present. Long external rays, which are circular in cross section, are located on the external side of both poles of the long axis. The polar spines lie in the plane of the short axis of the ellipse. The cortical shell is oval, its long axis coincident with that of the saturnal ring. The cortical shell bears small rounded pores in a hexagonal–pentagonal arrangement. The pore frames are either pentagonal or irregularly hexagonal. The polar spines and the ring, except for a very small area around the auxiliary rays, are covered by the cortical shell.

Measurements. Diameter of the cortical shell, 100–80; greatest length of the saturnal ring, including auxiliary rays, 110–60.

Comparison. *V. morini* differs from other species of the genus *Vitorfus* Pessagno, 1977 in the smaller saturnal ring, which is almost entirely hidden under the cortical shell.

Occurrence. Upper Campanian of the Pacific; Lower Turonian of Italy; Lower Turonian of the Crimean Mountains.

Material. Six specimens.

Order Entactinaria Kozur et Mostler, 1982

Family Polyentactiniidae Nazarov, 1975

Genus *Cuboctostylus* Bragina, 1999

Etymology. From the Latin *cub* (cubic), *octo* (eight), and *stylos* (spine).

Type species. *Cuboctostylus sakhalinensis* Bragina, 1999.

Explanation of Plate 41

Figs. 1 and 6. *Triactoma fragilis* Bragina, 1996, ×200, specimens: (1) GIN, no. 4870/169; and (6) GIN, no. 4870/170.

Fig. 2. *Triactoma parva* (Squinabol, 1903), GIN, no. 4870/171, ×200.

Fig. 3. *Cuboctostylus pontidus* sp. nov., GIN, no. 4870/172, ×250.

Figs. 4 and 5. *Orbiculiforma ornata* sp. nov., ×200: (4) holotype GIN, no. 4870/173; and (5) paratype GIN, no. 4870/174.

Figs. 7 and 16. *Acaeniotyle diaphorogona* Foreman, 1973, ×100, specimens: (7) GIN, no. 4870/175; and (16) GIN, no. 4870/176.

Fig. 8. *Acaeniotyle umbilicata* (Rust, 1898), GIN, no. 4870/177, ×200.

Fig. 9. *Patellula helios* (Squinabol, 1903), GIN, no. 4870/178, ×100.

Fig. 10. *Dactyliodiscus longispinus* (Squinabol, 1904), GIN, no. 4870/179, ×75.

Fig. 11. *Dactyliodiscus lenticulatus* (Jud, 1994), GIN, no. 4870/180, ×100.

Fig. 12. *Becus regius* O'Dogherty, 1994, GIN, no. 4870/181, ×100.

Fig. 13. *Stylodictya insignis* Campbell et Clark, 1944, GIN, no. 4870/182, ×100.

Fig. 14. *Spongodiscoidea* gen. et sp. indet., GIN, no. 4870/183, ×100.

Fig. 15. *Triactoma cellulosa* Foreman, 1973, GIN, no. 4870/184, ×100.

Fig. 17. *Praeconocaryomma lipmanae* Pessagno, 1976, GIN, no. 4870/185, ×150.

Diagnosis. Large-sized hexahedron. Spicule with very short median beam positioned at shell center. Eight primary spines extending from beam have apices in shape of two or three cubes within each other. Neighboring spines connected by parallel beams serving as cube ribs. Beyond cortical shell, primary spines thickened and becoming Y-shaped in cross section. Occasionally, narrow branching apophyses depart from primary spines to form an additional subspherical cover of external or internal cube.

Species composition. *C. kasinzovae* Bragina, 1999, *C. sakhalinensis* Bragina, 1999, *C. trifurcatus* Bragina, 1999, and *C. pontidus* sp. nov.; Upper Cretaceous of the Tethys and Pacific.

Comparison. *Cuboctostylus* differs from *Pyloctostylus* Dumitrica, 1994 in the shorter median beam placed in the shell center rather than eccentrically, and in the absence of the pylome.

Remarks. Diagnostic characters of *Cuboctostylus* include a variant with three covers, as evidenced by photos and drawings of *Pyloctostylus apenninicus* Dumitrica (1994), which should be transferred to the genus *Cuboctostylus*, based on some shared characters (the short median beam, the presence of spines with apices arranged in a cube shape, and three covers).

Cuboctostylus bears a close similarity to the genus *Pyloctostylus* Dumitrica known from the Middle Cretaceous. Both genera have a spicule with eight primary spines. They are closely similar in shell structure to the Paleozoic genus *Polyentactinia*, which has the same number of primary spines (although they are differently orientated). *Pyloctostylus* Dumitrica, 1994 has two groups of primary spines (apical and basal). In distinction, *Cuboctostylus* has a shorter and centrally positioned median beam and lacks a pylome. The distinguishing structural feature of the *Cuboctostylus* spicule is that the primary spines form two groups (four spines in each) that are distinguished by their position relative to any plane crossing the shell center parallel to the cube wall. These groups cannot be differentiated into apical and basal. The short median beam and the absence of a pylome may be due to the same reason.

If the lineage of Polyentactiniidae–Orosphaeridae actually existed (Petrushevskaya, 1984; Dumitrica, 1994), there might be a peculiar branch represented by members of the genus *Cuboctostylus* and comprising taxa that have lost the pylome. It is premature to indicate unequivocally which genus could be a descendant of *Cuboctostylus*. However, the genus *Hexacromyum* (from the family Cubosphaeridae Haeckel, 1887) is similar to *Cuboctostylus* in certain significant morphological characteristics, such as its large size, the Y-shaped cross section of the primary spines connecting in the shell center (Bragina, 1991a), and the polygonal surface of the outer and inner covers. The similarity, however, may be a result of homeomorphism.

Occurrence. Cenomanian–Coniacian of the Naiba and Bykov formations of southern Sakhalin; Middle–Upper Cenomanian of northern Turkey; Lower Turonian of the Crimean Mountains.

Cuboctostylus pontidus Bragina, sp. nov.

Plate 30, figs. 4, 6, and 7; Plate 35, figs. 1, 2, and 8

Etymology. From the Latin *pontidus* (after the place of the first finding).

Holotype. GIN, no. 4871/333; northern Turkey, Ürküt section; Upper Cretaceous, Middle Cenomanian, Tomalar Formation.

Description. The spicule is narrow and has a very short median beam (MB) and eight spines, Y-shaped in cross section and arranged with their apices tracing the shape of two cubes within one another. Each of the eight spines is connected to a neighboring spine by a rounded angular beam forming a rib of the inner cube. The beams of the outer cube are almost twice as long as those of the inner cube. A narrow spine, rounded in cross section extends from each rib at the junction between the spine and the beam of the outer cube. These spines are oriented to the adjacent side of the cube at an angle of 90°. Each cube face shows a meshwork of large pores one-fifth to one-seventh the length of the cube edge. The secondary spines, analogous to those located at the junction of the spine and the cube beam (described above), may extend from the pore vertices. As the distance from the center increases, the spines become more and more massive and distinctly Y-shaped in cross section; however, outside the outer cube, they lose precise outlines and gradually become smooth towards the apices.

Measurements. Spine length, 400–500; diameter of the cortical shell, 350; diameter of the medullary shell, 180.

Comparison. *C. pontidus* can be distinguished from *C. trifurcatus* Bragina, 1999 by the lack of branching apophyses that cover the outer cube and of branches on the spines; however, on the middle part of the beams of the cortical shell, it develops secondary spines, which are oriented at 90° and extend toward the adjacent cube side.

Occurrence. Middle–Upper Cenomanian of northern Turkey; Lower Turonian of the Crimean Mountains.

Material. Three complete and numerous incomplete specimens.

Order Collodaria Haeckel, 1881

Family Orosphaeridae Haeckel, 1887

Genus *Archaeoplegma* Bragina, gen. nov.

Etymology. From the Latin *archaeo* (ancient) and the extant orosphaerid genus *Oroplegma*.

Type species. *Archaeoplegma pontidae* Bragina, sp. nov.

Diagnosis. Shell large-sized, subspherical, and reticulate, with one to three poorly developed covers.

Inner spicule absent. Numerous spines smooth, branching, unconnected in shell center but connected to shell covers by apophyses.

Species composition. Type species.

Comparison. The new genus differs from *Oroplegma* Haeckel in the absence of the finely reticulated polyhedral medullary shell.

***Archaeoplegma pontidae* Bragina, sp. nov.**

Plate 29, figs. 1–6; Plate 30, figs. 1–3 and 5

Etymology. From the Pontic Mountains, the place of the first finding.

Holotype. GIN, no. 4871/322; northern Turkey, Ürküt section; Upper Cenomanian, Tomalar Formation.

Description. The shell is very large and indistinctly polyhedral in outline. The cortical shell is composed of curved beams rounded in cross section. The irregular faces of the cortical shell display triangular, tetragonal, and pentagonal joints. The ribbed secondary spines with variously branching terminations extend from the cortical shell. The primary spines are rounded in cross section, oriented to the shell center, and reach the medullary shell. This shell is connected with the cortical shell by branching apophyses. A characteristic feature is the unstable shell shape and a high variability in patterns of connections between the poorly differentiated shells.

Measurements. Length of the external spines, 200; diameter of the cortical shell, 600–800.

Occurrence. Middle–Upper Cenomanian of northern Turkey; Lower Turonian of the Crimean Mountains.

Material. Several dozen complete and fragmentary specimens.

CONCLUSIONS

In the course of this investigation, the Cenomanian and Turonian radiolarians of northern Turkey and the Crimean Mountains have been monographically studied for the first time. The studies produced the following results:

(1) The abundant and diverse radiolarian assemblages at many stratigraphic levels of five sections (two in Turkey and three in the Crimea) were studied. Radiolarians were associated with other fossils (foraminifers, inoceramids, and nanoplankton), which will allow the revision of the stratigraphic ranges of various radiolarian species.

(2) In the type section of the Tomalar Formation (Turkey), a radiolarian assemblage has been recognized that is assigned to the upper part of the *Dactyliosphaera silviae* Zone established in the western Mediterranean (Middle–Upper Cenomanian). The Ürküt section (Turkey) yielded an abundant assemblage corresponding to the upper and lower parts of the *Dactyliosphaera silviae* Zone. The Crimean Mountains sections demonstrate the following succession of radiolarian assemblages (from the base upsection): (1) Beds with *Triactoma parva–Patulibracchium ingens* (Upper Cenomanian) correlating with the upper part of the *Dactyliosphaera silviae* Zone and (2) Beds with *Alievium superbum* (Early Turonian), correlating with the synonymous circumtropical zone.

(3) Units of the Mediterranean Middle Cretaceous radiolarian zonation (O'Dogherty, 1994) were recognized not only in the axial areas of the Mediterranean belt (Turkey) but also in its periphery (the Crimea), making the refinement of the Upper Cretaceous radiolarian zonation possible.

(4) 193 radiolarian species belonging to 4 orders, 28 families, and 77 genera were described. Of these, one genus (*Cuboctostylus*) and three species were previously described by the author. One new genus (*Archaeoplegma*) and 36 new species were described. The diagnoses of 5 genera, and 28 species were emended. This study also emended the stratigraphic and geographic ranges of the majority of radiolarians under discussion.

ACKNOWLEDGMENTS

I am grateful to M.A. Akhmetiev, N.Yu. Bragin, Yu.B. Gladenkov, N.V. Goreva (Geological Institute of the Russian Academy of Sciences), A.S. Alekseev, L.F. Kopaevich, D.P. Naidin (Moscow State University), V.S. Vishnevskaya (Institute of Lithosphere of Marginal Seas of the Russian Academy of Sciences), and M.S. Afanasieva (Paleontological Institute of the Russian Academy of Sciences) for their support and valuable advice during the preparation of the monograph. I would like to thank A.I. Zhamoida, L.I. Kazintsova (VSEGEI) and G.E. Kozlova (VNIGRI) for helpful remarks. C. Tunoğlu and U.K. Tekin (Hacettepe University of Ankara) provided the field work in Turkey. Photos of a part of the microfossil material were made in Belgium thanks to the courtesy of A. Dhoundt (University of Brussels). I thank N.V. Gor'kova (Geological Institute of the Russian Academy of Sciences) for help with the electron microscope.

This study was supported by the Russian Foundation for Basic Research, project no. 00-05-64618.

REFERENCES

1. Y. Aita, K. Ogata, H. Murakami, *et al.*, "Late Cretaceous and Eocene Radiolarians from the Goshoura and Maki-shima Islands, Amakusa, Kumamoto, Japan," News Osaka Micropaleontol. **10**, 267–283 (1997).
2. A. S. Alekseev, V. S. Vengertsev, L. F. Kopaevich, and T. A. Kuz'micheva, "Lithology and Micropaleontology of the Cenomanian–Turonian Boundary Beds of the Southwestern Crimea," Tr. Krym. Geol. Nauchno-Issled. Tsentra, No. 1, 54–73 (1997).

3. Kh. Sh. Aliev, *Radiolarians of the Lower Cretaceous Deposits of Northeastern Azerbaijan and Their Stratigraphic Significance* (Akad. Nauk Azerb. SSR, Baku, 1965) [in Russian].
4. Kh. Sh. Aliev, "New Species of Valanginian and Albian Radiolarians of Northeastern Azerbaijan," in *Cretaceous Deposits of the Eastern Caucasus and Adjacent Areas* (Nauka, Moscow, 1967), pp. 69–72 [in Russian].
5. Kh. Sh. Aliev, "New Species of the Subfamily Lithocampinae from the Albian and Cenomanian of Northeastern Azerbaijan," Izv. Akad. Nauk Azerb. SSR, Ser. Nauk Zemle, No. 2, 26–32 (1968).
6. Kh. Sh. Aliev and R. F. Smirnova, "New Radiolarian Species from the Deposits of the Albian Stage in the Central Areas of the Russian Platform," in *Fossil and Recent Radiolarians: Materials of the Second All-Union Seminar on Radiolarians* (L'vov Univ., Lvov, 1969), pp. 62–72.
7. E. O. Amon, "Upper Cretaceous Radiolarians of the Ural Mountains," in *Materials on the Stratigraphy and Paleontology of the Ural Mountains* (Inst. Geol. Geokhim., Ural. Otd. Ross. Akad. Nauk, Yekaterinburg, 2000), Vol. 5, pp. 1–207 [in Russian].
8. *Atlas of Upper Cretaceous Fauna from the Northern Caucasus and Crimea* (Gostoptekhizdat, Moscow, 1959) [in Russian].
9. "Atlas of Mesozoic Index Faunal Groups of the Southern and Eastern USSR," Tr. Vseross. Nauchno-Issled. Geol. Inst. **350**, 1–375 (1992).
10. *Atlas of Cretaceous Index Faunal Groups of Sakhalin* (Nedra, St. Petersburg, 1993) [in Russian].
11. M. Bak, "Late Albian–Early Cenomanian Radiolaria from the Czorsztyn Succession of Pieniny Klippen Belt, Carpathians," Studia Geol. Pol., No. 102, 177–207 (1993).
12. P. O. Baumgartner, L. O'Dogherty, S. Gorican, *et al.*, "Middle Jurassic to Lower Cretaceous Radiolaria of Tethys: Occurrences, Systematics, Biochronology," Mem. Geol. Lausanne, No. 23, 1–1172 (1995).
13. N. Yu. Bragin, L. G. Bragina, and K. A. Krylov, "Albian–Cenomanian Deposits of the Mamonia Complex, Southwestern Cyprus," in *Proceedings of the Third International Conference on the Geology of the Eastern Mediterranean, Nicosia, Cyprus, 1998*, Ed. by I. Panayides, C. Xenophontos, and J. Malpas, (Geol. Surv., Nicosia, 2000), pp. 309–315.
14. N. Yu. Bragin, L. G. Bragina, C. Tunoğlu, and K. Tekin, "The Cenomanian (Upper Cretaceous) Radiolarians from the Tomalar Formation, Central Pontides, Northern Turkey," Geol. Carpath. **52** (6), 349–360 (2001).
15. L. G. Bragina, "Late Campanian–Maastrichtian Radiolarians from Shikotan Island," in *Paleontological–Stratigraphic Studies of the Far East Phanerozoic* (Dal'nevost. Geol. Inst. Dal'nevost. Otd. Akad. Nauk SSSR, Vladivostok, 1991a), pp. 100–103.
16. L. G. Bragina, "Radiolarians from the Santonian–Campanian Bystraya Formation of the Northwestern Kamchatka," Izv. Akad. Nauk SSSR, Ser. Geol., No. 7, 129–136 (1991b).
17. L. G. Bragina, "Radiolarians and Stratigraphy of the Upper Cretaceous Khotkovo Group of the Moscow Region," Byull. Mosk. O–va Izpyt. Prir., Otd. Geol. **69** (2), 91–100 (1994).
18. L. G. Bragina, "Cenomanian–Turonian Radiolarians of the Crimean Mountains," Byull. Mosk. O–va Izpyt. Prir., Otd. Geol. **74** (3), 43–50 (1999a).
19. L. G. Bragina, "*Cuboctostylus* n. gen., a New Late Cretaceous Spicule-Bearing Spumellarian Radiolaria from Southern Sakhalin (Russia)," Geodiversitas **21** (4), 571–580 (1999b).
20. L. G. Bragina, "Radiolarians and Stratigraphy of the Cenomanian and Turonian of the Crimean Mountains and Southern Sakhalin," Candidate's Dissertation in Geology–Mineralogy (Geol. Inst. Ross. Akad. Nauk, Moscow, 2001).
21. L. G. Bragina, "New Radiolarian Species from the Upper Cretaceous Naiba Reference Section (Southern Sakhalin)," Paleontol. Zh., No. 3, 25–30 (2003) [Paleontol. J., No. 3, 244–251 (2003)].
22. L. G. Bragina and N. Yu. Bragin, "Radiolarians and Stratigraphy of the Campanian–Maastrichtian Deposits in Southwestern Cyprus," Stratigr. Geol. Korrel. **3** (2), 147–155 (1995) [Stratigr. Geol. Correlation **3** (2), 143–151 (1995)].
23. L. G. Bragina and N. Yu. Bragin, "Stratigraphy and Radiolarians from the Type Section of the Perapedhi Formation (Upper Cretaceous of Cyprus)," Stratigr. Geol. Korrel. **4** (3), 38–45 (1996) [Stratigr. Geol. Correlation **4** (3), 346–353 (1996)].
24. L. G. Bragina and N. Yu. Bragin, "Radiolaria from the Upper Cretaceous Section near the Village of Novodevich'e (Samara Region, Middle Volga)," Stratigr. Geol. Korrel. (in press).
25. L. G. Bragina and D. I. Vitukhin, "Radiolarians from Cretaceous Deposits of the Maini-Kakyine Ridge, Koryak Highland," Stratigr. Geol. Korrel. **5** (2), 176–179 (1997) [Stratigr. Geol. Correlation **5**, 171–174 (1997)].
26. A. S. Campbell and B. L. Clark, "Radiolaria from the Upper Cretaceous of Middle California," Spec. Pap. Geol. Soc. Am., No. 57, 1–61(1944).
27. L. Cayeux, "Contribution a l'etude micrographique des terrains sedimentaires: 1. Etude de quelques depots siliceux secondaires et tertiaires du Basin de Paris et de la Belgique, 2. Craie du Basin de Paris," Mem. Soc. Geol. Nord. **4** (2), 1–591 (1897).
28. P. De Wever, C. Bourdillon-De Grissac, and M. Beurrier, "Radiolaries senonies de la Nappe de Samail (Oman)," Rev. Micropaleontol. **31** (3), 166–177 (1988).
29. I. V. Dolitskaya, "Facies-Controlled Distribution of Foraminifers in the Upper Cretaceous of the Crimean Mountains," Izv. Akad. Nauk SSSR, Ser. Geol., No. 4, 123–135 (1972).
30. D. Donofrio and H. Mostler, "Zur Verbreitung der Saturnalidae (Radiolaria) im Mesozoikum der Nordlichen Kalkalpen und Sudalpen," Geol. Paläontol. Mitt. Innsbruck **7** (5), 1–55 (1978).
31. P. Dumitrica, "Cryptocephalic and Cryptothoracic Nassellaria in Some Mesozoic Deposits of Romania," Rev. Roum. Geol. Geophys. Geogr., Ser. Geol. **14** (1), 45–124 (1970).
32. P. Dumitrica, "Cretaceous and Quaternary Radiolaria in Deep-Sea Sediments from the Northeast Atlantic Ocean

and Mediterranean Sea," in *Initial Reports of the Deep Sea Drilling Project* (US Gov. Print. Off., Washington, 1972), Vol. 13, No. 2, pp. 829–901.

33. P. Dumitrica, "Cenomanian Radiolaria at Podul Dimbovitei," in *Micropaleontological Guide to the Mesozoic and Tertiary of the Romanian Carpathians: Abstracts of the 14th Micropaleontological Colloquium* (Inst. Geol. Geophys., Bucharest, 1975), pp. 87–89.
34. P. Dumitrica, "Internal Morphology of the Saturnalidae (Radiolaria); Systematic and Phylogenetic Consequences," Rev. Micropaleontol. **28** (3), 181–196 (1985).
35. P. Dumitrica, "*Pyloctostylus* n. gen., a Cretaceous Spumellarian Radiolarian Genus with Initial Spicule," Rev. Micropaleontol. **37** (4), 235–244 (1994).
36. P. Dumitrica, "Systematic Framework of Jurassic and Cretaceous Radiolaria," Mem. Geol. Lausanne, No. 23, 19–35 (1995).
37. C. G. Ehrenberg, "Ueber die mikroskopisschen kieselschaligen Polycystinen als machtige Gebirgsmasse von Barbados und uber das Verhaltniss der aus mehr als 300 neuen Arten bestehenden ganz eigenthumlichen Formengruppe jener Felsmasse zu den jetzt lebenden Thieren und zur Kreidebildung Eine neue Anregung zur Erforschung des Erdlebens," in *Jahrbuch Königlich Preussischen Akademie der Wissenschaften* (Berlin, 1847), pp. 40–60.
38. C. G. Ehrenberg, "Die systematische Charakteristik der neun mikroskopischen Organismen des tiefen atlantischen Oceans," in *Jahrbuch Königlich Preussischen Akademie der Wissenschaften* (Berlin, 1854), pp. 236–250.
39. C. G. Ehrenberg, "Fortsetzung der mikrogeologischen Studien als Gesammt-Uebersichtder mikroskopischen Paläontologie gleichartig analysirter Gebirgsarten der Erde, mit specieller Rucksicht auf den Polycystinen-Mergel von Barbados," in *Jahrbuch Königlich Preussischen Akademie der Wissenschaften* (Berlin, 1875), pp. 1–225.
40. K. M. Empson-Morin, "Campanian Radiolaria from DSDP Site 313, Mid-Pacific Mountains," Micropaleontology **27** (3), 249–292 (1981).
41. K. M. Empson-Morin, "Depth and Latitude Distribution of Radiolaria in Campanian (Late Cretaceous) Tropical and Subtropical Oceans," Micropaleontology **30** (1), 87–115 (1984).
42. J. Erbacher, "Entwicklung und Palaoozeanographic mittelkretazischer Radiolarien der westlichen Tethis (Italien) und des Nordatlantiks," Tubinger Mikropaleontol. Mitt. Tubingen, No. 12, 1–119 (1994).
43. H. Foreman, "Two Cretaceous Radiolarian Genera," Micropaleontology **12** (3), 355–359 (1966).
44. H. Foreman, "Upper Maastrichtian Radiolaria of California," Spec. Pap. Paleontol., No. 3, 1–82 (1968).
45. H. Foreman, "Cretaceous Radiolaria, Leg 7, in *Initial Reports of the Deep Sea Drilling Project* (US Gov. Print. Off., Washington, 1971), Vol. 7, Part 2, pp. 1673–1693.
46. H. Foreman, "Radiolaria from DSDP Leg 20," in *Initial Reports of the Deep Sea Drilling Project* (US Gov. Print. Off., Washington, 1973), Vol. 20, pp. 249–305.
47. H. Foreman, "Radiolaria from the North Pacific, DSDP, Leg 32," in *Initial Reports of the Deep Sea Drilling Project* (US Gov. Print. Off., Washington 1975), Vol. 32, pp. 579–676.
48. H. Foreman, "Cretaceous Radiolaria in the Eastern South Atlantic, DSDP, Leg 40," in *Initial Reports of the Deep Sea Drilling Project* (US Gov. Print. Off., Washington, 1978a), Vol. 40, pp. 839–843.
49. H. Foreman, "Mesozoic Radiolaria in the Atlantic Ocean off the Northwest Coast of Africa, Leg 41," in *Initial Reports of the Deep Sea Drilling Project* (US Gov. Print. Off., Washington, 1978b), Vol. 41, pp. 739–761.
50. *Geological Structure of the Kacha Upland of the Crimean Mountains* (Mosk. Gos. Univ., Moscow, 1989) [in Russian].
51. T. N. Gorbatchik and L. I. Kazintsova, "Radiolarians and Foraminifers from the Upper Albian of the Village of Mar'ino (Simferopol Region, Crimea)," Stratigr. Geol. Korrel. **6** (6), 44–51 (1998) [Stratigr. Geol. Correlation **6**, 541–548 (1998)].
52. H. Gorka, "Les radiolaires du Turonien inferieur du sondage de Leba IG 1 (Pologne)," Cah. Micropaleontol. **6** (1), 39–45 (1991).
53. E. Haeckel, *Die Radiolarien (Rhizopoda Radiolaria)* (Reiner, Berlin, 1862), Part 1, Vol. 14.
54. E. Haeckel, "Entfurt eines Radiolarien-Systems auf Grund von Studien der Challenger-Radiolarien," Z. Naturwiss. Jena, Ser. 8, **15** (3), 418–472 (1881).
55. E. Haeckel, "Exploration of the Faroe Channel, during the Summer of 1880, in H.M. Shired Ship *Knight Errant*: List of Radiolaria," Proc. R. Soc. Edinburgh **11**, 638–677 (1882).
56. E. Haeckel, "Report on the Radiolaria Collected by H.M.S. Challenger during the Years 1873–76," Rep. Sci. Res. Voyage H.S.M. Challenger., Ser. Zool. **18**, 1–1803 (1887).
57. J. M. Hancock, W. J. Kennedy, and C. W. Wright, "Towards a Correlation of the Turonian Sequences of Japan with Those of North-West Europe," Spec. Pap. Paleontol. Soc. Jpn., No. 21, 151–158 (1977).
58. H. Hashimoto and K. Ishida, "Correlation of Selected Radiolarian Assemblages of the Upper Cretaceous Izumi and Sotoizumi Groups and Shimanto Supergroup in Shikoku," News Osaka Micropaleontol., Vol. Spec., No. 10, 245–257 (1997).
59. C. J. Hollis, "Cretaceous–Paleocene Radiolaria from Eastern Marlborough, New Zealand," Paleontol. Bull. New Zeal. Geol. Surv., No. 73, 1–152 (1997).
60. W. M. Holmes, "On Radiolaria from the Upper Chalk at Coulsdon (Surrey)," Quart. J. Geol. Soc. London **56**, 694–704 (1900).
61. K. Iwata and J. Tajika, "Late Cretaceous Radiolarians of the Yubetsu Group, Tokoro Belt, Northeast Hokkaido," J. Fac. Sci. Hokkaido Univ., Ser. 4, **21** (4), 619–644 (1986).
62. K. Ishida and H. Hashimoto, "Radiolarian Assemblage from the Kushibuchi Formation of the Sotoizumi Group in East Shikoku," J. Geol. Soc. Jpn. **102** (4), 361–364 (1996).
63. R. Jud, "Biochronology and Systematics of Early Cretaceous Radiolarians of the Western Tethys," Mem. Geol. Lausanne, No. 19, 1–147 (1994).

127. A. Schaaf, "Late Early Cretaceous Radiolaria from Deep Sea Drilling Project Leg 62," in *Initial Reports of the Deep Sea Drilling Project* (US Gov. Print. Off., Washington 1981), Vol. 62, pp. 419–470.

128. A. Schaaf, "Les Radiolaires du Cretace inferieur et Moyen: Biologie et Systematique," Sci. Geol. Mem., No. 75, 1–189 (1984).

129. A. Schaaf, "Un nouveau canevas biochronologique du Cretace inferieur et moyen: les biozones a radiolaires," Sci. Geol. Bull. Strasbourg **38** (3), 227–269 (1985).

130. R. Schmidt-Effing, "Radiolarien der Mittel-Kreide aus dem Santa Elena-Massiv von Costa Rica," Neues Jahrb. Geol. Paläontol. Abh. **160** (2), 241–257 (1980).

131. A. M. C. Sengor, "Structural Classification of the Tectonic History of Turkey," in *Proceedings of Ketin Symposium* (Turkish Geol. Soc., Ankara, 1984), pp. 37–62.

132. S. I. Shumenko and V. P. Stetsenko, "The Crimean Upper Cretaceous Zonation Based on Calcareous Nannofossils," Dokl. Akad. Nauk SSSR **241** (5), 1160–1162 (1978).

133. K. Sporli and Y. Aita, "Tectonic Significance of Late Cretaceous Radiolaria from the Abducted Matakaoa Volcanics, East Cape, North Island, New Zealand," Geosci. Rep. Shizuoka Univ., No. 20, 115–133 (1994).

134. S. Squinabol, "Le Radiolarie dei noduli selciosi nella Scaglia degli Euganei: Contribuzione 1," Riv. Ital. Paleontol. **9**, 105–151 (1903).

135. S. Squinabol, "Radiolaria cretacee degli Euganei," Atti Mem. Accad. Sci. Lett. Arti Padova, New. Ser. **20**, 171–244 (1904).

136. S. Squinabol, "Contributo alla conoscenza dei Radiolarii fossili del Veneto: Appendice—Di un genera di Radiolari caratteristico del Secondario," Mem. Ist. Geol. R. Univ. Padova **2**, 249–306 (1914).

137. M. Sykora, L. Ozwoldova, and D. Boorova, "Turonian Silicified Sediments in the Czorsztyn Succession of the Pieniny Klippen Belt (Western Carpathian Slovakia)," Geol. Carpath. **48** (4), 243–261 (1997).

138. Y. Taketani, "Cretaceous Radiolarian Biostratigraphy of the Urakawa and Obira Areas, Hokkaido," Sci. Rep. Tohoku Univ., 2nd Ser. (Geol.) **52** (1–2), 1–76 (1982).

139. Y. Taketani and Y. Kanie, "Radiolarian Age of the Lower Yezo Group and the Upper Part of the Sorachi Group in Hokkaido," in *Centenary of Japanese Micropaleontology*, Ed. by K. Ishizaki and T. Saito (Terra Sci., Tokyo, 1992), pp. 365–373.

140. Tan Sin Hok, "Over de sommenstelling en het onstaan van Krijten mergelgesteenten van de Molukken," in *Jaarbook van het mijnwezen in Nederlandsch Oost-Indie*, Ed. by H. A. Brouwer (S'Gravenhage, 1927), pp. 1–165.

141. Y. Teraoka and C. Kurimoto, "Cretaceous Stratigraphy of the Shimanto Terrane in the Uwajima Area, West Shikoku, Southwest Japan, with Reference to the Stratigraphic Distribution of Mega- and Radiolarian Fossils," Bull. Geol. Surv. Jpn. **37** (8), 417–453 (1986).

142. J. Thurow, "Cretaceous Radiolarians of the North Atlantic Ocean: ODP Leg 103 (Sites 638, 640 and 641) and DSDP Legs 93 (Site 603) and 47B (Site 398)," Proc. Final Rep. Oc. Dril. Progr., Part B **103**, 379–418 (1988).

143. J. Thurow and R. Anderson, "An Interpretation of Skeletal Growth Patterns of Some Middle Cretaceous and Modern Radiolarians," Micropaleontology **32** (4), 289–302 (1986).

144. J. Thurow and W. Kuhnt, "North Atlantic Palaeoceanography: Mid-Cretaceous of the Gibraltar Arch Area," Spec. Publ. Geol. Soc. London **22**, 423–445 (1986).

145. F. Tumanda, "Cretaceous Radiolarian Biostratigraphy in the Eashi Mountain Area, Northern Hokkaido, Japan," Sci. Rep. Inst. Geosci. Univ. Tsukuba **10**, 1–44 (1989).

146. F. Tumanda and K. Sashida, "On the Occurrence of Inoceramid Bivalves and Radiolarians from the Manokawa Formation, Esashi Mountain Area, Northern Hokkaido," Annu. Rep. Inst. Geosci., Univ. Tsukuba **14**, 56–63 (1988).

147. C. Tunoğlu, "Geological Investigations of Northern Devrekani (Kastamonu)," PhD Thesis (Hacettepe Univ., Ankara, 1991) [in Turkish, English abstract].

148. C. Tunoğlu, "Microfacies Analysis of the Upper Paleocene–Middle Eocene Carbonate Sequence of Devrekani Basin (Northern Kastamonu)," Geol. Bull. Turkey **37** (2), 43–51 (1994).

149. E. Urquhart and F. T. Banner, "Biostratigraphy of the Supra-Ophiolite Sediments of the Troodos Massif, Cyprus: The Cretaceous Perapedhi, Kannaviou, Moni and Kathikas Formations," Geol. Mag. **131** (4), 499–518 (1994).

150. E. Urquhart and A. H. F. Robertson, "Radiolarian Evidence of Late Cretaceous Exotic Blocks at Mangaleni, Cyprus and Implications for the Origin and Emplacement of the Related Moni Melange," in *Proceedings of the Third International Conference on Geology of Eastern Mediterranean, Nicosia, Cyprus, 1998* (Geol. Surv. Dep. Print., Nicosia, 2000), pp. 299–307.

151. P. E. Vinassa de Regny, "Radiolari Cretacei dell'Isola di Karpathos," Mem. Accad. Sci. Ist. Bologna **9**, 497–512 (1901).

152. V. S. Vishnevskaya, "Jurassic and Cretaceous Radiolarian Biostratigraphy in Russia," Micropaleontol. Spec. Publ., No. 6, 175–200 (1993).

153. V. S. Vishnevskaya, *Jurassic to Cretaceous Radiolarian Biostratigraphy of Russia* (GEOS, Moscow, 2001) [in Russian].

154. K. Wakita, Munasri, and Bambang, "Cretaceous Radiolarians from the Luk Ulo Melange Complex in the Karangsambung Area, Central Java, Indonesia," J. Southeast Asian Earth Sci. **9** (1–2), 29–43 (1994).

155. M. P. White, "Some Index Foraminifera of the Tampico Embayment Area of Mexico," J. Paleontol. **2** (4), 280–317 (1928).

156. H. R. Wu, "Some New Genera and Species of Cenomanian Radiolaria from Southern Xizang (Tibet)," Acta Micropalaeontol. Sin. **3** (4), 347–360 (1986).

157. V. P. Zinkevich, E. A. Konstantinovskaya, R. M. Magakyan, and L. G. Bragina, "Tectonics of the Ozernyi Peninsula (Eastern Kamchatka)," in *Essays on Geology of the Kamchatka and Koryak Upland* (Nauka, Moscow, 1988), pp. 87–102 [in Russian].

158. K. A. Zittel, "Ueber einige fossile Radiolarien aus der norddeutschen Kreide," Z. Deutsch. Geol. Gesellschaft **28**, 75–86 (1876).